DNA METHYLATION STATUS OF IMPRINTED GENE H19 AND IGF2 IN AMNIOTIC FLUID STEM CELLS

SUJEEPORN SRIPRADITE

**A THESIS SUBMITTED IN PARTIAL FULFILLMENT
OF THE REQUIREMENTS FOR
THE DEGREE OF MASTER OF SCIENCE (BIOCHEMISTRY)
FACULTY OF GRADUATE STUDIES
MAHIDOL UNIVERSITY
2010**

Thesis
entitled

DNA METHYLATION STATUS OF IMPRINTED GENE H19 AND IGF2 IN AMNIOTIC FLUID STEM CELLS

……..
Sujeeporn Sripradite,
Candidate

……..
Assoc. Prof. Nednapis Tirawanchai,
Ph.D.
Major advisor

……..
Lect.Tassanee Phermthai,
Ph.D.
Co-advisor

……
Lect.Wanna Thongnoppakhun,
Ph.D.
Co-advisor

……
Assoc. Prof. Vitaya Titapant,
M.D.
Co-advisor

……..
Prof. Banchong Mahaisavariya,
M.D., Dip Thai Board of Orthopedics
Dean
Faculty of Graduate Studies
Mahidol University

……..
Asst. Prof. Vorapan Sirivatanauksorn,
M.D., Ph.D.
Program Director
Master of Science
Program in Biochemistry
Faculty of Medicine, Siriraj Hospital
Mahidol University

Thesis
entitled

DNA METHYLATION STATUS OF IMPRINTED GENE H19 AND IGF2 IN AMNIOTIC FLUID STEM CELLS

was submitted to the Faculty of Graduate Studies, Mahidol University
for the degree of Master of Science (Biochemistry)
on

……....
Sujeeporn Sripradite,
Candidate

……....
Assist.Prof.Chatri Settasatian, Ph.D.
Chair

……....
Assoc. Prof. Nednapis Tirawanchai,
Ph.D.
Member

……....
Lect.Tassanee Phermthai,
Ph.D.
Member

……....
Lect. Wanna Thongnoppakhun,
Ph.D.
Member

……....
Assoc. Prof. Vitaya Titapant,
M.D.
Member

……....
Prof. Banchong Mahaisavariya,
M.D., Dip Thai Board of Orthopedics
Dean
Faculty of Graduate Studies
Mahidol University

……....
Prof.Teerawat Kulthanan,
M.D., Cert of Orthopedics
Dean
Faculty of Medicine Siriraj Hospital
Mahidol University

ACKNOWLEDGEMENTS

I would like to express my sincere gratitude and deep appreciation to Assoc. Prof. Nednapis Tirawanchai, my advisor, for her creative guidance, helpful suggestions, valuable advice, supervision and encouragement throughout this thesis work. Again, I am appreciated and thank you for everything.

I am so much indebted to Lect.Tatsanee Phermthai, my co-advisor, for her kindness, valuable guidance, suggestions and comments in everything throughout my work. She always shows me for being leader and experience me many things including how to dealing with thesis problem. I would like to apologize for whatever I have done the mistake and made her disappointed.

I am also very grateful to Lect.Wanna Thongnoppakhun, my co-advisor, for her suggestions and comments on this work that would always be remembered.

My grateful appreciation is extended to Assoc. prof. Vitaya Titapant, chairman of the thesis examination committees and Assist. Prof. Chatri Settasatian, external members of the thesis examination committees, for their expert guidance, valuable comments and suggestions.

Sincere appreciation is expressed to staffs of Stem Cell Research and Development for Medical Therapy, Department of Obstetrics & Gynecology, Faculty of Medicine Siriraj Hospital, for their help, suggestions and laboratory instruments.

I would like to express my thankfulness to staffs in Unit of Molecular Genetics, Reseach and Development Institute, for their kindness and suggestions in bisulfite conversion techniques including sharing of chemical reagents and laboratory instruments.

I also wish to express my appreciation to Miss Anchaleekorn Somkasetrin and staffs in Department of Biochemistry, Faculty of Medicine Siriraj Hospital, for their kindly help and suggestions in laboratory techniques including preparation of chemical reagents and laboratory instruments.

Many thanks are given to the graduate students and members of Department of Biochemistry, Faculty of Medicine Siriraj Hospital, especially Miss Aussara Panya, Miss Lanka Ranaweera and Mr. Aung Win Tun for their friendships and generous helps in many ways.

This thesis is partially supported by Graduate Thesis scholarship, Faculty of Medicine Siriraj Hospital, Mahidol University

Last but not least, I would like to express my sincere gratitude and deepest appreciation to my beloved parents, my brother, sister and all the members of ours family for their infinite love, attention, concerning care, understanding and encouragement throughout my life which will never be forgotten.

Sujeeporn Sripradite

DNA METHYLATION STATUS OF IMPRINTED GENE H19 AND IGF2 IN AMNIOTIC FLUID STEM CELLS

SUJEEPORN SRIPRADITE 4936481 SIBC/M

M.Sc. (BIOCHEMISTRY)

THESIS ADVISORY COMMITTEE: NEDNAPIS TIRAWANCHAI, Ph.D. (BIOCHEMISTRY), TATSANEE PHERMTHAI, Ph.D. (BIOTECHNOLOGY), WANNA THONGNOPPAKHUN, Ph.D. (BIOCHEMISTRY), VITAYA TITAPANT, M.D.

ABSTRACT

The amniotic fluid stem cell is the intermediate stem cell between the embryonic stem cell (ESC) and adult stem cell (ASC). This stem cell gives more advantages for medical therapy than other stem cells due to its appropriate proliferation potential, it has no teratoma formation as reported in ESC and it has higher proliferation potential than ASC to generate an adequate cell. Therefore, the factor that regulates AFS proliferation is quite interesting. DNA methylation is the one major mechanism of epigenetics that controls cell activity by regulation of gene action. The DNA methylation pattern is stable and has inheritable characteristics. Once it is established, it is maintained and passed through the daughter cells. The unique gene called the imprinted gene is also affected by DNA methylation mechanism. This gene is a susceptible gene due to its monoallelic methylation. The alteration of DNA methylation status on only one allele can lead to different cell characteristics. Some imprinted genes are involved in cell proliferation. The intensively studied imprinting cluster which regulates cell proliferation is the IGF2-H19 imprinting cluster. This imprinting cluster comprises 2 homeostatic imprinted genes. The *IGF2* encodes an insulin-like growth factor to trigger cell proliferation whereas the non-translated *H19* downregulates cell proliferation. The gene action of *IGF2* and *H19* is regulated by a DNA methylation pattern at the CTCF6 binding region upstream of H19, which has been suggested as the Imprinting Control Region (ICR). In addition, the Differentially Methylated Region (DMR) within IGF2 is also suggested as the regulatory region due to its imprinting methylation pattern. The methylation pattern at these regions was studied in various cell types including embryonic stem cells, embryonic tissues, various cancer cells and cells from patients suffering growth retardation such as from Bechwith-Weidmann Syndrome (BWS), and Silver Russel Syndrome. However, the DNA methylation at these regions in AFS has never been reported. Therefore, this study investigated the DNA methylation pattern at both DMR and ICR in the IGF2-H19 imprinting cluster in AFS using bisulfite sequencing technique. It also defined the methylation pattern separately at different passages, P8 and P15. The results showed that all CpG sites in both DMR and ICR are differentially methylated. Only some CpG sites in ICR at passage8 (P8) displayed biallelic methylation. The study concluded that the DNA methylation at DMR and ICR in the IGF2-H19 imprinting cluster of AFS cell was imprinting pattern. Additionally, the change of methylation pattern at ICR can occur during *in vitro* cultured process.

KEY WORDS: AMNIOTIC FLUID STEM CELL/ DNA METHYLATION/ IMPRINTING/ IGF2/ H19

135 pages

การศึกษารูปแบบ DNA METHYLATION ของยีนฝังจำ H19 และ IGF2 ในเซลล์ต้นกำเนิดน้ำคร่ำ (DNA METHYLATION STATUS OF IMPRINTED GENE H19 AND IGF2 IN AMNIOTIC FLUID STEM CELLS)

ศุจีภรณ์ ศรีประดิษฐ์ 4936481 SIBC/M

วท.ม.(ชีวเคมี)

คณะกรรมการที่ปรึกษาวิทยานิพนธ์: เนตรนภิส ธีระวัลย์ชัย, Ph.D., ทัศนีย์ เพิ่มไทย, Ph.D.,
วรรณา ทองนพคุณ, Ph.D., วิทยา ถิฐาพันธ์, M.D.

บทคัดย่อ

เซลล์ต้นกำเนิดน้ำคร่ำจัดเป็นเซลล์ต้นกำเนิดทารก ซึ่งมีศักยภาพอยู่ระหว่างเซลล์ต้นกำเนิดตัวอ่อนและเซลล์ต้นกำเนิดตัวเต็มวัย เมื่อพิจารณาถึงศักยภาพในการแบ่งตัวและการเปลี่ยนแปลงไปเป็นเซลล์ทำหน้าที่นั้นจะเห็นได้ว่าเซลล์ต้นกำเนิดน้ำคร่ำมีความสามารถในการเปลี่ยนแปลงไปเป็นเซลล์อื่นได้น้อยกว่าเซลล์ต้นกำเนิดตัวอ่อน ดังนั้น เซลล์ต้นกำเนิดน้ำคร่ำจึงมีศักยภาพในการนำไปใช้ในการรักษาต่ำกว่าเซลล์ต้นกำเนิดตัวอ่อนในแง่ของความหลากหลายในการสร้างเซลล์ทำหน้าที่ แต่ในแง่ของการแบ่งตัวเพิ่มจำนวนนั้น เซลล์ต้นกำเนิดน้ำคร่ำกลับมีความได้เปรียบในการนำไปใช้รักษามากกว่าเซลล์ต้นกำเนิดตัวอ่อนและตัวเต็มวัยเนื่องจากมีศักยภาพที่ไม่มากเกินไปจนก่อให้เกิดมะเร็งดั่งเช่นเซลล์ต้นกำเนิดตัวอ่อนและไม่น้อยเกินดั่งที่เป็นข้อจำกัดของเซลล์ต้นกำเนิดตัวเต็มวัย ดังนั้นการศึกษานี้จึงได้สนใจถึงปัจจัยควบคุมการแบ่งตัวเพิ่มจำนวนของเซลล์ ซึ่งการทำงานของยีนฝังจำใน IGF2-H19 imprinting cluster เป็นปัจจัยหนึ่งที่มีการศึกษาอย่างมากและมีรายงานว่ามีความสัมพันธ์กับความบกพร่องทางการเจริญเติบโตหลายๆโรคด้วยกัน โดยยีนฝังจำในกลุ่มนี้ประกอบด้วย 2 ยีนที่ทำหน้าที่ควบคุมสมดุลของการแบ่งเซลล์ ได้แก่ ยีน Insulin-like growth factor 2 (*IGF2*) ซึ่งส่งเสริมการแบ่งเซลล์ และ ยีน H19 ซึ่งยับยั้งการแบ่งเซลล์ ยีนในกลุ่มนี้จะมีการทำงานสัมพันธ์กันภายใต้การควบคุมของ DNA methylation ที่บริเวณ ICR เหนือยีน *H19* และ DMR ของยีน *IGF2* ดังนั้น เราจึงสนใจศึกษารูปแบบ methylation ที่บริเวณ ICRและ DMR ในเซลล์ต้นกำเนิดน้ำคร่ำซึ่งยังไม่เคยมีรายงานมาก่อน และนอกจากนี้ยังได้ทำการเปรียบเทียบรูปแบบ methylation ระหว่างเซลล์ต้นกำเนิดน้ำคร่ำที่ passage ต่างกันด้วย (passage8 และ passage15) การศึกษานี้ใช้เทคนิค Bisulfite sequencing เพื่อระบุถึงรูปแบบ methylation ของ CpG ทุกตำแหน่งในบริเวณที่สนใจ จากการศึกษาแสดงให้เห็นว่ารูปแบบ methylation ที่บริเวณ ICR เหนือ *H19* ของเซลล์ต้นกำเนิดน้ำคร่ำเป็นแบบ imprinting คือมีความแตกต่างกันระหว่างอัลลีล แต่อย่างไรก็ตามบางตัวอย่างพบรูปแบบ hypermethylation แทนที่ CpG บางตำแหน่ง ซึ่งเมื่อพิจารณาต่อไปพบว่า เซลล์ต้นกำเนิดที่มี hypermethylation CpG นั้นเป็นเซลล์ต้นกำเนิดน้ำคร่ำ passage8 ทั้งหมด และสำหรับการศึกษารูปแบบ methylation ที่บริเวณ DMR ของ *IGF2* พบว่ามีรูปแบบ methylation เป็นแบบ imprinting ทั้งหมด แต่ imprinting methylation นั้นไม่ได้เกิดขึ้นบนอัลลีลเดียวกัน CpG บางตำแหน่งเกิด methylation ขึ้นที่อัลลีลหนึ่งแต่ CpG ใกล้เคียงกลับ methylation ที่อัลลีลอื่น ดังนั้นจึงสรุปได้ว่ารูปแบบ methylation ของเซลล์ต้นกำเนิดน้ำคร่ำเป็นแบบ imprinting ทั้งที่บริเวณ ICR และ DMR ซึ่งรูปแบบ methylation ที่ ICR อาจเปลี่ยนแปลงได้ระหว่างการเพาะเลี้ยงในห้องปฏิบัติการ

135 หน้า

CONTENTS

CONTENTS (cont.)

CONTENTS (cont.)

LIST OF TABLES

LIST OF FIGURES

LIST OF FIGURES (cont.)

LIST OF ABBREVIATIONS

%	Percent
^{o}C	Celsius degree
µL	Microliter
A	Adenine
$A_{260/280}$	Absorbance at 260 nm per 280 nm
ADP	Allele discrimination protein
ADS	Allele discrimination signal
AF	Amniotic fluid
AFS	Amniotic fluid stem cell
Amp	Ampicillin
AS	Angelman Syndrome
ASC	Adult stem cell
BEG	Biallelic expressed gene
BSA	Bovine serum albumin
BWS	Beckwith-Weidmann Syndrome
C	Cytosine
CGIs	CpG islands
CO_2	Carbon dioxide
CpG	CG dinucleotide
CTCF	CCCTC-binding factor
CTCF binding region	CCCTC-factor binding region
DMR	Differentially methylated region
DNMT	DNA methyltransferase
DNP	*De novo* methylation protein
DNS	*De novo* methylation signal
dNTP	Deoxynucleoside triphosphate
EC	Embryonic carcinoma

LIST OF ABBREVIATIONS (cont.)

EG	Embryonic germ cell
ESC	Embryonic stem cell
F primer	Forward primer
G	Guanine
HDAC	Histone deacetylase
HSC	Hematopoietic stem cell
ICM	Inner cell mass
ICR	Imprinting control region
IGF2	Human insulin-like growth factor 2
igf2	Mouse insulin-like growth factor 2
IPs	Induced pluripotent stem cell
M	Molar
MACS	Magnetic activated cell sorting
MEG	Maternal expressed gene
miRNA	Micro RNA
mL	Milliliter
mM	Millimolar
mm^2	Millimeter square
mRNA	Messenger RNA
MSC	Mesenchymal stem cell
NCSC	Neural crest stem cell
NSC	Neural stem cell
O_2	Oxygen
P	Passage
PBS	Phosphate buffer saline
PCR	Polymerase chain reaction
PEG	Paternal expressed gene
PWS	Prader Willi Syndrom

LIST OF ABBREVIATIONS (cont.)

R primer	Reverse primer
rpm	Round per minute
SDS	Sodium dodecylsulfate
SRS	Silver Russel Syndrome
T	Thymidine
TBE buffer	Tris borate EDTA buffer
Tm	Melting temperature
U	Unit
V	Voltz

CHAPTER I
INTRODUCTION

Amniotic fluid stem cell is one of promising cells implicated in regenerative medicine due to its high proliferative potential and wide-range of differentiation capability. Before the discovery stem cell from amniotic fluid[1], the main sources of stem cells are from both embryonic and adult tissues. The embryonic stem cell (ESC) is pluripotent cell which is capable of differentiation into almost all cell types, except placenta. The ESC also possesses the great proliferative potential that has been expandable over 100 passages [2-5]. Therefore, the ESC has been anticipated as the powerful tool for regenerative medicine. However, the utilization of ESC has an ethical concern[6] and some evidences of teratoma formation after transplantation[7]. Regarding to such limitation of ESC, the adult stem cell (ASC) becomes an alternative choice. The ASC is derived from adult tissue and has been suggested as multipotent cell [8-10] which is capable of differentiation only into many cell types but not all cell types as derived from 3 embryonic germ layers. Furthermore, it also possesses low proliferative potential. Therefore, the ASC is limited in utilization for medical application because of its restricted potency of proliferation and differentiation. The discovery of amniotic fluid stem cell (AFS) may provide an alternatibe choice for stem cell therapy. This stem cell is derived from fetal tissue and has been reported as having capability of differentiation into various cell types of 3 germ layers [11, 12] which is benefit for stem therapy. Furthermore, AFS possesses high proliferative potential. The prior study has shown that AFS can form colony from single cell resulting in the homogenous AFS cell population. According to the stem cell property, the different of proliferative potential of each stem cell source may be influenced by the different proliferative regulatory factors.

Cell proliferation is controlled in part by epigenetic mechanism such as DNA methylation, histone modification, and chromatin remodeling. The most intensive epigenetic study is DNA methylation because of the direct relevant between

exact methylation pattern with gene action whereas other epigenetic shows complicate pattern. The important methylated region to switch on or off the action of general gene is at promoter region. For the special gene set called imprinted gene, the important methylated region is differentially methylated region (DMR) which is methylated differently between paternal and maternal allele and concordance with the action of imprinted gene. The methylation pattern of imprinted gene is very interesting because this characteristic is susceptible, the mutation of methylation pattern only on one allele may lead to the different cell property.

In human, there are several imprinted genes play role in various cell actions but this study interested to the imprinted gene involving in cell proliferation regulation[13, 14]. The imprinted gene is normally control specific characteristic in cluster. The IGF2-H19 imprinting cluster is the most intensive study to regulate cell proliferation. This imprinting cluster composes of 2 antagonistic proliferation regulated genes. The insulin-like growth factor 2 (*IGF2*) encodes growth factor to trigger cell proliferation[13-15] whereas the *H19* encodes non-translated RNA to inhibit cell proliferation by siRNA action[16]. The imprinted gene action in this cluster is regulated by DNA methylation at DMR especially at 2 kb on the upstream of *H19*, called CTCF binding region[17]. This CTCF binding region recruits the CTCF insulator protein and switch gene action between 2 gene members in IGF2-H19 imprinting cluster, *IGF2* and *H19*. The CTCF binding region can be divided into 7 sub-regions, CTCF1 to 7. Only the sixth CTCF binding region is reported as DMR[17]. The methylation pattern at this DMR plays role in regulation of gene action of both IGF2 and H19 according to the insulator model. Thus, the CTCF6 binding region is called imprinting control region (ICR). Furthermore, another DMR in IGF2-H19 imprinting cluster locates between exon 2 and 3 of *IGF2*. This region shows unique of methylation pattern specific to each cell types. Therefore, the methylation pattern at ICR and DMR is important to regulated imprinted gene action and it is specific to each cell types.

This study explores the methylation pattern at ICR and DMR in IGF2-H19 imprinting cluster which has never been reported in amniotic fluid stem cell. We would like to know the methylation pattern at both ICR and DMR in IGF2-H19 imprinting cluster of amniotic fluid stem cell and whether the methylation pattern of

this intermediate stem cell differs from those of embryonic stem cell and adult stem cell or not. Furthermore, this study also compares the methylation pattern between the different passages of the cell culture to determine if the methylation pattern is changed by in vitro culture condition.

Objective

1. This study is the first report of the DNA methylation pattern at Differentially Methylated Region (DMR) and Imprinting Control Region (ICR) in IGF2-H19 imprinting cluster in Amniotic Fluid Stem Cell (AFS).

2. This study compares the DNA methylation pattern at Differentially Methylated Region (DMR) and Imprinting Control Region (ICR) in IGF2-H19 imprinting cluster between early passage and late passage of Amniotic Fluid Stem Cell.

CHAPTER II
LITERATURE REVIEW

1. Stem Cells

Stem cells are unspecialized cells with uncommitment on cell morphology and function. These cells possess capability to undergo self-renewal and can be induced to become at least one or more functional cell types after exposure to appropriate signal to trigger differentiation[(1)]. According to these unique properties, stem cells may play pivotal role in homeostasis to balance between regenerative cells and degenerative cells. Furthermore, they are involved in repair system for injury and some diseases[(2)].

1.1 The unique properties of stem cell

Stem cells from various organs and various developmental stages have 3 shared common characteristics. First, they are unspecialized cells. Second, they are capable to renew themselves for long periods. And third, they can differentiate to functional cells[(3)].

1.1.1 Unspecialized cell

The word “stem” in stem cells is like stem of tree before branching to various stalks. These cells have not, yet, been specified for cell morphology and function. However, they can be induced to differentiate into various cell lineages under appropriate situation.

1.1.2 Self-renewal property

One unique stem cell property is self-renewal. Stem cells can replicate themselves and maintain their characteristic in cell population along proliferation process, for example, the stem cell can maintain telomere length during proliferation process whereas the differentiated cells change telomere length after undergo each cell division. The stem cells contain unlimited proliferation capability[(4)]. The ability to produce a large amount of cell population is attractive for therapeutic usage.

The previous study showed that the high self-renewal potential was found in embryonic stem cell[5]. This cell was able to proliferate for a year or even longer without developing to specialized cells.

1.1.3 Differentiation property

Another unique stem cell property is differentiation, the ability to differentiate unspecialized cells into specific morphology and carry out specific function. Differentiation process can occurred after receive appropriate signal. The internal signals from their gene action are the one factor to trigger differentiation process [6]. These signals are specific to each cell lineage and were reported as differentiation protein marker in several previous studies [7-10]. Furthermore, the external signal[11] such as chemicals in extracellular matrix and physical connections[12] are also involved in differentiation process.

1.2 Classification of Stem Cell

1.2.1 Based on differentiation capability

Stem cells can be categorized according to the differentiation capability.

1.2.1.1. Totipotent stem cells

Stem cells in this category contain the highest differentiation potential. They can give rise to all cell types in a fully human development including placenta. The totipotent stem cell can be derived from the fertilized oocyte and premorula blastomeres [13].

1.2.1.2. Pluripotent stem cells

Stem cells in this category contain lower differentiation potential than totipotent stem cells. Though, they can give rise to 3 primordial germ layers but not placenta[14]. The pluripotent stem cell can be derived various sources. The embryonic stem (ES) cell is derived from inner cell mass (ICM) in blastocyst stage [15] whereas the embryonic germ (EG) cell and embryonic carcinoma (EC) are derived from in vitro germ cell culture and tumorigenic germinal tissue, respectively. Furthermore, the induced pluripotent stem cell (IPs) technology was discovered to restore pluripotency in adult cells[16, 17].

1.2.1.3. Multipotent stem cells

Stem cells in this category contain lower differentiation potential than totipotent and pluripotent stem cells. They can give rise at least 2 or more cell types in specific lineages. The neural stem cell (NSC) [18] and neural crest stem cell (NCSC)[19] can differentiate to neural cell lineage such as oligodendrocytes, dopaminergic neurons and astrocytes. Hematopoietic stem cell (HSC) [20, 21] can be derived to blood lineage such as red blood cells, white blood cells and lymphocytes. Mesenchymal stem cell (MSC)[22] can give rise to mesenchymal cell such as adipocytes, chondrocytes, osteocytes and myocytes.

1.2.1.4. Unipotent stem cells

Stem cells in this category contain limited differentiation potential. They can give rise to only one mature cell type[23]. The keratinocyte stem cell is one example of this category. This cell can give rise to closely related keratinocytes.

1.2.2 Based on their origin

Another way to classify stem cells is regarding the source they were derived from. Generally, stem cells are classified as: embryonic, fetal or adult stem cells. Besides, the umbilical cord blood stem cells sometimes called neonatal stem cells. Therefore, stem cells are categorized into 4 groups according to their origin.

1.2.2.1. Embryonic stem cells

Embryonic stem cells are isolated from embryo during development. They can be either totipotent or pluripotent stem cell depending on embryonic stage. Stem cell derived from fertilized egg and cell at early development contain totipotency whereas stem cell derived from 4 or 5 day-old, called blastocyst[15, 24], contain pluripotency. The inner cell mass of blastocyst will develop into 2 layers; epiblast and hypoblast. Only the part of epiblast can give rise to 3 primordial germ layers; ectoderm, mesoderm and endoderm [25].

Even though these stem cells have advantage due to the highest differentiation potential however they have limitation about ethical concern and show teratomas formation evidence.

1.2.2.2. Fetal stem cells

Fetal stem cells are isolated from the organs of fetuses. These stem cells can be isolated either from abortuses directly or from releasing cells in amniotic fluid. Previous study found fetal neural stem cells which can differentiate into neurons and glial cells in neural lineage [(26)]. Furthermore, the fetal blood was rich sources of fetal hematopoietic stem cells [(27)]. According to these discoveries, most stem cell derived from fetal is multipotent stem cells.

1.2.2.3. Neonatal stem cells

The neonatal stem cells are isolated from newborn baby such as umbilical cord which is collected after birth. The umbilical cord blood is a rich source of hematopoietic stem cells. Cord blood cells hold advantages over embryonic stem cells because of there are no ethical debate. In addition, cord blood stem cells hold an advantage over adult stem cells because they do not have the DNA mutations which accumulated along development[(28)].

1.2.2.4. Adult stem cells

Adult stem cells, or somatic stem cells, are isolated from adult organs. In humans, the key functions of adult stem cells are to maintain and repair the specific tissues where they reside[(29)]. Adult stem cells have been found in many tissues but their numbers are very small. It is suggested that stem cells will remain in a particular area of a tissue for years without dividing. They are then triggered to divide by disease or tissue damage. These stem cells contain low proliferation potential therefore cell population number is inadequate for using. Moreover, they possess limited differentiation capability.

Even though these stem cells have disadvantages as mention before however there are some advantages of avoiding ethical concern and no evidence of teratomas formation.

1.3 Amniotic fluid stem cell

Amniotic fluid stem cell (AFS) is fetal stem cell[(30)]. Its stem cell potential, both proliferation and differentiation, is intermediate between ESC and ASC. For the differentiation potential, the AFS can differentiate to wide range of functional cell types more than ASC which is restricted differentiation potential to a few cell lineages. However, the AFS cannot derive to all cell types; it does not have high differentiation

potential as ESC. Therefore, the AFS is less advantage for medical therapy than ESC in term of differentiation potential. For the proliferation potential, the AFS contains higher proliferation potential than ASC. The single AFS cell can give rise to the large stem cell population (up to 10^7). The large cell population is benefit for therapeutic usage. The comparing to ESC, the AFS contains lower proliferation potential than ESC. The teratoma formation, due to the excess proliferation potential as shown in ESC, does not exist after AFS transplantation.

In conclusion, the AFS contains appropriate proliferation potential to avoid teratoma formation and to generate an adequate cell. This statement reveals that the AFS is more advantage for medical therapy than both ESC and ASC in term of proliferation potential.

Table1. The comparison of stem cell properties among ESC, AFS, and ASC

Property	**Embryonic stem cell**	**Amniotic fluid stem cell**	**Adult stem cell**
Differentiation potential	High potential	Intermediate (ESC>AFS>ASC)	Low potential
proliferation potential	High potential (resulting in teratomas formation)	Intermediate (ESC>AFS>ASC) (resulting in adequate cell for therapy and no evidence of teratomas formation)	Low potential (resulting in lack of cell for therapy)
Feeder cell contamination	Yes	No	No
Ethical concerned	Yes	No	No

This study interested to the regulatory factor of cell proliferation. A high relevant factor to cell proliferation is the imprinted genes action in IGF2-H19 imprinting cluster under the influence of DNA methylation. Therefore, the DNA methylation pattern to control those imprinted genes' action becomes our interesting proliferation regulatory factor.

2. Epigenetic – DNA methylation

DNA methylation is an inheritable epigenetic modification in which methyl group is covalently added to the cytosine residue in CpG dinucleotides. The DNA methylation is stable characteristic due to the covalent modification. Once established, the DNA methylation tends to be inherited in a clonal fashion by all daughter cells [31] under the effect of DNA methyltransferases enzyme.

2.1 DNA methyltransferase (DNMT) enzyme

The DNA methyltransferase plays important role to define DNA methylation pattern. Thus far, five Dnmts are known: Dnmt1, Dnmt2 and the Dnmt3 family a,b and L. The Dnmt1, Dnmt3a and Dnmt3b contain functional methyltransferase activity.

The Dnmt1 was the first metyltransferase to be discovered. The deletion of this gene was shown to cause demethylation of the genome and embryonic lethality in mouse [32, 33]. Even though Dnmt1 has the ability to methylate DNA *de novo*, it is generally thought of as a maintenance methyltransferase. It has been shown to be part of the replication machinery, responsible for restoring the methylation pattern on the newly synthesized hemimethylated DNA after replication [34-37].

The Dnmt3a and Dnmt3b constitute the class of *de novo* methyltransferases. Dnmt3a was shown *de novo* methylation activity when its expression was induced in *Drosophila* assays [38]. The deletion of *Dnmt3a* or *Dnmt3b* or both was shown to affect the methylation of ES cells and early mouse embryos [39]. These methyltransferases are therefore considered to be involved in establishing the methylation patterns of the genome during post-implantation development (Figure1). These enzymes might also be responsible for the aberrant methylation patterns during tumourogenesis, since overexpression of these genes, especially *DNMT3B*, can be seen in several cancer forms [40, 41].

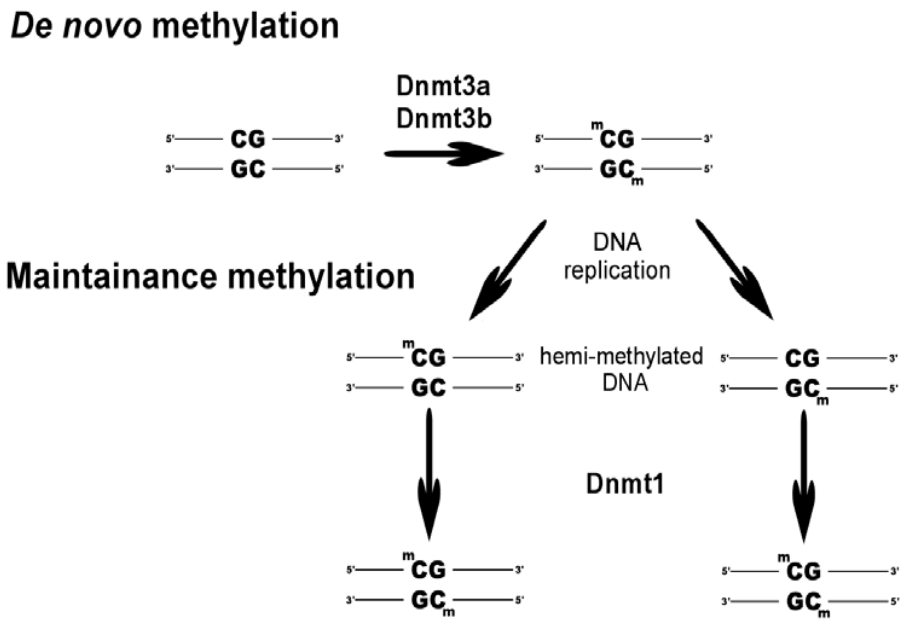

Figure1. The role of DNMT enzyme in establishment and maintenance the DNA methylation pattern.

The DNMT3 is known as de novo methyltransferase, it adds methyl group to the target CpG in both strand. The DNMT1 is known as maintenance methyltransferase, it adds methyl group to the CpG on the newly synthesized strand along the methyl mark on the old strand resulting in the symmetric methylation as before DNA replication.

The Dnmt2 and Dnmt3L have so far not been shown to have any methyltransferase activity. The *Dnmt2* is expressed at low levels and the function of expressed protein is still largely unknown, since the inactivation of this gene does not affect the methylation status of genome and show no phenotypic disturbances [42, 43]. Dnmt2 has, however, been shown to bind strongly to DNA and its biological significance has yet to be determined [42].

The Dnmt3L share several features with the rest of the Dmnt3 family, and despite its inability to methylate DNA, it has been shown to be important in the establishment of maternal methylation imprints. This was shown when the deletion of the *Dnmt3L* gene only affected maternal specific methylation marks without affecting the global methylation levels [44]. Dnmt3L emerges therefore as a regulator of maternal specific methylation patterns. Although the mechanisms behind this process remains

unknown, it has been shown that Dnmt3L co-localizes with both Dmnt3a and Dnmt3b [45] and binds directly to HDAC [46].

2.2 DNA methylation region

The majority of CpG dinucleotides throughout the mammalian genome is methylated [47]. Functional groups of DNA that can acquire methylation are repetitive sequences, CGIs, genes and imprinted regions. The CGIs are often unmethylated and thus diverge from other sequence types where methylation is the default state. The CGIs tend to co-localize with 5' promoter regions in around 30-70% of human genes [48-51]. *In silico* approaches strictly based on sequence composition are used to define CGIs (e.g., region >500 bp, GC-content >55%, and CpG observed/expected >0.6) and thus their function has to be proven experimentally [52]. For the imprinted gene regulation, the influence of DNA methylation and special methylation pattern will be informed in "Imprinting" section.

2.3 Role of DNA methylation

DNA methylation plays critical roles in diverse biological processes. In prokaryotes DNA methylation is a component of the restriction system, which protects the host from the effects of foreign DNA [53]. In mammal, DNA methylation is known to play important roles in gene regulation [50]. Several lines of evidence suggest that DNA methylation is associated with gene silencing [54-57]. DNA methylation is crucial for embryonic and post-birth development. Mouse embryos having homozygous deletion of DNA methyltransferases *DNMT1* and *DNMT3b* die before birth [58, 59]. Knocking out *DNMT3a* leads to death in ~ 4 weeks [59]. The alteration of DNA methylation is the cause of several disease causing germline mutations [60], and somatic mutations that lead to cancer [61]. Aberrant promoter methylation has been shown to be associated with cancer [62, 63]. Methylation has also been implicated in immunodeficiency, centromeric instability, facial anomalies (ICF) syndrome. Study of ICF patients'cells showed the mutations in the gene encoding the DNA methyltransferase *DNMT3b*, which leads to specific chromosomal decondensation and reduced levels of methylation in satellite DNA [64, 65]. Rett syndrome patients have mutations in the methyl-CpG binding protein *MeCP2*, suggesting a possible role of the inability to decode methylation signals in causing this disease [66].

In addition, a role for DNA methylation in imprinting was first demonstrated by defective imprinting observed in the *Dnmt1*-/- mice, where imprinting of the *H19*, *Igf2*, and *Igf2r* genes was disrupted [67, 68]. This study showed that methylated CpG maintenance was mandatory for imprinted expression. The DNMT3 family of proteins has also been demonstrated to be vital for imprinting. As more and more imprinted genes have been identified, the effect of DNA methylation on imprinting has developed into a more complex picture, where some murine genes can maintain placental parent-of-origin specific expression in a DNA methylation independent manner [69, 70].

3. Imprinting phenomenon

3.1 Imprinting characteristic

Imprinting phenomenon refers to the unequal of gene expression of two different parental alleles. The imprinted gene is susceptible gene to lose function because of its monoallelic expression. The alteration of gene expression only on one allele of imprinted gene can lead to abnormal characteristic [71-74]. Therefore, the alteration of imprinted gene can be noticed easier than non-imprinted gene which requires biallelic mutation to cause the abnormal characteristic.

The imprinted genes disperse throughout whole genome, they locate and action in group, called imprinting cluster (Table2). The consideration at each imprinted genes, it can be divided into 2 sub-classes depending on the allelic methylation and allelic expression. One is the maternal imprinted genes which are methylated at imprinting box only on maternal allele and resulting in maternal allele silencing. These genes are normally expressed from unmethylated paternal allele, thus, this gene set is called paternal expressed genes (PEGs). Another one is paternal imprinted genes which are methylated at imprinting box of paternal allele and resulting in paternal allele silencing. These genes are expressed from unmethylated maternal allele, called maternal expressed genes (MEGs) [75].

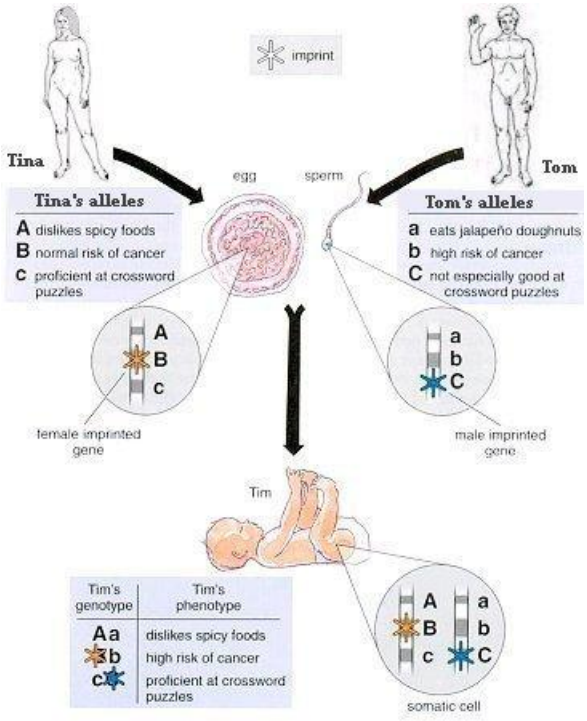

Figure2. Imprinting phenomenon is parental specific gene modification (star mark). The gene modification is specifically defined to parental sex along gametogenesis. B gene is marked in maternal allele, called maternal imprinted gene. C gene is marked in paternal allele, called paternal imprinted gene.

Table2. The list of human imprinted gene

Gene	Gene name	Cyto-band	Expressed Allele	Imprinting Syndromes*
TP73	tumor protein p73	1p36.3	Maternal	
DIRAS3	DIRAS family, GTP-binding RAS-like 3	1p31	Paternal	
PLAGL1	pleiomorphic adenoma gene-like 1	6q24.2	Paternal	TND1
HYMAI	hydatidiform mole associated and imprinted (non-protein coding)	6q24.2	Paternal	TND1
SLC22A2	solute carrier family 22 (organic cation transporter), member 2	6q25.3	Maternal	
SLC22A3	solute carrier family 22 (extraneuronal monoamine transporter), member 3	6q25.3	Maternal	
GRB10	growth factor receptor-bound protein 10	7p12.2	Isoform	SRS?
TFPI2	tissue factor pathway inhibitor 2	7q21.3	Maternal	
SGCE	sarcoglycan, epsilon	7q21.3	Paternal	
PEG10	paternally expressed 10	7q21.3	Paternal	
PPP1R9A	protein phosphatase 1, regulatory (inhibitor) subunit 9A	7q21.3	Maternal	
CPA4	carboxypeptidase A4	7q32	Maternal	SRS?
MEST	mesoderm specific transcript homolog (mouse)	7q32	Paternal	SRS?
MESTIT1	MEST intronic transcript 1 (non-protein coding)	7q32	Paternal	SRS?
COPG2IT1	coatomer protein complex, subunit gamma 2, intronic transcript 1	7q32	Paternal	SRS?
KLF14	Kruppel-like factor 14	7q32.2	Maternal	SRS?
DLGAP2	discs, large (Drosophila) homolog-associated protein 2	8p23	Paternal	
KCNK9	potassium channel subfamily K member 9	8q24.3	Maternal	
H19	H19, imprinted maternally expressed transcript (non-protein coding)	11p15.5	Maternal	BWS & SRS
IGF2	insulin-like growth factor 2	11p15.5	Paternal	BWS & SRS
IGF2AS	insulin-like growth factor 2 antisense	11p15.5	Paternal	BWS & SRS
INS	insulin	11p15.5	Paternal	BWS & SRS
KCNQ1	potassium voltage-gated channel, subfamily Q, member 1	11p15.5	Maternal	BWS (SRS)
KCNQ1OT1	KCNQ1 overlapping transcript 1 (non-protein coding)	11p15.5	Paternal	BWS (SRS)
KCNQ1DN	KCNQ1 downstream neighbor	11p15.4	Maternal	BWS (SRS)
CDKN1C	cyclin-dependent kinase inhibitor 1C (p57, Kip2)	11p15.4	Maternal	BWS (SRS)
SLC22A18	solute carrier family 22, member 18	11p15.4	Maternal	BWS (SRS)
PHLDA2	pleckstrin homology-like domain, family A, member 2	11p15.4	Maternal	BWS (SRS)
OSBPL5	oxysterol binding protein-like 5	11p15.4	Maternal	BWS (SRS)
WT1-AS	Wilms tumor 1 antisense	11p13	Paternal	

Gene	Names	Cyto-band	Expressed Allele	Imprinting syndrome
DLK1	delta-like 1 homolog (Drosophila)	14q32	Paternal	Mat and patUPD14
MEG3	maternally expressed 3 (non-protein coding)	14q32	Maternal	Mat and patUPD14
MKRN3	makorin ring finger protein 3	15q11.2	Paternal	AS, PWS
MAGEL2	MAGE-like 2	15q11.2	Paternal	AS, PWS
NDN	necdin homolog (mouse)	15q11.2	Paternal	AS, PWS
SNRPN	small nuclear ribonucleoprotein polypeptide N	15q11.2	Paternal	AS, PWS
SNURF	SNRPN upstream reading frame	15q11.2	Paternal	AS, PWS
SNORD107	small nucleolar RNA, C/D box 107	15q11.2	Paternal	AS, PWS
SNORD64	small nucleolar RNA, C/D box 64	15q11.2	Paternal	AS, PWS
SNORD108	small nucleolar RNA, C/D box 108	15q11.2	Paternal	AS, PWS
SNORD116@	small nucleolar RNA, C/D box 116 cluster	15q11.2	Paternal	PWS
SNORD115@	small nucleolar RNA, C/D box 115 cluster	15q11.2	Paternal	AS, PWS
SNORD109A	small nucleolar RNA, C/D box 109A	15q11.2	Paternal	AS, PWS
SNORD109B	small nucleolar RNA, C/D box 109B	15q11.2	Paternal	AS, PWS
UBE3A	ubiquitin protein ligase E3A	15q11.2	Maternal	AS
ATP10A	ATPase, class V, type 10A	15q12	Maternal	AS
TCEB3C	transcription elongation factor B polypeptide 3C (elongin A3)	18q21.1	Maternal	
ZIM2	zinc finger, imprinted 2	19q13.4	Paternal	
PEG3	paternally expressed 3	19q13.4	Paternal	
ZNF264	zinc finger protein 264	19q13.4	Maternal	
NNAT	neuronatin	20q11.23	Paternal	
L3MBTL	l(3)mbt-like (Drosophila)	20q13.11-12	Paternal	
GNASAS	GNAS antisense RNA (non-protein coding)	20q13.32	Paternal	
GNAS	GNAS complex locus	20q13.32	Maternal	PHP-1b

3.2. Imprinting regulation

The action of imprinted gene is regulated by DNA methylation mechanism. The differentially methylated CpG-rich regions with methylation specific to maternal or paternal chromosomes are typically found in the vicinity of imprinted genes [76, 77]. Some differentially methylated regions are called imprinting control regions (ICR). The ICRs further have to be proven experimentally, through, e.g., knockout experiments in animal models, where the loss of the ICR disrupts the imprinting [78-80]. The ICR can function in different ways, but direct tandem repeats containing highly conserved core transcription factor binding sites are typical [81]. ICRs are relatively long (murine average 3.2 kb) compared to normal regulatory elements such as promoters and enhancers which rarely are longer than 500 bp [82, 83]. Additional differentially methylated regions, called DMR, undergo significant

reprogramming through development, and are thought to be hierarchically regulated by the ICR [98]. DMRs are thought to aid the stabilization of allele-specific expression at the level of individual genes and can constitute functional units such as promoters. It is noteworthy that all ICRs/DMRs would not formally be defined as CGIs and differences in GC and CpG content have been reported between maternal and paternal ICRs [82].

3.3 The establishment and maintenance of imprinting methylation

Along development, the DNA methylation level is fluctuating. The global demethylation happens twice during development: first in gametogenesis and the second time immediately following conception, where the paternal genome is rapidly demethylated while the maternal genome is demethylated at a slower rate (Figure4) [84].

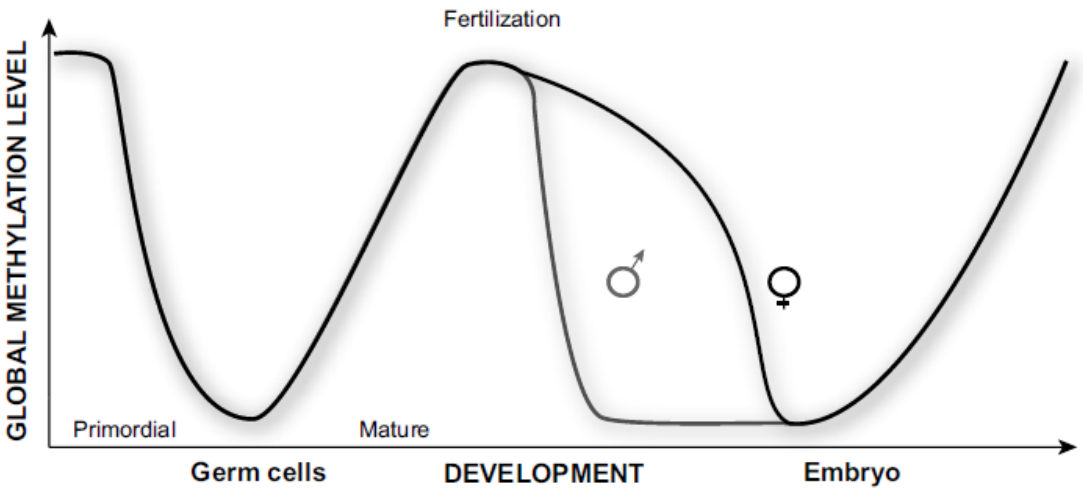

Figure3. The DNA methylation level along development is fluctuation in both male (grey line) and female (black line). The lowest methylation level causes by the global demethylation. The graph showed the lowest methylation level at 2 times, thus, it implies to global demethylation twice.

The escape of the global methylation can be observed at imprinted methylation region including ICR and DMR. This exception was explained by the action of two regulatory factors, both allele-discremination protein (ADP) and *de novo* methylation protein (DNP) which can bind to different *cis-acting* elements allele-discremination signal (ADS) and *de novo* methylation signal (DNS) respectively [85].

In case of maternal imprinting or PEG, the DNP mask the DNS on maternal allele to protect methylation pattern from global demethylation during

preimplantation stage and prevent *de novo* methylation on paternal allele at implantation stage by masking ADS from ADP, and vice versa in case of paternal imprinting of MEG.

For the non-imprinted genes (biallelically expressed genes, or BEG), they may also contain differentially methylated regions (DMRs). However, the DMRs of non-imprinted genes are subjected to the genome-wide demethylation. Some regions especially at promoter and CGIs are prevented from de novo methylation by the action of ADP on both parental alleles. The low-level methylation leads to biallelic expression of either tissue-specific genes or housekeeping genes.

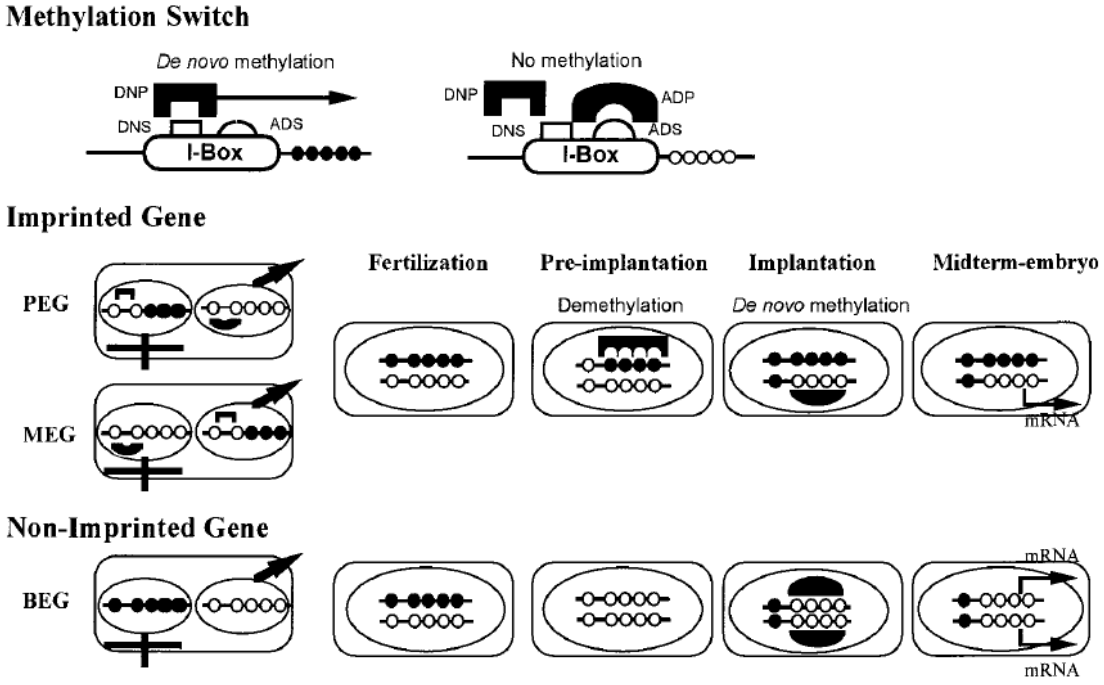

[Genomics, 2000;64(2):132-43]

Figure4. The exception of global demethylation. DNA methylation pattern is established during gametogenesis. This pattern is inherited and maintained throughout of life, thus, it required some mechanism to retain this pattern when undergo to global demethylation and remethylation after fertilization. The hypothesis of 2 protein masks was suggested to protect methylation pattern.

Once established, the methyl marks are typically maintained through cell divisions in a clonal manner. It does not follow Mendelian laws of inheritance. This enables a cellular memory and the methylation pattern is often specific for distinct cell types, and a range of tissue-specific differentially methylated regions have been

described before. The alteration of DNA methylation to control imprinted gene action has been reported in various diseases such as Prader-Willi Syndrome (PWS) [102], Angelman Syndrom (AS) [86], Beckwith-Weidmann Syndrome (BWS) [87], Silver Russel Syndrome (SRS) [88], etc. Some diseases are growth and development retardation. Some of them are metabolic diseases. Therefore, the imprinted gene involves in various cell function which will be described in "Imprinting Function" section.

3.4 Imprinting function

The nuclear transfer experiments creating parthenogenetic and androgenetic embryos were not only incompatible with development, but striking differences in the phenotype between the two types of conceptions were reported, with parthenogenetic embryos showing clear underdevelopment of extra-embryonic tissues and the opposite phenotype in androgenetic embryos. Further studies of chimeric mice created from normal cells in combination with parthenogenetic or androgenetic cells, revealed embryonal growth and skeletal defects and biased cell type contributions, underlining the functional inequality [89-91]. Subsequent knockout studies of imprinted genes have revealed different specific functions, with the general conclusion that imprinted genes foremost affect mammalian growth, metabolism, and behavioral traits [92]. The parent-offspring model (kinship theory) for the evolution of imprinting relates to the fact that imprinting is specific to placental animals, and that paternally expressed genes tend to be growth-promoting. The placenta enables a continuous maternal-fetal nutrition exchange throughout gestation, where in the model the mother strives to preserve resources for future pregnancies (potentially with a different father), while the interest of the paternal genome is to maximize nutrient allocation to his offspring [93]. Clearly, this is just a theory and all imprinted genes do not support this model in an obvious way, and other models for the evolution of imprinting have been proposed including protection against parasitic DNA and maternal protection from invasive trophoblasts [92]. This study interested to the factor controlling cell proliferation. The outstanding imprinting cluster involving in proliferation regulation is IGF2-H19 imprinting cluster, the major abnormal characteristic in many growth retardation diseases such as BWS, SRS, and various cancers.

4. IGF2-H19 imprinting cluster

4.1 Composition of IGF2-H19 imprinting cluster

The IGF2-H19 imprinting cluster locates on chromosome 11p15.5 and composes of 2 homeostatic imprinted genes including *IGF2* and *H19*. The *IGF2* embeds on the upstream of this imprinting cluster. This imprinted gene encodes insulin-like growth factor 2 (IGF2) to trigger cell proliferation. The *H19* embeds at downstream of *IGF2*. This imprinted gene encodes untransgated RNA which acts as miRNA to limit *IGF2* action resulting in decreased of cell proliferation.

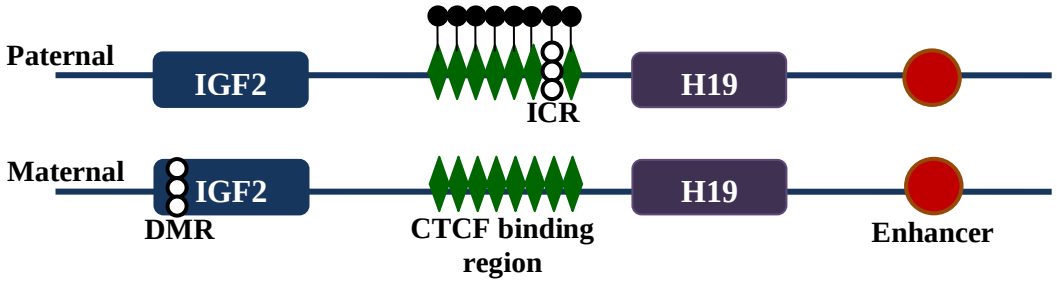

Figure5. IGF2-H19 imprinting cluster compose of 2 imprinted gene members, *IGF2* (blue square) and *H19* (purple square). The 7 sub-CTCF binding regions locate between those 2 gene members (green diamond). The enhancer (red circle) locates at downstream of *H19*. The methylation region (white circle) in this cluster is DMR in the *IGF2* and the sixth CTCF binding site, which is suggested as imprinting control region (ICR).

H19 is flanked by 2 regulatory regions. The upstream regulatory region of *H19* is CCCTC-binding factor (CTCF) binding site and the downstream regulatory region of the *H19* is shared enhancer.

4.1.1 Insulin-like growth factor 2 gene (*IGF2*)

Insulin-like growth factor II (*IGF2*) gene is maternal imprinted gene which locates on the upstream of H19/IGF2 imprinting cluster. This gene consists of 9 exons and its expression is regulated by 4 promoters (Figure6). Each promoter is active in different tissues and different developmental stage; for example, promoter1 (P1) is active predominantly in fetal and adult liver tissue. It is always transcripted from both parental alleles. In contrast to promoter 2-4 (P2-P4) are active in imprinting fashion [(94)]. These promoters express throughout all stage of fetal

development. The *IGF2* encodes insulin-like growth factor II (IGF2) protein. This IGF2 protein involve in proliferation, cell survival, and metastasis.

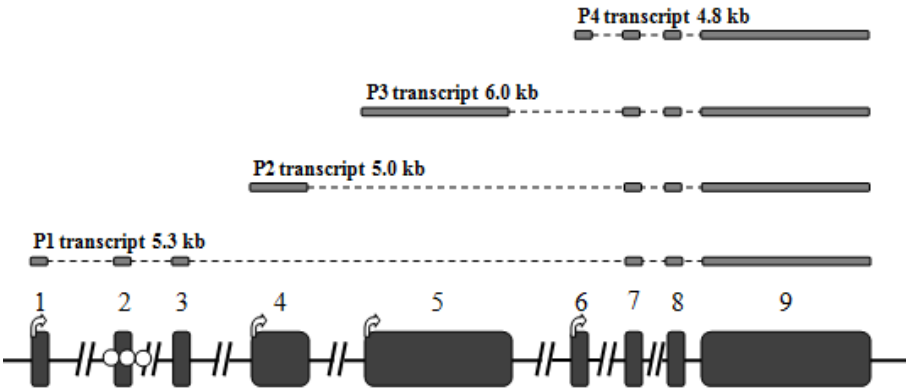

Figure6. IGF2 gene composes of 9 exons. This gene encodes 4 IGF2 isoformed proteins under the influence of 4 promoters.

4.1.2 *H19*

H19 is paternal imprinted gene on the downstream of IGF2. This gene consists of 5 exons and 4 small introns. The *H19* encodes non-coding RNA but its exact function is still unclear. Xuezhong Cai and Bryan R. Cullen [(95)] suggest that this non-coding RNA function as miRNA. This miRNA results in downregulation of specific mRNA and acts as tumor-suppressor gene. This gene is highly expressed since early stage of embryogenesis until fetal stage in many organs such as fetal adrenal, fetal liver, and placenta, but is approximately completely downregulated at postnatal stage.

4.1.3 CCCTC-binding factor

The CCCTC-binding factor, known as CTCF, is a zinc finger transcription factor that functions to preclude potential associations between promoters and enhancers by inducing formation of chromatin structure that physically separates the relevant sequences [(96)]. The CTCF protein is methylation-specific factor. It can bind to the unmethylated but not methylated region. The docking of CTCF protein at CTCF binding site can act as insulator to prevent accessing of enhancers to promoter of farther neighbor gene. In case of CTCF binding at upstream of *H19*, this protein can block the influence of H19 downstream enhancer to the IGF2 promoter. Acquisition of methylation on the maternal chromosome in this region or loss of methylation from

the paternal chromosome occurs in a highly tumor-specific manner. For example, in bladder cancer, paternal hypomethylation leads to biallelic H19 expression [97].

4.1.4 Enhancer

IGF2-H19 imprinting cluster has one shared enhancer at downstream. This shared enhancer can trigger both IGF2 and H19 gene expression. The mechanism to switch gene action of these 2 imprinted gene members in this cluster has been described in the insulator model.

4.1.5 Differentially methylated region (DMR) of IGF2

The position of DMR of *igf2* was previously defined in mouse. Three DMRs disperse along igf2, the DMR0 locates between exon1 and 2, the DMR1 locates on the upstream of exon3, and the DMR3 locates on exon8 of *igf2*. In human, there are 3 homologous regions to the mouse DMR. However, the methylation study using methylated specific enzyme digestion showed that the DMR1 was not differentially methylated between parental allele. Therefore, only the homologous region to mouse DMR0 and DMR2 were suggested as DMR in human.

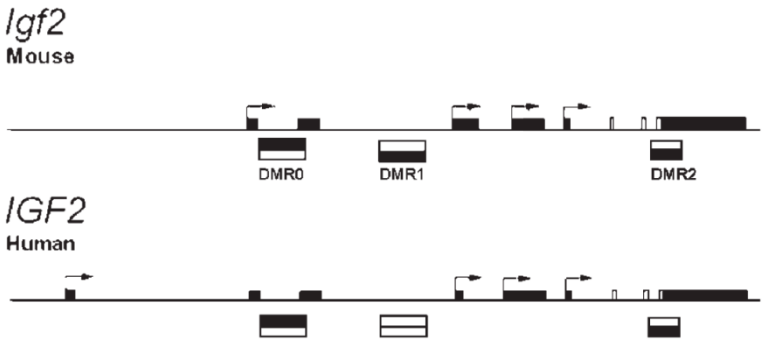

[Human Molecular Genetics, 2004; 13(2): 247–55]

Figure7. The differentially methylated region (DMR) of *IGF2*. The human IGF2 has 3 homologous regions to the *igf2* DMR in mouse. The methylation study using methylation specific enzyme restriction technique showed the different pattern at DMR1 between mouse and human. The DMR1 homologous region is not DMR in human.

Thus far, the methylation studied technique has been improved. The bisulfite sequencing technique can determine methylation status of every CpG site in the interesting region. This technique showed the conflict

methylation pattern at DMR1 from the previous technique [98]. They discussed that the differential methylation at DMR2 as reported by methylation specific enzyme digestion technique may false due to the limitation of enzyme restriction. The methylation status could be determined only at the CpG in restriction region. In conclusion, the DMR of human *IGF2* referred to the homologous region to DMR0 of *igf2* which locates between exon2 and 3 of *IGF2*.

4.1.6 Imprinting control region on the upstream of *H19*

The previous study screened methylation status on the upstream of H19 including the CTCF binding region and promoter of H19. The CTCF binding region can be divided into 7 sub-CTCF binding region (CTCF1 to CTCF7 binding region). Only the CTCF6 binding region showed the percent methylation approximate to 50% whereas other CTCF binding regions showed hypermethylation. This region was suggested as DMR of *H19*.

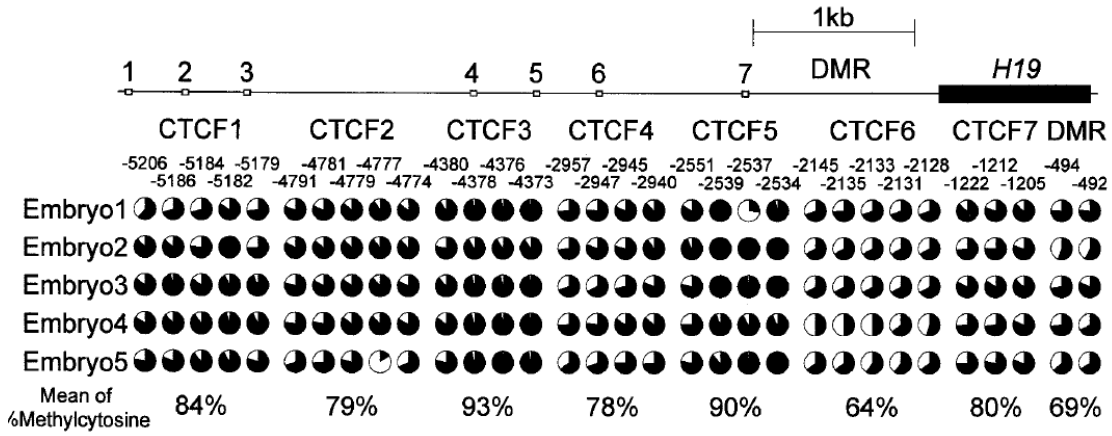

[Human Molecular Genetics, 2001; 10(23): 2619–26]

Figure8. The methylation pattern on the upstream of *H19*. The CTCF6 binding region showed percent methylation approximate to 50%. This region was suggested as imprinting control region (ICR).

Many studies showed the association between DNA methylation at this region and the gene expression of imprinted gene members in IGF2-H19 imprinting cluster. The CTCF6 was hypothesized to be imprinting regulatory region of IGF2-H19 imprinting cluster, called imprinting control region (ICR).

4.2 The regulatory mechanism to control imprinted gene action in IGF2-H19 imprinting cluster (Insulator model)

The insulator model interprets the cooperation between enhancer and the CTCF insulator protein to regulate imprinted gene action in IGF2-H19 imprinting cluster [(99)]. The CTCF6 binding region, or ICR, locates on the upstream of *H19*. The CTCF protein is recruited to bind this region; however, the binding can be interrupted by methylation at this region. This CTCF protein acts as insulator protein to block the action of long distance downstream enhancer to upregulate IGF2 expression, then, switching on the H19 action instead. In normally, the CTCF6 binding region is methylated on paternal allele. Therefore, the CTCF protein cannot bind to this region on paternal allele. The disappearance of insulator protein allows the downstream enhancer to reach IGF2 promoter, but not H19 promoter, resulting in the upregulate IGF2 expression. For the maternal allele which is normally unmethylated, the CTCF protein can bind to this region. The CTCF insulator protein blocks the interaction between downstream enhancer and IGF2 promoter. The downstream enhancer reach to the H19 promoter instead and upreguates H19 expression.

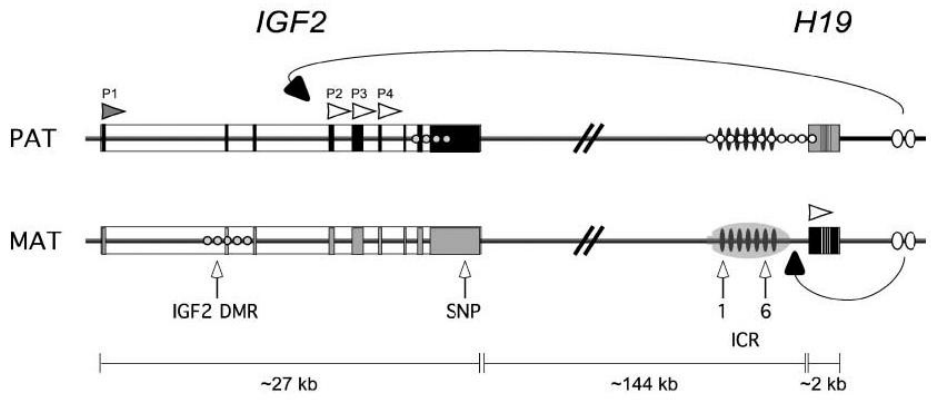

[Mol Cancer Res 2006;4(4):283-92]

Figure9. The imprinted gene action in IGF2-H19 imprinting cluster is regulated by DNA methylation. At ICR, the methylation appears on the paternal allele but not maternal allele. The CTCF insulator protein binds to this region on maternal allele and blocks the interaction between downstream enhancer and IGF2 imprinting promoter. Therefore, the downstream enhancer binds to H19 promoter and trigger H19 expression instead. For the paternal allele, the downstream enhancer can reach to imprinting IGF2 promoter due to the absence of insulator protein.

According to the insulator model, the DNA methylation at CTCF6 binding region, or ICR, is major regulatory factor to control imprinted gene action in IGF2-H19 imprinting cluster. In addition, the imprinting methylation at DMR is concordance with imprinting expression manner. Therefore, the DNA methylation pattern at DMR and ICR is interesting factor to control imprinted gene expression in IGF2-H19 imprinting cluster which involving in proliferation regulation. The methylation at these regions has been study in various cell types such as embryonic stem cell, differentiated cells, cancer cells, cells from growth retardation patients' cells. However, it has never been reported in AFS. Therefore, this study would like to define methylation at both DMR and ICR in IGF2-H19 imprinting cluster in AFS cells. In addition, this study also define methylation pattern separately at different passage because the previous studies suggested that the *in vitro* environment might affect to the DNA methylation pattern by the observation the change of imprinting methylation pattern in the prolonged *in vitro* cultured cells [(100)].

5. Bisulfite sequencing technique

Bisulfite sequencing technique is a useful tool for DNA methylation study. These techniques can define methylation status of every cytosine residue along interesting region.

DNA was treated with sodium bisulfite. This sodium bisulfite react to cytosine residue and results in deamination of cytosine to become uracil. The bisulfite reaction starts from sulfonation of cytosine at C-6 position followed by hydrolytic deamination at C-4 position to produce uracil-sulfonate and end up with desulfonation under alkaline conditions.

However, not all cytosine are affected equally. The reaction for methylated cytosine is extremely slow when compare to unmethylated cytosine. Therefore, the bisulfite treating at appropriate time can distinguish methylated cytosine from unmethylated cytosine.

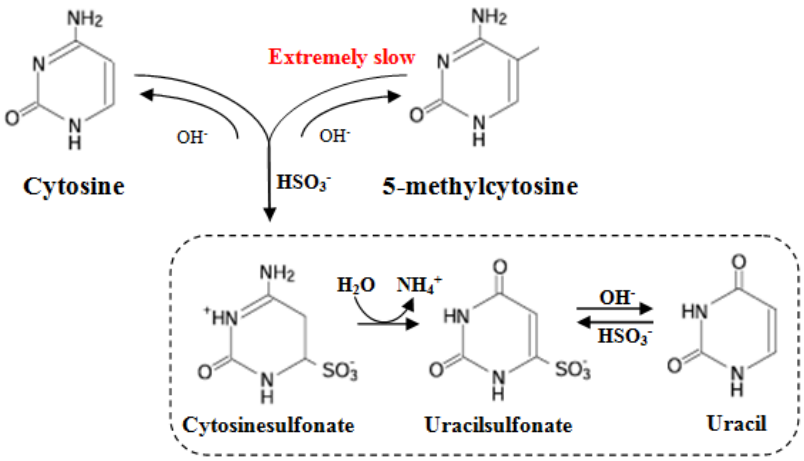

Figure10. The bisulfite reaction

After bisulfite reaction, the treated DNA was amplified and detected by sequencing technique with or without cloning. Cytosine (C) signal from sequencing technique refer to unconverted cytosine of methylated cytosine whereas thymidine (T) signal refer to converted cytosine of unmethylated cytosine.

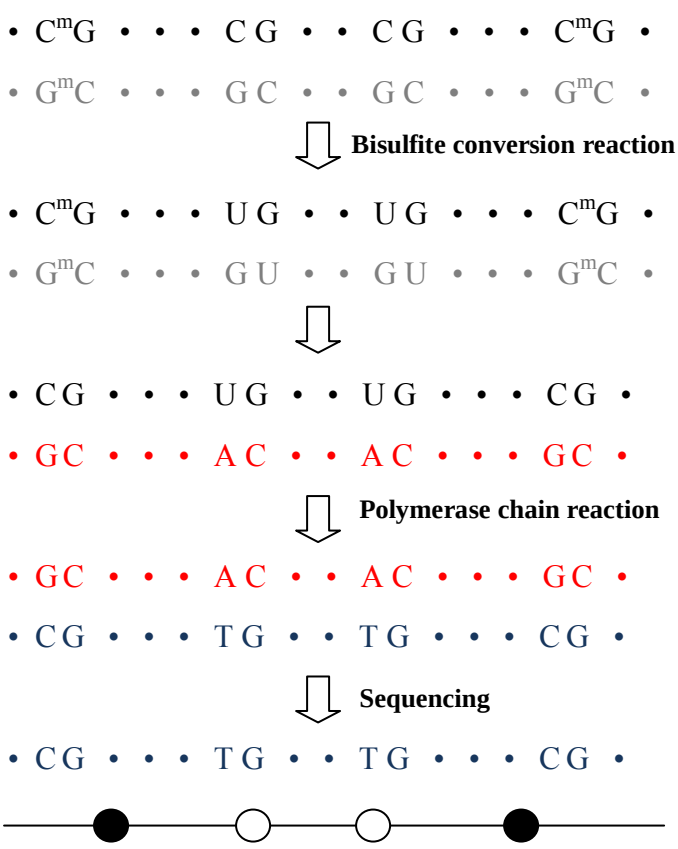

Bisulfite conversion reaction:

- Unmethylated cytosine residues in both sense and antisense strand were converted to uracil.
- Both strands become uncomplimentary to each other.

Polymerase chain reaction:

- Uracil, by conversion of unmethylated cytosine, compliment to adenine in 1st PCR cycle.
- Adenine compliment to thymine in next PCR cycle.
- Therefore, uracils in template strand are replaced by thymine in PCR product

Sequencing:

- C signal represent to methylated cytosine.
- T signal represent to unmethylated cytosine.

Figure11. Characterization of methylated and unmethylated cytosine after bisulfite treatment

This study uses bisulfite sequencing with cloning process to determine methylation status of interesting CpGs. The cloning step purposes to separate two parental alleles in each clone before sequencing. The sequencing information from one clone referred to sequence of single allele. Therefore, DNA methylation status can be determined in individual allele.

CHAPTER III
MATERIALS & METHODS

Materials and Reagents

1. Chemicals and reagents

Name	Catalog No.	Company
Agar	FB0010	Bio Basic, Canada
Agarose	1170A	Research Organics, USA
Ampicillin	1A6750	GPO, Thailand
Boric acid	B-6768	Sigma, USA
Chloroform	1.02445.2500	MERCK, Germany
dNTP mix	MBD00R0191	Fermentas, Canada
Dream *Taq* polymerase	EP0702	Fermentas, Canada
EDTA	E-5134	MERCK, Germany
Ethanol	1.00893.2500	Sigma, USA
Ethidium bromide	160539	Sigma, USA
EZ DNA methylation kit	D5001	Zymo research, USA
Fast start *Taq* polymerase	12032902001	Roche, USA
Hundred basepair ladder	MBDOSM0241	Fermentas, Canada
IPTG	DB0168	Bio Basic, Canada
pGEM-T-easy system	A1360	Promega, USA
Phenol	1.00206.0250	MERCK, Germany
Potassium acetate	P-1190	Sigma, USA
Potassium chloride	P-9541	Sigma, USA
Potassium phosphate	P-0662	Sigma, USA
Primers	HAP-100	Bio Basic, Canada
Proteinase K	03115879001	Roche, USA
Pureyield plasmid miniprep	A1221	Promega, USA
Sodium chloride	S-3214	Sigma, USA
Sodium phosphate	S-9763	Sigma, USA

Name	Catalog No.	Company
Sodiumdodecylsulfate	L-4390	Sigma, USA
Sucrose	21938	Amersham, USA
Trizma base	T-1503	Sigma, USA
Tryptone powder	G-211	Bio Basic, Canada
X-gal	DB0083	Bio Basic, Canada
Yeast extract	G-0961	Bio Basic, Canada

2. Equipments and instruments

Name	Company
Autopipette pipetman (20, 100, 1000)	Gilson, France
Electrophoresis	Biorad, Italy
Gel document	Biorad, Italy
Hot air oven	Heraeus,UK
Hot plate stirrer	Thermolyne, USA
Microcentrifuge	Heraeus,UK
Milli Q	Millipore, USA
Nanophotometer	Implen, Germany
pH meter	Thermo, USA
Refrigerator (-20^{o}C)	Sanyo, Japan
Refrigerator (4^{o}C)	Sharp, Japan
Refrigerator (-80^{o}C)	Sanyo, Japan
Shaker	Hoefer, USA
Spindown	Wealtec, USA
Thermocycler	Labnet, USA
Waterbath	GFL, USA

3. Miscellaneous

Name	Company
Liquid Nitrogen	Taylor-Wharton, USA
Microcentrifuge tube (0.5, 1.5 ml)	Axygen Scientific Inc., USA
Pipette tips (P10, P200, P1000)	Axygen Scientific Inc., USA
Autoclave	Huxley, Germany

Methods

1. Amniotic fluid stem cell sample

The amniotic fluid stem cell was expanded by Unit of Stem Cell Research and Development for Medical Therapy, Department of Obstetrics and Gynecology, Faculty of Medicine of Siriraj Hospital. Two amniotic fluid stem cell lines were derived from the isolated cell from MACS technique using human CD117 Microbead kit (no.130-091-332, Miltenyi Biotec, Germany) according to Manufacturer's instruction. Briefly, five milliliters of amniotic fluid from 14-18 weeks pregnancy was centrifuged at 2,000 rpm for 10 minutes, then, resuspended in 300 µL buffer (Phosphate buffer saline at pH 7.2, 0.5% BSA and 2 mM EDTA by diluting MACS BSA Stock Solution 1:20 with AutoMACS Rinsing Solution). A hundred microliters FcR Blocking reagent and 100 µL CD117 Microbeads was then added to cell suspension followed by incubation at 4^{o}C for 15 minutes. After incubation, cell was washed with 1 mL buffer and collected by centrifugation at 2,000 rpm for 10 minutes. During centrifugation, the magnetic separation column was placed in magnetic field and rinsed with 500 µL of buffer. After that, the collected cell was resuspended in 500 µL buffer and transferred to prepared magnetic column. It was left at room temperature until it was empty and followed by rinsing with 500 µL buffer for three times. The column was removed from the magnetic field and placed on a collection tube containing α-MEM medium followed by elution with 1 mL buffer before seeding on culture flask. These c-kit positive cell was cultured in AFS medium until it was 80% confluent before subculturing to the next passage. For subculturing process, the cell was washed twice with phosphate buffer saline (PBS^{-}) before it was detached by 0.25% tripsin-EDTA. Trypsinization reaction was stopped by the addition 2 volume of AFS medium. Following centrifugation at 2,800 rpm for 5 minutes, the cell pellet was resuspended in 1 mL AFS medium before seeding onto a 25 cm^2 culture flask. This cell was expanded until harvesting at passage 8 (P8) and passage 15 (P15).

Another six amniotic fluid stem cell lines were isolated and expanded by the starter cell technique. In brief, five milliliters of the amniotic fluid was obtained from 14-18 weeks pregnant women. The amniotic cell was collected by centrifugation at 2,800 rpm for 5 minutes, then, resuspension in AF culture medium before seeding onto a 60 mm^2 non-treated tissue culture dish. Following incubation at 37^{o}C, 5%CO_2,

5%O_2 for 48-60 hours, the cell was further cultured in AFS medium for 48 hours. Each clone was detached by trypsinization using fine pipette tip to handle directly. It was seeded onto a 24-well non-treated plate and cultured until the cells reached 70% confluence. Following trypsinization, the cell was diluted to 3% cell concentration in a total volume of 10 mL. A hundred microliters was applied to each well of a 96-well non-treated plate. After culturing at 37^{o}C, 5%CO_2, 5%O_2 for 7 days, the AFS medium was changed and further cultured until 70% cell confluent before the cell was expanded gradually in a 24-well plate, a 6-well plate, a 25 mm^2 flask and a 75 mm^2 flask. The Amniotic fluid stem cell was harvested at P8 and P15.

2. DNA extraction

Amniotic fluid stem cell was harvested by trypsinization. It was washed twice with 1 mL phosphate buffer saline (PBS^-) and recovered by centrifugation for 5 minutes at 10,000 rpm (75008162 rotor, Heraeus labofuge 400R, UK). The pellet was resuspended with 500 µL homogenized buffer (0.1M NaCl, 0.2M sucrose, 0.01M EDTA, 0.3M Tris-base pH8.0) followed by adding 40 µL of 10% SDS and 10 µL Proteinase K, and incubation at 37^{o}C overnight (8-12 hours) or 52^{o}C for 3 hours. Then, 8M potassium acetate 100 µL was added and incubated at 4^{o}C for 1 hour (vortex every 10 minutes) followed by centrifugation at 4^{o}C, 10,000 rpm for 15 minutes. The clearance supernatant was mixed with 1 mL of phenol:chloroform (1:1), centrifuged at 4^{o}C, 10,000 rpm for 5 minutes. Then, the upper phase was mixed with 500 µL of chloroform before centrifugation at 4^{o}C, 10,000 rpm for 5 minutes. After that, the upper phase was mixed with 1 mL of absolute ethanol and left at room temperature for 2 hours (or at -20^{o}C overnight) before DNA pellet recovering by centrifugation at 4^{o}C, 12,000 rpm for 15 minutes. The DNA pellet was washed with 1 mL of 70% ethanol and recovered by centrifugation at 4^{o}C, 10,000 rpm for 15 minutes and dried in room temperature. DNA pellet was finally solubilized with 20-30 µL of deionized distilled water. The DNA suspension was further analyzed by nanodrop spectrophotometry to define Purity ($A_{260/280}$ approximate to 1.8) and concentration.

3. Bisulfite treatment

The DNA was treated using commercially available EZ DNA methylation kit (D5001, zymo research) according to the manufacturer's instruction manual. First, the DNA was calculated for 1 µg. This DNA was mixed with 5 µL of M-dilution buffer and adjusted the total volume up to 50 µL with deionized distilled water before incubation at 42^{o}C for 30 minutes. A hundred microliters of CT-conversion buffer was mixed to the DNA sample and followed by incubation at 50^{o}C for 16 hours in the dark. After incubation, the sample was further incubated at 4^{o}C for 10 minutes (DNA thermal cycler 480, Perkin Elmer). A few minute before reach incubation time, 400 µL M-binding buffer was transferred into Zymo-spin IC™ column, which placed on collecting tube. Then, the treated DNA was mixed with M-binding buffer in column, and centrifugation at 13000 rpm for 30 seconds. The column was washed once with 100 µL of M-wash buffer followed by adding 200 µL of M-desulphonation buffer and left at room temperature for 20 minutes. After incubation, it was centrifuged and washed twice with 200 µL of M-wash buffer. Finally, the column was placed on 1.5 mL microtube before adding 20 µL of M-elution buffer directly to the filter and centrifuged at 13000 rpm for 1 minute. The bisulfite treated DNA were kept at -20^{o}C.

4. Defining of interesting region and gene information

4.1 Differentially methylated region (DMR) of *IGF2*

The sequence of DMR of IGF2 referred to GenBank accession no.Y13633. The methylation pattern in this region has been studied in several cell types. The interesting site in this region composed of 3 CpGs which shown as yellow label in Figure12.

Homo sapiens IGF2 gene, exon 3

Locus: Y13633

Definition: Homo sapiens IGF2 gene, exon 3.

```
   1 ggatcctggt ttctgaagga ggggaagaac ttctgctgct ggagggtgca ggaagcctcc
  61 tgagagcagc ctcaacttca ggggatgggg tgtgcaggaa aggccattgt ggagagggtt
 121 ctcctttagg gctgcacaaa gccactgagg cttttgcaag gaaaataggt tttccttgtc
 181 taattcacca agcaaaatgg gaggggtagg ggaggagggc taggccgctc ttcccagcgg
 241 gaacacacag ctgtcttcac aagtgtgaaa ggaagagtct ttctgtgtga aaagtttcct
 301 cccgttgcat cccccatccc attcccagag acaaacagga gactttgcag aggagccagg
 361 ggcccgagat tctggcgcag agattttatt tatacatata tacaccattt tacaggtaaa
 421 gcttccttcc ctcctgcctc cctatgcctg ctgaccacca gcaagaaatt ggacaggaga
 481 ctgaggagaa acgccgggag aggcaacaac cgccctccat gtccccccta ggtttagctt
 541 ctctcctcct gatggcgcac ctggtccccc ttgctgctct cccagcctcc ctggcacaga
 601 gaggcaccct ggggccaagg cagtttccct gggaatgctc attcatgcat gaagttttc
 661 tctgttgcac cctggaccca gactcctcaa tccacccagg gtggtgtctg tggggagggg
 721 gttcacttcc ccaggaagca cagccacgcc gtccctcact ggcctcgtca agcagagctg
 781 tgtgtccagt ggcttttgct ggggcccccc ccttatctcc ttccaaggtg gggtgtttg
 841 gaggtggagg aggctttcat attccgtgcc atgacccctc aaggcgggcc attcgtgtgc
 901 accctccacc cccagtgcca ggcagaagcc catcctcacc caggaacagg gcagcctgtc
 961 caacagaagg gtctcggcct ctccatcagc accgggaagc cctttctagg caaacttctc
```

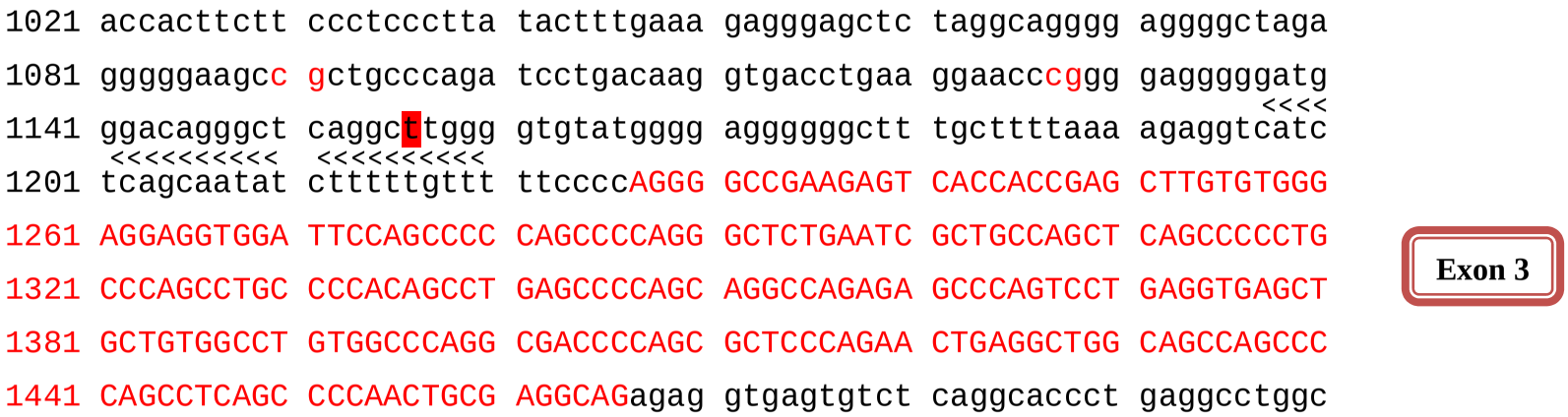

Figure12. Human IGF2 gene. The red label referred to SNPs, the yellow label referred to the interesting CpG site, the red capital alphabet referred to exon region, and (>) and (<) referred to primer annealing site.

4.2 CTCF6 binding region on the upstream of *H19*

The CTCF6 binding region was intensively studied region. There were several reference sequences to define gene information in this region such as GenBank accession no.AF087017, AF125183, AC004556, U50731 and M32053. All reference sequences were aligned to each other, then, defining the interesting CpGs in the chosen reference sequence, GenBank accession no.AF087017. The interesting site in this region was 5 CpGs of CTCF6 binding region, yellow label in Figure14.

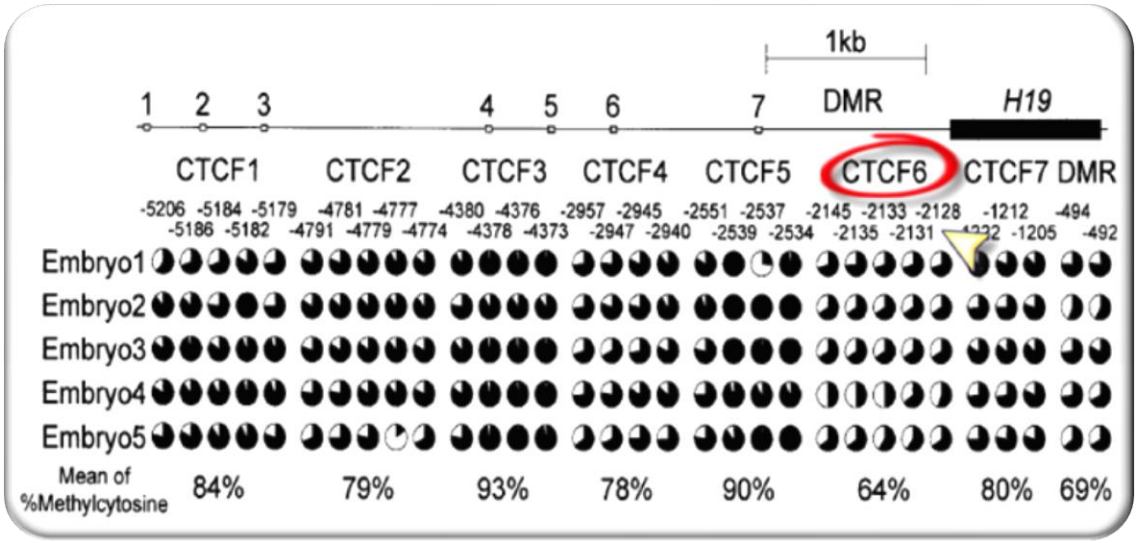

Figure13. CpG position of individual CTCF binding site within CTCF binding region on the upstream of *H19* gene

Homo sapiens H19 gene, complete sequence

Locus: AF087017

Definition: Homo sapiens H19 gene, complete sequence

```
3001 gtatttctgg aggcttccca ttcagtcttg gatgccagcc tcaccaaggg cggcccatct
3061 tgctgacctc accaagggag gcccgtctca ctgccctgat ggcgcagaat cggctgtacg
3121 tgtggaatca gaagtggccg cgcggcggca gtgcaggctc acacatcaca gcccgagcac
3181 gcctggctgg ggttcaccca cagaaacgtc ccaggtctcc caggccaggt gccgcattgg
3241 ttcccgaggg ttgtcagaga tagacactca tgcgactaac atcgggctat gtgtttgatt
3301 caccccaggg tgcattgttg aaggttgggg agattggagg agatgcttgg gggacaatga
3361 ggtgtcccag ttccttggat gatagggatc tcggcctaag cgtgagaccc ctcctacagg
3421 gtctctggca ggcacagagc ctgggggctc ttgcatagca catgtgtatt tctggaggct
3481 tccccttcgg tctcaccgcc ccgatggtgc agaatcggtt gtagttgtgg aatcggaagt
3541 ggccgcgcgcgg cggcagtgca ggctcccaca tcacagctca agcccgcccc agctgaggtt
3601 cacccgcgga aacgtcccgg gtcacgcaag ctaggtgccg caaggttcac gggggtagtg
3661 agggatagaa cactcatggg agccacattg ggctacgtgt ctgattcacc ccagggtgca
3721 ctattgaggg ttggggagat gagatacttt ggtgacaatg aggtgtcccc attctttgga
3781 tgatggggat ctcggcctca gcgtgaggcc cctcccacag ggtctctggc aggcacagaa
3841 actgggggct cttgcgtagc acatgggtat ttgtggacgc ttccccttct gtctcaccac
3901 ccggatggca cagaatcggt tgtaagtgtg gactcaaaag tggccgcgcgcg gcggcagtgc
3961 aggctcacac atcacagccc aagccctccc tggatggggt tcgcccgcgg aaacgtcctg
```

1st CTCF binding site

2nd CTCF binding site

3rd CTCF binding site

```
4021 ggtcacccaa gccaggtgcc gcagggttct cggaggtctt ctgggaatag gacgctcatg
4081 ggagccacac cacgtcttcg tatcgggcca tatccacggc cgcgtggccc caggtcacac
4141 tctgagggct tcagtgtcat ggcctgggac tcaagtcacg cctacccgcg tgatgagcac
4201 agcaaattcc aacaaaagct tatactttcc acatccatcc cagagcacag atccgactaa
4261 ggacagcccc caaatcccga gccttttct gaactgacaa ttgcctcccc agtgaacact
4321 ctgagcttgt caatcttaag tggccagaca ttaacattcc cattcagtgc aggtttgaga
4381 tgctaattta ggagcttgag atgctaaaga gctgggagtg ccactgctgc tttattctgg
4441 ggtctaggat ccttgtgttg gctgagataa tctgctaatg tgggtgcagc agacatcccg
4501 cggtttgtgg aatcgataaa ggatggggat caatggtgtt tgtgcactgt gcggtctgtg
4561 cccaattgcc tgccttgtgc tgtggaatct gtacacctgg ccaacatgtg cttgtgtgag
4621 cctgacagtg cattttccag agcctcacct cggctctgcc ctggaggctc tgtgctgctg
4681 gaatcagact caaggacctc atcagaggac catggccccg tatcacctgg gtcaggcact
4741 gaagctggga caggagagca gagacttcca aaatgaggga tccctgtgtt ctgaggtgat
4801 catgactggg acccaaggac tcaagcgcat gctccagagg gaatcgtttc ccacaaggcc
4861 tttggcagga acagggatcc tgggagcctg ccaagcagag cgcacagtgt tcctggagtc
4921 tcgctgccca gatgccacgg aatcagttga aggtatggaa acacaggtgg ccacgtggta
4981 gcagggcagg ctcaggcgtc atagcccgag cccggctacc tgtggtttgc ctgcagaaac
5041 atcccgggtc aacaggccag gcaccgcatt ggttcgcgag ggtcatcggg ggtaggaccc
5101 ttgtacgagc cacatcgggc tacgtgcctg attcacccca gggtgcactg ttgaaggttg
5161 gggagatgag aggagatact tgggggacag tgaagtgtcc ccattctttg gatgatgggg
```


5221 atctcggcct cagcgtgaga cccctcccac agggtctctg gcaggctcaa gagcccaggg
5281 gctcttgcat agcacatgaa tatttctgga ggcttcccct tcagtctcac cacccggatg
5341 gtgcagaatt ggttgtagct gtggaatcgg aagtggccgc gtggcggcag tgcaggctca
5401 cacatcacag cccgagccca ccccagctgg ggttcgcccg cggaaacgtc ccgggtcccg
5461 caagccaggc gccgcagggt tcacgggggt catcagggat aggacattca tgggagccac
5521 atcgggctat gtgtctgatt caccccaggg tgcactattg agggttggga agatgagagg
5581 agatgcttgg gggacaatga agtgtcccca ttctttggat gatggggatc ttggcctcag
5641 ggtgagatcc ttcttgcagg gtctatggca ggcacagagc ccgggggctc ttgcatagca
5701 catgtgtatt tctggaggct tcccttcag tctcaccgcc cggatggcac ggaattggtt
5761 gtagttgtgg aatcggaggt ggctgcgcgg cggcagtgca ggctcacaca tcacagcccg
5821 agcccgcccc agctggggtt cgcccgtgga aacatcccag gtcatccaag ccgggcgcca
5881 cagggttcac aggggtcgtg aggtatagga cactcatggg agccatatcg ggctacgtgt
5941 ctgattcacc ccagggtgca ctgttgaagg ttggggagat gggaggagat actaggggaa
6001 caatgaggtg tcccagttcc atggatgatg gggatctcgg ccctagtgtg aaacccttct
6061 cgcagggtct ctggcaggca cagagcccgg gggctcttgc atagcacatg ggtatttctg
6121 gaggcttctc cttcggtctc accgcctgga tggcacggaa ttggttgtag ttgtggaatc
6181 ggaagtggcc gcgcggcggc agtgcaggct cacacatcac agcccgagcc cgcccaact
6241 ggggttcgcc cgtggaaacg tcccgggtca cccaagccac gcgtcgcagg gttcacgggg
6301 gtcatctggg aataggacac tcataggagc cgcaccagat cttcaggtcg ggcattatcc
6361 acagccccgt ggccccgggt cacactccga gggcttcagt gtcatggcct gggactcaag
4th CTCF binding site
5th CTCF binding site
6th CTCF binding site

Figure14. Human *H19* gene. The red label referred to SNPs, the yellow label referred to the interesting CpG site, and the red (>) and (<) referred to outer primer annealing site whereas black (>) and (<) referred to inner primer annealing site.

5. Primer design

The primer for methylation study was designed using online MethPrimer program (http://www.urogene.org/ methprimer/index1.html). The genomic sequence in FASTA format of interesting region was input to the program and marked "Pick primers for bisulfite sequencing PCR or restriction PCR"..

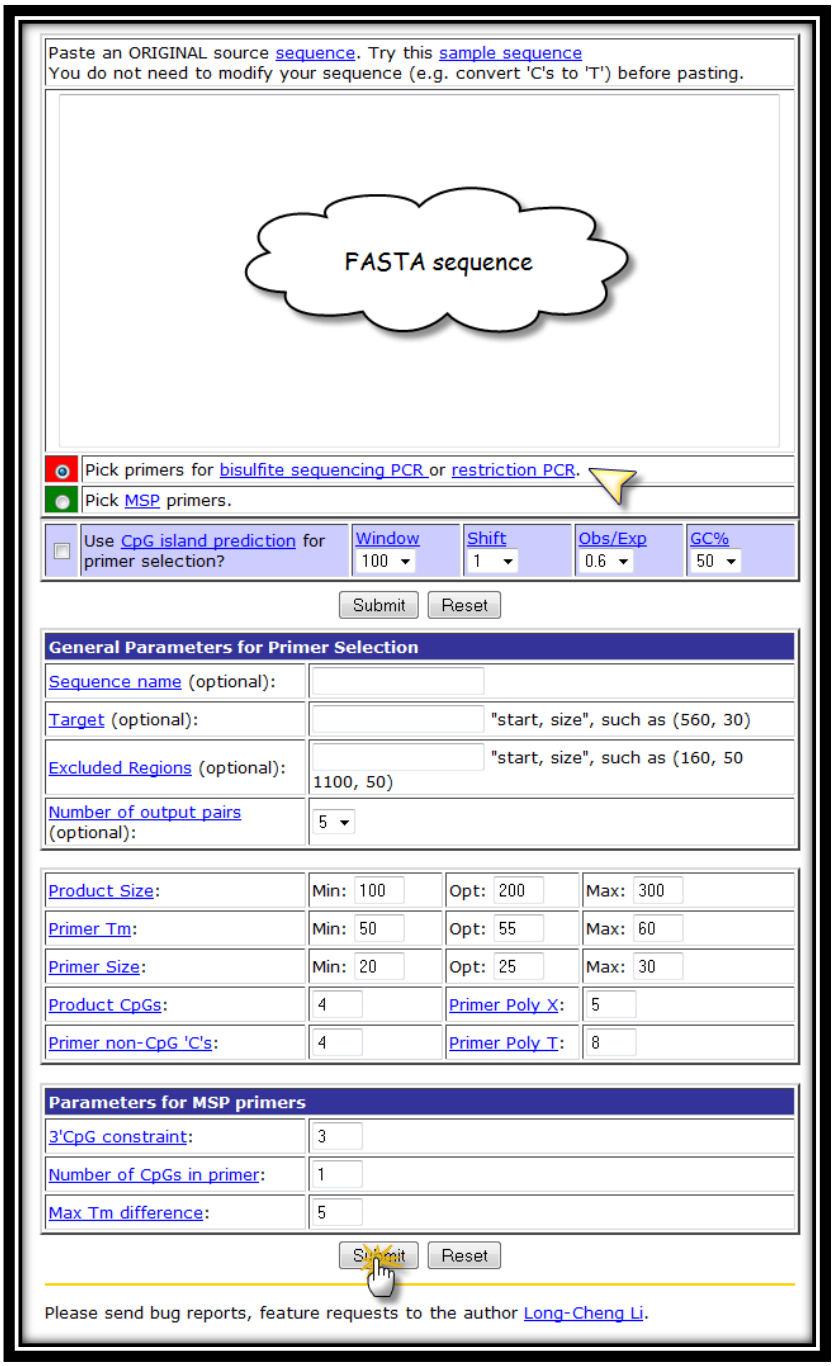

Figure15. The feature of online MethPrimer program which is a bioinformatics tool to design primer for methylation studied

This program could specify forward and reverse annealing sites by numbering in the "target" blank. Moreover, the advance options were able to set up for more specific parameters such as product size, primer Tm, primer size, etc. After setting all parameters properly, the "submit" button was clicked. The program would take a few minutes before the appropriate primer pair sequences were shown.

The specificity of each primer was further validated using online MethBLAST program (http://medgen.ugent.be/methBLAST/).

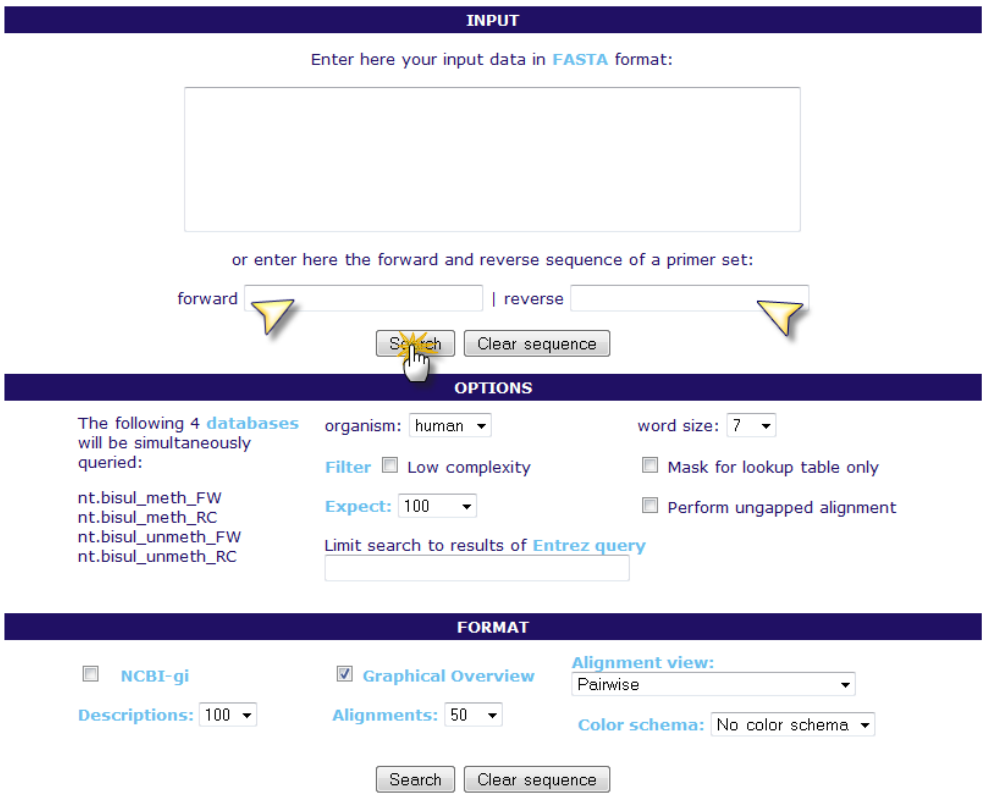

Figure16. The feature of MethBlast online program the bioinformatics tool to calculate specificity of primer pairs

The forward primer sequence from MethPrimer program was filled in "forward" blank whereas the reverse primer sequence was filled in "reverse" blank. After submitting the data, the program showed the probable amplified region in the whole genome. Only the primer pairs which specific to the interesting region were chosen (Table3).

Table3. Oligonucleotide primers for methylation studied

Gene (region)	Direction		Sequence	GenBank database	Annealing start site	Annealing end site	primer Size
H19 (CTCF6)	outer	forward	GGAATAATGAGGTGTTTTAGTTTTA	AF087017	5997	6021	25
		reverse	CTAACCACTTAAAACTAAAAAAATC		6574	6598	25
	inner	forward	GTAGGGTTTTTGGTAGGTATAGAGT		6062	6086	25
		reverse	CACTAAAAAAACAATTATCAATTC		6542	6566	24
IGF2 (DMR)	forward		TAATTTATTTAGGGTGGTGTTTGTG	Y13633	688	712	25
	reverse		CAAACCTAAACCCTATCCCATC		1137	1158	22

6. Polymerase chain reaction (PCR)

The nested-touchdown PCR was performed to amplify the CTCF6 binding region. For the first reaction of nested PCR, 4 µL of bisulfite treated DNA was mixed with PCR reagent containing 1X Fast Start *Taq* Buffer with 2 mM $MgCl_2$, 0.5 µM H19outer F primer (5'-GGAATAATGAGGTGTTTTAGTTTTA-3'), 0.5 µM H19outer R primer (5'-CTAACCACTTAAAACTAAAAAAATC-3'), 0.2 mM dNTP, and 1U Fast Start *Taq* polymerase in total volume 20 µL. The reaction was started with an initial step at 95^{o}C for 4 minutes followed by 10 cycles of touchdown PCR (denaturation step at 95^{o}C for 45 seconds, annealing step at 57^{o}C for 1 minute at first cycle and gradually decrease 1^{o}C in each cycle and ended up with another extension step at 72^{o}C for 1 minute). Then, the reaction continued to 40 cycles of general PCR (denaturation at 95^{o}C for 45 seconds, annealing at 51^{o}C for 1 minute, extension at 72^{o}C for 1 minute) and ended up with final extension at 72^{o}C for 10 minutes before holding the reaction at 4^{o}C. Furthermore, 5 µL of PCR product from the first reaction was amplified using the same condition except H19inner F primer (5'-GTAGGGTTTTTGGTAGGTATAGAGT-3') and H19inner R primer (5'-CACTAAAAAAACAATTATCAATTC-3') were added.

The touchdown PCR was used to amplify the IGF2 gene. Its reaction was composed of 6 µL of bisulfite treated DNA, 1X Fast Start *Taq* Buffer, 1.5 mM $MgCl_2$, 0.2 mM dNTP, 0.5 µM IGF2 F primer (5'-TAATTTATTTAGGGTGGTGTTTGTG-3'), 0.5 µM IGF2 R primer (5'-CAAACCTAAACCCTATCCCATC-3') and 1U Fast Start *Taq* Polymerase in total volume 20 µL. Reaction was preheated at 95^{o}C for 3 minutes and followed by PCR 50 cycles with 3 different annealing temperatures. The first annealing temperature was at 65^{o}C (denaturation at 95^{o}C for 45 seconds, annealing at 65^{o}C for 45 seconds, extension at 72^{o}C for 1 minute) for 5 cycles and followed by another 5 cycles with annealing temperature at 62^{o}C (denaturation at 95^{o}C for 45 seconds, annealing at 62^{o}C for 45 seconds, extension at 72^{o}C for 1 minute) and continue to 45 cycles with annealing temperature at 57^{o}C (denaturation at 95^{o}C for 45 seconds, annealing at 57^{o}C for 45 seconds, extension at 72^{o}C for 1 minute) and end up with final extension at 72^{o}C for 10 minutes before holding at 4^{o}C.

The PCR product was further detected by horizontal agarose gel electrophoresis. Three percent agarose gel was prepared and sank in 1X TBE in

electrophoresis chamber. The mixing of 6X loading dye to 1 µL of 100 basepair-DNA molecular weight marker, and 3 µL PCR product was loaded separately into each well. Then, the chamber was given electricity 100V for 60 minutes. After that, the gel was stained with ethidium bromide (EtBr) for 1 minute and destained in 1X TBE for 4 minutes. Finally, the electrophoretic result was detected and recorded using GelDocument (Figure17).

(A) **(B)**

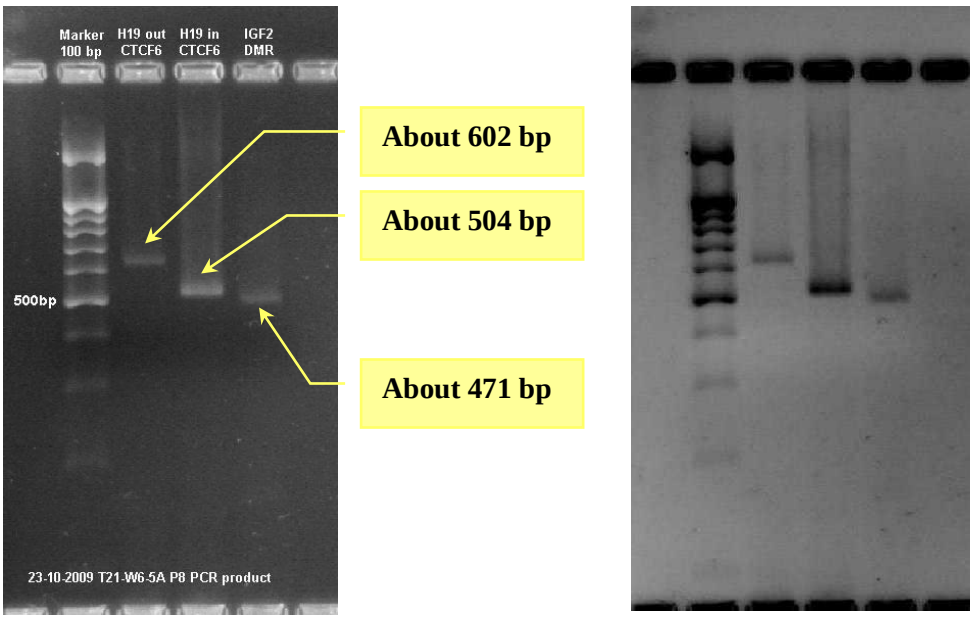

Figure17. (A) PCR product detection by electrophoresis technique. PCR product was separated in 3% agarose gel under electric field 80 volts for 90 minutes. The 1st lane was 100 bp DNA marker, 2nd lane was PCR product 602 bp of H19 outer CTCF6, 3rd lane was PCR product 504 bp of H19 inner CTCF6 and 4th lane was PCR product 471 bp of IGF2 DMR. **(B) Invert image of PCR product.**

7. DNA cloning

7.1. Competent cell preparation

The *E.coli* JM109 cells were thawed and streaked onto LB agar without ampicillin (LB w/o Amp^- agar) followed by incubation at 37°C for 14-16 hours. A single colony was picked up into 3 mL of LB broth without ampicillin (LB w/o Amp^- broth) and shaked at 37°C for 12-14 hours. One milliliter cell suspension was inoculated into 100 mL of LB w/o Amp^- broth and shaked at 37°C for 8 hours. After

incubation, each 45 mL cultured cells were aliquoted to 50 mL-tube and stored on ice for 10 minutes. The cells were pelleted by centrifugation at 3,000 rpm at 4^{o}C for 10 minutes. Then, the cell pellet was resuspended in 10 mL of cold RF1 and placed on ice for 30 minutes. After that, the cell was pelleted and resuspended in 2.5 mL of cold RF2 followed by stored on ice for 15 minutes. Each 100 µL of cell suspension was aliquoted to 1.5 mL-microcentrifuge tube and rapidly frozen in liquid nitrogen before stored at -80^{o}C.

7.2. Recombinant DNA construction

The PCR product was ligated to pGEM plasmid using pGEM-T-easy vector system (A3600, Promega, WI) as manufacturer's instruction. Ligation reaction was composed of 5 µL of 2X Rapid Ligation Buffer, 1 µL of 50 ng/µL pGEM-T-easy vector, 1 µL of 3Weiss units/µL T4 DNA Ligase and 3 µL of PCR product. This solution was incubated at 16^{o}C for 12 hours and could be stored at -20^{o}C until transformation.

7.3. Transformation

One-hundred µL of JM109 competent cell in a 1.5 mL-microcentrifuge tube was thawed on ice for 5 minutes before mixing with the ligation reaction followed by stirring gently using a pipette tip and incubated on ice for 30 minutes. After incubation, the cells were heated at 42^{o}C for 50 seconds before they were placed on ice immediately and further stored on ice for 5 minutes. Then, 900 µL of LB broth without ampicillin was added before shaking the cells at 37^{o}C for 1 hour. IPTG/X-gal/ampicillin LB agar was freshly prepared in the dark. Forty microliters of 100 mM IPTG, 40 µL of 20% X-gal and LB broth without ampicillin were mixed together before spreading onto LB agar containing ampicillin. The incubated cells were then collected by centrifugation at 10,000 rpm for 5 minutes. Nine hundred microliters of supernatant was pipetted out before spreading the left 100 µL cell suspension onto the IPTG/X-gal/ampicillin LB agar plate and incubated at 37^{o}C for 16-20 hours.

7.4. Colony selection

The LB agar containing ampicillin was prepared and poured into petri dishes. The table was drawn under this plate. Each block was numbered sequentially (Figure18). This plate was called a master plate. Only white colonies detected on the Amp^{+}/X-gal/IPTG LB agar from the transformation step (step 6.3) was subcultured to

the master plate. Then, it was cultured at 37°C for 12 hours. After incubation, DNA insert in individual clones were further verified by PCR. The PCR reaction composed of 1X Dream Taq buffer with 2 mM $MgCl_2$, 0.5 µM primer (H19 inner primer pair or IGF2 primer pair depending on the inserted fragment in recombinant construction step), 0.2 mM dNTP and 0.5U Dream Taq polymerase in a total volume of 10 µL. Each clone was picked up and resuspended in a PCR master mix solution. The reaction was started with preheated step at 95°C for 5 minutes followed by 30 cycles of denaturation at 95°C for 45 seconds, annealing at 52°C for 45 seconds, extension at 72°C for 1 minute and followed by a final extension at 72°C for 10 minutes before holding at 4°C. The PCR product was further analyzed by 3% agarose gel electrophoresis under 100V for 60 minutes. Only clones with the appropriate PCR product were picked up from the master plate and cultured in 3 mL of LB broth with ampicillin at 37°C for 12 hours. For each sample, at least 8 clones were selected.

(A) **(B)**

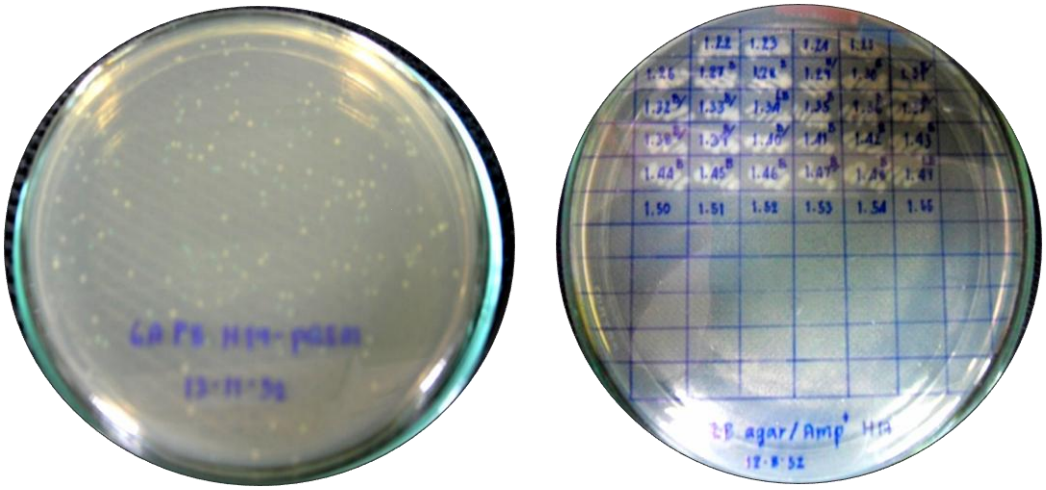

Figure18. (A) colony screening blue and white colony formation on IPTG/x-gal/amplicillin LB agar plate **(B) master plate** the numbering colony for further recombinant DNA selection

(A) **(B)**

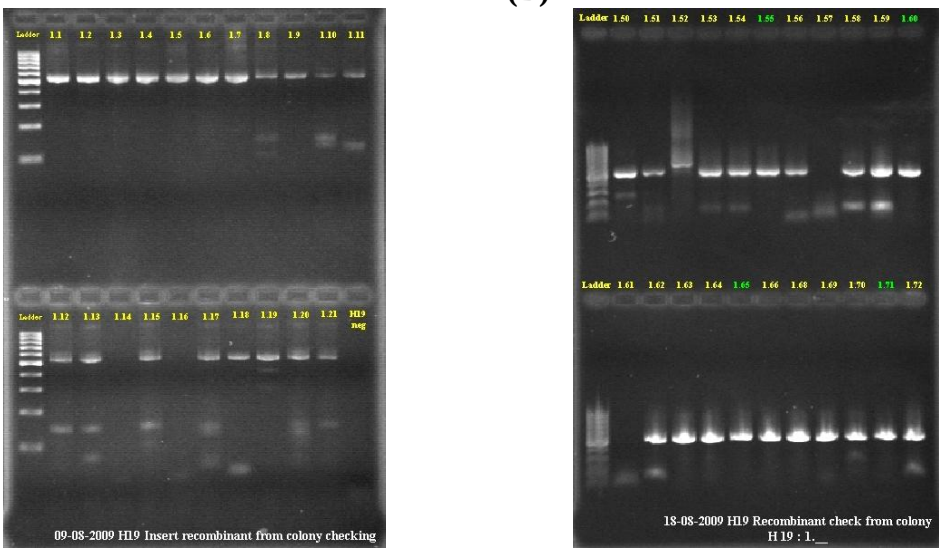

Figure19. Recombinant DNA selection by PCR technique

8. Plasmid minipreparation

Plasmid DNA was extracted from the selected clones using PureYield Plasmid Miniprep System (A1221 Promega, USA) according to the Manufacturer's instruction. The 1.5 mL of cultured cell were transferred to a 1.5 mL microtube and harvested by centrifugation at 13,000 rpm for 5 minutes before removal of supernatant and followed by adding another 1.5 mL of cultured cell into the same tube and mixed with 100 µL of cell lysis buffer. After that, 350 µL of cold neutralization solution was mixed before centrifugation at maximum speed for 3 minutes. The supernatant was then transferred to the column which placed into the collecting tube before centrifugation at maximum speed for 15 seconds. Two-hundred µL of the Endotoxin Removal Wash was subsequently added into the column and centrifuged for 15 seconds before the column was washed with 400 µL using the Column Wash Solution and centrifuged for 30 seconds. Finally, the column was placed into a new 1.5 mL microtube and let stand for 1 minute at room temperature before centrifugation at maximum speed for 15 seconds.

9. Sequencing

Totally the 256 plasmids of the selected clone (8 clons x 8 cell lines x 2 passages x 2 regions) were analyzed using sequencing technique. Details of each plasmid i.e. the sample name, vector name, primer name, plasmid concentration, and product size were shown in Figure20 before sending to Ramathibodi Hospital, Thailand, and 1st Base Company, Malaysia, for commercially sequencing

For the clones containing CTCF6 binding region, the H19 inner forward primer was used as a sequencing primer. For the clones containing DMR of IGF2, the IGF2 DMR forward primer was used as sequencing primer.

1st BASE
Your Research, Our Business

Ward Medic Ltd., Part
19/28 Sukhumvit 65 Chaiyaprik
Prakanong-Nua
Vadhana Bangkok 10110

Order Form – Automated DNA Sequencing Service

Online order is available at https://order.base-asia.com

Name (English)	:	Sujeeporn Sripradite
Supervisor	:	Assoc.Prof.Nednapis Tirawanchai
Institute	:	Mahidol University
Department	:	Biochemistry
PO or Standing Order #	:	
Contact No.	:	
E-mail (*important*)	:	Sugie_Palm@hotmail.com
Date	:	
Total no. of Reactions	:	164

For Office Use Only

Data Entry:	Date Received:	OrderID Tracking:	Remarks:

Please check (X) in the ☐ for the type of services:

- ☐ Regular cycle sequencing reaction
- ☒ Difficult templates (Please circle: GC-rich / AT-rich / GT-rich / repetitive sequence)
- ☐ Ready-to-load samples (we only accept BDTv3.1)
- ☐ Primer walking of constructs (Single Pass or Bi-directional)
- ☐ Others (_____)

For pre-treatment services, please fill in Pretreatment form in the next sheet.

No	Template Information						Primer Information					
	Name of Sample(s)	* Type of DNA	Conc (ng/µl)	Size (bp)	Vol (µl)	Vector Name (for plasmid DNA only)	Primer Used	@Check (X) if using Free Universal Primers?		# Conc (pmol/µl)	Tm (^{o}C)(50mM Na^{+})	Vol (µl)
1	CL9P8 2.1	*1 - Purified Plasmid*	4753	3471	10	pGEM	IGF2-F		Yes	10	55.42	5
2	CL9P8 2.6	*1 - Purified Plasmid*	5105	3471	10	pGEM	IGF2-F		Yes	10	55.42	5
3	CL9P8 2.9	*1 - Purified Plasmid*	5430	3471	10	pGEM	IGF2-F		Yes	10	55.42	5
4	CL9P8 2.10	*1 - Purified Plasmid*	1715	3471	10	pGEM	IGF2-F		Yes	10	55.42	5
5	CL9P8 2.31	*1 - Purified Plasmid*	5320	3471	10	pGEM	IGF2-F		Yes	10	55.42	5
6	CL9P8 2.33	*1 - Purified Plasmid*	4910	3471	10	pGEM	IGF2-F		Yes	10	55.42	5
7	CL9P8 2.37	*1 - Purified Plasmid*	2735	3471	10	pGEM	IGF2-F		Yes	10	55.42	5
8	CL9P8 2.40	*1 - Purified Plasmid*	5193	3471	10	pGEM	IGF2-F		Yes	10	55.42	5
9	CL8P15 2.3	*1 - Purified Plasmid*	4708	3471	10	pGEM	IGF2-F		Yes	10	55.42	5
10	CL8P15 2.4	*1 - Purified Plasmid*	4735	3471	10	pGEM	IGF2-F		Yes	10	55.42	5

* 1 = Purified Plasmid; 2 = Purified PCR product; 3 = Purified M13 ssDNA; 4 = Others (please specify)

5uL of 10uM (or 10pmol/uL) of primer provided per reaction for regular sequencing.
5uL of 30uM (or 30pmol/uL) of primer provided per reaction for direct genomic DNA sequencing

Quick reference of sample requirement *per reaction* :

Purified PCR Product [90-250bp]	: 10 ng/µL, min 10 µL per rxn in dH2O
Purified PCR Product [251-500bp]	: 20 ng/µL, min 10 µL per rxn in dH2O
Purified PCR Product [>500bp]	: 40 ng/µL, min 10 µL per rxn in dH2O
Purified Plasmid	: 50 ng/µL, min 10 µL per rxn in dH2O
Purified M13 ssDNA	: 50 ng/µL, min 10 µL per rxn in dH2O
Purified Genomic DNA	: 400 ng/µL, min 20 µL per rxn in dH2O
Primer Walking [≤ 3kb]	: 50 – 200ng/µL, in 50µL sdH2O
Primer Walking [> 3kb]	: Whole bacterial colony; or 50 – 200ng/µL, in 50 µL sdH2O

Note: Additional quantity of sample will be required for quantification.

@ Free universal primers provided:

M13F (-20)	5' GTAAAACGACGGCCAGT 3'	T7 Terminator	5' GCTAGTTATTGCTCAGCGG 3'
M13F (-29)	5' CACGACGTTGTAAAACGAC 3'	T3	5' ATTAACCCTCACTAAAG 3'
M13F-pUC (-40)	5' GTTTTCCCAGTCACGAC 3'	SP6	5' ATTTAGGTGACACTATAG 3'
M13R (-20)	5' GCGGATAACAATTTCACACAGG 3'	BGH-rev	5' CTAGAAGGCACAGTCGAGGC 3'
M13R (-24)	5' GGAAACAGCTATGACCATG 3'	AOX1 Forward	5' GACTGGTTCCAATTGACAAGC 3'
M13R-pUC (-26)	5' CAGGAAACAGCTATGAC 3'	AOX1 Reverse	5' GCAAATGGCATTCTGACATCC 3'
T7	5' AATACGACTCACTATAG 3'	pBRrevBam	5' GGTGATGTCGGCGATATAGG 3'
T7 Promoter	5' TAATACGACTCACTATAGGG 3'		

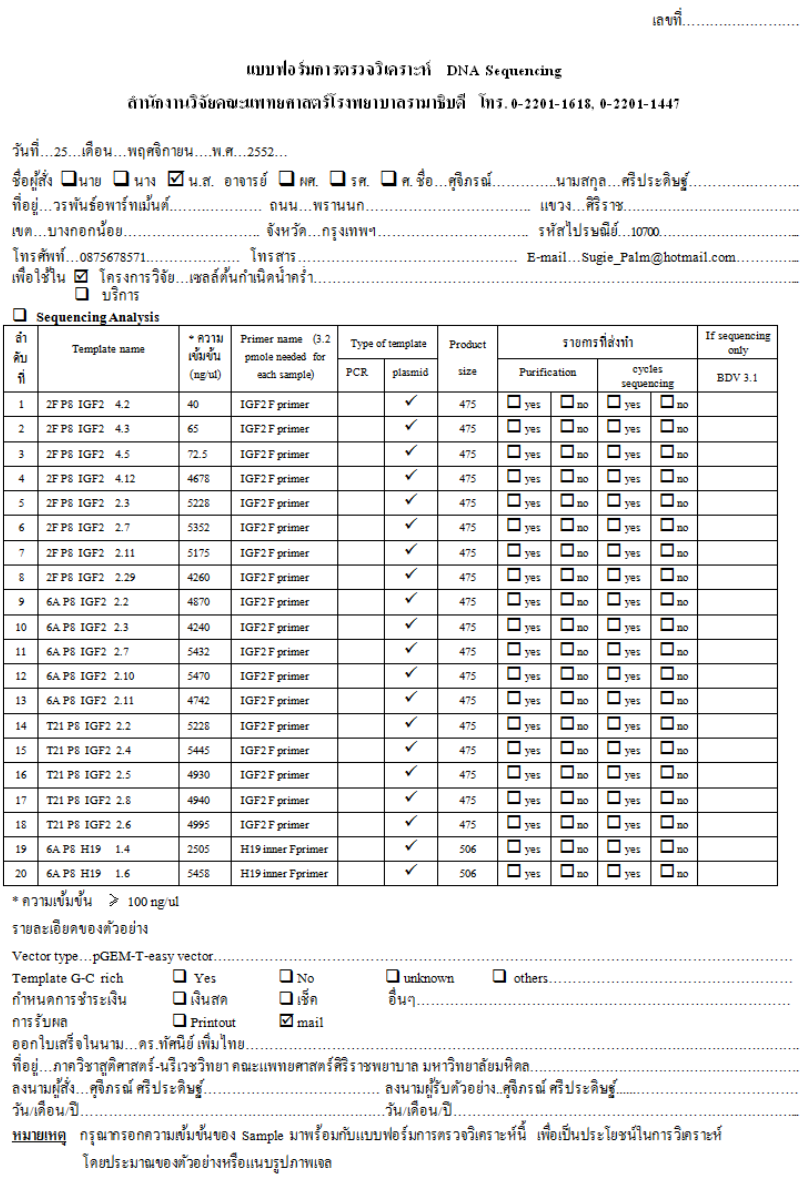

เลขที่.....

แบบฟอร์มการตรวจวิเคราะห์ DNA Sequencing

สำนักงานวิจัยคณะแพทยศาสตร์โรงพยาบาลรามาธิบดี โทร. 0-2201-1618, 0-2201-1447

วันที่...25...เดือน...พฤศจิกายน....พ.ศ...2552...

ชื่อผู้สั่ง ☐นาย ☐ นาง ☑ น.ส. อาจารย์ ☐ ผศ. ☐ รศ. ☐ ศ. ชื่อ...ศุจิภรณ์.....นามสกุล...ศรีประดิษฐ์.....

ที่อยู่...วรพันธ์อพาร์ทเม้นต์..... ถนน...พรานนก..... แขวง...ศิริราช.....

เขต...บางกอกน้อย..... จังหวัด...กรุงเทพฯ..... รหัสไปรษณีย์...10700.....

โทรศัพท์...0875678571..... โทรสาร..... E-mail...Sugie_Palm@hotmail.com.....

เพื่อใช้ใน ☑ โครงการวิจัย...เซลล์ต้นกำเนิดน้ำคร่ำ.....
☐ บริการ

☐ **Sequencing Analysis**

ลำดับที่	Template name	* ความเข้มข้น (ng/ul)	Primer name (3.2 pmole needed for each sample)	Type of template		Product size	รายการที่สั่งทำ				If sequencing only
				PCR	plasmid		Purification		cycles sequencing		BDV 3.1
1	2F P8 IGF2 4.2	40	IGF2 F primer		✓	475	☐ yes	☐ no	☐ yes	☐ no	
2	2F P8 IGF2 4.3	65	IGF2 F primer		✓	475	☐ yes	☐ no	☐ yes	☐ no	
3	2F P8 IGF2 4.5	72.5	IGF2 F primer		✓	475	☐ yes	☐ no	☐ yes	☐ no	
4	2F P8 IGF2 4.12	4678	IGF2 F primer		✓	475	☐ yes	☐ no	☐ yes	☐ no	
5	2F P8 IGF2 2.3	5228	IGF2 F primer		✓	475	☐ yes	☐ no	☐ yes	☐ no	
6	2F P8 IGF2 2.7	5352	IGF2 F primer		✓	475	☐ yes	☐ no	☐ yes	☐ no	
7	2F P8 IGF2 2.11	5175	IGF2 F primer		✓	475	☐ yes	☐ no	☐ yes	☐ no	
8	2F P8 IGF2 2.29	4260	IGF2 F primer		✓	475	☐ yes	☐ no	☐ yes	☐ no	
9	6A P8 IGF2 2.2	4870	IGF2 F primer		✓	475	☐ yes	☐ no	☐ yes	☐ no	
10	6A P8 IGF2 2.3	4240	IGF2 F primer		✓	475	☐ yes	☐ no	☐ yes	☐ no	
11	6A P8 IGF2 2.7	5432	IGF2 F primer		✓	475	☐ yes	☐ no	☐ yes	☐ no	
12	6A P8 IGF2 2.10	5470	IGF2 F primer		✓	475	☐ yes	☐ no	☐ yes	☐ no	
13	6A P8 IGF2 2.11	4742	IGF2 F primer		✓	475	☐ yes	☐ no	☐ yes	☐ no	
14	T21 P8 IGF2 2.2	5228	IGF2 F primer		✓	475	☐ yes	☐ no	☐ yes	☐ no	
15	T21 P8 IGF2 2.4	5445	IGF2 F primer		✓	475	☐ yes	☐ no	☐ yes	☐ no	
16	T21 P8 IGF2 2.5	4930	IGF2 F primer		✓	475	☐ yes	☐ no	☐ yes	☐ no	
17	T21 P8 IGF2 2.8	4940	IGF2 F primer		✓	475	☐ yes	☐ no	☐ yes	☐ no	
18	T21 P8 IGF2 2.6	4995	IGF2 F primer		✓	475	☐ yes	☐ no	☐ yes	☐ no	
19	6A P8 H19 1.4	2505	H19 inner Fprimer		✓	506	☐ yes	☐ no	☐ yes	☐ no	
20	6A P8 H19 1.6	5458	H19 inner Fprimer		✓	506	☐ yes	☐ no	☐ yes	☐ no	

* ความเข้มข้น ≥ 100 ng/ul

รายละเอียดของตัวอย่าง

Vector type...pGEM-T-easy vector.....

Template G-C rich ☐ Yes ☐ No ☐ unknown ☐ others.....

กำหนดการชำระเงิน ☐ เงินสด ☐ เช็ค อื่นๆ.....

การรับผล ☐ Printout ☑ mail

ออกใบเสร็จในนาม...ดร.ทัศนีย์ เพิ่มไทย.....

ที่อยู่...ภาควิชาสูติศาสตร์-นรีเวชวิทยา คณะแพทยศาสตร์ศิริราชพยาบาล มหาวิทยาลัยมหิดล.....

ลงนามผู้สั่ง...ศุจิภรณ์ ศรีประดิษฐ์..... ลงนามผู้รับตัวอย่าง..ศุจิภรณ์ ศรีประดิษฐ์.....

วัน/เดือน/ปี.....วัน/เดือน/ปี.....

หมายเหตุ กรุณาทรอกความเข้มข้นของ Sample มาพร้อมกับแบบฟอร์มการตรวจวิเคราะห์นี้ เพื่อเป็นประโยชน์ในการวิเคราะห์โดยประมาณของตัวอย่างหรือแนบรูปภาพเจล

Figure20. The sequencing order form. The sample's name, plasmid's name, plasmid concentration was filled in the form.

10. Data analysis

The sequencing result was converted to FASTA format by Chromas program.

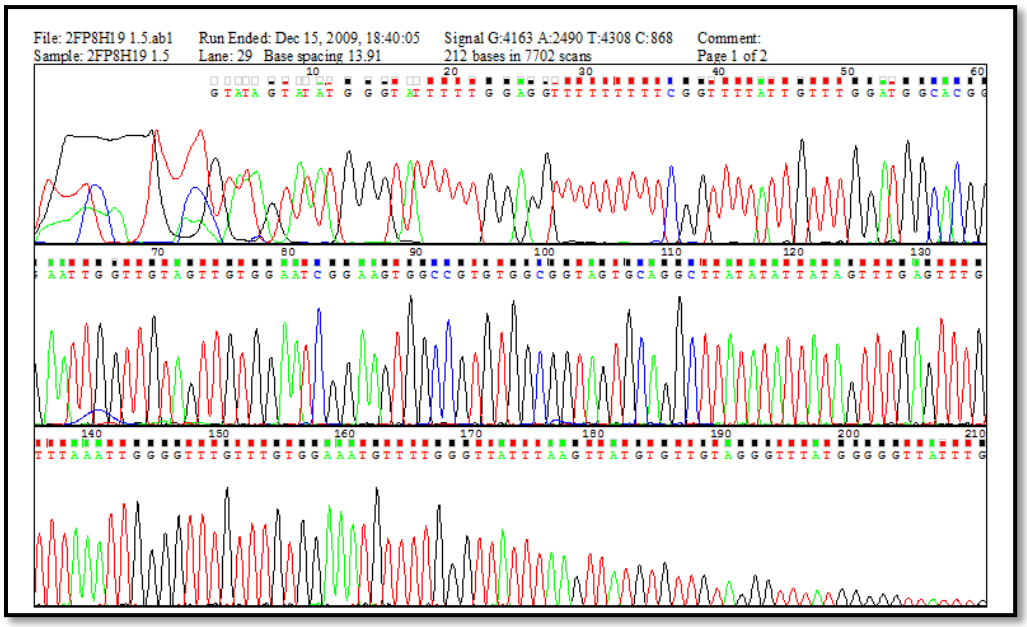

Figure21. Sequencing data. The result from an automate sequencer is .abl file

This sequence in FASTA format was further aligned to gene reference sequence, H19 (GenBank accession no.AF087017 nucleotide 6001-6600) or IGF2 gene (GenBank accession no.Y13633 nucleotide 601-1200) according to the type of sequencing primer, using BiQ Analyzer program. This program converted cytosine (C) of non-CpG in reference sequence to thymine (T) before pairwise alignment with the sequencing result. Stars were marked underneath the perfect match nucleotide sequence between reference sequence and test sequence. The remaining cytosine at CpG site implied the methylated pattern (orange color label) whereas the converted thymine at CpG site implied the unmethylated pattern (purple color label).

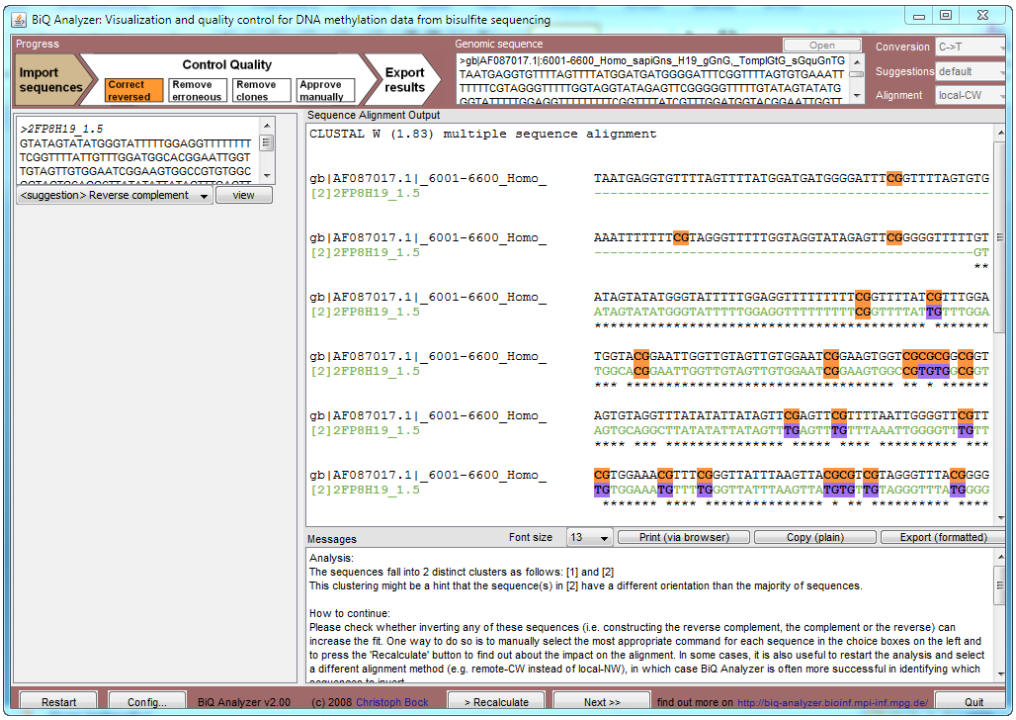

Figure22. DNA methylation pattern was analyzed by BiQ Analyzer program

Methylation pattern from BiQ Analyzer program could be symbolized by filled and blank circle. The methylated pattern (orange label) was represented by filled circle (●) whereas the unmethylated pattern (purple label) was represented by blank circle (○). For the CTCF6 binding region on the upstream of *H19*, there are 5 interesting CpG sites and their methylation status were represented by 5 continuous circles. For the DMR of *IGF2*, there are 3 interesting CpG sites and their methylation status were represented by 3 continuous circles (Figure23)

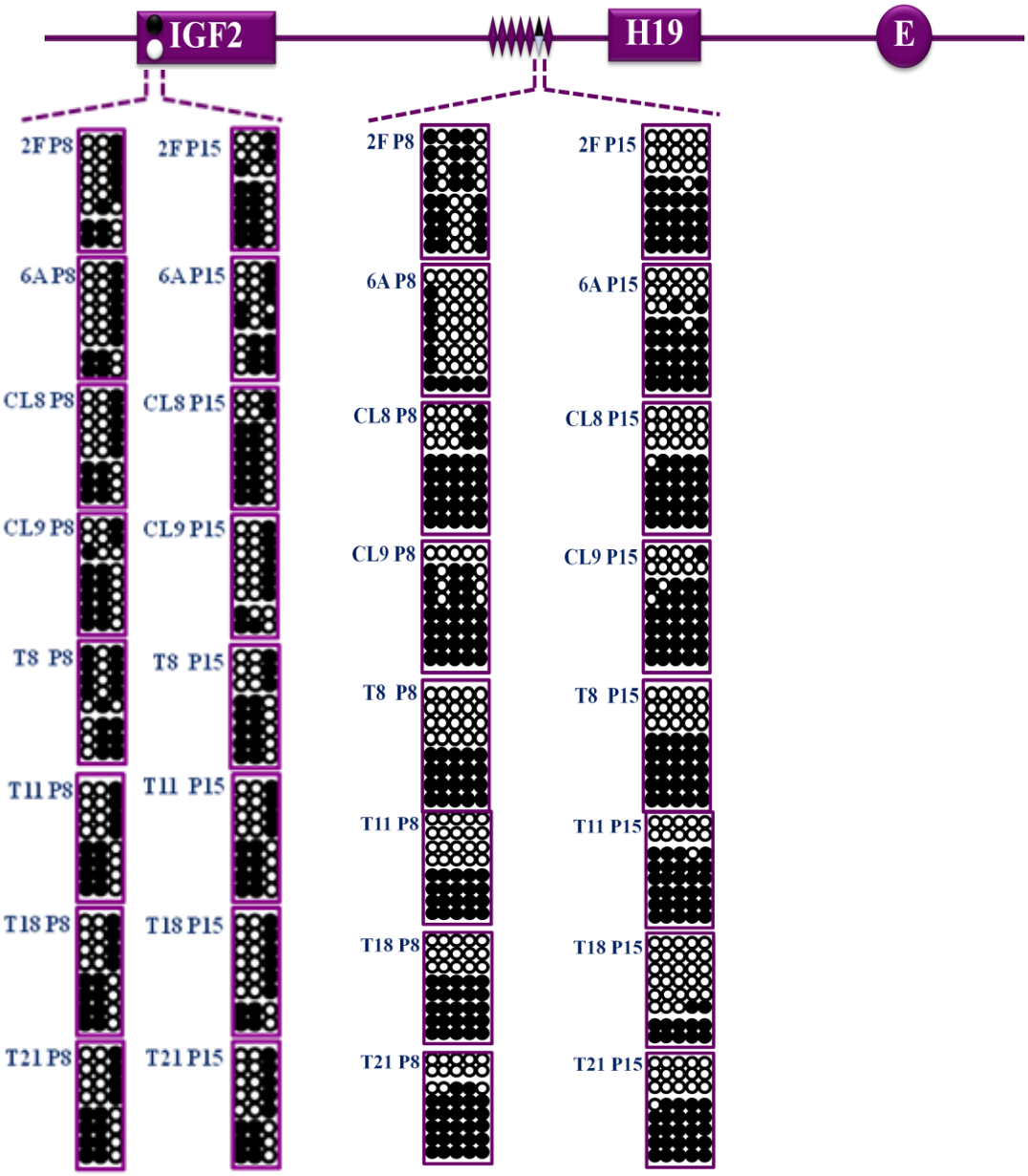

Figure23. Methylation pattern of interesting CpG dinucleotide. Filled circle referred to methylated CpG, blank circle referred to unmethylated CpG.

The methylation patterns of 256 clones were categorized into individual cell line at each passage. Therefore, each sample showed 8 methylation patterns. Some methylation patterns were found repeatly in several clones from the same sample, thus, the methylation pattern could be grouped. Each group of methylation pattern which found in each sample represented the methylation pattern of that sample.

CHAPTER IV
RESULT

1. The exploration of DNA methylation pattern at ICR and DMR in IGF2-H19 imprinting cluster of Amniotic Fluid Stem Cell (AFS)

This study explored the DNA methylation pattern at Imprinting Control Region (ICR) and Differentially Methylated Region (DMR) in IGF2-H19 imprinting cluster in Amniotic Fluid Stem Cell (AFS). The ICR of this cluster locates about 2 kb on the upstream of *H19*, known as CTCF6 binding site, whereas the DMR locates between exon2 and 3 of *IGF2*.

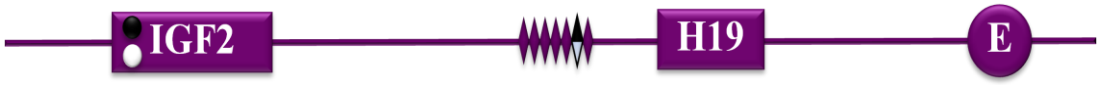

Figure24. Location of the interesting ICR and DMR in IGF2-H19 imprinting cluster. The IGF2-H19 imprinting cluster composes of 2 imprinted gene members; the *IGF2* locates on the upstream-side whereas *H19* locates on the downstream of *IGF2* (each boxes). The CTCF1 to 7 binding sites embeds between those two gene members (diamonds) and the enhancer is on the downstream of cluster (E-circle). The interesting ICR is represented by black-white diamond of the sixth CTCF binding site whereas the DMR is represented by black-white circle in *IGF2*.

1.1. Imprinting Control Region (ICR) on the upstream of *H19*

The bisulfite sequencing analysis showed methylation pattern of every CpGs in the interesting region. The methylated cytosine was detected as CpG from sequencing technique and represented by black circle (●) whereas the unmethylated cytosine was detected as TpG and represented by white circle (○). The exploring of the DNA methylation pattern at CTCF6 binding region and other CpG nearby this region included 3 CpGs on the upstream of CTCF6 binding region followed by 5 CpGs of CTCF6 binding region and 2 CpGs on the downstream of CTCF6 binding region. It showed the fully methylated pattern (●●● ●●●●● ●●) in almost all samples, except for 2FP8. This fully methylated pattern (●●● ●●●●● ●●) with ●○● ○○○○○ ○○ was

found as major pattern in 11 samples such as T8P8, T11P8, T18P8, T21P8, 2FP15, 6AP15, CL8P15, CL9P15, T8P15, T11P15, T18P15, and T21P15. For sample 6AP8, the major methylation pattern was similar to those 11 samples but there was gain of methylation at CpG1 of CTCF6 binding region of pattern ●○● ○○○○○ ○○ therefore the major methylation pattern of 6AP8 was the combination of fully methylated pattern (●●● ●●●●● ●●) with pattern ●○● ●○○○○ ○○. For the sample 2FP8, the major methylation pattern was quite different from others. There was not any fully methylated or unmethylated pattern in 2FP8, only the alternative pattern (●●● ●○●●○ ●● and ●○● ●●○○● ○○) was found. The alternative pattern ●●● ●○●●○ ●● was also found as one major methylation pattern of CL9P8 and in T21P8. The other methylation pattern such as ●○○ ○○○●● ○○ was found in CL8P8 and T18P15 whereas fully unmethylated pattern was found in T18P15.

According to this exploring of DNA methylation pattern at CTCF6 binding region, it could be concluded that the highest frequent major methylation pattern (11/16) of amniotic fluid stem cell was ●●● ●●●●● ●● with ●○● ○○○○○ ○○ even though some other patterns were also found occasionally such as major pattern ●●● ●○●●○ ●● with pattern ●○● ●●○○● ○○ in 2FP8 and the major pattern of ●●● ●●●●● ●● with ●○○ ○○○●● ○○ in CL8P8. Most samples (10/16) could be found only 2 major methylation patterns; however, some samples (6/16) appeared methylation pattern more than 2 patterns.

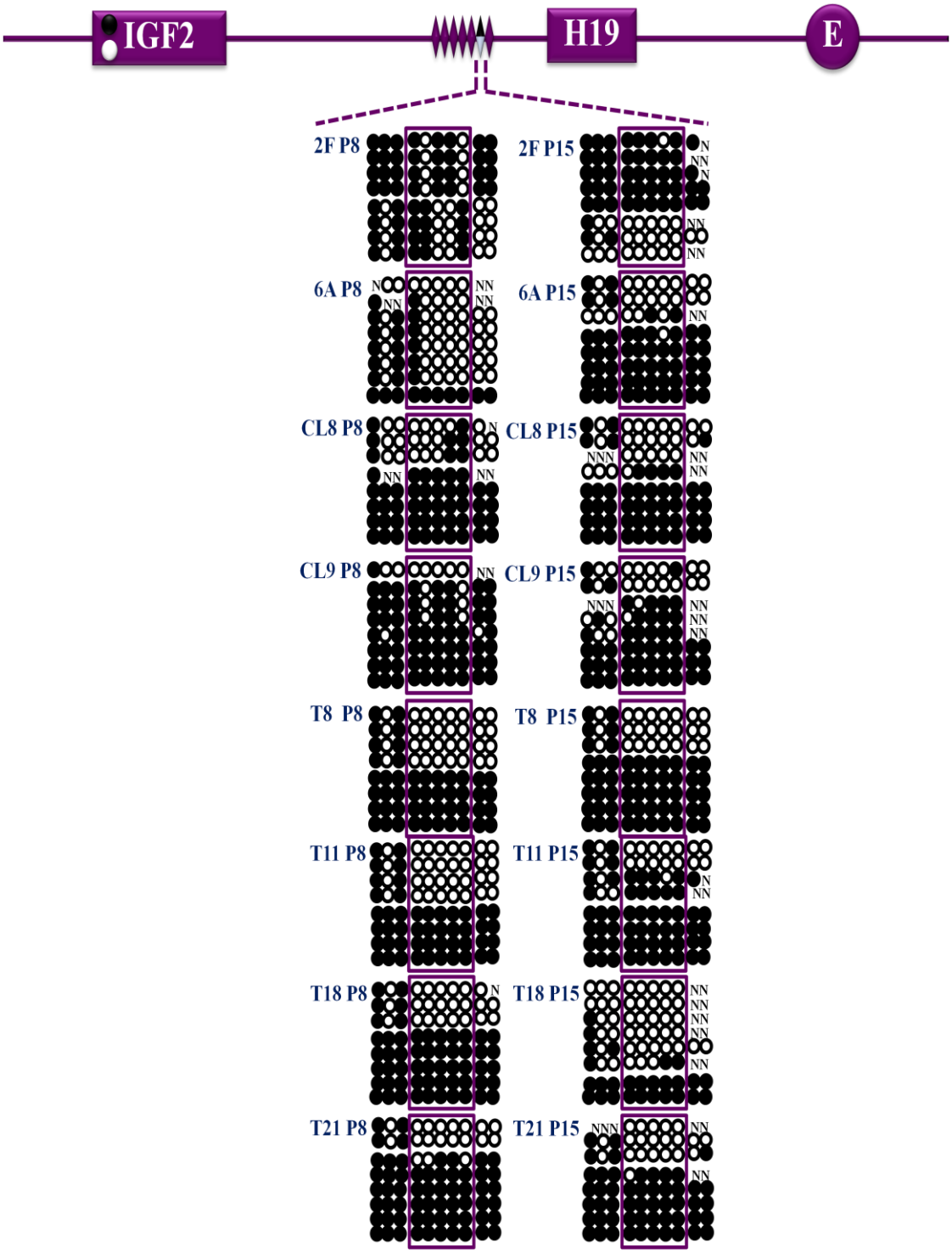

Figure25. Methylation pattern around CTCF6 binding region on the upstream of *H19*. The methylated CpG is represented by filled circle (●) whereas the unmethylated CpG is represented by blank circle (○). Five CpGs of CTCF6 binding region showed in square.

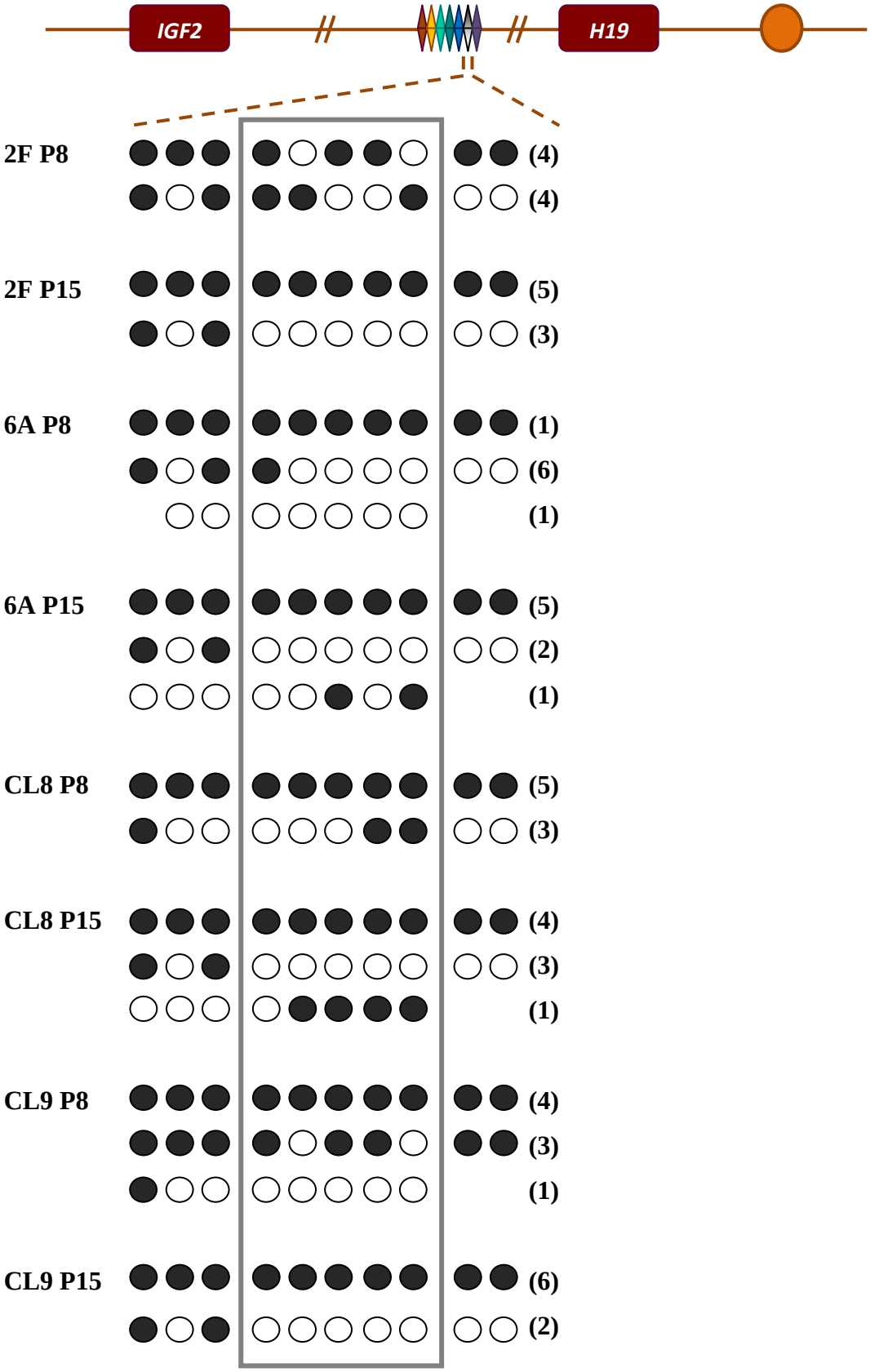
IGF2
H19
2F P8
(4)
(4)
2F P15
(5)
(3)
6A P8
(1)
(6)
(1)
6A P15
(5)
(2)
(1)
CL8 P8
(5)
(3)
CL8 P15
(4)
(3)
(1)
CL9 P8
(4)
(3)
(1)
CL9 P15
(6)
(2)

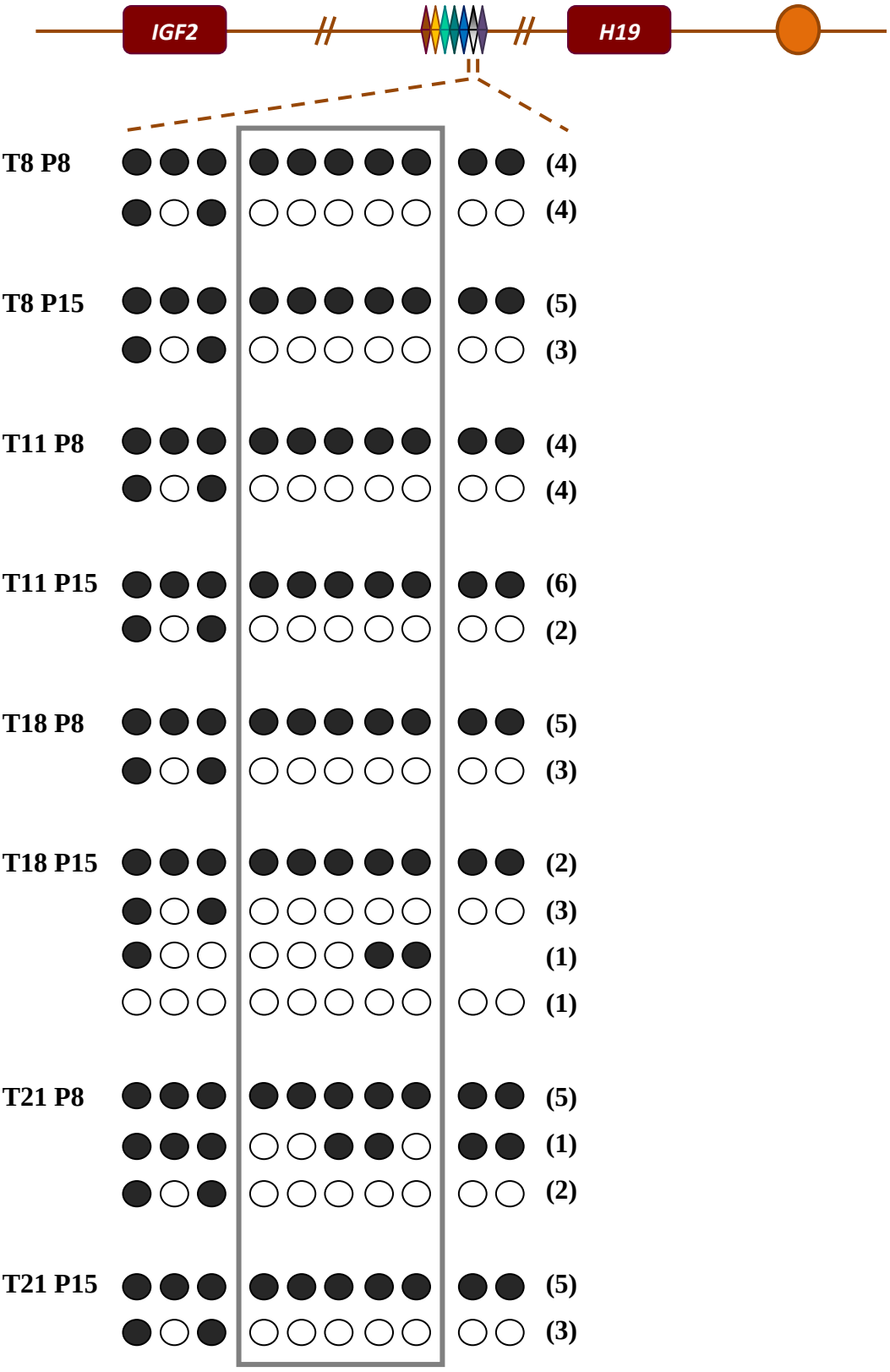

Figure26. The frequency of particular DNA methylation pattern around CTCF6 binding region of individual AFS samples

For the consideration of methylation pattern at CpG site by site, both methylated pattern and unmethylated pattern could be found at same CpG from the different major methylation patterns. This pattern was called the differentially methylated pattern and represented by black-white circle (◑). Besides, some sample showed only methylated pattern at the same CpG from all major methylation pattern, called hypermethylated CpG and represented by filled circle (●). The definition of methylation pattern around CTCF6 binding region found that the first and third of 3 CpGs on the upstream of CTCF6 binding region was hypermethylated in 13/16 samples (81.25%) and 10/16 samples (62.5%), respectively, whereas the second of 3 CpGs on the upstream of CTCF6 binding region showed the differentially methylated pattern. In CTCF6 binding region, the CpG1, 4 and 5 was hypermethylated in 1/16 samples (6.25%) whereas the CpG2 and 3 was differentially methylated pattern. For the downstream of CTCF6 binding region, both 2 CpGs showed hypermethylation in 1 of 16 samples (6.25%).

Therefore, the hypermethylation was frequently found at the first and third of 3 CpGs on the upstream of CTCF6 binding region whereas the CpG1, 4, and 5 of CTCF6 binding region and 2 CpGs on the downstream was rarely found hypermethylation. The different methylation pattern without any hypermethylation from all samples could be found at the second CpG on the upstream of CTCF6 binding region and the CpG2 and 3 of CTCF6 binding region.

Sample	CpG	CpG	CpG	CTCF6 binding region					CpG	CpG
				CpG1	CpG2	CpG3	CpG4	CpG5		
2F P8	●	◑	●	●	◑	◑	◑	◑	◑	◑
2F P15	●	◑	●	◑	◑	◑	◑	◑	◑	◑
6A P8	●	◑	◑	◑	◑	◑	◑	◑	◑	◑
6A P15	◑	◑	◑	◑	◑	◑	◑	◑	◑	◑
CL8 P8	●	◑	◑	◑	◑	◑	●	●	◑	◑
CL8 P15	◑	◑	◑	◑	◑	◑	◑	◑	◑	◑
CL9 P8	●	◑	◑	◑	◑	◑	◑	◑	●	●
CL9 P15	●	◑	●	◑	◑	◑	◑	◑	◑	◑
T8 P8	●	◑	●	◑	◑	◑	◑	◑	◑	◑
T8 P15	●	◑	●	◑	◑	◑	◑	◑	◑	◑
T11 P8	●	◑	●	◑	◑	◑	◑	◑	◑	◑
T11 P15	●	◑	●	◑	◑	◑	◑	◑	◑	◑
T18 P8	●	◑	●	◑	◑	◑	◑	◑	◑	◑
T18 P15	◑	◑	◑	◑	◑	◑	◑	◑	◑	◑
T21 P8	●	◑	●	◑	◑	◑	◑	◑	◑	◑
T21 P15	●	◑	●	◑	◑	◑	◑	◑	◑	◑

Table4. Methylation status at each CpG site around CTCF6 binding region. The methylation status at each CpG site (each circle) came from the overall methylation pattern from all 8 selected clones in individual samples. The specific CpG site which showed methylation pattern in all 8 selected clones was called hypermethylated CpG site, represented by fully filled circle (●). The specific CpG site which showed both methylation and unmethylation pattern in 8 selected clones was called differential methylated CpG, represented by half filled circle (◑).

1.2. Differentially Methylated Region (DMR) of *IGF2*

The exploring of the DNA methylation pattern at DMR of *IGF2* and other CpGs nearby this region included 3 CpGs in DMR of *IGF2* followed by 3 CpGs on the downstream of this region. The detectable methylation pattern was mainly in DMR of IGF2 whereas the methylation pattern of further CpG could be defined only in some clones. The pattern ○○● was found in almost all samples, except for the T8P8. This methylation pattern (○○●) with pattern ●●○ was the major methylation pattern in 14 samples such as 2FP8, 6AP8, CL8P8, CL9P8, T11P8, T18P8,, T21P8, 2FP15, CL8P15, CL9P15, T8P15, T11P15, T18P15, and T21P15. For the other 2 samples, their methylation patterns were various. The methylation pattern in T8P8 showed ●○●, ○●○ and ○●● whereas the methylation pattern of 6AP15 was ○○●, ○●●, ●○● and ●○○.

According to this exploring of DNA methylation pattern at DMR of *IGF2*, it could be concluded that the highest frequent major methylation pattern (14/16) of DMR of *IGF2* was ○○● with ●●○ even though some other patterns were also found occasionally such as pattern ●○● in T8P8 and 6AP15, pattern ○●○ in 2FP8 and T8P8, pattern ●○○ in 2FP15, 6AP15 and CL9P15, and pattern ○●● in T8P8 and 6AP15. Most samples (10/16) could be found only 2 major methylation patterns; however, some samples (6/16) appeared methylation pattern more than 2 patterns.

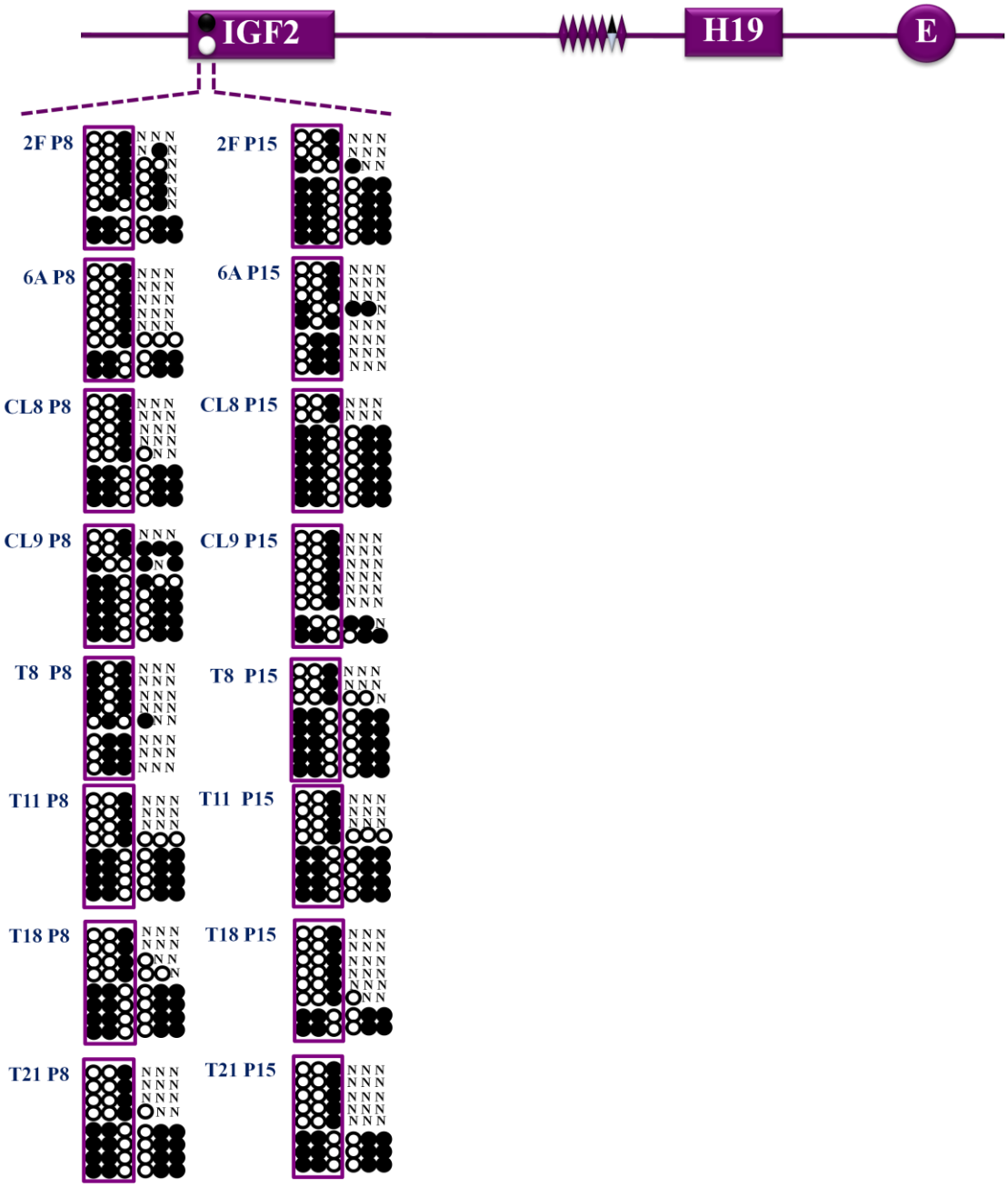

Figure27. Methylation pattern around the DMR of *IGF2*. The methylated CpG is represented by filled circle (●) whereas the unmethylated CpG is represented by blank circle (○). Three CpGs of DMR of *IGF2* showed in square.

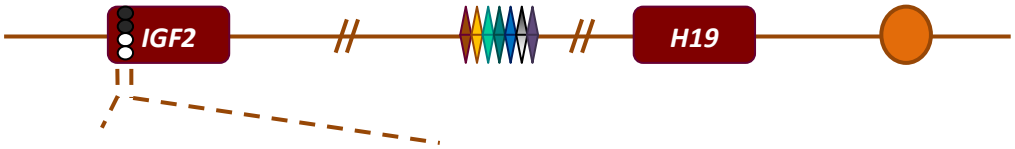

2F P8	○○● ○●N	**(5)**
	●●○ ○●●	**(2)**
	○●○ ○●N	**(1)**
2F P15	○○● NNN	**(2)**
	●●○ ○●●	**(5)**
	●○○ ●NN	**(1)**
6A P8	○○● ○○○	**(6)**
	●●○ ○●●	**(2)**
6A P15	○○● NNN	**(3)**
	○●● NNN	**(3)**
	●○○ ●●N	**(2)**
CL8 P8	○○● ○NN	**(5)**
	●●○ ○●●	**(3)**
CL8 P15	○○● NNN	**(2)**
	●●○ ○●●	**(6)**
CL9 P8	○○● ●●●	**(2)**
	●●○ ○●●	**(5)**
	●○○ ●N●	**(1)**
CL9 P15	○○● NNN	**(6)**
	●●○ ○●●	**(1)**
	●○○ ●●N	**(1)**

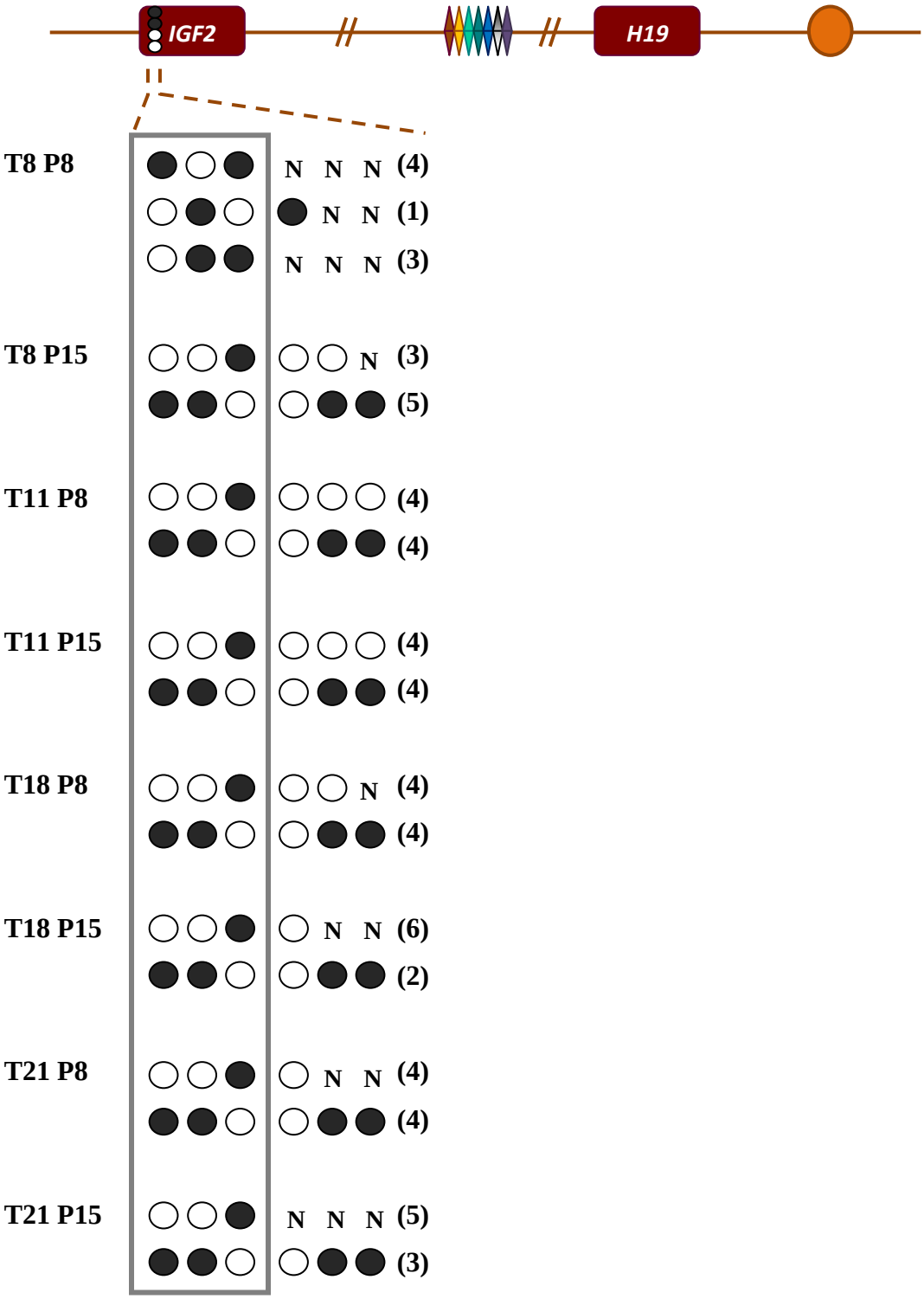

Figure28. The frequency of particular DNA methylation pattern around DMR of *IGF2* of individual AFS samples

For the consideration of methylation pattern at CpG site by site, both methylated pattern and unmethylated pattern could be found at same CpG from the different major methylation patterns. This pattern was called the differentially methylated pattern and represented by black-white circle (◑). Besides, some sample showed only unmethylated pattern at the same CpG from all major methylation pattern, called hypomethylated CpG and represented by blank circle (○). The definition of methylation pattern around DMR of *IGF2* found that all 3 CpGs at DMR of *IGF2* was differential methylation in all samples (100%). For the downstream of DMR, the detectable methylation pattern showed high frequency (11/16 samples) of hypomethylation at the first CpG next to DMR of *IGF2*.

The study showed that the methylation pattern of this region was differential methylated therefore this region was DMR in amniotic fluid stem cell.

Sample	DMR of *IGF2*			CpG	CpG	CpG
	CpG1	CpG2	CpG3			
2F P8	◑	◑	◑	○	●	●
2F P15	◑	◑	◑	◑	●	●
6A P8	◑	◑	◑	○	◑	◑
6A P15	◑	◑	◑	●	●	N
CL8 P8	◑	◑	◑	○	●	●
CL8 P15	◑	◑	◑	○	●	●
CL9 P8	◑	◑	◑	◑	●	●
CL9 P15	◑	◑	◑	◑	●	●
T8 P8	◑	◑	◑	●	N	N
T8 P15	◑	◑	◑	○	◑	●
T11 P8	◑	◑	◑	○	◑	◑
T11 P15	◑	◑	◑	○	◑	◑
T18 P8	◑	◑	◑	○	◑	●
T18 P15	◑	◑	◑	○	●	●
T21 P8	◑	◑	◑	○	●	●
T21 P15	◑	◑	◑	○	●	●

Table5. Methylation status at each CpG site around DMR of *IGF2*. The methylation status at each CpG site (each circle) came from the overall methylation pattern from all 8 selected clones in individual samples. The specific CpG site which showed methylation pattern in all 8 selected clones was called hypermethylated CpG site, represented by fully filled circle (●). The specific CpG site which showed both methylation and unmethylation pattern in 8 selected clones was called differential methylated CpG, represented by half filled circle (◑).

2. The comparing of DNA methylation pattern at ICR and DMR in IGF2-H19 imprinting cluster between AFS passage8 (P8) and passage15 (P15)

2.1. Imprinting Control Region (ICR) on the upstream of *H19*

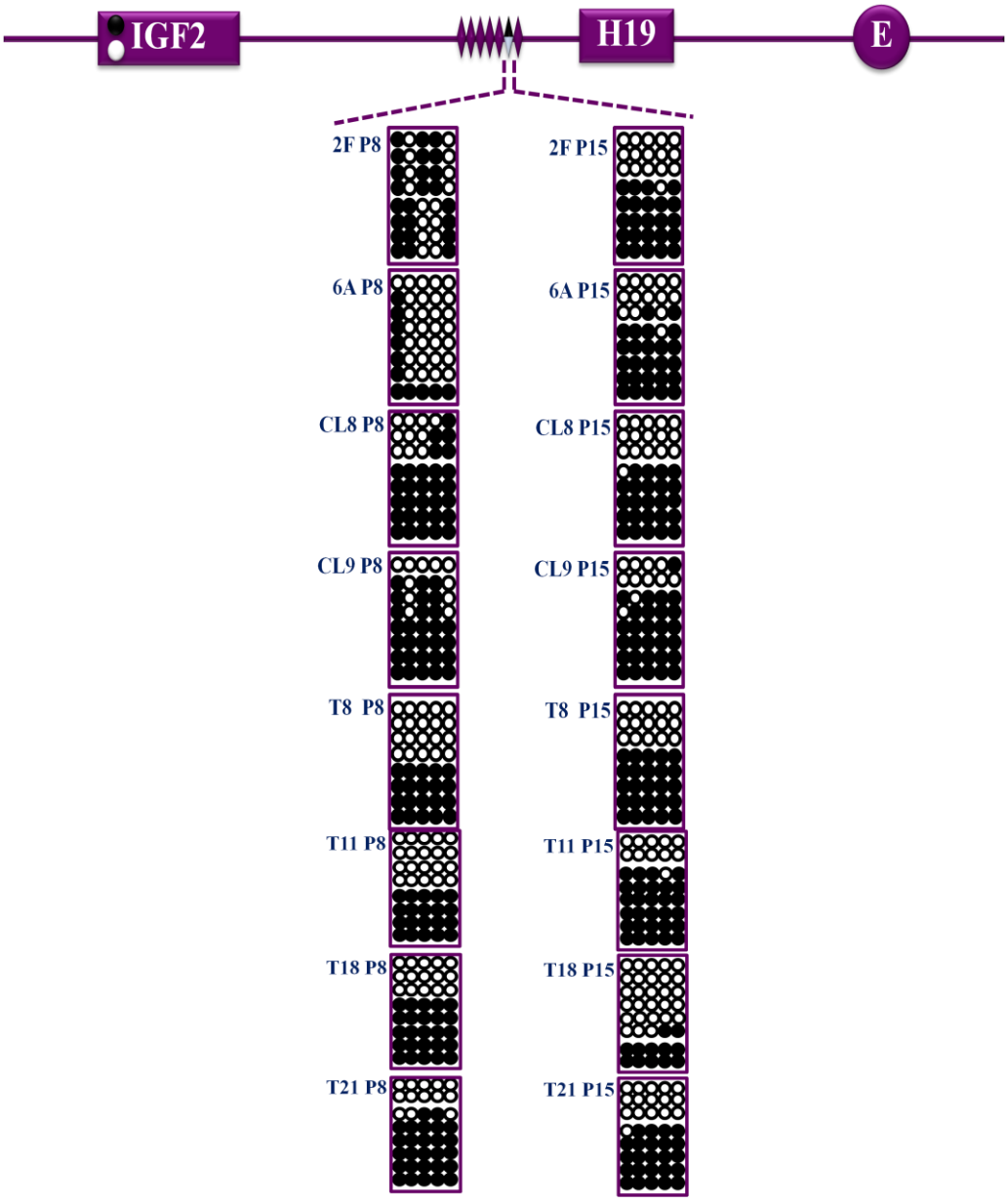

Figure29. Methylation pattern of CTCF6 binding region on the upstream of *H19*. The methylated CpG is represented by filled circle (●) whereas the unmethylated CpG is represented by blank circle (○). Five CpGs of CTCF6 binding region showed in the square.

The methylation pattern of CpGs in CTCF6 binding region was shown in pair of P8 and P15 sample by sample (Figure30). This section would interpret the alteration of methylation pattern of CpG in CTCF6 binding region between P8 and P15 using flanking region to indicate the different pattern. For the AFS 2F, the major methylation pattern at P8 was (●●●)●○●●○(●●) with (●○●)●●○○●(○○) and the major methylation pattern at P15 was (●●●)●●●●●(●●) with (●○●)○○○○○(○○). The pattern ●○●●○ at P8 might gain more methylation and become ●●●●● at P15 whereas the other major pattern ●●○○● at P8 lost some methylation and become ○○○○○ at P15. For the AFS 6A, the pattern (●●●)●●●●●(●●) remained in both P8 and P15 whereas other 2 major methylation patterns at P8 were similar to 2 major methylation patterns at P15, the pattern (●○●)●○○○○(○○) at P8 similar to (●○●)○○○○○(○○) at P15 and the pattern (○○○)○○○○○ at P8 similar to (○○○)○○●○● at P15. For the AFS CL8, the pattern (●●●)●●●●●(●●) was found in both P8 and P15 whereas another major pattern (●○○)○○○●●(○○) at P8 did not appear at P15 but the pattern (●○●)○○○○○(○○) and (○○○)○●●●● were found at P15 instead. For the AFS CL9, the fully methylated (●●●)●●●●●(●●) and unmethylated pattern (●○○)○○○○○ were found in both P8 and P15 whereas the pattern (●●●)●○●●○(●●) was found only at P8. This ●○●●○ pattern might gain methylation and become ●●●●● at P15. For the AFS T8, T11, T18, and T21, the major methylation pattern at P8 was same as P15. The pattern (●●●)●●●●●(●●) with (●○●)○○○○○(○○) was found in both different passages. However, the other patterns appeared in some samples such as the pattern (○○○)○○○○○(○○) at P15 of T18 and the pattern (●●●)○○●●○(●●) at P8 of T21. The pattern (●●●)○○●●○(●●) of T21 was found at P8 and disappeared at P15 as same as AFS CL9.

The comparative of methylation pattern between P8 and P15 showed that the highest frequent pattern was (●●●)●●●●●(●●) with (●○●)○○○○○(○○). However, there were gain and loss of methylation in some pattern along *in vitro* culture.

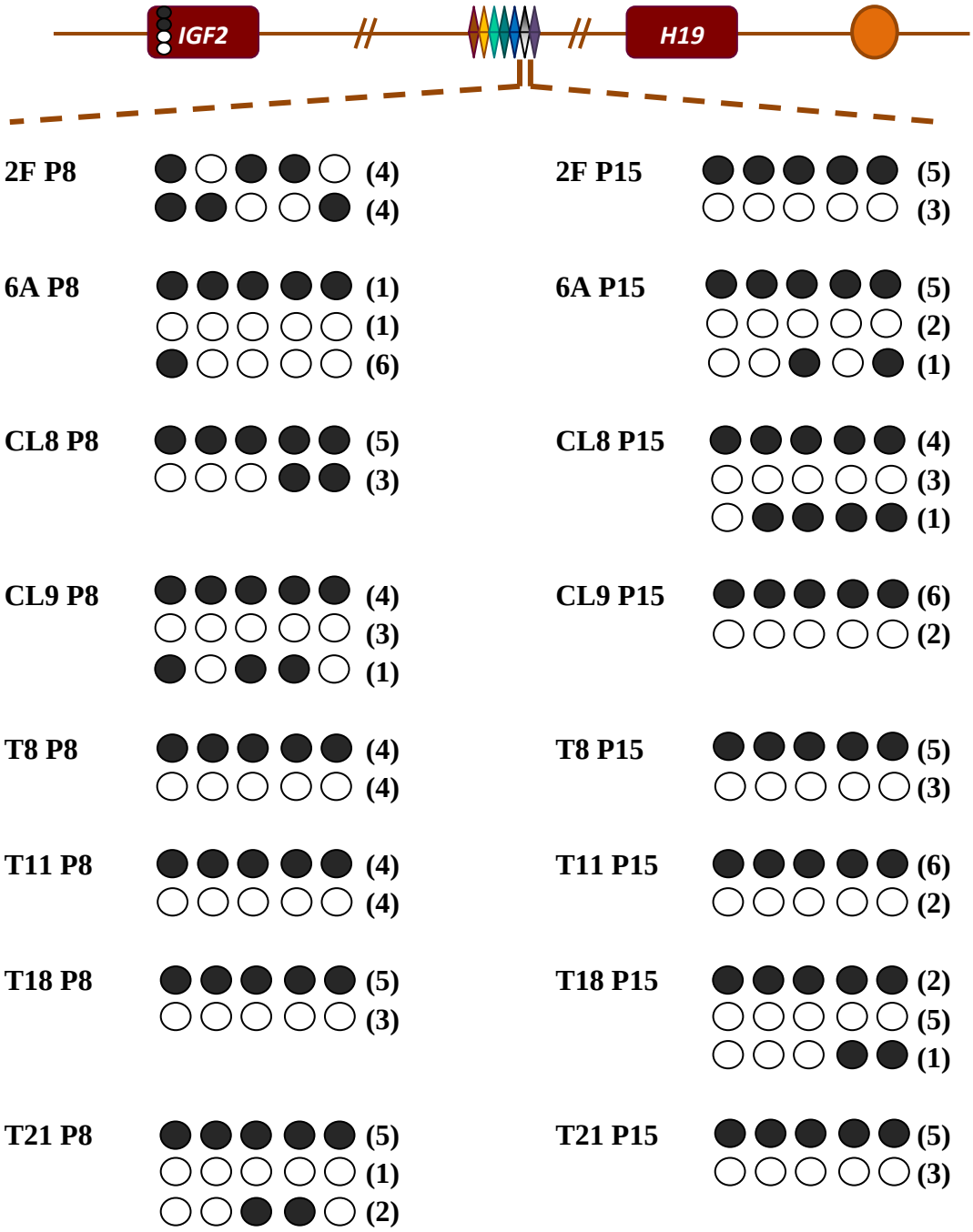

Figure30. The frequency of particular DNA methylation pattern of interesting CpG site in CTCF6 binding region

For the consideration of methylation pattern at CpG site by site**,** both methylated pattern and unmethylated pattern could be found at same CpG from the different major methylation patterns. This pattern was called the differentially methylated pattern and represented by black-white circle (◑). Besides, some sample showed only methylated pattern at the same CpG from all major methylation pattern, called hypermethylated CpG and represented by filled circle (●). The definition of methylation pattern at CTCF6 binding region in each 2 different passages found that only P8 could be found hypermethylation at some CpGs in CTCF6 binding region. The hypermethylation at CpG1, CpG4, and CpG5 was found in 1 of 8 AFS lines (12.5%) at P8 whereas the others showed differentially methylated pattern.

Therefore, the CTCF6 binding region was DMR in amniotic fluid stem cell even though some hypermethylation was found in P8.

Sample P8	CTCF6 binding region					Sample P15	CTCF6 binding region				
	CpG1	CpG2	CpG3	CpG4	CpG5		CpG1	CpG2	CpG3	CpG4	CpG5
2F P8	●	◑	◑	◑	◑	2F P15	◑	◑	◑	◑	◑
6A P8	◑	◑	◑	◑	◑	6A P15	◑	◑	◑	◑	◑
CL8 P8	◑	◑	◑	●	●	CL8 P15	◑	◑	◑	◑	◑
CL9 P8	◑	◑	◑	◑	◑	CL9 P15	◑	◑	◑	◑	◑
T8 P8	◑	◑	◑	◑	◑	T8 P15	◑	◑	◑	◑	◑
T11 P8	◑	◑	◑	◑	◑	T11 P15	◑	◑	◑	◑	◑
T18 P8	◑	◑	◑	◑	◑	T18 P15	◑	◑	◑	◑	◑
T21 P8	◑	◑	◑	◑	◑	T21 P15	◑	◑	◑	◑	◑

Table6. Methylation status of each interesting CpG site in CTCF6 binding region at different passages. The methylation status at each CpG site (each circle) came from the overall methylation pattern from all 8 selected clones in individual samples. The specific CpG site which showed methylation pattern in all 8 selected clones was called hypermethylated CpG site, represented by fully filled circle (●)**.** The specific CpG site which showed both methylation and unmethylation pattern in 8 selected clones was called differential methylated CpG, represented by half filled circle (◑).

2.2. Differentially Methylated Region (DMR) of *IGF2*

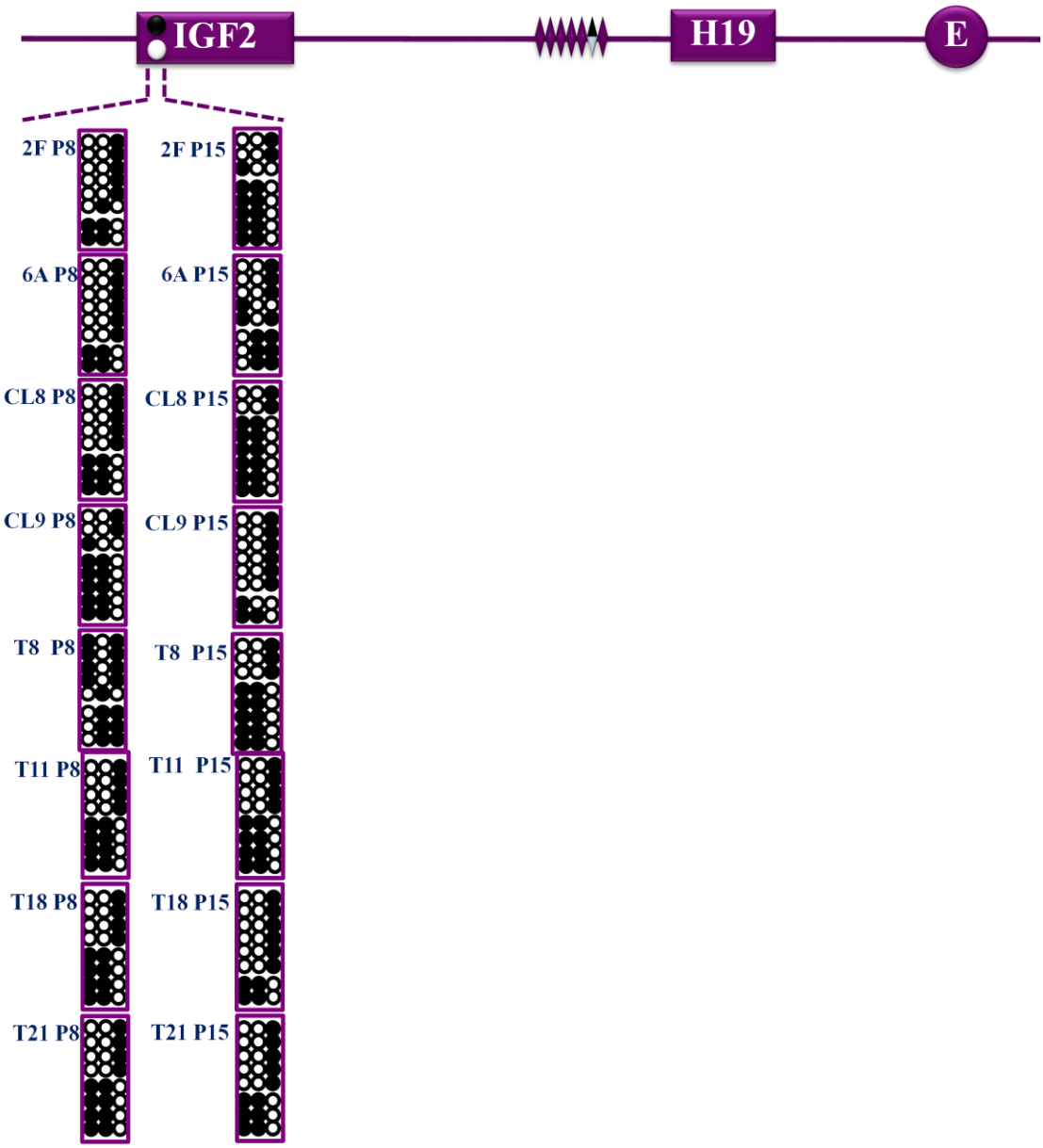

Figure31. Methylation pattern of the DMR of *IGF2*. The methylated CpG is represented by filled circle (●) whereas the unmethylated CpG is represented by blank circle (○). Three CpGs of DMR of *IGF2* showed in square.

The methylation pattern of CpGs in DMR of *IGF2* was shown in pair of P8 and P15 sample by sample (Figure32). This section would interpret the alteration of methylation pattern of CpG in DMR between P8 and P15. For the AFS 2F, the pattern ○○● and ●●○ were found at both passages whereas another methylation pattern was different between P8, ○●○, and P15, ●○○. For the AFS 6A, the pattern ○○● remained in both P8 and P15 whereas the pattern ●●○ at P8 was not found at P15 but there were the pattern ○●●, ●○●, and ●○○ instead. For the AFS T8, all methylation patterns at P8 and P15 were totally different. The pattern ○●●, ●○●, and ○●○ were found at P8 whereas the methylation pattern at P15 was ○○● and ●●○. For the AFS CL8, CL9, T11, T18, and T21, the methylation pattern at P8 was same as the methylation pattern at P15. In AFS CL8, T11, T18, and T21, the pattern ○○● and ●●○ remained in both P8 and P15 whereas the AFS CL9 found the pattern ○○●, ●○○, and ●●○ in both passages.

The comparative of methylation pattern between P8 and P15 showed that the highest frequent pattern was ○○● and ●●○. However, there were gain and loss of methylation in some pattern along *in vitro* culture.

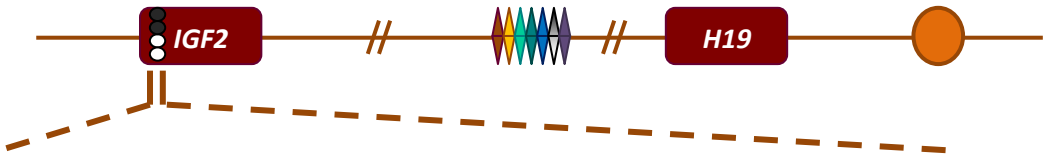

2F P8	○○●	**(5)**	**2F P15**	○○●	**(2)**
	●●○	**(2)**		●●○	**(5)**
	○●○	**(1)**		●○○	**(1)**
6A P8	○○●	**(6)**	**6A P15**	○○●	**(3)**
	●●○	**(2)**		○●●	**(3)**
				●○○	**(2)**
CL8 P8	○○●	**(5)**	**CL8 P15**	○○●	**(2)**
	●●○	**(3)**		●●○	**(6)**
CL9 P8	○○●	**(2)**	**CL9 P15**	○○●	**(6)**
	●●○	**(5)**		●●○	**(1)**
	●○○	**(1)**		●○○	**(1)**
T8 P8	●○●	**(4)**	**T8 P15**	○○●	**(3)**
	○●○	**(1)**		●●○	**(5)**
	○●●	**(3)**			
T11 P8	○○●	**(4)**	**T11 P15**	○○●	**(4)**
	●●○	**(4)**		●●○	**(4)**
T18 P8	○○●	**(4)**	**T18 P15**	○○●	**(6)**
	●●○	**(4)**		●●○	**(2)**
T21 P8	○○●	**(4)**	**T21 P15**	○○●	**(5)**
	●●○	**(4)**		●●○	**(3)**

Figure32. The frequency of particular DNA methylation pattern of interesting CpG site in DMR of *IGF2*

For the consideration of methylation pattern at CpG site by site**,** both methylated pattern and unmethylated pattern could be found at same CpG from the different major methylation patterns. This pattern was called the differentially methylated pattern and represented by black-white circle (◑). The definition of methylation pattern at DMR of *IGF2* in each 2 different passages found that all CpG site of DMR of IGF2 showed differential methylated pattern in both P8 and P15.

Therefore, this region also was DMR in amniotic fluid stem cell.

Sample P8	DMR of *IGF2*			Sample P15	DMR of *IGF2*		
	CpG1	CpG2	CpG3		CpG1	CpG2	CpG3
2F P8	◑	◑	◑	2F P15	◑	◑	◑
6A P8	◑	◑	◑	6A P15	◑	◑	◑
CL8 P8	◑	◑	◑	CL8 P15	◑	◑	◑
CL9 P8	◑	◑	◑	CL9 P15	◑	◑	◑
T8 P8	◑	◑	◑	T8 P15	◑	◑	◑
T11 P8	◑	◑	◑	T11 P15	◑	◑	◑
T18 P8	◑	◑	◑	T18 P15	◑	◑	◑
T21 P8	◑	◑	◑	T21 P15	◑	◑	◑

Table7. Methylation status of each interesting CpG site in DMR of *IGF2* at different passages. The methylation status at each CpG site (each circle) came from the overall methylation pattern from all 8 selected clones in individual samples. The specific CpG site which showed methylation pattern in all 8 selected clones was called hypermethylated CpG site, represented by fully filled circle (●)**.** The specific CpG site which showed both methylation and unmethylation pattern in 8 selected clones was called differential methylated CpG, represented by half filled circle (◑).

CHAPTER V
DISCUSSION

This study explored the DNA methylation pattern at Imprinting Control Region and Differentially Methylated Region in IGF2-H19 imprinting cluster using bisulfite sequencing technique. The methylation pattern of every CpGs at interesting regions including flanking region was defined. For CTCF6 binding region, the major methylation pattern of CpGs around the CTCF6 binding region was outstanding. The unmethylation at second and methylation at first and third of CpGs on the upstream-side of CTCF6 binding region with 2 unmethylated CpGs on the downstream (●○●) NNNNN(○○) was the one major pattern. Another major pattern of flanking region was fully methylation of 3 CpGs on the upstream-side of CTCF6 binding region with 2 methylated CpGs on the downstream (●●●)NNNNN(●●). These 2 major surrounding methylation patterns benefit to distinguish the different methylation pattern in CTCF6 binding region. The exploring of methylation pattern at CTCF6 binding region found that highest frequent methylation pattern (11/16 samples) of CTCF6 binding region was fully methylation (●●●●●) and fully unmethylation (○○○○○). Therefore, the main methylation pattern of this region in amniotic fluid stem cell was (●●●)●●●●●(●●) and (●○●)○○○○○(○○). In theoretically, each samples supposed to show only 2 different methylation patterns because the amniotic fluid stem cell was diploid cell and the *H19* was imprinted gene. However, more than 2 various methylation patterns were found in some samples which might because of the pool of cultured cell population. The unexpecting little mutate cell might include in sample population. Further than the consideration of methylation pattern along allele, the methylation pattern at each CpG site was digested. This pattern was hardly measure in quantitative due to the random error in colony selection process. The unequal between methylation patterns was found in most samples. Therefore, the methylation pattern at each CpG site from all clones was defined as disappearance or appearance only methylation including the combination of both methylated and unmethylated pattern.

The result showed that most samples found both methylated and unmethylated pattern at the same CpG, called differential methylation, except for the 2FP8 at CpG1 and CL8P8 at CpG4 and 5 which found only methylation pattern, called hypermethylation. Therefore, the CTCF6 binding region was DMR in amniotic fluid stem cell

Furthermore, this study compared the methylation pattern at CTCF6 binding region between P8 and P15. This work was inspired from the previous study on the influence of *in vitro* culture to epigenetic of imprinted gene and the previous report of the alteration of imprinting after prolonged culture (at P66 to P76) of human Embryonic Stem Cell (hESC). Therefore, we would like to investigate whether the methylation pattern at CTCF6 binding region has been altered after in vitro culture or not. The study showed that some patterns were remained in both P8 and P15. The pattern (●●●)●●●●●(●●) was found in both passages in almost all sample, except for AFS 2F which found this pattern only at P15. The pattern (●○●)○○○○○(○○) was shown at both passages in AFS T8, T11, T18, and T21. The consideration sample by sample, some patterns was found only at P8 but not at P15 such as pattern (●●●)●○●●○(●●) and (●○●)●●○○○●(○○) in line 2F, pattern (●○●)●○○○○(○○) and (N○○)○○○○○ in line 6A, pattern (●○○)○○○●●(○○) in line CL8, pattern (●●●)●○●●○(●●) and (●○○)○○○○○ in line CL9, pattern (●●●)○○●●○(●●) in line T21. On the other hand, some patterns was found only at P15 such as pattern (●●●)●●●●●(●●) and (●○●)○○○○○(○○) in line 2F, pattern (●○●)○○○○○(○○) and (○○○)○○●○● in line 6A, pattern (●○●)○○○○○(○○) and (○○○)○●●●● in line CL8, pattern (●○●)○○○○○(○○) in line CL9, pattern (●○○)○○○●● and (○○○)○○○○○(○○) in line T18. Therefore, the methylation pattern at CTCF6 binding region got alteration after *in vitro* culture. The methylation pattern at P8 gain more methylation or lost some methylation to become the pattern at P15. The definition of methylation pattern at each CpG site at separate passages showed the hypermethylation pattern of CpG1, 4, and 5 only in some samples (12.5%) at P8 whereas all CpGs at P15 was differentially methylated.

For the study of methylation pattern at DMR of *IGF2*, the methylation status of CpGs in DMR of *IGF2* and surrounding CpGs were determined. Unfortunately, the CpGs on the downstream embedded far apart from the CpG of DMR; the sequencing result was able to define methylation pattern in this region only

in some clones. Therefore, the downstream region was rarely help to distinguish the different methylation of DMR. However, the methylation pattern of CpGs in DMR was outstanding. The major pattern was ○○● and ●●○ in most samples (14/16 samples). In theoretically, each samples supposed to show only 2 different methylation patterns because the amniotic fluid stem cell was diploid cell and the *IGF2* was imprinted gene. However, more than 2 various methylation patterns were found in some samples which might because of the pool of cultured cell population. The consideration at each CpG site showed differential methylation in all samples of all CpG sites. Therefore, the DMR of *IGF2* was differentially methylated region in amniotic fluid stem cell.

In addition, this study compared the methylation pattern at DMR of *IGF2* between P8 and P15. The result showed that some patterns were remained in both P8 and P15. The pattern ○○● and ●●○ was found in both passages in almost all sample, except for 6A which found these patterns only at P8 and T8 which found these patterns only at P15. The consideration sample by sample, some patterns was found only at P8 but not at P15 such as pattern ○●○ in line 2F, pattern ○●○, ○●● and ●○● in line T8. On the other hand, some patterns was found only at P15 such as pattern ●○○ in line 2F, pattern ●○○, ○●● and ●○● in line 6A, pattern ○○● and ●●○ in line T8. Therefore, the methylation pattern at CTCF6 binding region got alteration in some samples after *in vitro* culture. The methylation pattern at P8 gain more methylation or lost some methylation to become the pattern at P15. The definition of methylation pattern at each CpG site at separate passages showed the differential methylation of all samples at all CpG sites in both passages.

The methylation patterns of imprinting regulatory region, both DMR and ICR, in IGF2-H19 imprinting cluster have been intensively studied in many cell types. The next section would discuss the methylation pattern of amniotic fluid stem cell which achieved from this study with the methylation pattern of other related cell types from previous studies region by region. The methylation pattern at CTCF6 binding region showed differential methylation pattern in human embryonic stem cell [115, 116], fetal tissue such as fetal brain, liver, kidney [100], and fetal ureteral tissue [17]. Rugg-Gunn and colleague determined the methylation pattern board region around the CTCF6 binding region in human embryonic stem cell showed the board differential

methylation region (Figure33). The major methylation patterns of this cell were fully methylated pattern, the methylation of all CpG along the same allele, and fully unmethylated pattern, the unmethylation of all CpG along the same allele. The study in fetal brain, kidney and liver of Thanh H Vu and colleague also showed the board differential methylation region (Figure33). The major methylation patterns of this cell were fully methylated pattern and fully unmethylated pattern even though some CpG was frequently found gain of methylation. Daiya and his colleague expanded the methylation determining region cover the CTCF6 binding region in fetal ureteral tissue (Figure33). Their result showed the board differential methylation region, started from 4 CpGs on the upstream of CTCF6 binding region until 10 CpGs on the downstream. The major methylation patterns in this cell were fully methylated pattern and fully unmethylated pattern. The methylation pattern in amniotic fluid stem cell in this study showed similar pattern to those cell types. The CTCF6 binding region and 2 downstream CpGs was differential methylation region whereas 2 of 3 CpG on the upstream of CTCF6 binding region found the loss of imprinting methylation pattern. In the differential methylation region in AFS, the CTCF6 binding region and 2 downstream CpGs, The major methylation pattern were fully methylated and fully unmethylated pattern as same as hESC and fetal tissue.

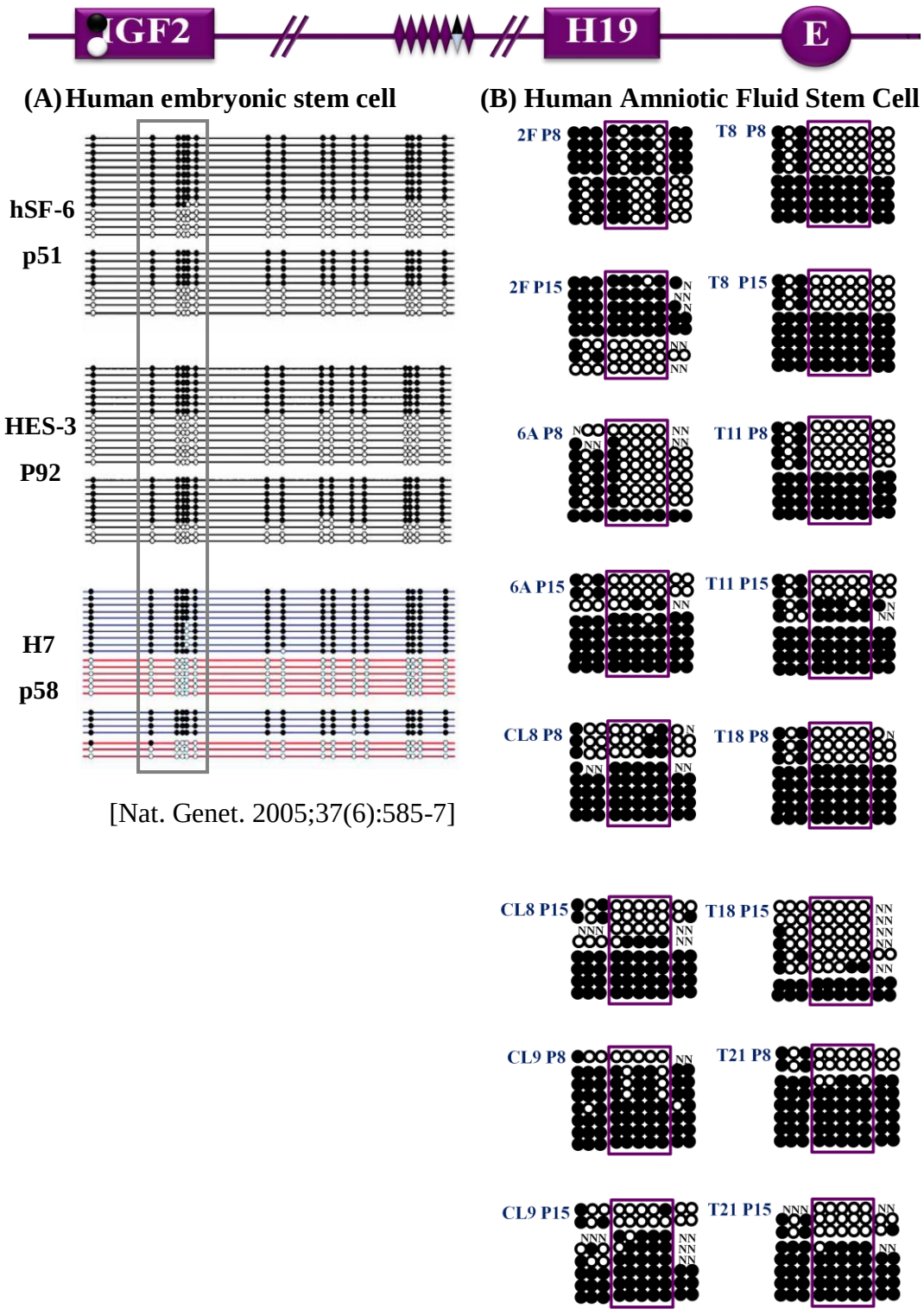

[Nat. Genet. 2005;37(6):585-7]

(C) Fetal Brain, Kidney, Liver

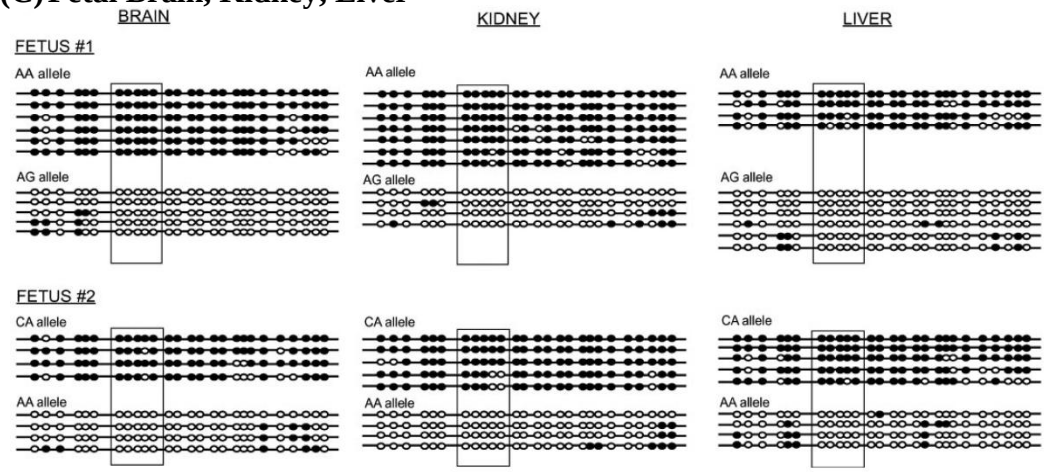

[Genom. 2000;64:132–143]

(D) Human fetal ureteral tissue

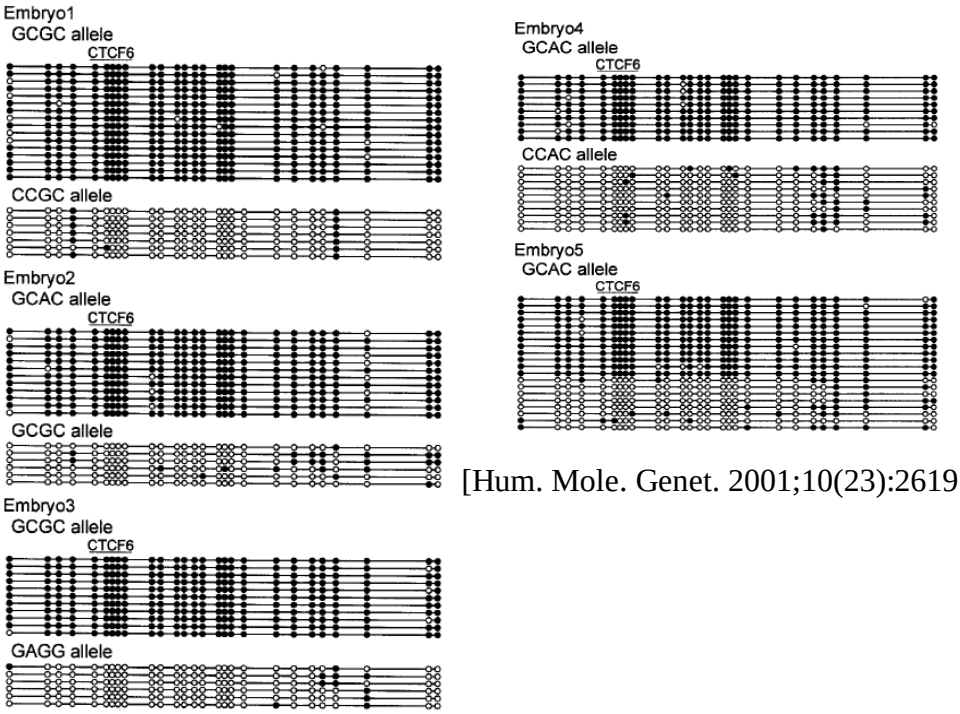

[Hum. Mole. Genet. 2001;10(23):2619-26]

Figure33. Methylation pattern around CTCF6 binding region in various cell types. The methylation status of every CpG around CTCF6 binding region was shown in each clone. The methylated CpGs were represented by black circle (●) whereas the unmethylated CpGs were represented by white circle (○). **(A)** Human embryonic stem cell (hESC) **(B)** Human amniotic fluid stem cell (AFS) **(C)** Fetal brain, kidney, liver **(D)** Fetal ureteral tissue

According to the comparative of methylation pattern between human embryonic stem cell, fetal tissue, and amniotic fluid stem cell (Figure34), most CpGs in CTCF6 binding region were differential methylation pattern which represented by black-white circle (◑). However, the hypermethylation was found in different frequency between human embryonic stem cell, fetal tissue, and amniotic fluid stem cell. In human embryonic stem cell, the hypermethylation could be found at 3 CpGs on the upstream of CTCF6 binding region and CpG2 to 5 in CTCF6 binding region. The frequency of hypermethylation in human embryonic stem cell was different at each CpG site, 3 CpGs on the upstream-side showed 100% hypermethylation (13/13 samples), 23% hypermethylation (3/13 samples), and 7% hypermethylation (1/13 samples), respectively. For the CTCF6 binding site, the hypermethylation was found 53% (7/13 samples) at CpG2, 38% (5/13 samples) at CpG3, 15% (2/13 samples) at CpG4, and 7% (1/13 samples) at CpG5. In amniotic fluid stem cell, the hypermethylation could be found at the first and third of 3 CpGs on the upstream of CTCF6 binding region, the CpG1, 4, and 5 of CTCF6 binding region and 2 CpGs on the downstream. The hypermethylation at first and third on the upstream-side of CTCF6 binding region were 81% (13/16 samples) and 62% (10/16 samples), respectively. For the CpG1, 4, 5 of CTCF6 binding region and the 2 CpGs on the downstream, the hypermethylation was found 7% (1/16 samples). Therefore, though this region showed differential methylation pattern in most CpG however the hypermethylation was also found at some CpG sites. The frequency of hypermethylation was different between human embryonic stem cell and amniotic fluid stem cell.

(A) Human Embryonic Stem Cell

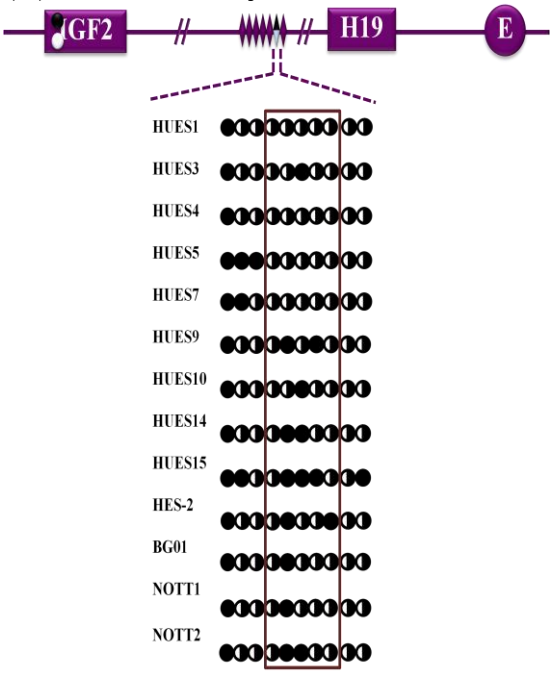

[Genome Res. 2007 17: 1731-1742]

(B) Human embryonic ureteral tissue

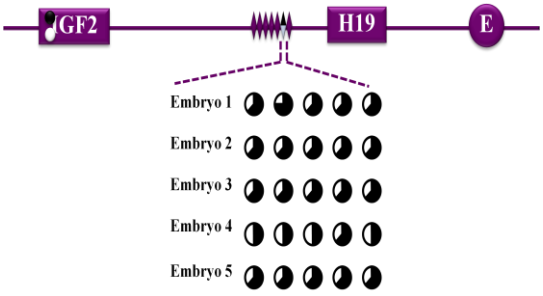

[Hum. Mole. Genet. 2001;10(23):2619-26]

(C) Human Amniotic Fluid Stem Cell

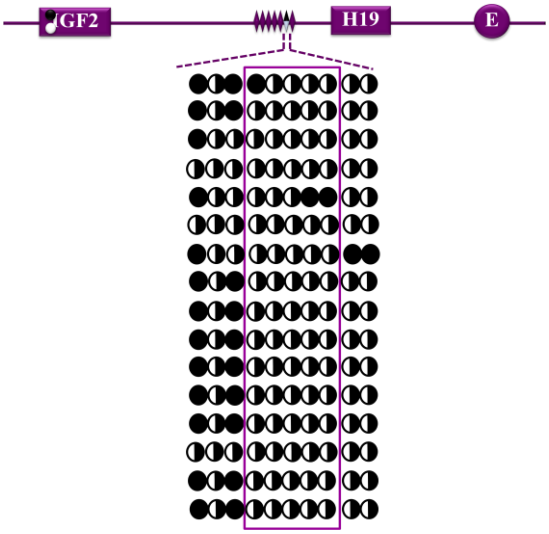

Figure34. The DNA methylation pattern of each CpG site around CTCF6 binding region in various cell types. The methylation pattern at each CpG from all clones in individual sample was analyzed. The CpG position which found both methylated and unmethylated pattern from all clones, called differential methylated CpG, was represented by black-white circle (◑). The CpG position which found only methylated pattern from all clones, called hypermethylated CpG, was represented by black circle (●).

The comparative the methylation pattern between different passages has been reported in some cell. Rugg-Gunn et al. compared the methylation pattern between early and late passages in human embryonic stem cell (Figure35). In his study, the embryonic stem cell approximate to passage100 represented to the late passage because of the high proliferation potential of embryonic stem cell. For this study, the amniotic fluid stem cell at passage15 represented for the late passage because its limited proliferation potential. Even though the amniotic fluid stem cell possessed high proliferation potential to generate stem cell population from single cell at early passage but its proliferation potential was decreased along *in vitro* culture and was limited around passage15.

The study in human embryonic stem cell showed the gain of methylation pattern after prolonged *in vitro* culture, the unmethylated pattern at earlier passage (P55) became more methylation at late passage (P89). For the study in human amniotic fluid stem cell, some pattern remained in both early and late passage such as pattern (●●●)●●●●●(●●) and (●○●)○○○○○(○○) whereas some pattern was found only at P8 or P15 as describe in prior part of discussion. The change of methylation between P8 and P15 could be the gain of methylation or loss of methylation. Therefore, the change of methylation in human amniotic fluid stem cell differed from the change in human embryonic stem cell.

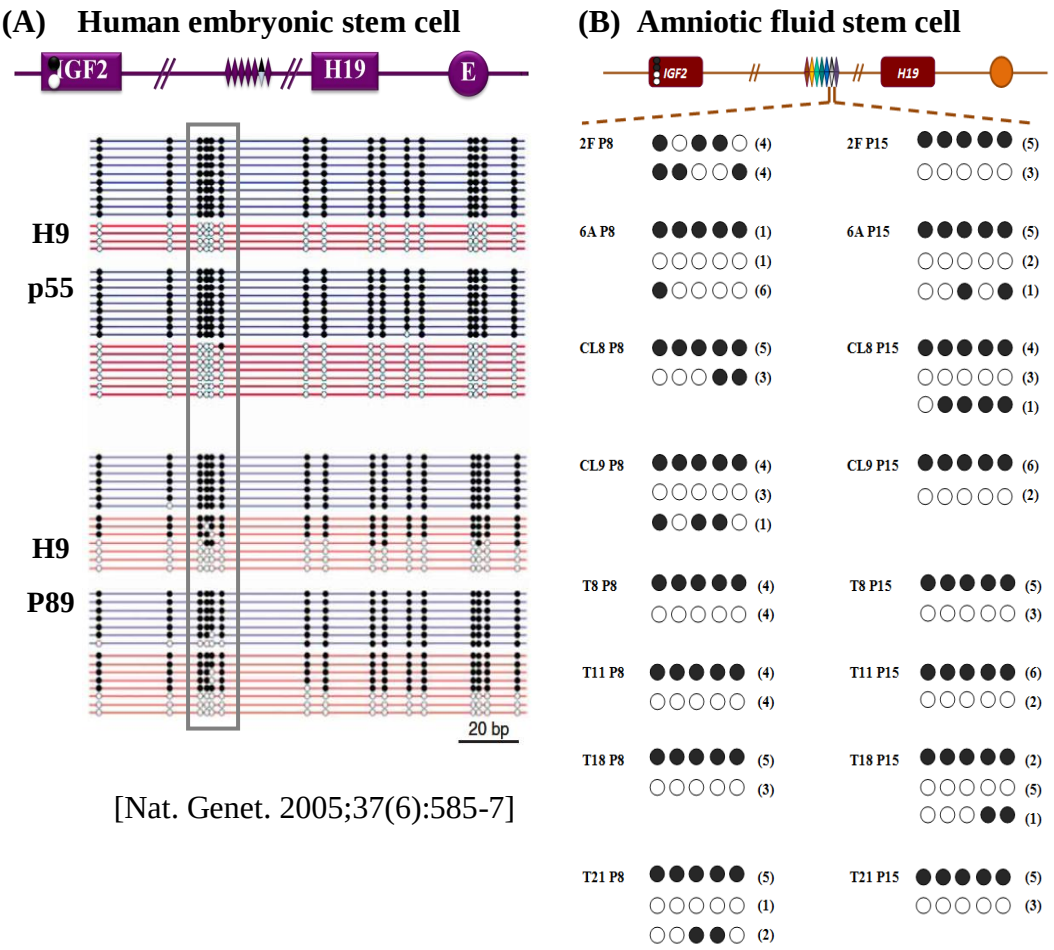

[Nat. Genet. 2005;37(6):585-7]

Figure35. The comparative methylation pattern between different passages in various cell types. (A) Human embryonic stem cell line (B) Amniotic fluid stem cell

For the Differentially Methylated Region (DMR) between exon2 and exon3 of *IGF2*, it was suggested as hot spot for cancer marker [117]. The global demethylation pattern in this region was found in many cancers. DNA methylation in this region was also investigated in ESCs. Kee-Pyo Kim and colleges [116] reported that the DMR of IGF2 was differentially methylated in all ESC lines as same as the methylation pattern in AFS in this study (Figure36).

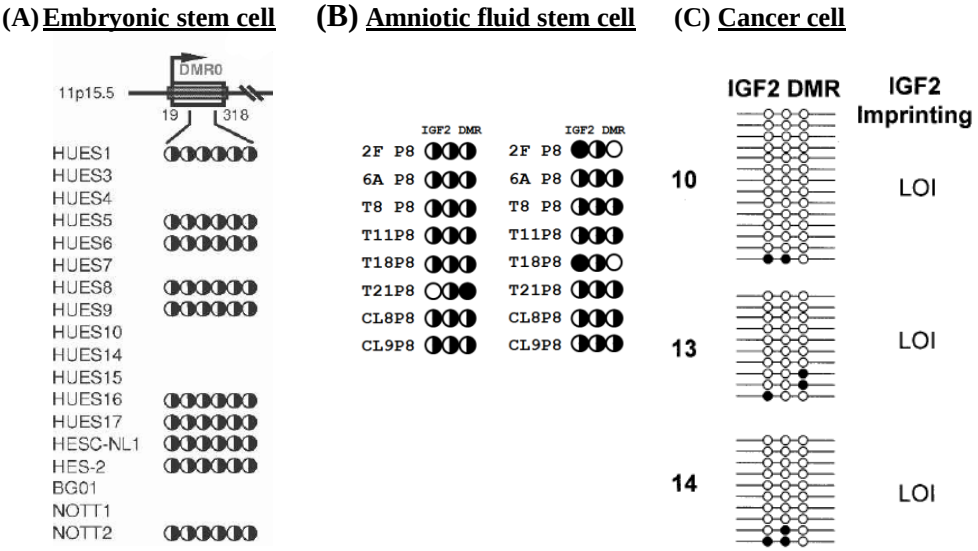

[Genome Res. 2007 17: 1731-1742] [Cancer Res 2002;62:6442–6]

Figure36. The DNA methylation pattern at DMR of IGF2 gene in various cell types. (A) Embryonic stem cell lines (B) Amniotic fluid stem cells (C) Colorectal cancer cells

CHAPTER VI
CONCLUSION

This study define methylation pattern at DMR and ICR in IGF2-H19 imprinting cluster in AFS cells. The DNA methylation pattern is unique characteristic of each gene and each cell types therefore the methylation pattern at the same region but different cell types may appear the different pattern. For the methylation pattern at DMR and ICR in IGF2-H19 imprinting cluster, it was previously defined in various cell types; however, it has never been defined in AFS cells. Therefore, this study is the first report of methylation pattern at these regions in AFS cells.

Sixteen AFS cell samples were represented for AFS cell population. These samples could be categorized into 2 sub-groups according to the different passages. The results showed that the ICR, or CTCF6 binding region, was differentially methylated between 2 parental alleles in most AFS samples. Only 3 of 16 samples showed biallelic methylation at some CpG site in ICR. Therefore, the overall of the DNA methylation pattern at ICR of AFS was differential methylation pattern. Furthermore, the consideration at different passages revealed that 3 AFS samples which found biallelic methylation pattern were AFS at passage8. This statement showed little mutation of methylation pattern during *in vitro* culture process.

For the methylation pattern at DMR of *IGF2*, all 16 AFS samples showed differential methylation pattern. However, this differential methylation pattern was not the same allele specific methylation. Two of 3 CpG sites of *IGF2* DMR were methylated on the same allele whereas one CpG site of *IGF2* DMR was methylated on different allele.

In conclusion, the methylation pattern at ICR of IGF2-H19 imprinting cluster was differential methylation with allelic specificity in AFS cells and it was slightly mutated during *in vitro* culture process. For the methylation pattern at DMR of IGF2 was differential methylation non allelic specificity.

The mutation of methylation pattern at ICR implied to the change of some characteristic, cell proliferation. This methylation pattern might utilize as indicator to determine AFS cell property.

REFERENCES

1. Prusa AR, Marton E, Rosner M, Bernaschek G, Hengstschlager M. Oct-4-expressing cells in human amniotic fluid: a new source for stem cell research? Hum Reprod2003 Jul;18(7):1489-93.
2. Lopez Moratalla N, Gonzalez de la Tajada I. [Human pluripotent stems cells I]. Rev Med Univ Navarra2003 Jul-Sep;47(3):34-42.
3. Trounson A. Human embryonic stem cells: mother of all cell and tissue types. Reprod Biomed Online2002;4 Suppl 1:58-63.
4. Sato M, Nakano T. Embryonic stem cell. Intern Med2001 Mar;40(3):195-200.
5. Itskovitz-Eldor J, Schuldiner M, Karsenti D, Eden A, Yanuka O, Amit M, et al. Differentiation of human embryonic stem cells into embryoid bodies compromising the three embryonic germ layers. Mol Med2000 Feb;6(2):88-95.
6. Waite L, Nindl G. Human embryonic stem cell research: an ethical controversy in the US & Germany. Biomed Sci Instrum2003;39:567-72.
7. Chambers I, Smith A. Self-renewal of teratocarcinoma and embryonic stem cells. Oncogene2004 Sep 20;23(43):7150-60.
8. Moe MC, Varghese M, Danilov AI, Westerlund U, Ramm-Pettersen J, Brundin L, et al. Multipotent progenitor cells from the adult human brain: neurophysiological differentiation to mature neurons. Brain2005 Sep;128(Pt 9):2189-99.
9. Murrell W, Feron F, Wetzig A, Cameron N, Splatt K, Bellette B, et al. Multipotent stem cells from adult olfactory mucosa. Dev Dyn2005 Jun;233(2):496-515.
10. Rodriguez AM, Elabd C, Amri EZ, Ailhaud G, Dani C. The human adipose tissue is a source of multipotent stem cells. Biochimie2005 Jan;87(1):125-8.

11. Perin L, Giuliani S, Jin D, Sedrakyan S, Carraro G, Habibian R, et al. Renal differentiation of amniotic fluid stem cells. Cell Prolif2007 Dec;40(6):936-48.
12. De Coppi P, Bartsch G, Jr., Siddiqui MM, Xu T, Santos CC, Perin L, et al. Isolation of amniotic stem cell lines with potential for therapy. Nat Biotechnol2007 Jan;25(1):100-6.
13. Burns JL, Hassan AB. Cell survival and proliferation are modified by insulin-like growth factor 2 between days 9 and 10 of mouse gestation. Development2001 Oct;128(19):3819-30.
14. Joyce JA, Schofield PN. Genomic imprinting and cancer. Mol Pathol1998 Aug;51(4):185-90.
15. Hartmann W, Koch A, Brune H, Waha A, Schuller U, Dani I, et al. Insulin-like growth factor II is involved in the proliferation control of medulloblastoma and its cerebellar precursor cells. Am J Pathol2005 Apr;166(4):1153-62.
16. Kim NH, Lee CH, Lee AY. H19 RNA downregulation stimulated melanogenesis in melasma. Pigment Cell Melanoma Res Feb;23(1):84-92.
17. Takai D, Gonzales FA, Tsai YC, Thayer MJ, Jones PA. Large scale mapping of methylcytosines in CTCF-binding sites in the human H19 promoter and aberrant hypomethylation in human bladder cancer. Hum Mol Genet2001 Nov 1;10(23):2619-26.
18. Gardner RL. Stem cells: potency, plasticity and public perception. J Anat2002 Mar;200(Pt 3):277-82.
19. Alison MR, Poulsom R, Forbes S, Wright NA. An introduction to stem cells. J Pathol2002 Jul;197(4):419-23.
20. Verfaillie CM, Pera MF, Lansdorp PM. Stem cells: hype and reality. Hematology Am Soc Hematol Educ Program2002:369-91.
21. Liu S, Dontu G, Wicha MS. Mammary stem cells, self-renewal pathways, and carcinogenesis. Breast Cancer Res2005;7(3):86-95.
22. Roman-Trufero M, Mendez-Gomez HR, Perez C, Hijikata A, Fujimura Y, Endo T, et al. Maintenance of undifferentiated state and self-renewal of embryonic neural stem cells by Polycomb protein Ring1B. Stem Cells2009 Jul;27(7):1559-70.

23. Khurdayan VK. Stem cells: therapeutic present and future. Timely Top Med Cardiovasc Dis2007;11:E14.
24. Pruszak J, Ludwig W, Blak A, Alavian K, Isacson O. CD15, CD24, and CD29 define a surface biomarker code for neural lineage differentiation of stem cells. Stem Cells2009 Dec;27(12):2928-40.
25. Islam MS, Tatsumi K, Okuda H, Shiosaka S, Wanaka A. Olig2-expressing progenitor cells preferentially differentiate into oligodendrocytes in cuprizone-induced demyelinated lesions. Neurochem Int2009 Mar-Apr;54(3-4):192-8.
26. Suter DM, Tirefort D, Julien S, Krause KH. A Sox1 to Pax6 switch drives neuroectoderm to radial glia progression during differentiation of mouse embryonic stem cells. Stem Cells2009 Jan;27(1):49-58.
27. Peh GS, Lang RJ, Pera MF, Hawes SM. CD133 expression by neural progenitors derived from human embryonic stem cells and its use for their prospective isolation. Stem Cells Dev2009 Mar;18(2):269-82.
28. Imamura O, Satoh Y, Endo S, Takishima K. Analysis of extracellular signal-regulated kinase 2 function in neural stem/progenitor cells via nervous system-specific gene disruption. Stem Cells2008 Dec;26(12):3247-56.
29. Hari L, Brault V, Kleber M, Lee HY, Ille F, Leimeroth R, et al. Lineage-specific requirements of beta-catenin in neural crest development. J Cell Biol2002 Dec 9;159(5):867-80.
30. Corley LS, Lavine MD. A review of insect stem cell types. Semin Cell Dev Biol2006 Aug;17(4):510-7.
31. Thomson JA, Itskovitz-Eldor J, Shapiro SS, Waknitz MA, Swiergiel JJ, Marshall VS, et al. Embryonic stem cell lines derived from human blastocysts. Science1998 Nov 6;282(5391):1145-7.
32. Germain D. [Induced pluripotent stem cells (iPS cells)]. Pathol Biol (Paris)2009 Nov-Dec;57(7-8):555-9.
33. Kim JB, Sebastiano V, Wu G, Arauzo-Bravo MJ, Sasse P, Gentile L, et al. Oct4-induced pluripotency in adult neural stem cells. Cell2009 Feb 6;136(3):411-9.

34. Snyder EY, Macklis JD. Multipotent neural progenitor or stem-like cells may be uniquely suited for therapy for some neurodegenerative conditions. Clin Neurosci1995;3(5):310-6.
35. Anderson DJ. Stem cells and transcription factors in the development of the mammalian neural crest. FASEB J1994 Jul;8(10):707-13.
36. Hoang T. The origin of hematopoietic cell type diversity. Oncogene2004 Sep 20;23(43):7188-98.
37. Hirschi KK, Goodell MA. Hematopoietic, vascular and cardiac fates of bone marrow-derived stem cells. Gene Ther2002 May;9(10):648-52.
38. Sukhikh GT, Malaitsev VV, Bogdanova IM, Dubrovina IV. Mesenchymal stem cells. Bull Exp Biol Med2002 Feb;133(2):103-9.
39. Shostak S. (Re)defining stem cells. Bioessays2006 Mar;28(3):301-8.
40. Wu DC, Boyd AS, Wood KJ. Embryonic stem cell transplantation: potential applicability in cell replacement therapy and regenerative medicine. Front Biosci2007;12:4525-35.
41. Sylvester KG, Longaker MT. Stem cells: review and update. Arch Surg2004 Jan;139(1):93-9.
42. Villa A, Snyder EY, Vescovi A, Martinez-Serrano A. Establishment and properties of a growth factor-dependent, perpetual neural stem cell line from the human CNS. Exp Neurol2000 Jan;161(1):67-84.
43. Hutton JF, D'Andrea RJ, Lewis ID. Potential for clinical ex vivo expansion of cord blood haemopoietic stem cells using non-haemopoietic factor supplements. Curr Stem Cell Res Ther2007 Sep;2(3):229-37.
44. Brown JA, Boussiotis VA. Umbilical cord blood transplantation: basic biology and clinical challenges to immune reconstitution. Clin Immunol2008 Jun;127(3):286-97.
45. Presnell SC, Petersen B, Heidaran M. Stem cells in adult tissues. Semin Cell Dev Biol2002 Oct;13(5):369-76.
46. Schubeler D, Lorincz MC, Cimbora DM, Telling A, Feng YQ, Bouhassira EE, et al. Genomic targeting of methylated DNA: influence of methylation on transcription, replication, chromatin structure, and histone acetylation. Mol Cell Biol2000 Dec;20(24):9103-12.

47. Lei H, Oh SP, Okano M, Juttermann R, Goss KA, Jaenisch R, et al. De novo DNA cytosine methyltransferase activities in mouse embryonic stem cells. Development1996 Oct;122(10):3195-205.

48. Li E, Bestor TH, Jaenisch R. Targeted mutation of the DNA methyltransferase gene results in embryonic lethality. Cell1992 Jun 12;69(6):915-26.

49. Vertino PM, Sekowski, J.A., Coll, J.M., Applegren, N., Han, S., Hickey,R.J. & Malkas, L.H. DNMT1 is a Component of a Multiprotein DNA Replication Complex. Cell Cycle2002;1:416-23.

50. Fuks F, Burgers WA, Brehm A, Hughes-Davies L, Kouzarides T. DNA methyltransferase Dnmt1 associates with histone deacetylase activity. Nat Genet2000 Jan;24(1):88-91.

51. Robertson KD, Ait-Si-Ali S, Yokochi T, Wade PA, Jones PL, Wolffe AP. DNMT1 forms a complex with Rb, E2F1 and HDAC1 and represses transcription from E2F-responsive promoters. Nat Genet2000 Jul;25(3):338-42.

52. Rountree MR, Bachman KE, Baylin SB. DNMT1 binds HDAC2 and a new co-repressor, DMAP1, to form a complex at replication foci. Nat Genet2000 Jul;25(3):269-77.

53. Lyko F, Ramsahoye BH, Kashevsky H, Tudor M, Mastrangelo MA, Orr-Weaver TL, et al. Mammalian (cytosine-5) methyltransferases cause genomic DNA methylation and lethality in Drosophila. Nat Genet1999 Nov;23(3):363-6.

54. Okano M, Bell DW, Haber DA, Li E. DNA methyltransferases Dnmt3a and Dnmt3b are essential for de novo methylation and mammalian development. Cell1999 Oct 29;99(3):247-57.

55. Xie S, Wang Z, Okano M, Nogami M, Li Y, He WW, et al. Cloning, expression and chromosome locations of the human DNMT3 gene family. Gene1999 Aug 5;236(1):87-95.

56. Robertson KD, Uzvolgyi E, Liang G, Talmadge C, Sumegi J, Gonzales FA, et al. The human DNA methyltransferases (DNMTs) 1, 3a and 3b: coordinate mRNA expression in normal tissues and overexpression in tumors. Nucleic Acids Res1999 Jun 1;27(11):2291-8.

57. Dong A, Yoder JA, Zhang X, Zhou L, Bestor TH, Cheng X. Structure of human DNMT2, an enigmatic DNA methyltransferase homolog that displays denaturant-resistant binding to DNA. Nucleic Acids Res2001 Jan 15;29(2):439-48.

58. Okano M, Xie, S. & Li, E. Dnmt2 is not required for de novo and maintenance methylation of viral DNA in embryonic stem cells. *Nucleic Acids Res*1998;26:2536-40.

59. Bourc'his D, Xu GL, Lin CS, Bollman B, Bestor TH. Dnmt3L and the establishment of maternal genomic imprints. Science2001 Dec 21;294(5551):2536-9.

60. Hark ATT, S.M. Chromatin conformation of the H19 epigenetic mark. *Hum Mol Genet*1998;7:1979-85.

61. Aapola U, Liiv, I. & Peterson, P. Imprinting regulator DNMT3L is a transcriptional repressor associated with histone deacetylase activity. *Nucleic Acids Res*2002;30:3602-8.

62. Suzuki MM BA. DNA methylation landscapes: provocative insights from epigenomics. Nat Rev Genet2008;9:465-76.

63. Costello JF PC. Methylation matters. J Med Genet2001;38:285-303.

64. Cross SH BA. CpG islands and genes. Curr Opin Genet Dev1995;5:309-14.

65. Klose RJ BA. Genomic DNA methylation: the mark and its mediators. Trends Biochem Sci2006;31:89-97.

66. Larsen F GG, Lopez R, Prydz H. CpG islands as gene markers in the human genome. Genomics1992;13:1095-107.

67. Takai D JP. Comprehensive analysis of CpG islands in human chromosomes 21 and 22. Proc Natl Acad Sci U S A2002;99:3740-5.

68. Noyer-Weidner M, and T. A. TRAUTNER. Methylation of DNA in prokaryotes. EXS1993;64:39-108.

69. BOYES J, and A. BIRD. DNA methylation inhibits transcription indirectly via a methyl-CpG binding protein. Cell1991;64:1123-34.

70. Compere SJ, and R. D. Palmiter. DNA methylation controls the inducibility of the mouse metallothionein-I gene lymphoid cells. Cell1981;25:233-40.

71. Kass SU, N. Landsberger and A. P. Woffe. DNA methylation directs a timedependent repression of transcription initiation. Curr Biol1997;7:157-65.

72. Siegfried Z, S. Eden, M. Mendelsohn, X. Feng, B. Z. Tsuberi *et al*. DNA methylation represses transcription in vivo. Nat Genet1999;22:203-6.

73. Li E, T. H. Bestor and R. Jaenisch. Targeted mutation of the DNA methyltransferase gene results in embryonic lethality. Cell1992;69:915-26.

74. Okano M, D. W. Bell, D. A. Haber and E. Li. NA methyltransferases Dnmt3a and Dnmt3b are essential for de novo methylation and mammalian development. Cell1999;99:247-57.

75. Cooper DN, and H. Youssoufian. The CpG dinucleotide and human genetic disease. Hum Genet1988;78:151-5.

76. Rideout, 3RD, G. A. Coetzee, A. F. Olumi and P. A. Jones. 5-Methylcytosine as an endogenous mutagen in the human LDL receptor and p53 genes. Science1990;**249**:1288-90.

77. Jones PA, and P. W. Laird. Cancer epigenetics comes of age. Nat Genet1999;21:163-7.

78. Oshiro MM, C. J. Kim, R. J. Wozniak, D. J. Junk, J. L. Munoz-Rodriguez *et al.* Epigenetic silencing of DSC3 is a common event in human breast cancer. Breast Cancer Res Treat2005;7:R669-80.

79. Okano M, D. W. Bell, D. A. Haber and E. Li. DNA methyltransferases Dnmt3a and Dnmt3b are essential for de novo methylation and mammalian development. Cell1999;99:247-57.

80. Xu GL, T. H. Bestor, D. Bourc'His, C. L. Hsieh, N. Tommerup *et al.* Chromosome instability and immunodeficiency syndrome caused by mutations in a DNA methyltransferase gene. Nature1999;402:187-91.

81. Amir RE, I. B. Van Den Veyver, M. Wan, C. Q. Tran, U. Francke *et al.* Rett syndrome is caused by mutations in X-linked MECP2, encoding methyl-CpGbinding protein 2. Nat Genet1999;23:185-8.

82. Li E, Beard C, Jaenisch R. Role for DNA methylation in genomic imprinting. Nature1993 Nov 25;366(6453):362-5.

83. Li E, Beard C, Forster AC, Bestor TH, Jaenisch R. DNA methylation, genomic imprinting, and mammalian development. Cold Spring Harb Symp Quant Biol1993;58:297-305.

84. Lewis A, Mitsuya K, Umlauf D, Smith P, Dean W, Walter J, et al. Imprinting on distal chromosome 7 in the placenta involves repressive histone methylation independent of DNA methylation. Nat Genet2004 Dec;36(12):1291-5.

85. Tanaka M, Puchyr M, Gertsenstein M, Harpal K, Jaenisch R, Rossant J, et al. Parental origin-specific expression of Mash2 is established at the time of implantation with its imprinting mechanism highly resistant to genome-wide demethylation. Mech Dev1999 Sep;87(1-2):129-42.

86. Cheng YW, Idrees K, Shattock R, Khan SA, Zeng Z, Brennan CW, et al. Loss of imprinting and marked gene elevation are 2 forms of aberrant IGF2 expression in colorectal cancer. Int J Cancer Aug 1;127(3):568-77.

87. Zhao R, DeCoteau JF, Geyer CR, Gao M, Cui H, Casson AG. Loss of imprinting of the insulin-like growth factor II (IGF2) gene in esophageal normal and adenocarcinoma tissues. Carcinogenesis2009 Dec;30(12):2117-22.

88. Martin-Trujillo A, van Rietschoten JG, Timmer TC, Rodriguez FM, Huizinga TW, Tak PP, et al. Loss of imprinting of IGF2 characterises high IGF2 mRNA-expressing type of fibroblast-like synoviocytes in rheumatoid arthritis. Ann Rheum Dis Jun;69(6):1239-42.

89. Wang Y, Li GW, Wen BG. [Loss of IGF2 imprinting in colorectal cancer]. Sheng Li Ke Xue Jin Zhan2005 Jan;36(1):71-3.

90. Wrzeska M, Rejduch B. Genomic imprinting in mammals. J Appl Genet2004;45(4):427-33.

91. Biliya S, Bulla LA, Jr. Genomic imprinting: the influence of differential methylation in the two sexes. Exp Biol Med (Maywood) Feb;235(2):139-47.

92. Holmes R, Soloway PD. Regulation of imprinted DNA methylation. Cytogenet Genome Res2006;113(1-4):122-9.

93. Yang T, Adamson TE, Resnick JL, Leff S, Wevrick R, Francke U, et al. A mouse model for Prader-Willi syndrome imprinting-centre mutations. Nat Genet1998 May;19(1):25-31.

94. Fitzpatrick GV, Soloway PD, Higgins MJ. Regional loss of imprinting and growth deficiency in mice with a targeted deletion of KvDMR1. Nat Genet2002 Nov;32(3):426-31.

95. Wutz A, Barlow DP. Imprinting of the mouse Igf2r gene depends on an intronic CpG island. Mol Cell Endocrinol1998 May 25;140(1-2):9-14.

96. Kim J, Kim JD. In vivo YY1 knockdown effects on genomic imprinting. Hum Mol Genet2008 Feb 1;17(3):391-401.

97. Kobayashi H, Suda C, Abe T, Kohara Y, Ikemura T, Sasaki H. Bisulfite sequencing and dinucleotide content analysis of 15 imprinted mouse differentially methylated regions (DMRs): paternally methylated DMRs contain less CpGs than maternally methylated DMRs. Cytogenet Genome Res2006;113(1-4):130-7.

98. Lopes S, Lewis A, Hajkova P, Dean W, Oswald J, Forne T, et al. Epigenetic modifications in an imprinting cluster are controlled by a hierarchy of DMRs suggesting long-range chromatin interactions. Hum Mol Genet2003 Feb 1;12(3):295-305.

99. Reik W, Dean W, Walter J. Epigenetic reprogramming in mammalian development. Science2001 Aug 10;293(5532):1089-93.

100. Vu TH, Li T, Nguyen D, Nguyen BT, Yao XM, Hu JF, et al. Symmetric and asymmetric DNA methylation in the human IGF2-H19 imprinted region. Genomics2000 Mar 1;64(2):132-43.

101. Aquino NH, Bastos E, Fonseca LC, Llerena JC, Jr. Angelman syndrome methylation screening of 15q11-q13 in institutionalized individuals with severe mental retardation. Genet Test2002 Summer;6(2):129-31.

102. Bourque DK, Penaherrera MS, Yuen RK, Van Allen MI, McFadden DE, Robinson WP. The utility of quantitative methylation assays at imprinted genes for the diagnosis of fetal and placental disorders. Clin Genet Apr 8.

103. Kagami M, Nagai T, Fukami M, Yamazawa K, Ogata T. Silver-Russell syndrome in a girl born after in vitro fertilization: partial hypermethylation

at the differentially methylated region of PEG1/MEST. J Assist Reprod Genet2007 Apr;24(4):131-6.

104. Ferguson-Smith AC, Cattanach BM, Barton SC, Beechey CV, Surani MA. Embryological and molecular investigations of parental imprinting on mouse chromosome 7. Nature1991 Jun 20;351(6328):667-70.
105. Fundele RH, Norris ML, Barton SC, Fehlau M, Howlett SK, Mills WE, et al. Temporal and spatial selection against parthenogenetic cells during development of fetal chimeras. Development1990 Jan;108(1):203-11.
106. Mann JR, Gadi I, Harbison ML, Abbondanzo SJ, Stewart CL. Androgenetic mouse embryonic stem cells are pluripotent and cause skeletal defects in chimeras: implications for genetic imprinting. Cell1990 Jul 27;62(2):251-60.
107. Bartolomei MS, Tilghman SM. Genomic imprinting in mammals. Annu Rev Genet1997;31:493-525.
108. Moore T, Haig D. Genomic imprinting in mammalian development: a parental tug-of-war. Trends Genet1991 Feb;7(2):45-9.
109. Chao W, D'Amore PA. IGF2: epigenetic regulation and role in development and disease. Cytokine Growth Factor Rev2008 Apr;19(2):111-20.
110. Cai X, Cullen BR. The imprinted H19 noncoding RNA is a primary microRNA precursor. RNA2007 Mar;13(3):313-6.
111. Gary A.U. YY, Ji-Fan H., et al. CTCF Binding at the Insulin-Like Growth Factor-II (IGF2)/H19 Imprinting Control Region Is Insufficient to Regulate IGF2/H19 Expression in Human Tissues. Endocrinology2003;144(10):4420–6.
112. Byun HM, Wong HL, Birnstein EA, Wolff EM, Liang G, Yang AS. Examination of IGF2 and H19 loss of imprinting in bladder cancer. Cancer Res2007 Nov 15;67(22):10753-8.
113. Murphy SK, Huang Z, Wen Y, Spillman MA, Whitaker RS, Simel LR, et al. Frequent IGF2/H19 domain epigenetic alterations and elevated IGF2 expression in epithelial ovarian cancer. Mol Cancer Res2006 Apr;4(4):283-92.

114. Suzuki J, Jr., Therrien J, Filion F, Lefebvre R, Goff AK, Smith LC. In vitro culture and somatic cell nuclear transfer affect imprinting of SNRPN gene in pre- and post-implantation stages of development in cattle. BMC Dev Biol2009;9:9.
115. Peter J Rugg-Gunn ACF-S, Roger A Pedersen. Epigenetic status of human embryonic stem cells. Nat Genet2005;37(6):585-7.
116. Kim KP, Thurston A, Mummery C, Ward-van Oostwaard D, Priddle H, Allegrucci C, et al. Gene-specific vulnerability to imprinting variability in human embryonic stem cell lines. Genome Res2007 Dec;17(12):1731-42.
117. Cui H, Onyango P, Brandenburg S, Wu Y, Hsieh CL, Feinberg AP. Loss of imprinting in colorectal cancer linked to hypomethylation of H19 and IGF2. Cancer Res2002 Nov 15;62(22):6442-6.

APPENDICES

APPENDIX A
REAGENT PREPARATION

1) Phosphate buffer saline (PBS^-)

1. Mixed solution as followed

NaCl	10 g
KCl	0.2500 g
Na_2HPO_4	1.4400 g
KH_2PO_4	0.2500 g
Ultra pure water up to	1 L
Total volume	1 L

2. Autoclaved at 120^{o}C under high pressure condition for 30 minutes

2) Homogenize buffer

1. Mixed solution as followed

NaCl	1.461 g
Sucrose	17.115 g
EDTA	0.9305 g
Tris base (pH 8.0)	9.0825 g
Ultra pure water up to	250 mL
Total volume	250 mL

2. Autoclave at 120^{o}C under high pressure condition for 30 minutes

3) 10% Sodiumdodecylsulfate (10%SDS)

1. Added 50 mL ultra pure water to 10 g of SDS (Lauryl sulfate)
2. Stirred at 37^{o}C until the solution turned to be clear.
3. Adjusted volume by adding ultra pure water up to 100 mL.
4. Shaked solution at 56^{o}C for 1 hour.
5. Filter through 0.22 µm (Corning)

4) 8M Potassium acetate

1. Mixed solution as followed

$KC_2H_3O_2$	39.257 g
Ultra pure water up to	100 mL
Total volume	100 mL

2. Autoclave at 120^{o}C under high pressure condition for 30 minutes

5) Phenol

1. Melt Phenol crystal at 65^{o}C for one hour
2. Added 0.25 g of 8-Hydroxyquinaline to the solution and
3. Added 1 volume (~250 mL) of 1M Tris HCl pH8 and shaked for 15 minutes
4. Let stand at room temperature until the phenol phase (lower phase) became transparent, then, removed the upper phase
5. Added another 1 volume of 1M Tris HCl pH8 and shaked for 15 minutes
6. Let stand at 4^{o}C overnight
7. Removed the upper phase
8. Added 1 volume of 0.1M Tris HCl pH8 and shaked for 15 minutes

6) TBE (Stock 5x)

1. Mixed the solution as followed

Trizma base	54.00 g
Orthoboric acid	27.50 g
EDTA	3.72 g
Ultra pure water up to	1 L
Total volume	1 L

7) RF1 solution

1. Mixed the solution as followed

$KC_2H_3O_2$(30 mM)	1.47 g
$CaCl_2$-2H_2O (10 mM)	0.75 g
Glycerol (15% w/v)	75 g
Ultra pure water up to	450 mL
Total volume	450 mL

2. Adjusted pH to 5.92 with 0.2 M acetic acid
3. Added

RbCl (100 mM)	6 g
$MnCl_2$-$4H_2O$ (50 mM)	4.59 g

4. Adjusted volume up to 500 mL
5. Filtrated through 0.2 µm filter

8) RF2 solution

1. Mixed solution as followed

RbCl (10 mM)	0.6 g
$CaCl_2$-$2H_2O$ (75 mM)	5.5 g
MOPS (10 mM)	1.05 g
Glycerol (15% w/v)	75 g
Ultra pure water up to	500 mL
Total volume	500 mL

2. Adjusted pH to 6.8 with NaOH
3. Filtrated through 0.2 µm filter

9) LB broth

1. Mixed solution as followed

Yeast extract	5 g
Tryptone powder	10 g
NaCl	5 g
Ultra pure water up to	1 L
Total volume	1 L

2. Autoclave at 120^{o}C under high pressure condition for 30 minutes

APPENDIX B:
SEQUENCING RESULT

1. 2F P8 H19

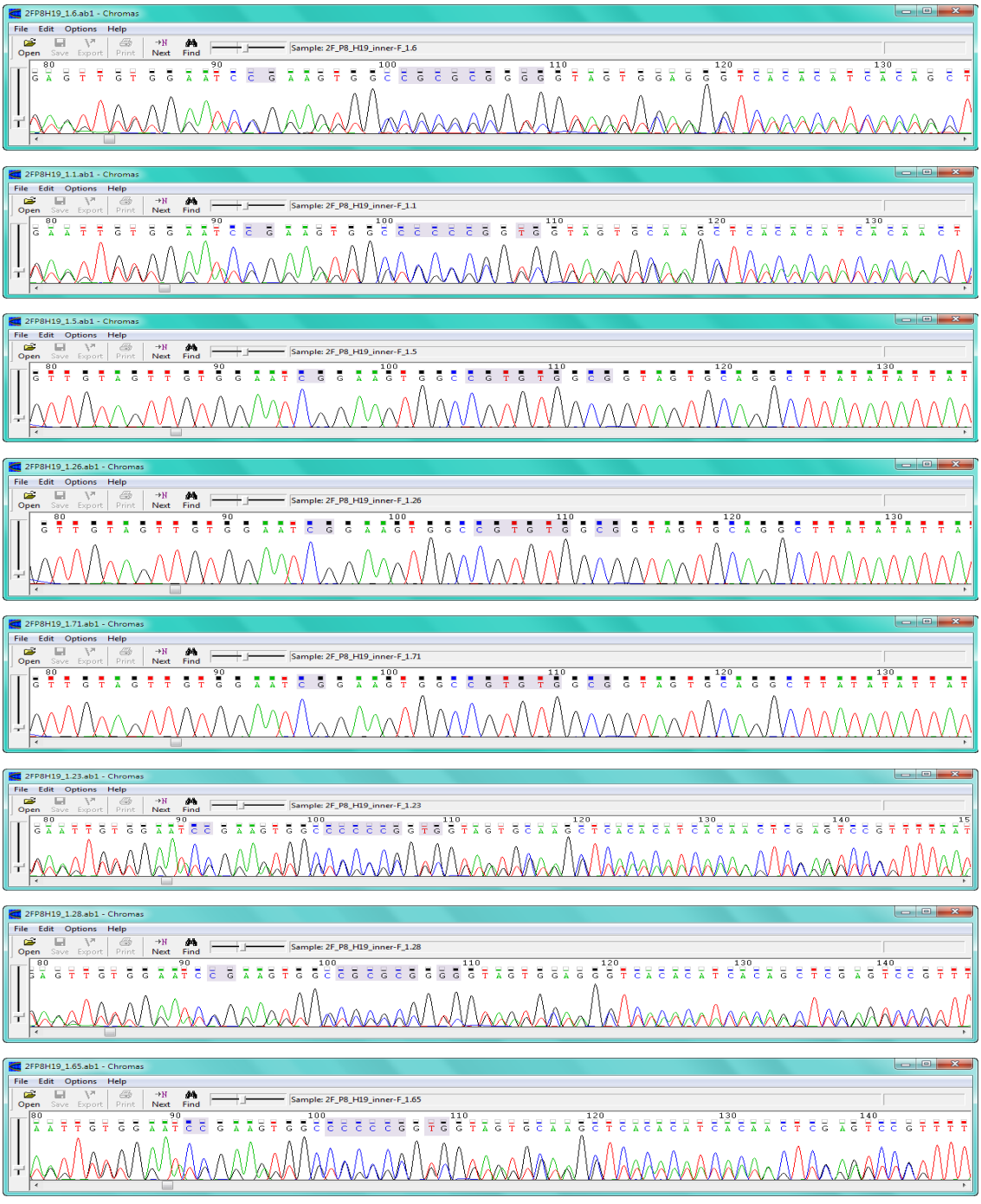

2. 2F P15 H19

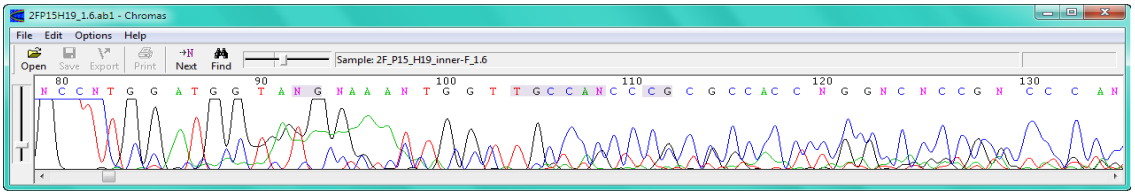
2FP15H19_1.6.ab1 - Chromas
Sample: 2F_P15_H19_inner-F_1.6

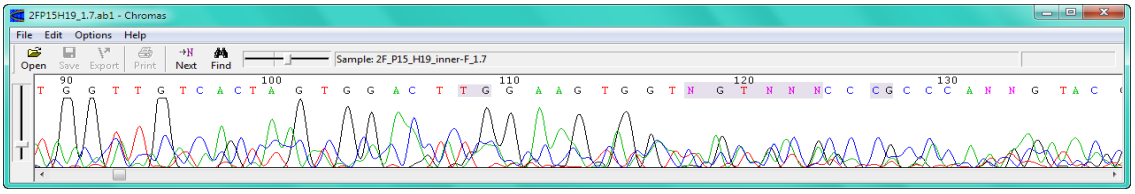
2FP15H19_1.7.ab1 - Chromas
Sample: 2F_P15_H19_inner-F_1.7

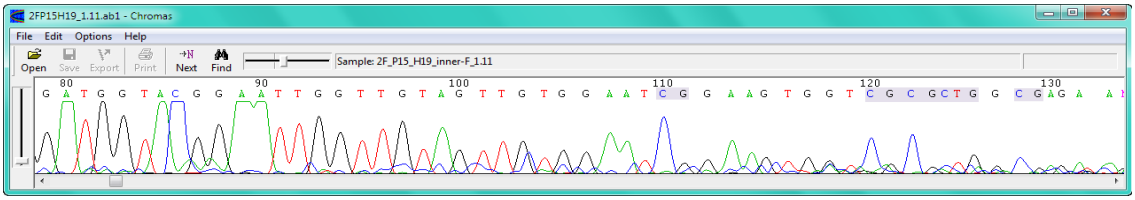
2FP15H19_1.11.ab1 - Chromas
Sample: 2F_P15_H19_inner-F_1.11

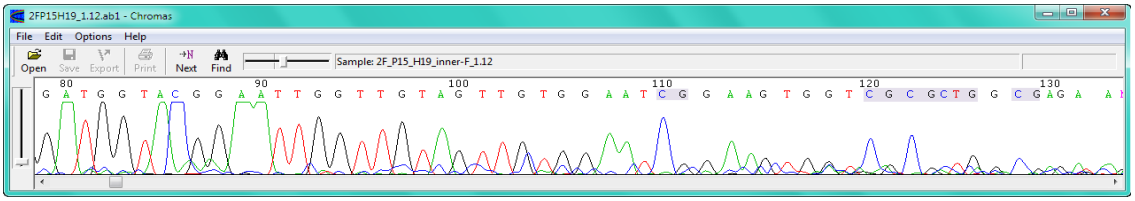
2FP15H19_1.12.ab1 - Chromas
Sample: 2F_P15_H19_inner-F_1.12

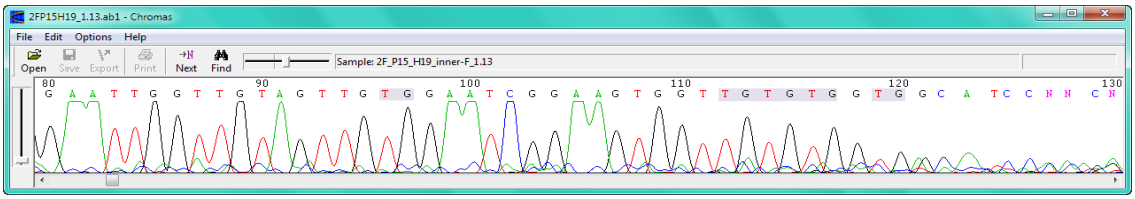
2FP15H19_1.13.ab1 - Chromas
Sample: 2F_P15_H19_inner-F_1.13

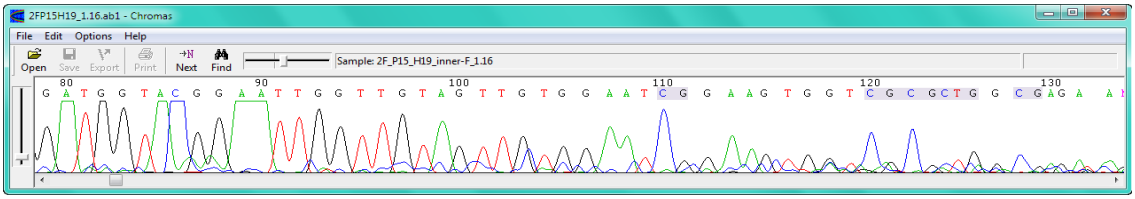
2FP15H19_1.16.ab1 - Chromas
Sample: 2F_P15_H19_inner-F_1.16

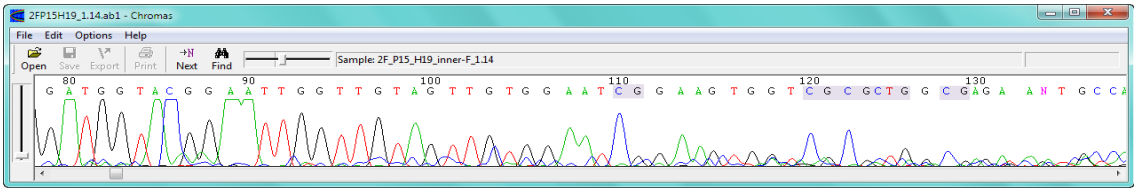
2FP15H19_1.14.ab1 - Chromas
Sample: 2F_P15_H19_inner-F_1.14

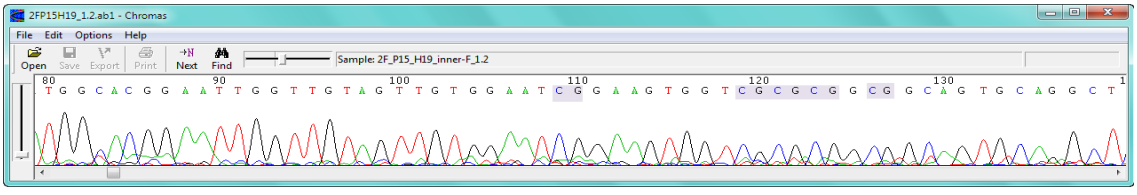
2FP15H19_1.2.ab1 - Chromas
Sample: 2F_P15_H19_inner-F_1.2

3. 6A P8 H19

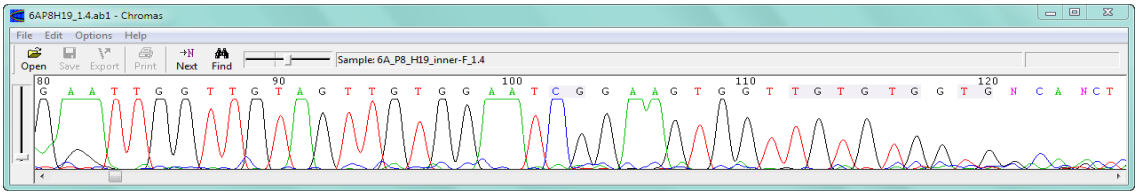
6AP8H19_1.4.ab1 - Chromas
Sample: 6A_P8_H19_inner-F_1.4

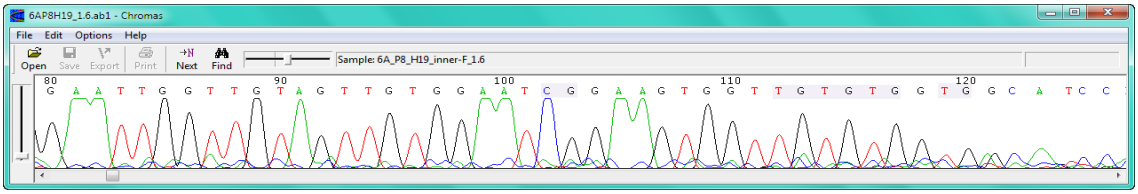
6AP8H19_1.6.ab1 - Chromas
Sample: 6A_P8_H19_inner-F_1.6

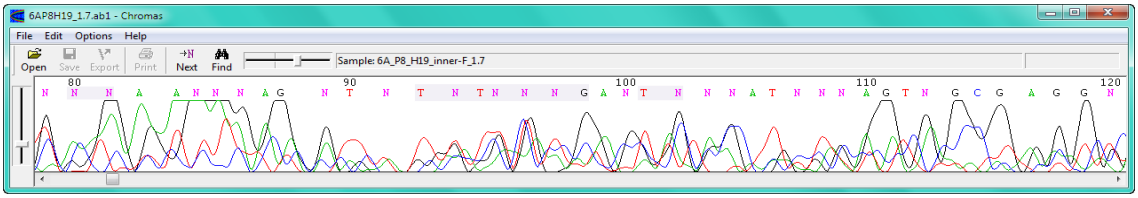
6AP8H19_1.7.ab1 - Chromas
Sample: 6A_P8_H19_inner-F_1.7

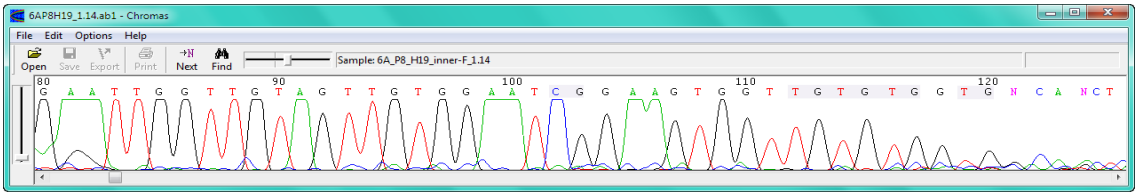
6AP8H19_1.14.ab1 - Chromas
Sample: 6A_P8_H19_inner-F_1.14

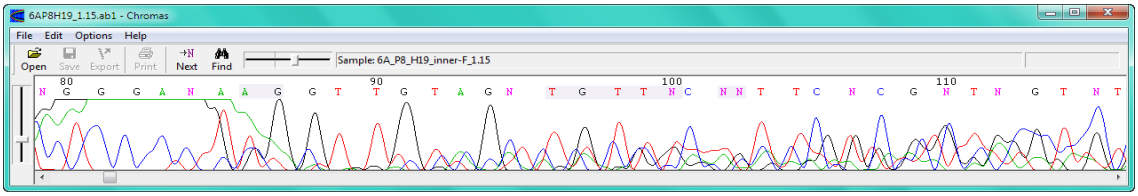
6AP8H19_1.15.ab1 - Chromas
Sample: 6A_P8_H19_inner-F_1.15

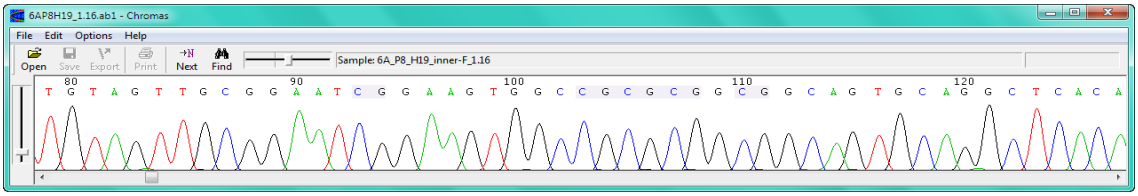
6AP8H19_1.16.ab1 - Chromas
Sample: 6A_P8_H19_inner-F_1.16

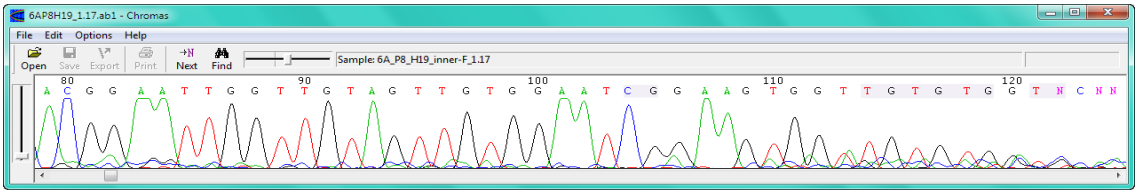
6AP8H19_1.17.ab1 - Chromas
Sample: 6A_P8_H19_inner-F_1.17

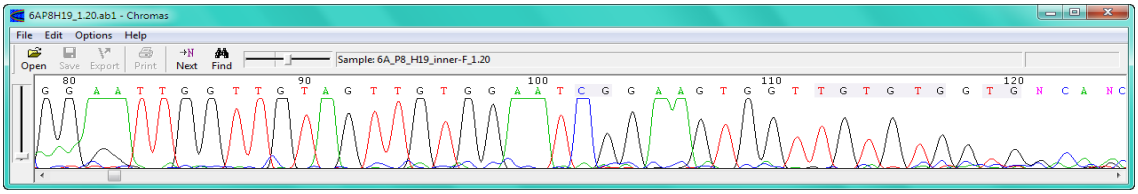
6AP8H19_1.20.ab1 - Chromas
Sample: 6A_P8_H19_inner-F_1.20

4. 6A P15 H19

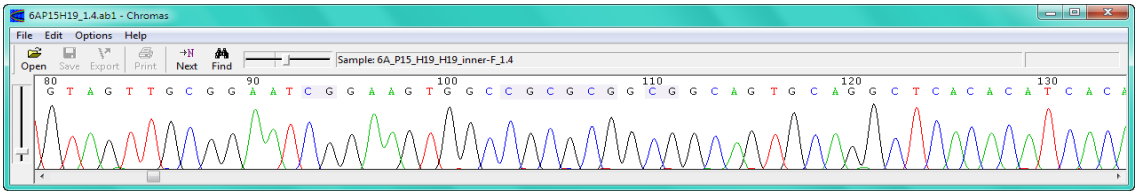
6AP15H19_1.4.ab1 - Chromas
Sample: 6A_P15_H19_H19_inner-F_1.4

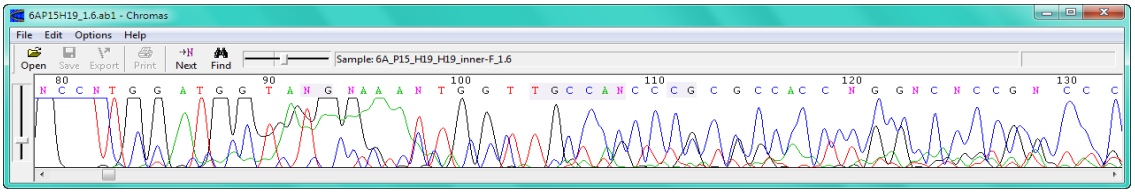
6AP15H19_1.6.ab1 - Chromas
Sample: 6A_P15_H19_H19_inner-F_1.6

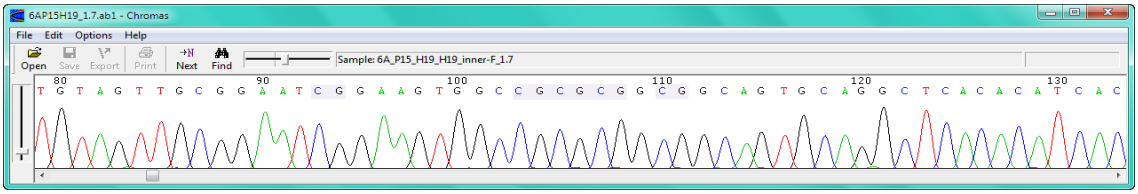
6AP15H19_1.7.ab1 - Chromas
Sample: 6A_P15_H19_H19_inner-F_1.7

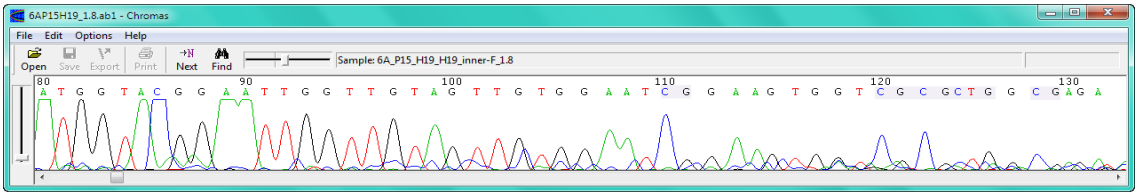
6AP15H19_1.8.ab1 - Chromas
Sample: 6A_P15_H19_H19_inner-F_1.8

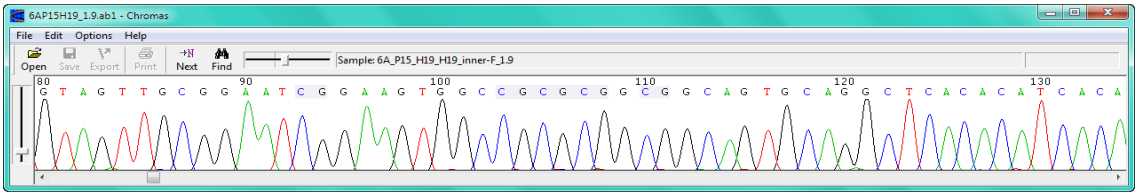
6AP15H19_1.9.ab1 - Chromas
Sample: 6A_P15_H19_H19_inner-F_1.9

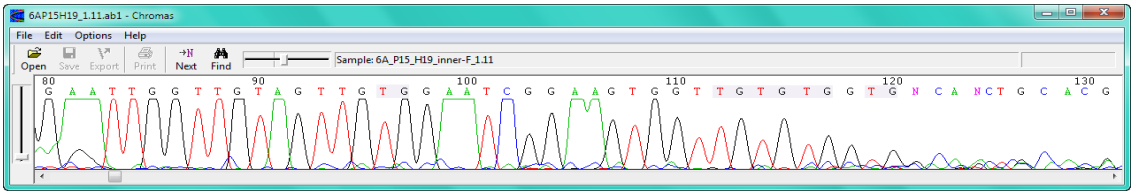
6AP15H19_1.11.ab1 - Chromas
Sample: 6A_P15_H19_inner-F_1.11

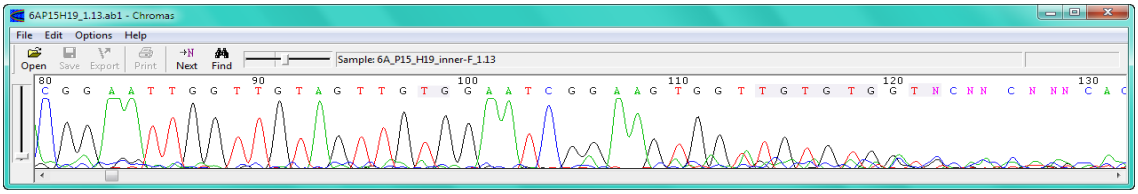
6AP15H19_1.13.ab1 - Chromas
Sample: 6A_P15_H19_inner-F_1.13

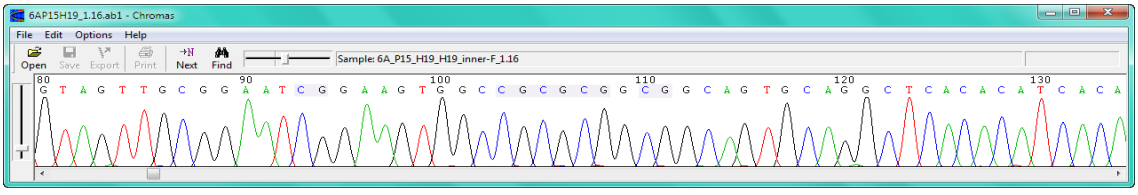
6AP15H19_1.16.ab1 - Chromas
Sample: 6A_P15_H19_H19_inner-F_1.16

5. CL8 P8 H19

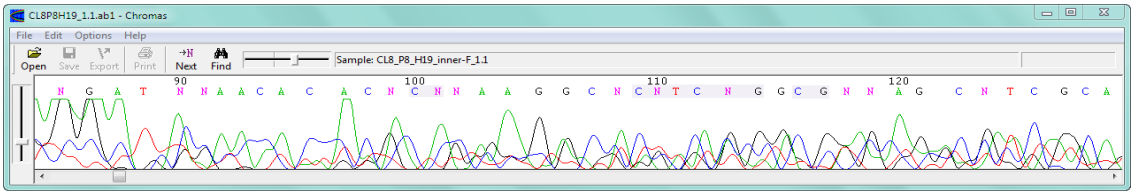
CL8P8H19_1.1.ab1 - Chromas
Sample: CL8_P8_H19_inner-F_1.1

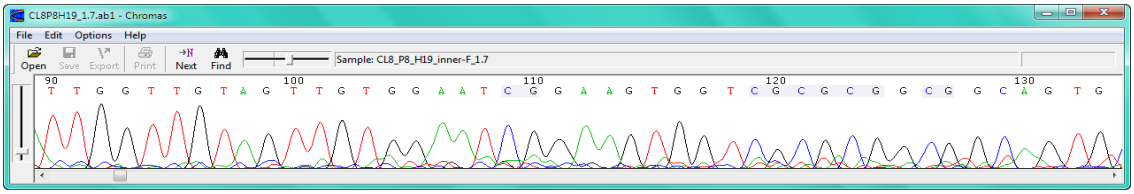
CL8P8H19_1.7.ab1 - Chromas
Sample: CL8_P8_H19_inner-F_1.7

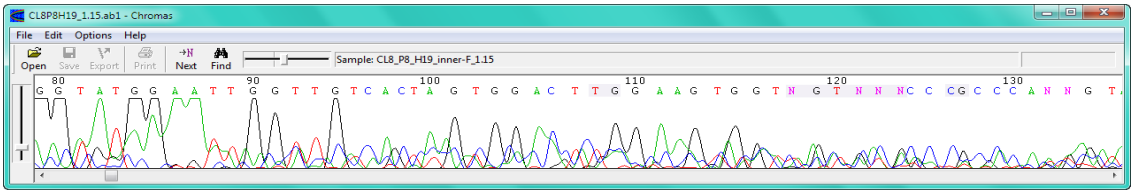
CL8P8H19_1.15.ab1 - Chromas
Sample: CL8_P8_H19_inner-F_1.15

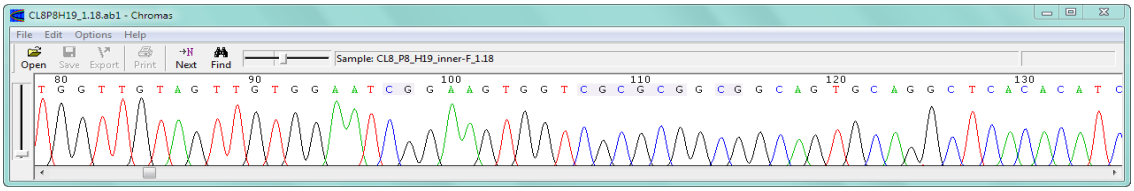
CL8P8H19_1.18.ab1 - Chromas
Sample: CL8_P8_H19_inner-F_1.18

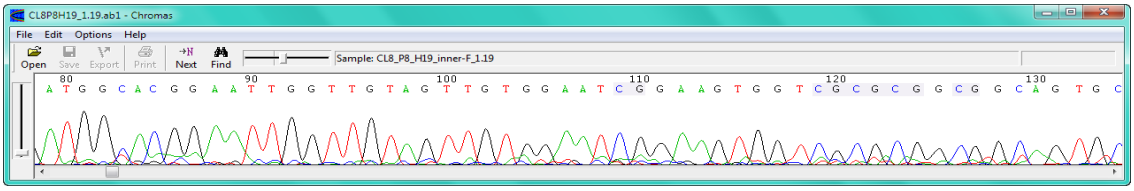
CL8P8H19_1.19.ab1 - Chromas
Sample: CL8_P8_H19_inner-F_1.19

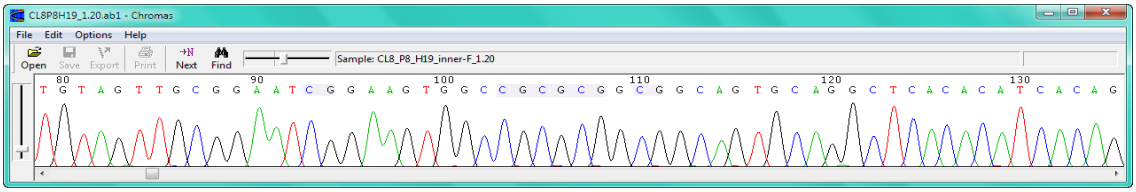
CL8P8H19_1.20.ab1 - Chromas
Sample: CL8_P8_H19_inner-F_1.20

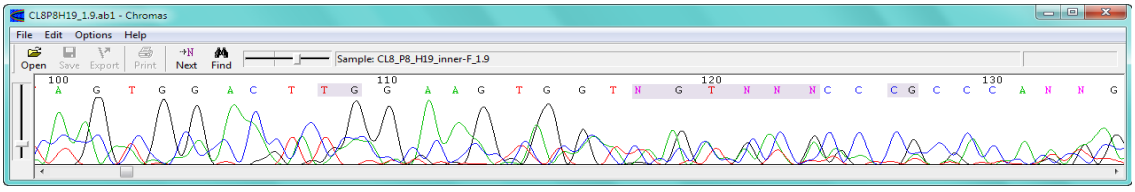
CL8P8H19_1.9.ab1 - Chromas
Sample: CL8_P8_H19_inner-F_1.9

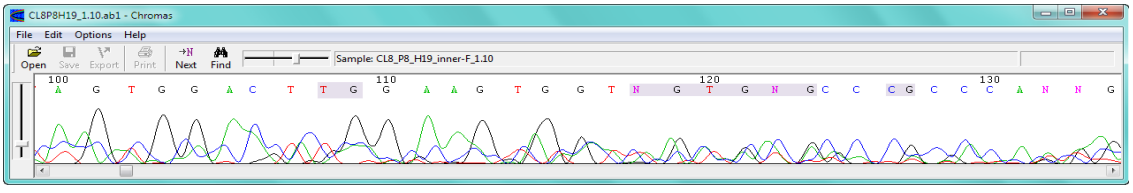
CL8P8H19_1.10.ab1 - Chromas
Sample: CL8_P8_H19_inner-F_1.10

6. CL8 P15 H19

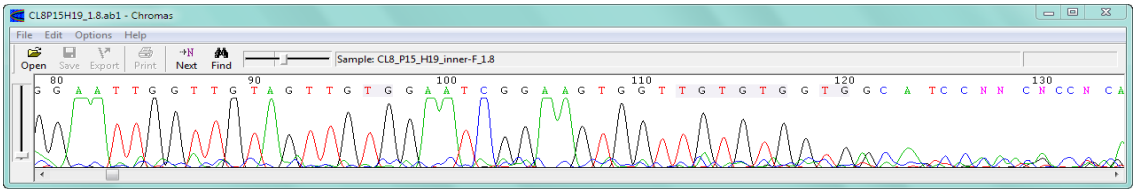
CL8P15H19_1.8.ab1 - Chromas
Sample: CL8_P15_H19_inner-F_1.8

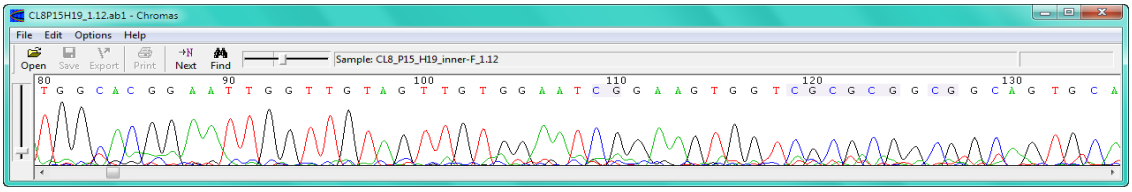
CL8P15H19_1.12.ab1 - Chromas
Sample: CL8_P15_H19_inner-F_1.12

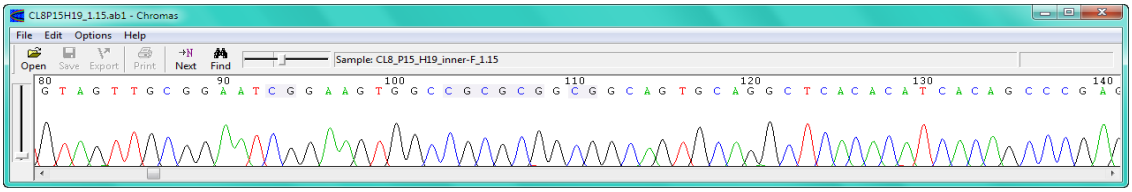
CL8P15H19_1.15.ab1 - Chromas
Sample: CL8_P15_H19_inner-F_1.15

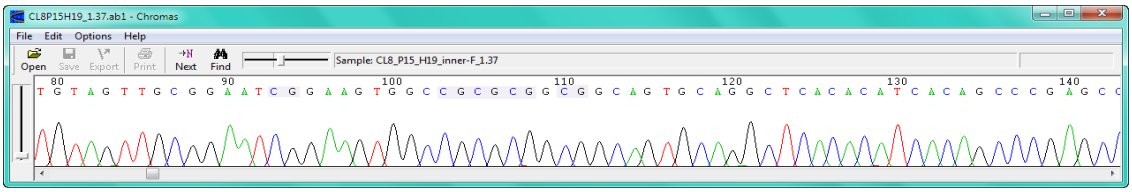
CL8P15H19_1.37.ab1 - Chromas
Sample: CL8_P15_H19_inner-F_1.37

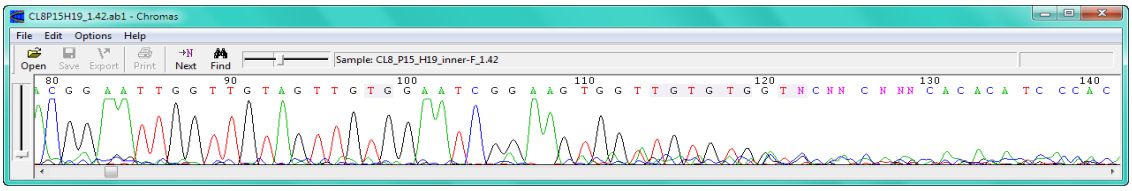
CL8P15H19_1.42.ab1 - Chromas
Sample: CL8_P15_H19_inner-F_1.42

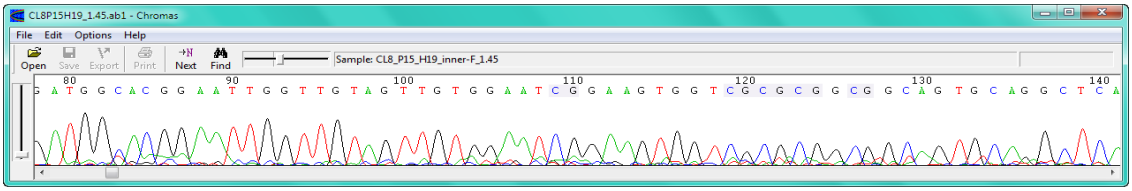
CL8P15H19_1.45.ab1 - Chromas
Sample: CL8_P15_H19_inner-F_1.45

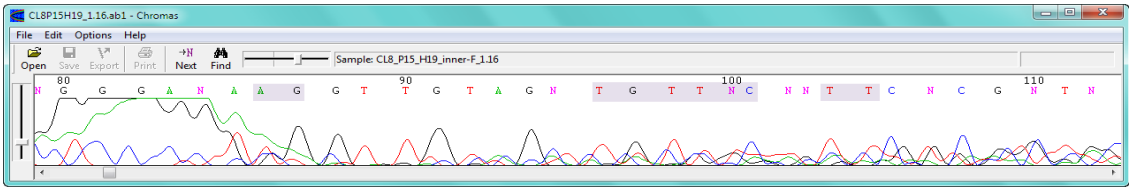
CL8P15H19_1.16.ab1 - Chromas
Sample: CL8_P15_H19_inner-F_1.16

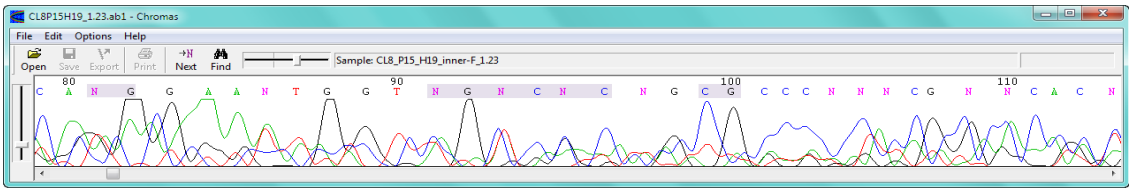
CL8P15H19_1.23.ab1 - Chromas
Sample: CL8_P15_H19_inner-F_1.23

7. CL9 P8 H19

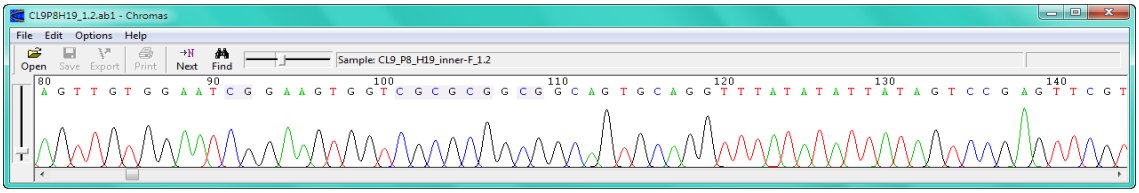
CL9P8H19_1.2.ab1 - Chromas
File Edit Options Help
Open Save Export Print Next Find
Sample: CL9_P8_H19_inner-F_1.2

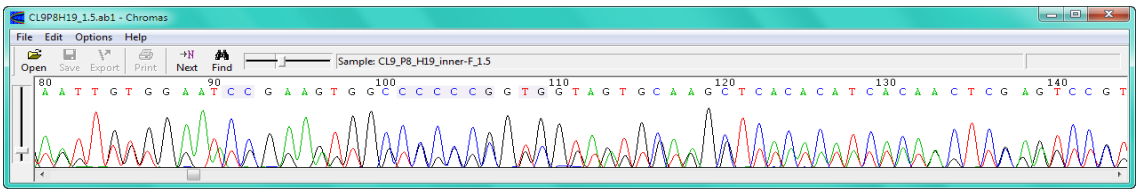
CL9P8H19_1.5.ab1 - Chromas
File Edit Options Help
Open Save Export Print Next Find
Sample: CL9_P8_H19_inner-F_1.5

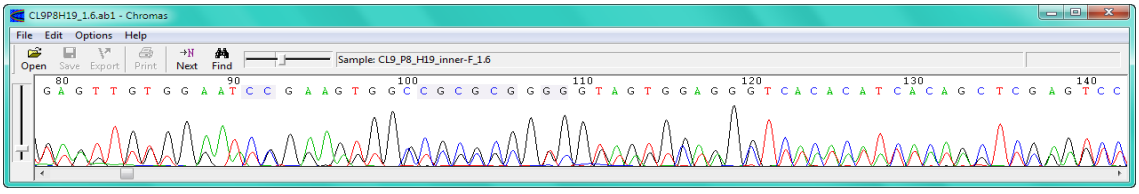
CL9P8H19_1.6.ab1 - Chromas
File Edit Options Help
Open Save Export Print Next Find
Sample: CL9_P8_H19_inner-F_1.6

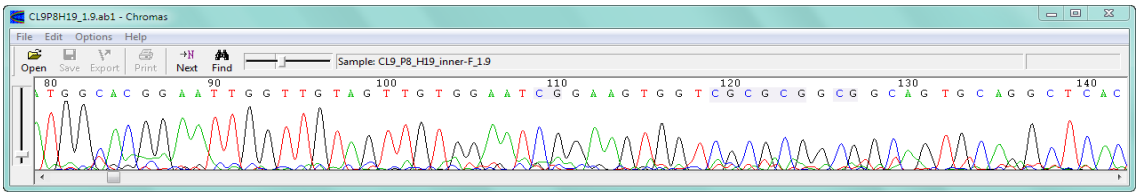
CL9P8H19_1.9.ab1 - Chromas
File Edit Options Help
Open Save Export Print Next Find
Sample: CL9_P8_H19_inner-F_1.9

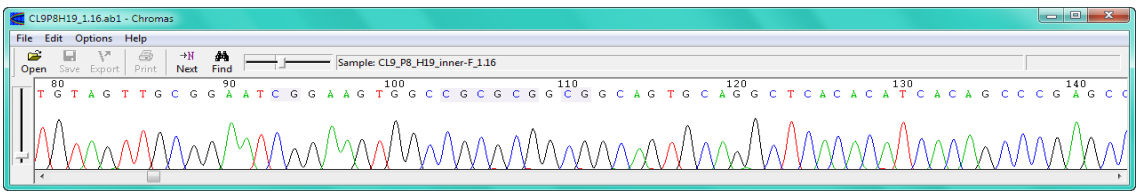
CL9P8H19_1.16.ab1 - Chromas
File Edit Options Help
Open Save Export Print Next Find
Sample: CL9_P8_H19_inner-F_1.16

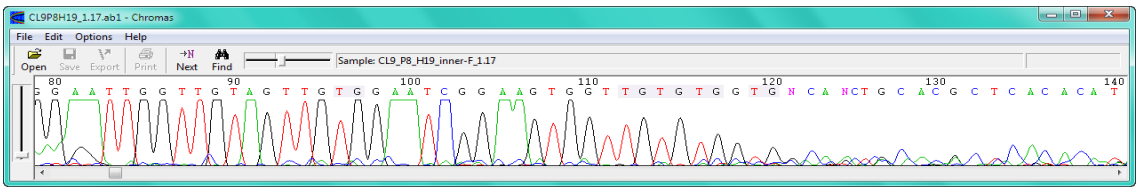
CL9P8H19_1.17.ab1 - Chromas
File Edit Options Help
Open Save Export Print Next Find
Sample: CL9_P8_H19_inner-F_1.17

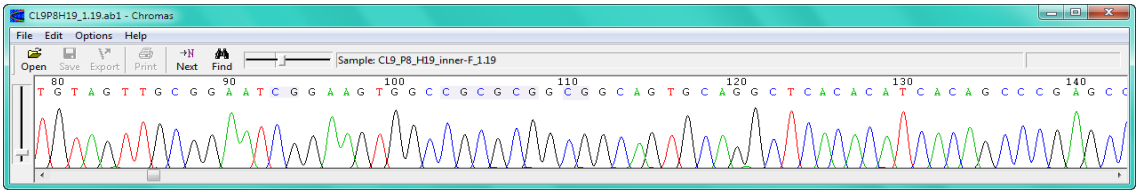
CL9P8H19_1.19.ab1 - Chromas
File Edit Options Help
Open Save Export Print Next Find
Sample: CL9_P8_H19_inner-F_1.19

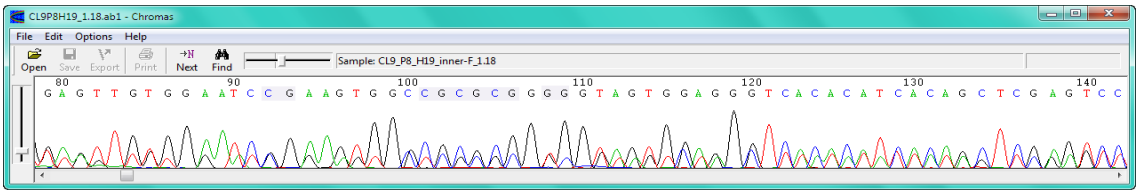
CL9P8H19_1.18.ab1 - Chromas
File Edit Options Help
Open Save Export Print Next Find
Sample: CL9_P8_H19_inner-F_1.18

8. CL9 P15 H19

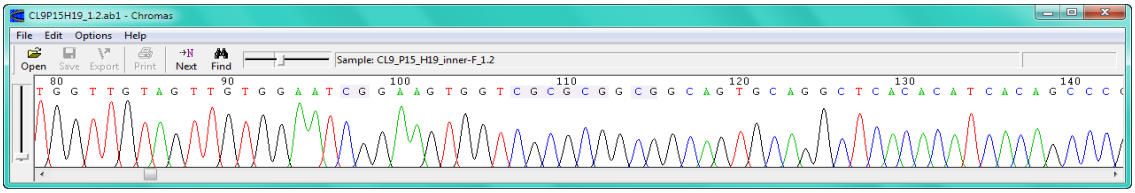
CL9P15H19_1.2.ab1 - Chromas
File Edit Options Help
Open Save Export Print Next Find
Sample: CL9_P15_H19_inner-F_1.2

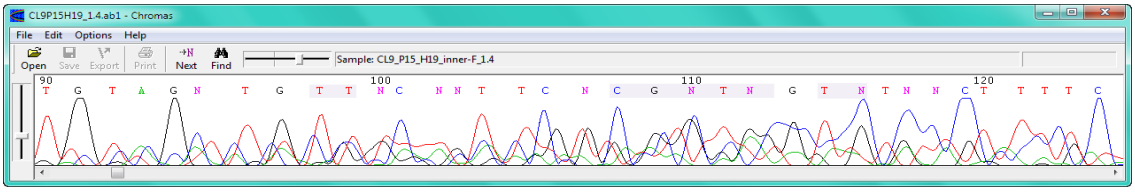
CL9P15H19_1.4.ab1 - Chromas
File Edit Options Help
Open Save Export Print Next Find
Sample: CL9_P15_H19_inner-F_1.4

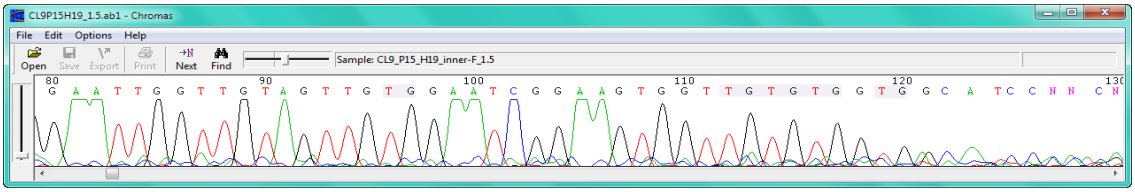
CL9P15H19_1.5.ab1 - Chromas
File Edit Options Help
Open Save Export Print Next Find
Sample: CL9_P15_H19_inner-F_1.5

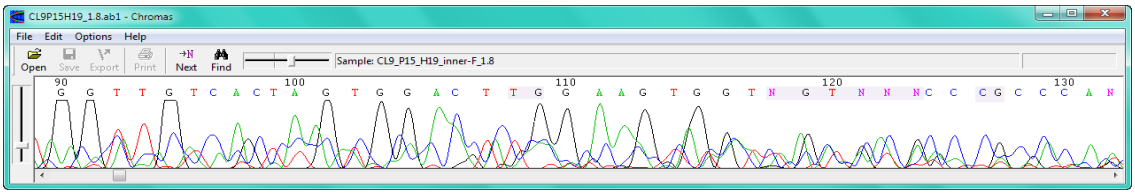
CL9P15H19_1.8.ab1 - Chromas
File Edit Options Help
Open Save Export Print Next Find
Sample: CL9_P15_H19_inner-F_1.8

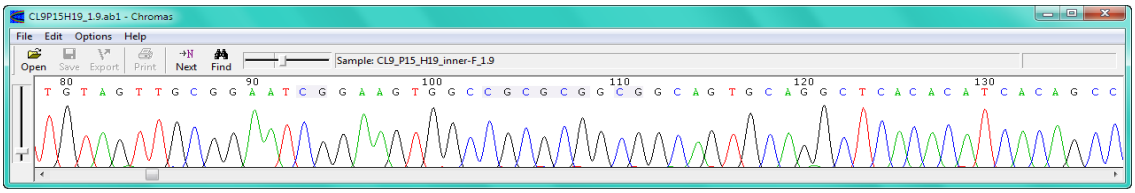
CL9P15H19_1.9.ab1 - Chromas
File Edit Options Help
Open Save Export Print Next Find
Sample: CL9_P15_H19_inner-F_1.9

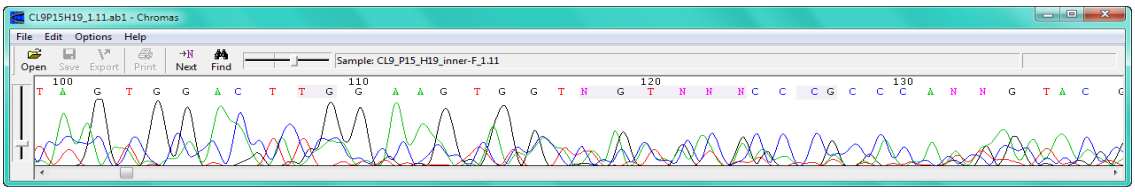
CL9P15H19_1.11.ab1 - Chromas
File Edit Options Help
Open Save Export Print Next Find
Sample: CL9_P15_H19_inner-F_1.11

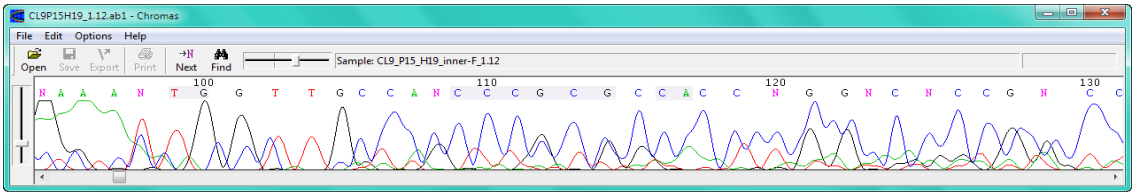
CL9P15H19_1.12.ab1 - Chromas
File Edit Options Help
Open Save Export Print Next Find
Sample: CL9_P15_H19_inner-F_1.12

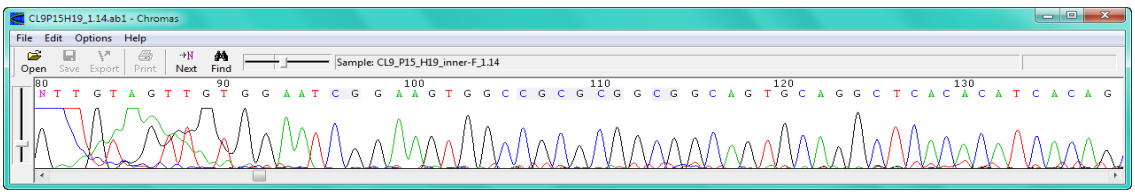
CL9P15H19_1.14.ab1 - Chromas
File Edit Options Help
Open Save Export Print Next Find
Sample: CL9_P15_H19_inner-F_1.14

9. T8 P8 H19

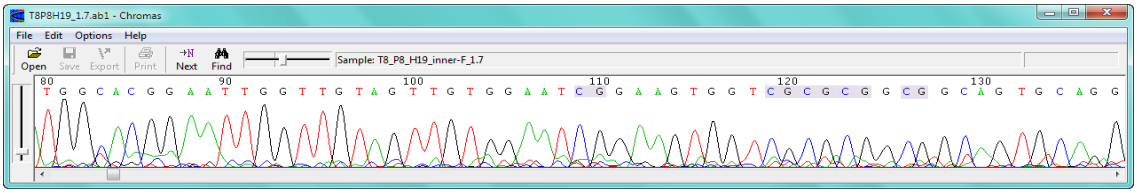
T8P8H19_1.7.ab1 - Chromas
File Edit Options Help
Open Save Export Print Next Find
Sample: T8_P8_H19_inner-F_1.7

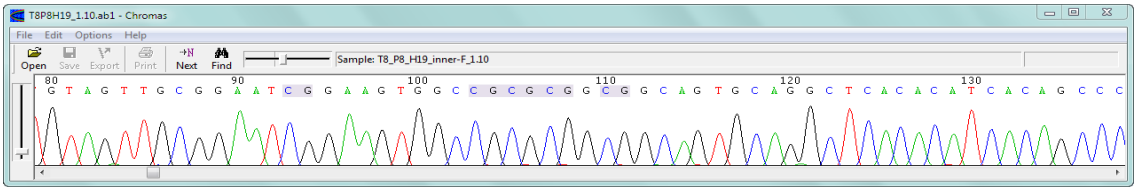
T8P8H19_1.10.ab1 - Chromas
File Edit Options Help
Open Save Export Print Next Find
Sample: T8_P8_H19_inner-F_1.10

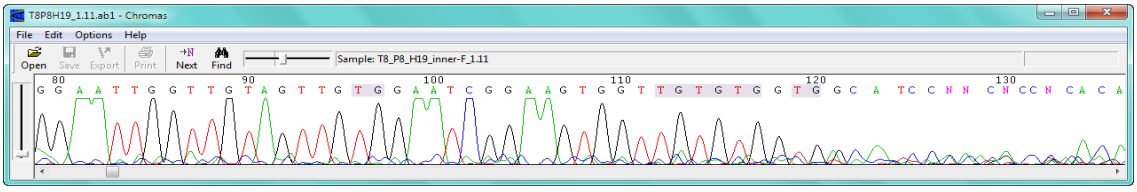
T8P8H19_1.11.ab1 - Chromas
File Edit Options Help
Open Save Export Print Next Find
Sample: T8_P8_H19_inner-F_1.11

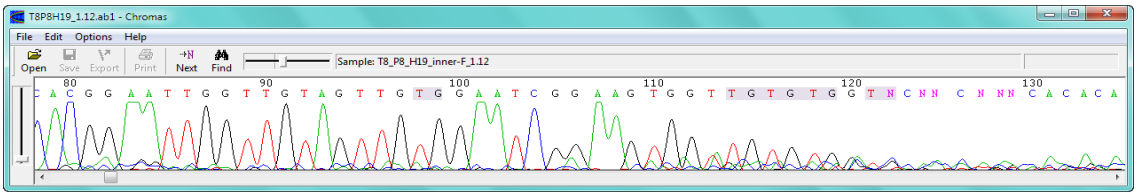
T8P8H19_1.12.ab1 - Chromas
File Edit Options Help
Open Save Export Print Next Find
Sample: T8_P8_H19_inner-F_1.12

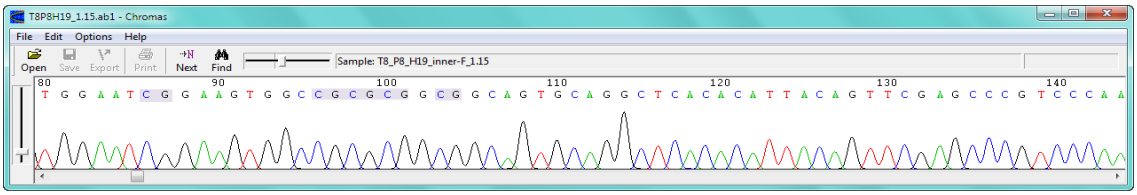
T8P8H19_1.15.ab1 - Chromas
File Edit Options Help
Open Save Export Print Next Find
Sample: T8_P8_H19_inner-F_1.15

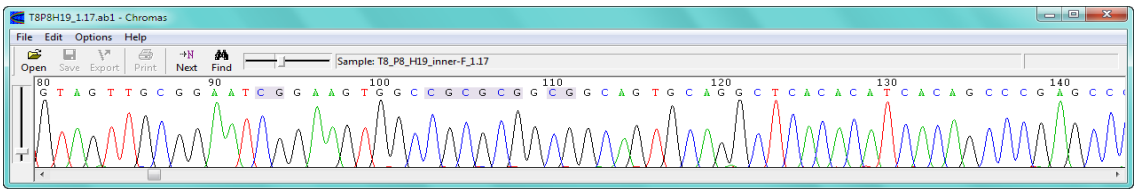
T8P8H19_1.17.ab1 - Chromas
File Edit Options Help
Open Save Export Print Next Find
Sample: T8_P8_H19_inner-F_1.17

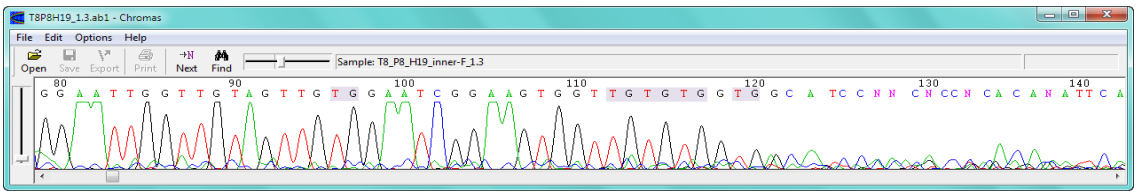
T8P8H19_1.3.ab1 - Chromas
File Edit Options Help
Open Save Export Print Next Find
Sample: T8_P8_H19_inner-F_1.3

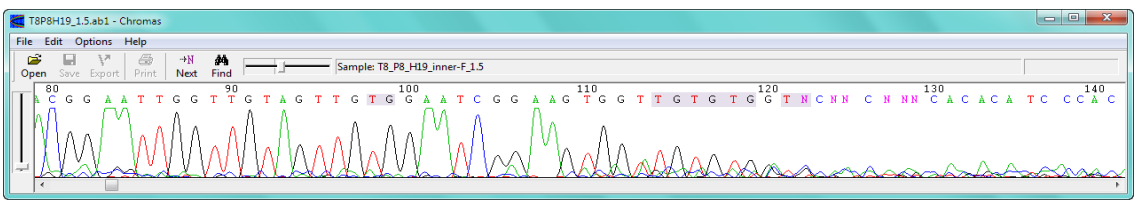
T8P8H19_1.5.ab1 - Chromas
File Edit Options Help
Open Save Export Print Next Find
Sample: T8_P8_H19_inner-F_1.5

10. T8 P15 H19

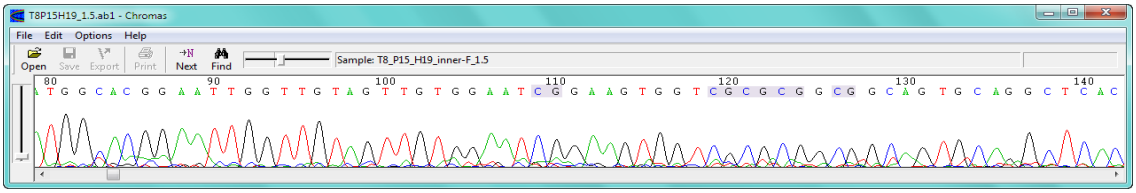
T8P15H19_1.5.ab1 - Chromas
Sample: T8_P15_H19_inner-F_1.5

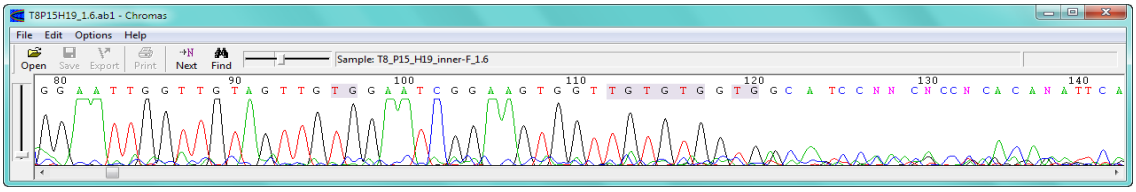
T8P15H19_1.6.ab1 - Chromas
Sample: T8_P15_H19_inner-F_1.6

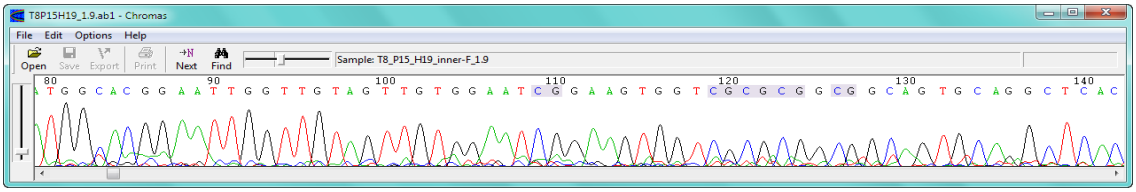
T8P15H19_1.9.ab1 - Chromas
Sample: T8_P15_H19_inner-F_1.9

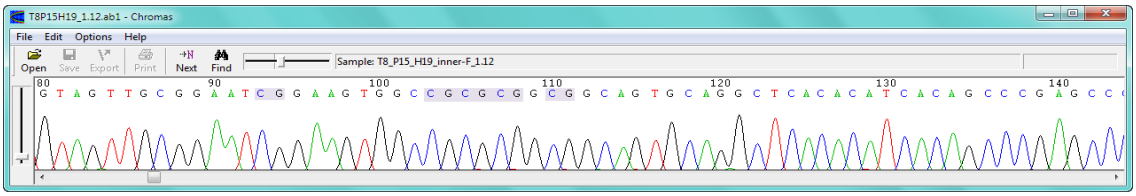
T8P15H19_1.12.ab1 - Chromas
Sample: T8_P15_H19_inner-F_1.12

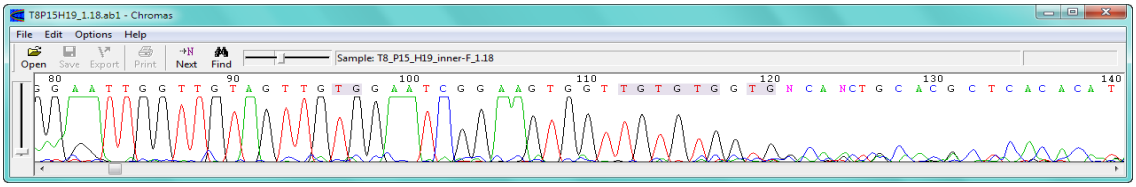
T8P15H19_1.18.ab1 - Chromas
Sample: T8_P15_H19_inner-F_1.18

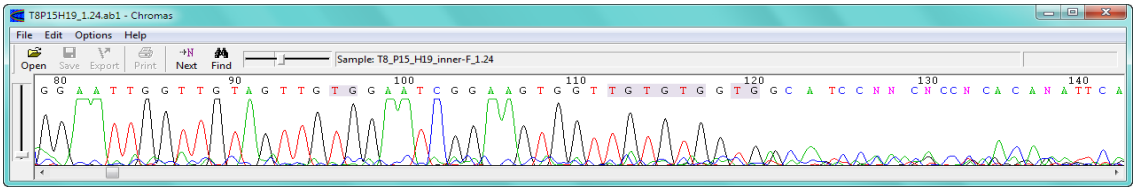
T8P15H19_1.24.ab1 - Chromas
Sample: T8_P15_H19_inner-F_1.24

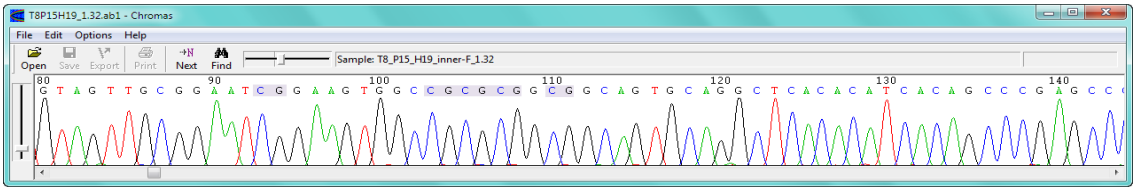
T8P15H19_1.32.ab1 - Chromas
Sample: T8_P15_H19_inner-F_1.32

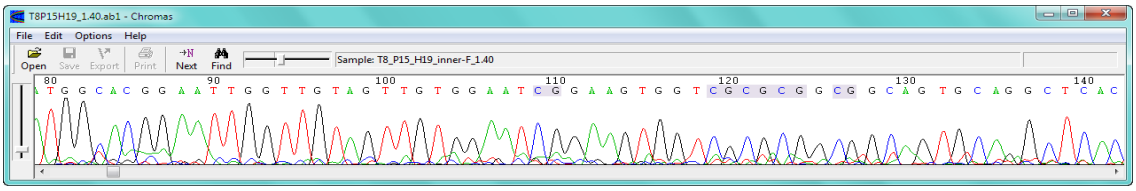
T8P15H19_1.40.ab1 - Chromas
Sample: T8_P15_H19_inner-F_1.40

11. T11 P8 H19

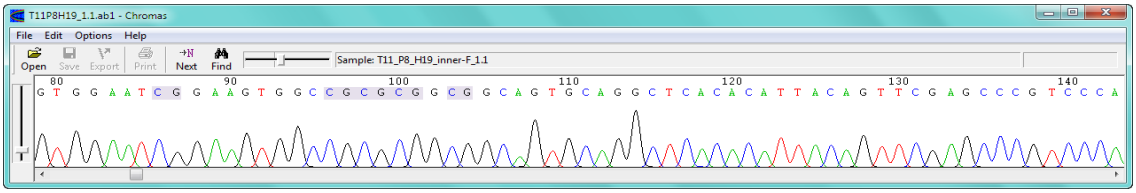
T11P8H19_1.1.ab1 - Chromas
File Edit Options Help
Open Save Export Print Next Find
Sample: T11_P8_H19_inner-F_1.1

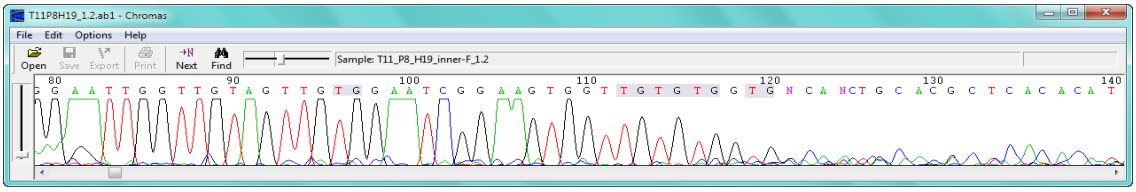
T11P8H19_1.2.ab1 - Chromas
File Edit Options Help
Open Save Export Print Next Find
Sample: T11_P8_H19_inner-F_1.2

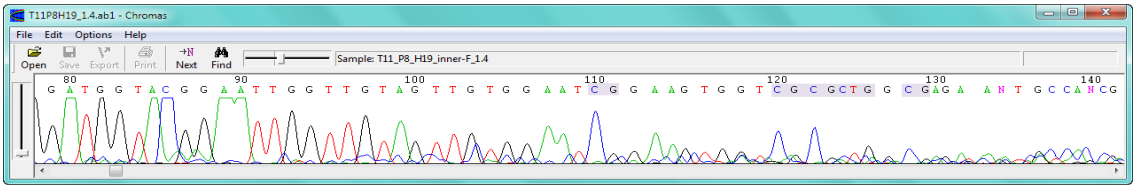
T11P8H19_1.4.ab1 - Chromas
File Edit Options Help
Open Save Export Print Next Find
Sample: T11_P8_H19_inner-F_1.4

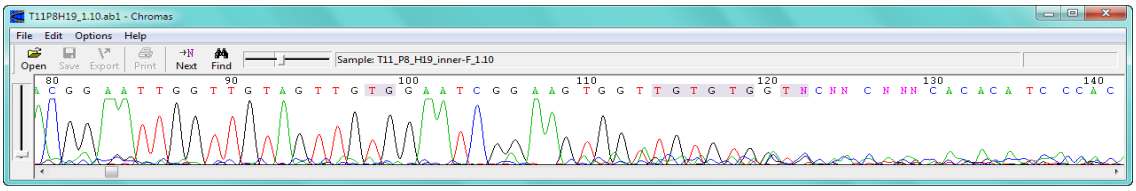
T11P8H19_1.10.ab1 - Chromas
File Edit Options Help
Open Save Export Print Next Find
Sample: T11_P8_H19_inner-F_1.10

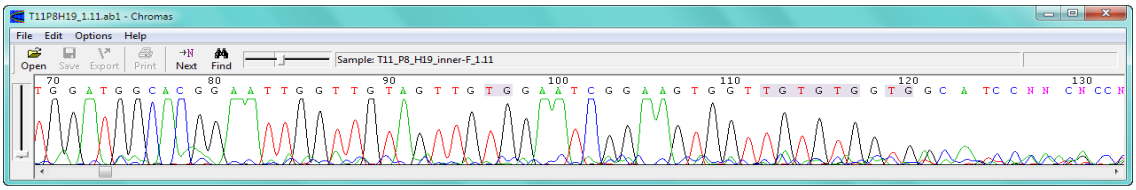
T11P8H19_1.11.ab1 - Chromas
File Edit Options Help
Open Save Export Print Next Find
Sample: T11_P8_H19_inner-F_1.11

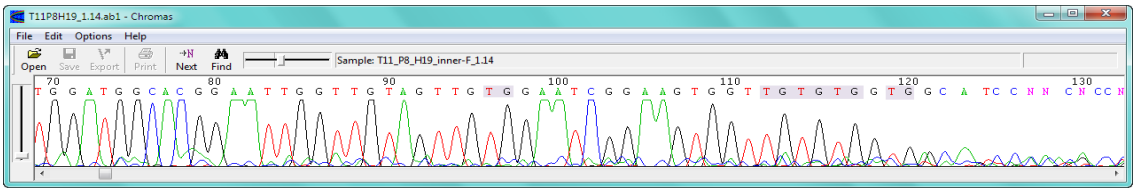
T11P8H19_1.14.ab1 - Chromas
File Edit Options Help
Open Save Export Print Next Find
Sample: T11_P8_H19_inner-F_1.14

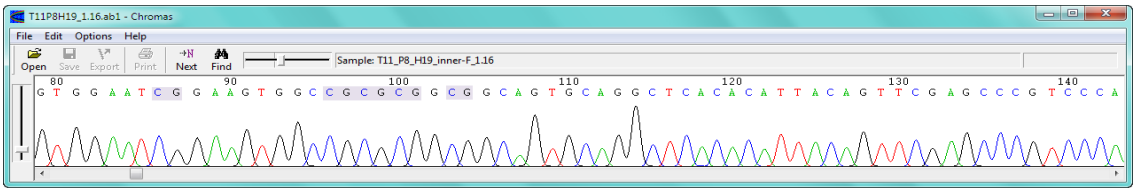
T11P8H19_1.16.ab1 - Chromas
File Edit Options Help
Open Save Export Print Next Find
Sample: T11_P8_H19_inner-F_1.16

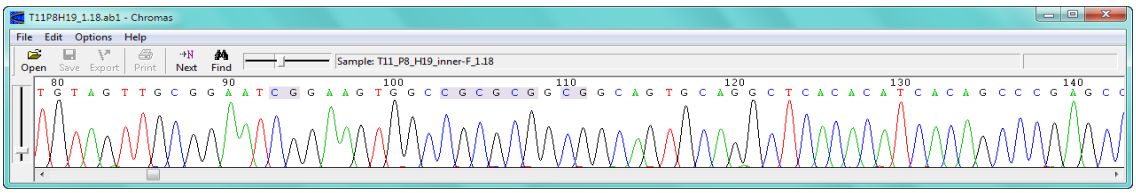
T11P8H19_1.18.ab1 - Chromas
File Edit Options Help
Open Save Export Print Next Find
Sample: T11_P8_H19_inner-F_1.18

12. T11 P15 H19

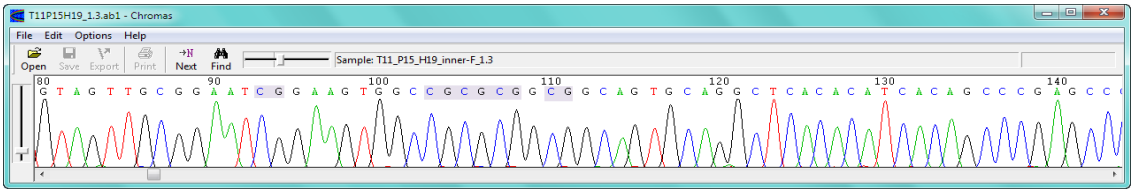

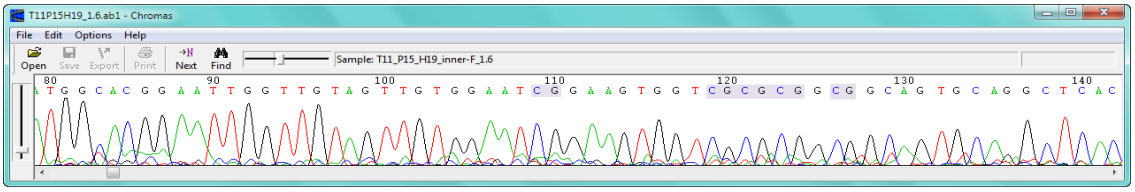

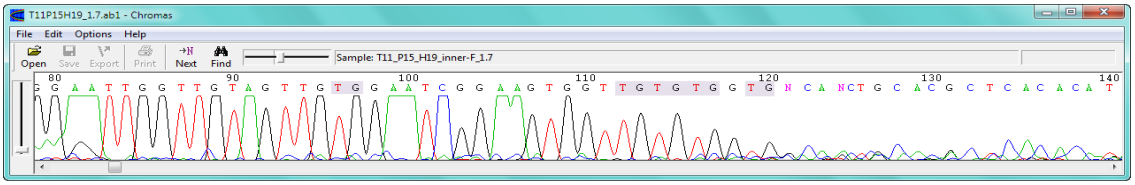

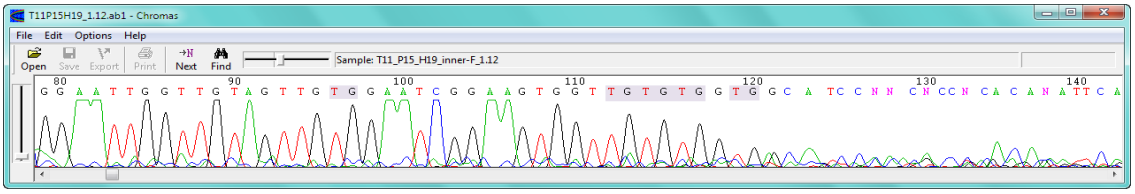

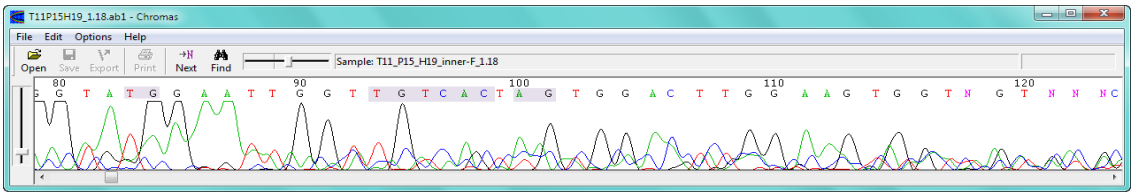

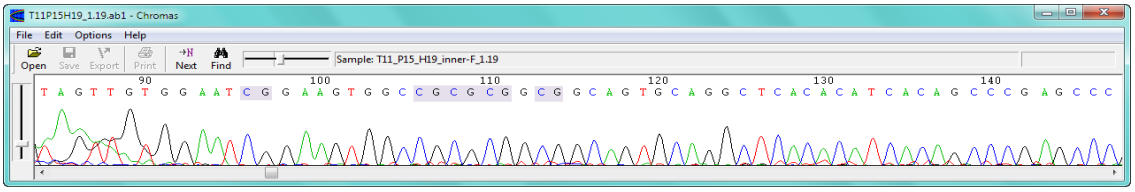

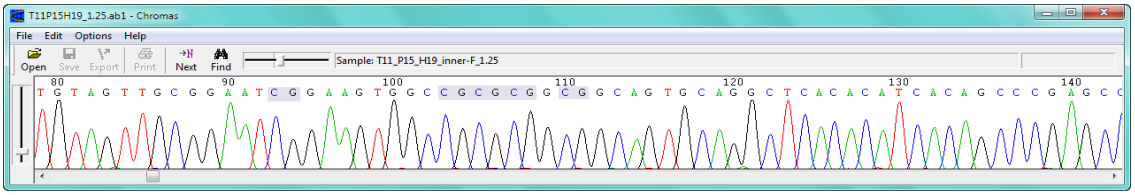

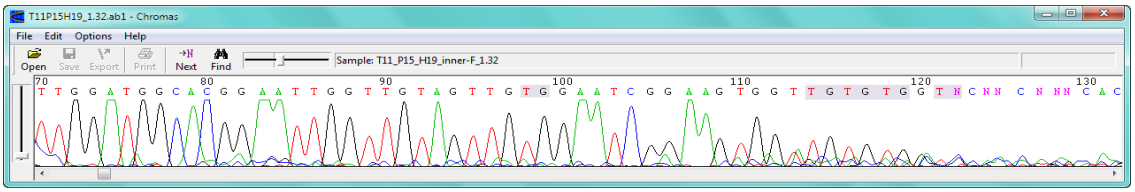

13. T18 P8 H19

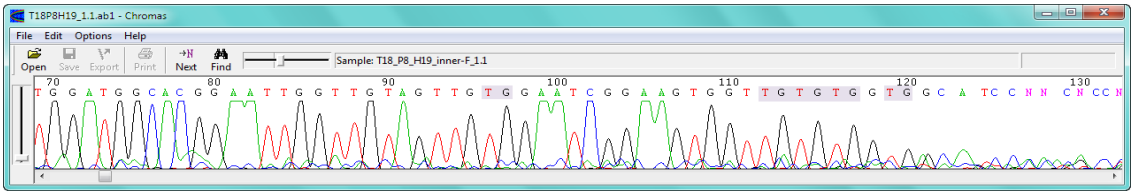
T18P8H19_1.1.ab1 - Chromas
Sample: T18_P8_H19_inner-F_1.1

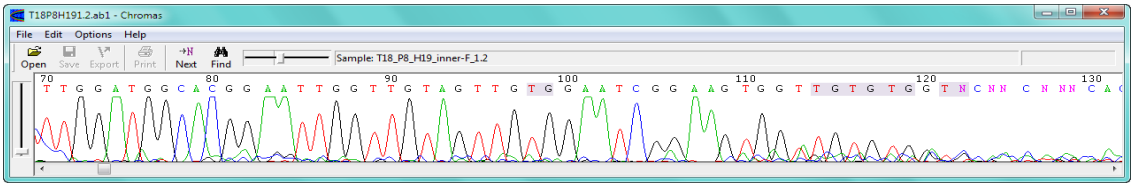
T18P8H191.2.ab1 - Chromas
Sample: T18_P8_H19_inner-F_1.2

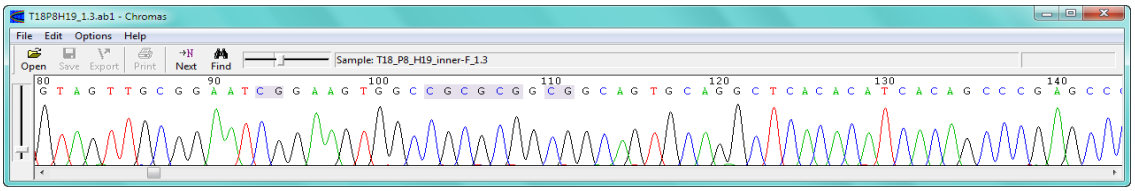
T18P8H19_1.3.ab1 - Chromas
Sample: T18_P8_H19_inner-F_1.3

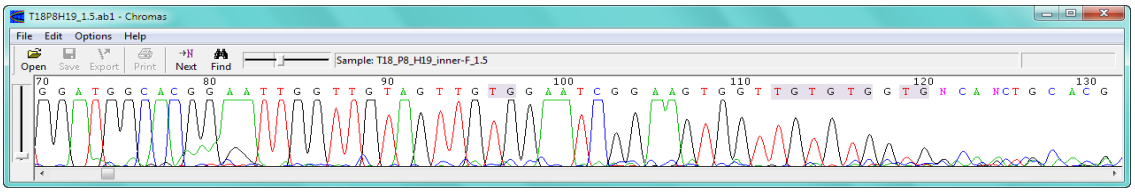
T18P8H19_1.5.ab1 - Chromas
Sample: T18_P8_H19_inner-F_1.5

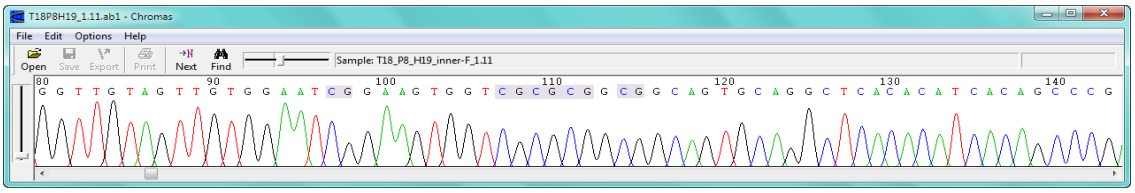
T18P8H19_1.11.ab1 - Chromas
Sample: T18_P8_H19_inner-F_1.11

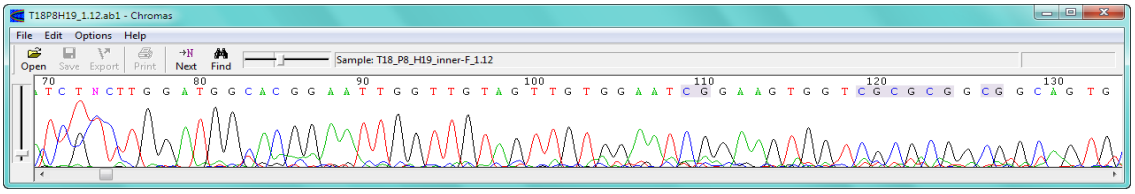
T18P8H19_1.12.ab1 - Chromas
Sample: T18_P8_H19_inner-F_1.12

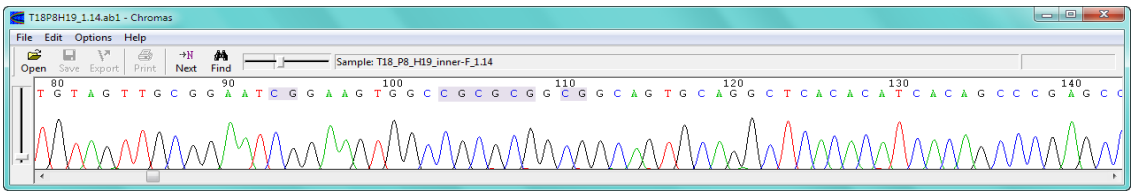
T18P8H19_1.14.ab1 - Chromas
Sample: T18_P8_H19_inner-F_1.14

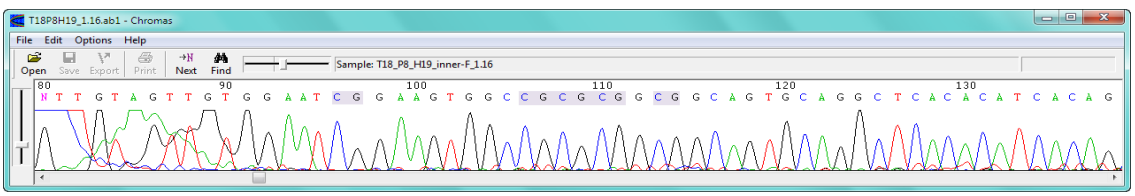
T18P8H19_1.16.ab1 - Chromas
Sample: T18_P8_H19_inner-F_1.16

14. T18 P15 H19

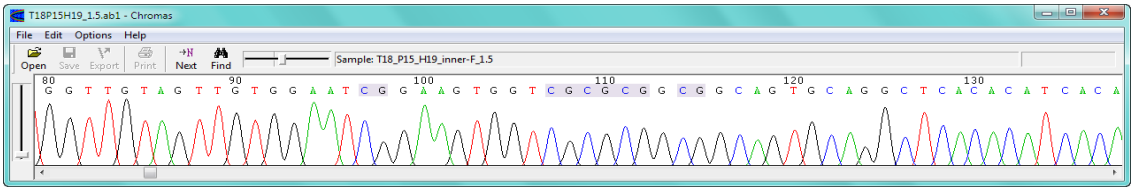

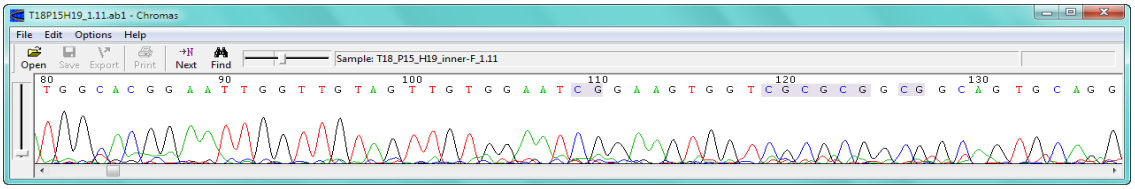

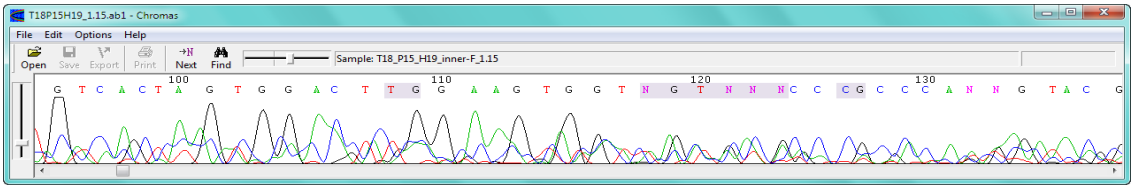

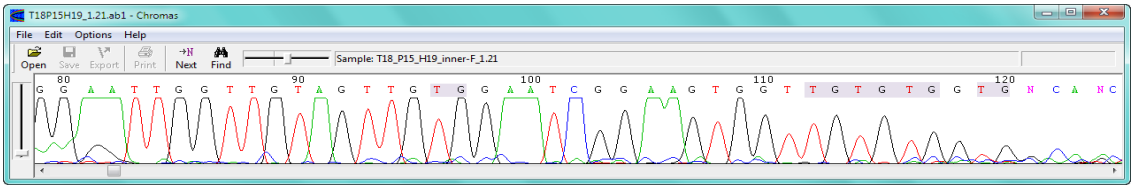

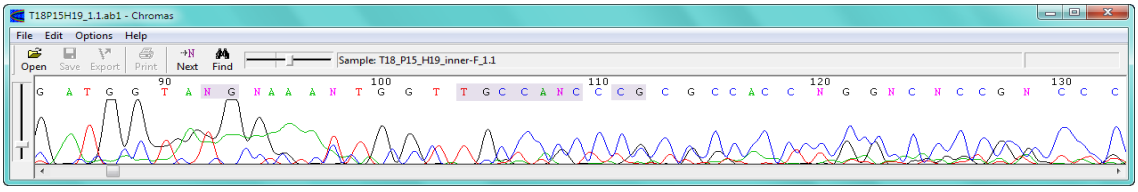

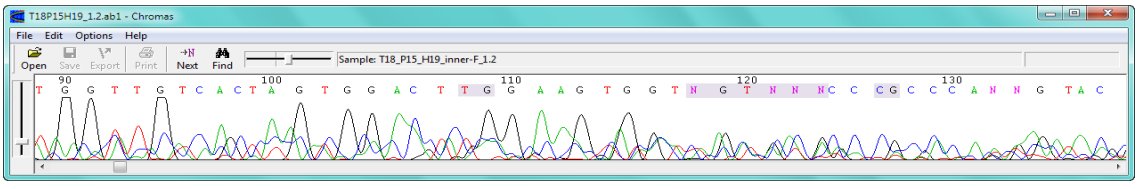

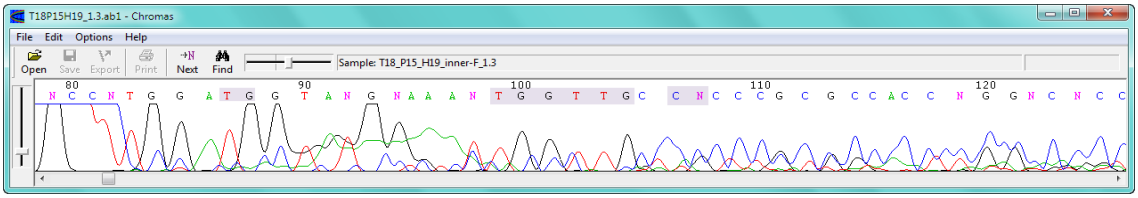

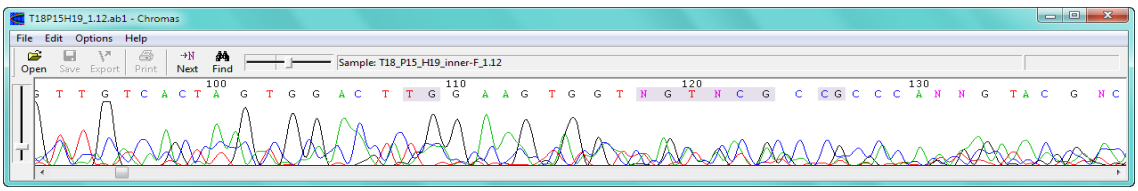

15. T21 P8 H19

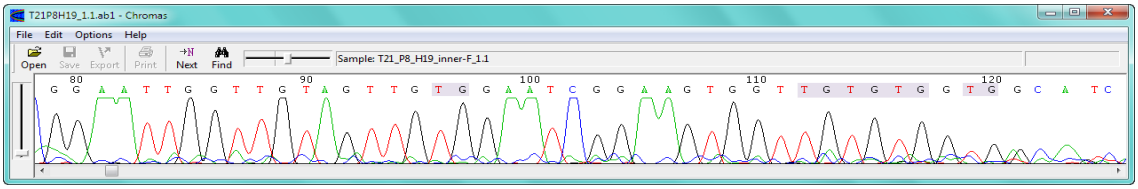
T21P8H19_1.1.ab1 - Chromas
Sample: T21_P8_H19_inner-F_1.1

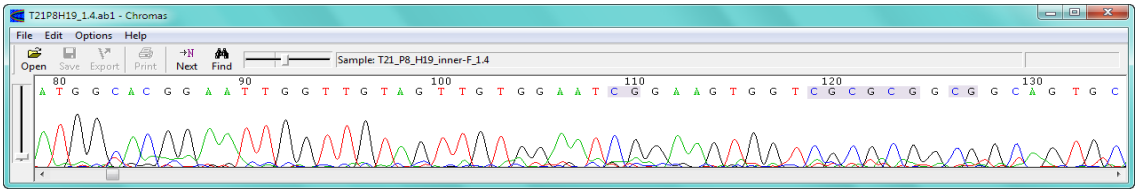
T21P8H19_1.4.ab1 - Chromas
Sample: T21_P8_H19_inner-F_1.4

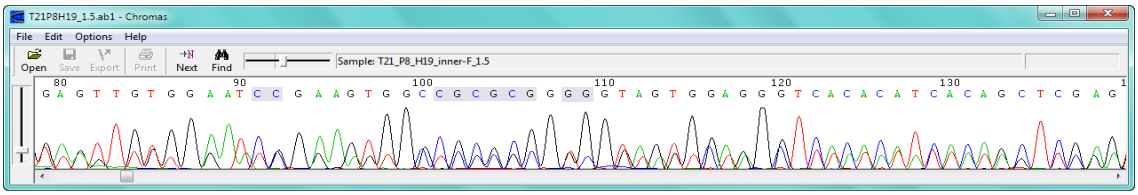
T21P8H19_1.5.ab1 - Chromas
Sample: T21_P8_H19_inner-F_1.5

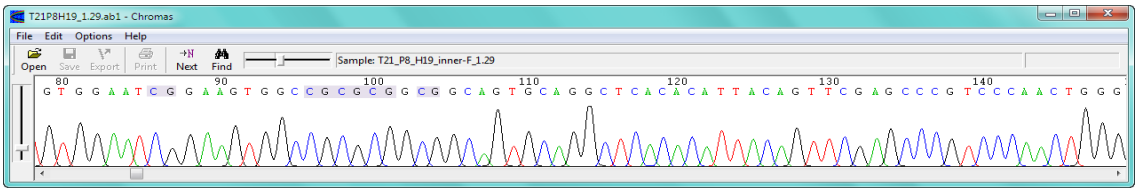
T21P8H19_1.29.ab1 - Chromas
Sample: T21_P8_H19_inner-F_1.29

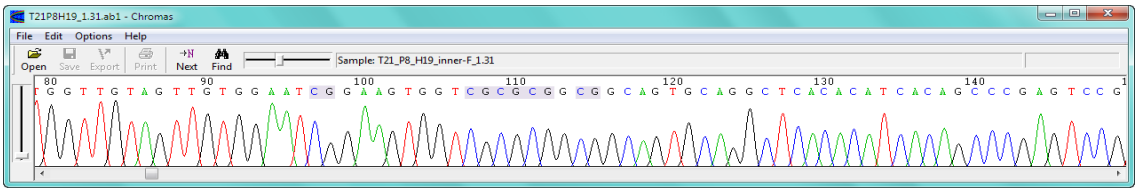
T21P8H19_1.31.ab1 - Chromas
Sample: T21_P8_H19_inner-F_1.31

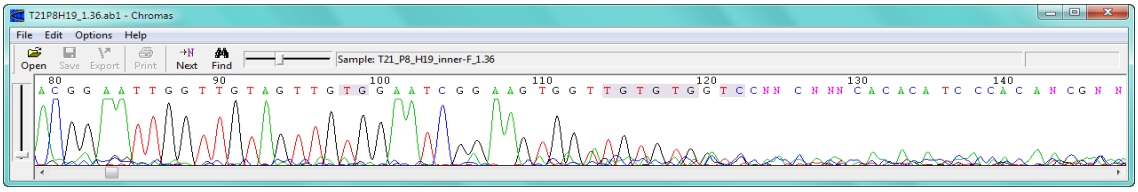
T21P8H19_1.36.ab1 - Chromas
Sample: T21_P8_H19_inner-F_1.36

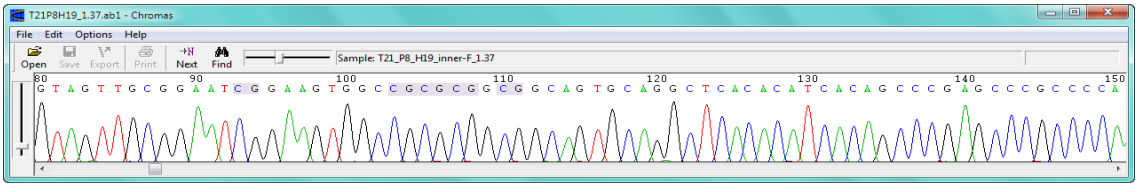
T21P8H19_1.37.ab1 - Chromas
Sample: T21_P8_H19_inner-F_1.37

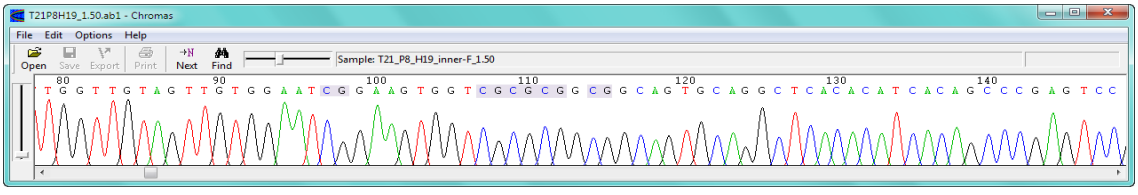
T21P8H19_1.50.ab1 - Chromas
Sample: T21_P8_H19_inner-F_1.50

16. T21 P15 H19

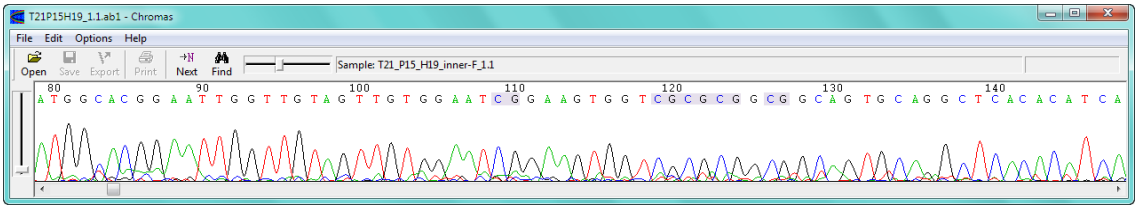

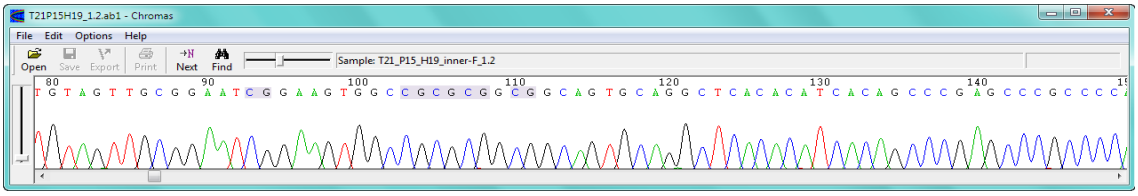

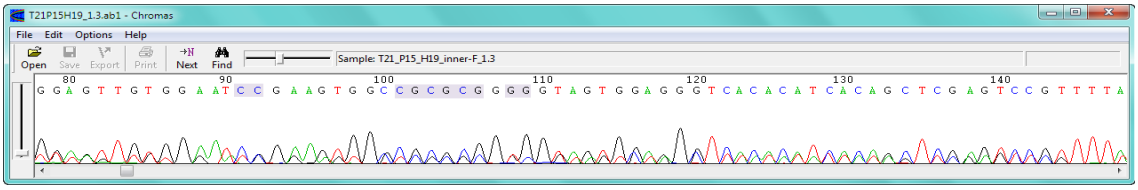

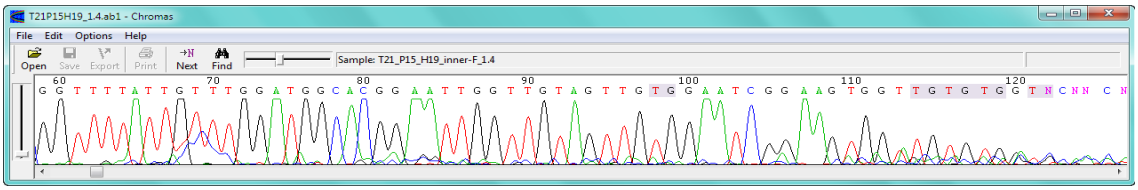

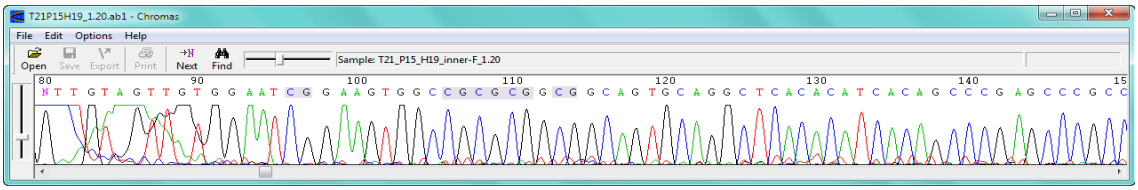

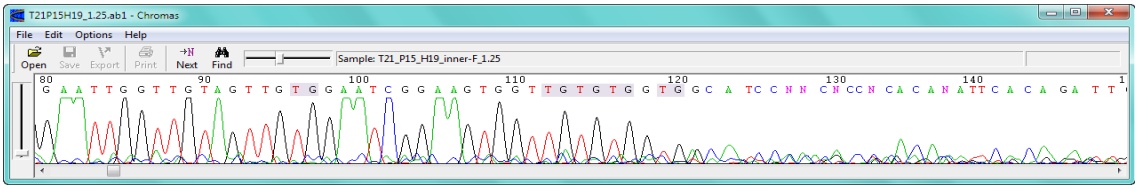

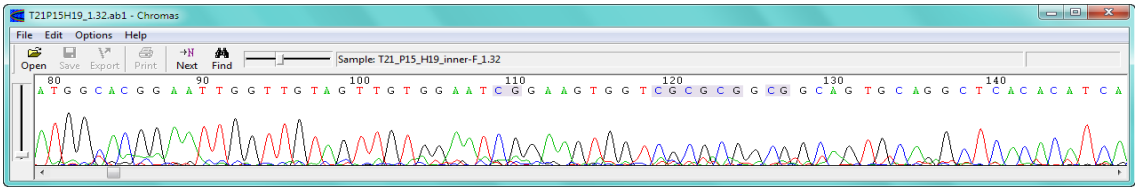

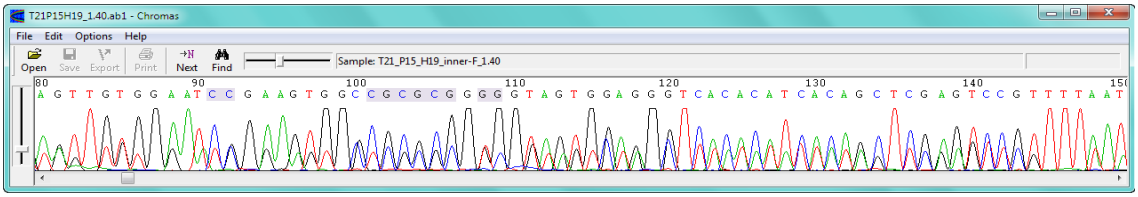

17. 2F P8 IGF2

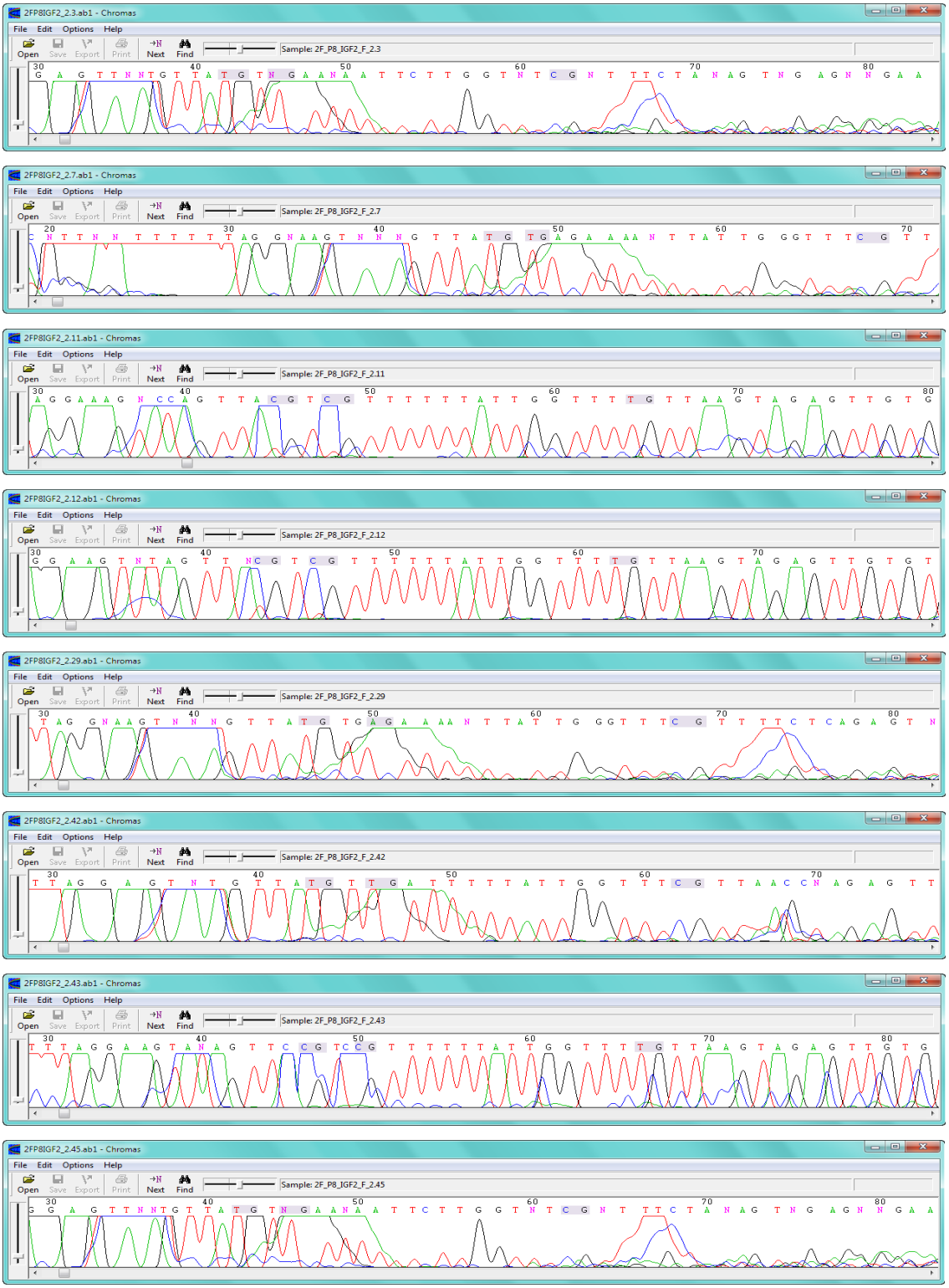
2FP8IGF2_2.3.ab1 - Chromas
2FP8IGF2_2.7.ab1 - Chromas
2FP8IGF2_2.11.ab1 - Chromas
2FP8IGF2_2.12.ab1 - Chromas
2FP8IGF2_2.29.ab1 - Chromas
2FP8IGF2_2.42.ab1 - Chromas
2FP8IGF2_2.43.ab1 - Chromas
2FP8IGF2_2.45.ab1 - Chromas

18. 2F P15 IGF2

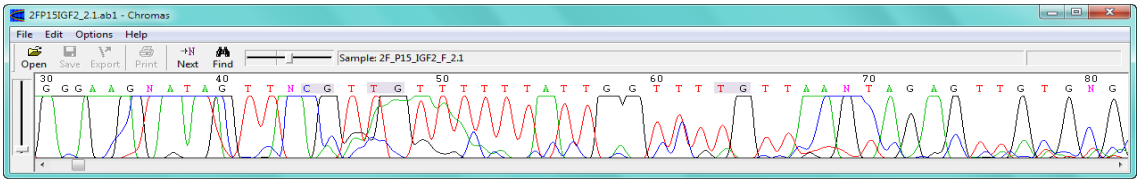

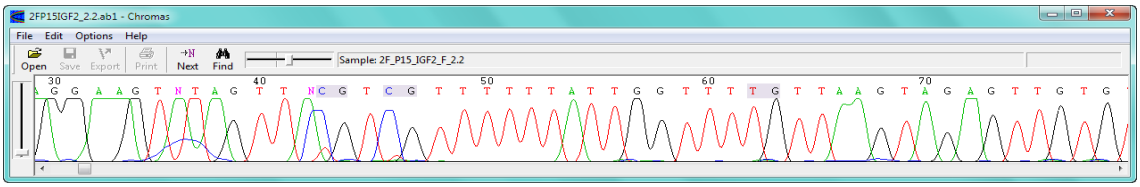

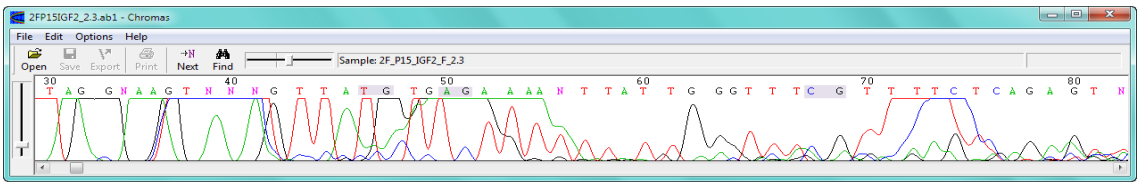

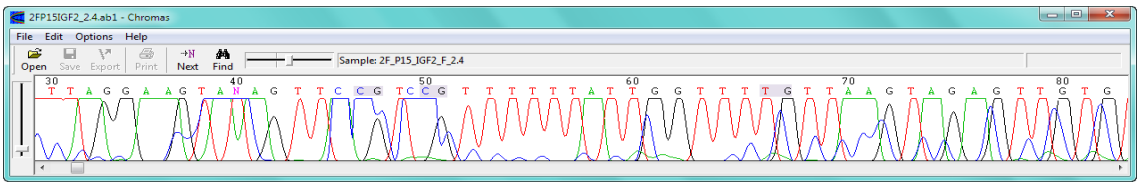

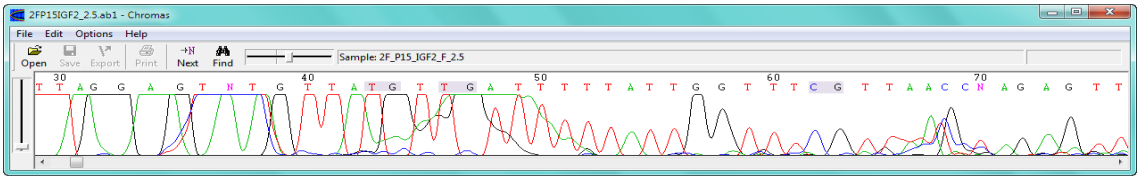

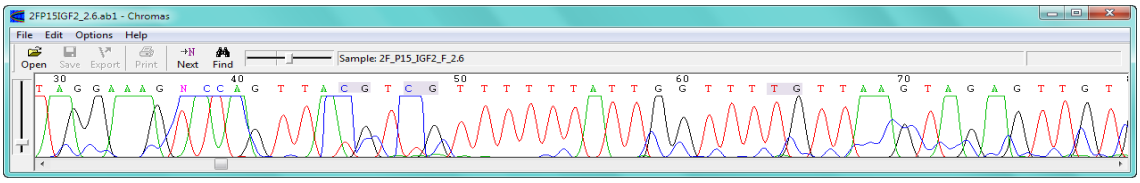

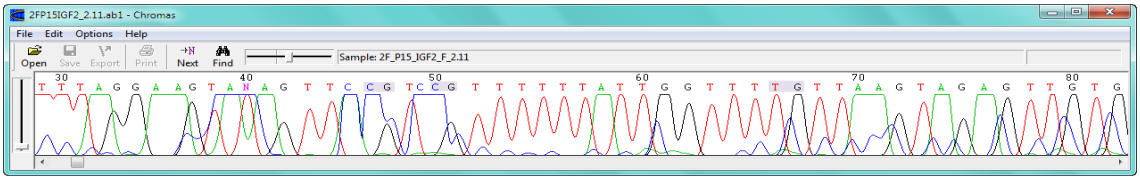

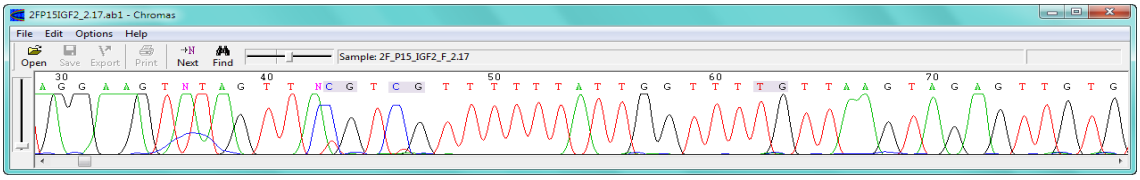

19. 6A P8 IGF2

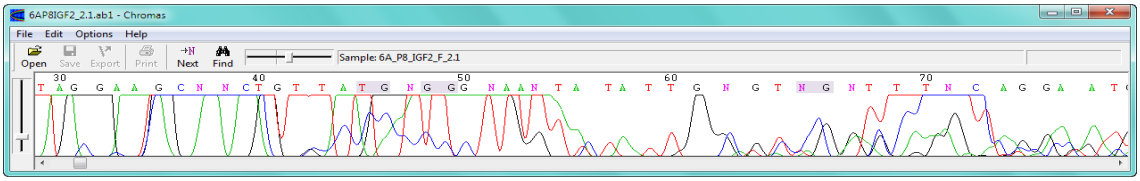
6AP8IGF2_2.1.ab1 - Chromas
File Edit Options Help
Open Save Export Print Next Find
Sample: 6A_P8_IGF2_F_2.1

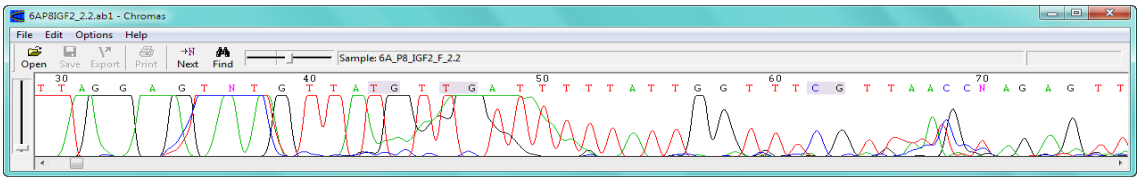
6AP8IGF2_2.2.ab1 - Chromas
File Edit Options Help
Open Save Export Print Next Find
Sample: 6A_P8_IGF2_F_2.2

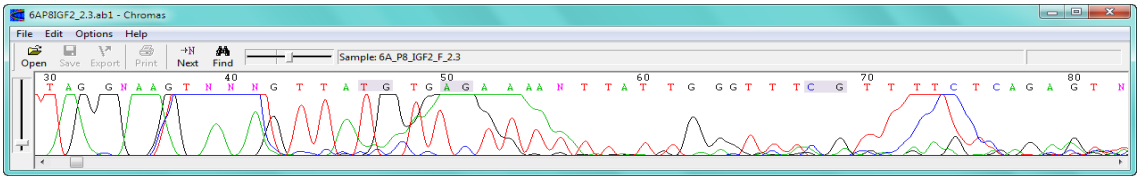
6AP8IGF2_2.3.ab1 - Chromas
File Edit Options Help
Open Save Export Print Next Find
Sample: 6A_P8_IGF2_F_2.3

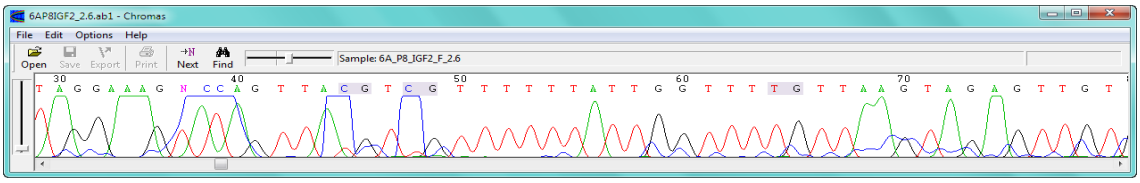
6AP8IGF2_2.6.ab1 - Chromas
File Edit Options Help
Open Save Export Print Next Find
Sample: 6A_P8_IGF2_F_2.6

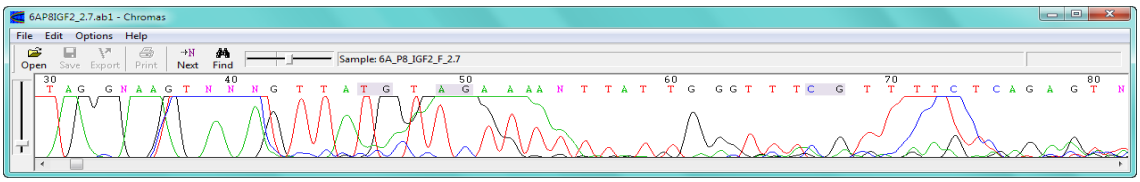
6AP8IGF2_2.7.ab1 - Chromas
File Edit Options Help
Open Save Export Print Next Find
Sample: 6A_P8_IGF2_F_2.7

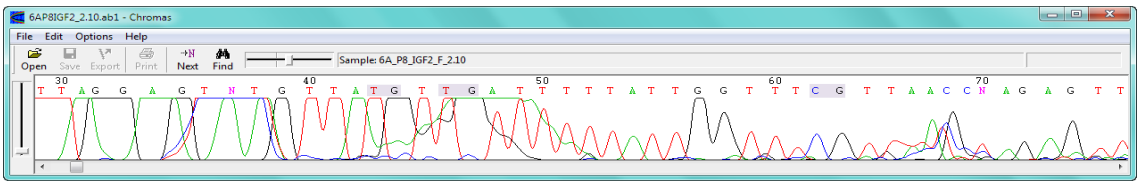
6AP8IGF2_2.10.ab1 - Chromas
File Edit Options Help
Open Save Export Print Next Find
Sample: 6A_P8_IGF2_F_2.10

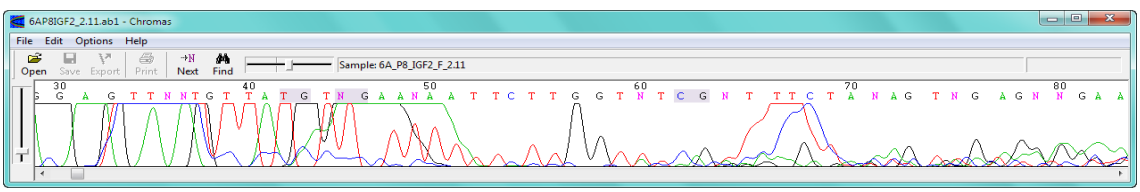
6AP8IGF2_2.11.ab1 - Chromas
File Edit Options Help
Open Save Export Print Next Find
Sample: 6A_P8_IGF2_F_2.11

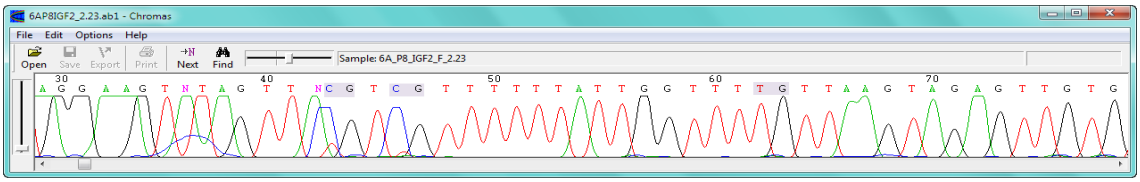
6AP8IGF2_2.23.ab1 - Chromas
File Edit Options Help
Open Save Export Print Next Find
Sample: 6A_P8_IGF2_F_2.23

20. 6A P15 IGF2

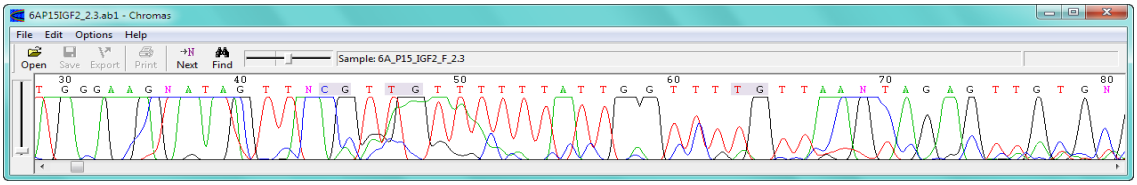

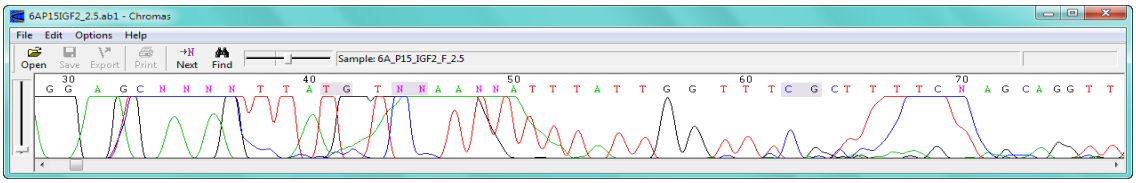

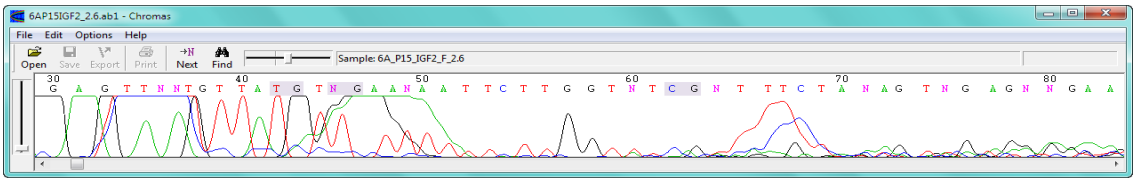

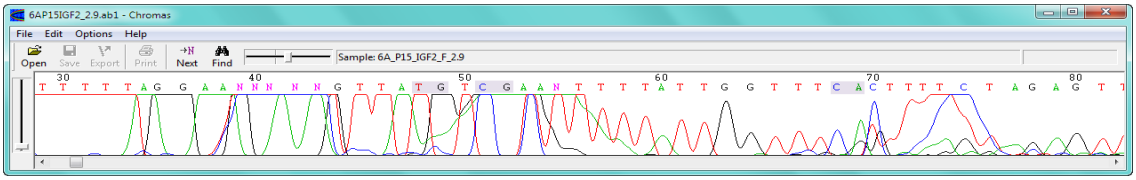

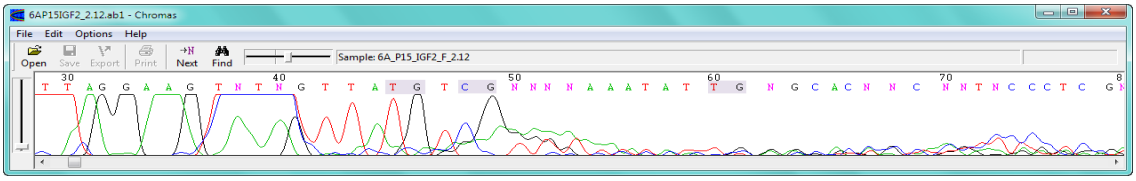

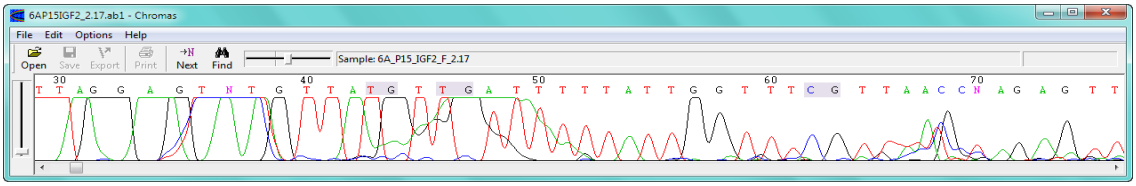

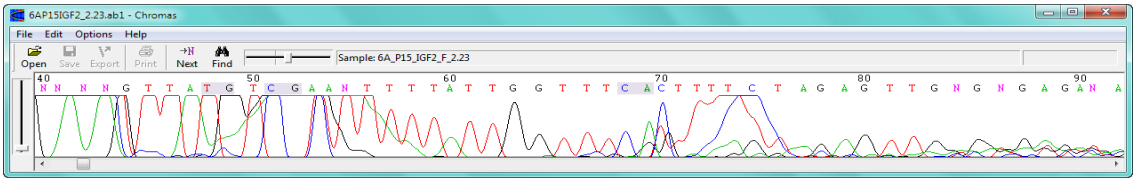

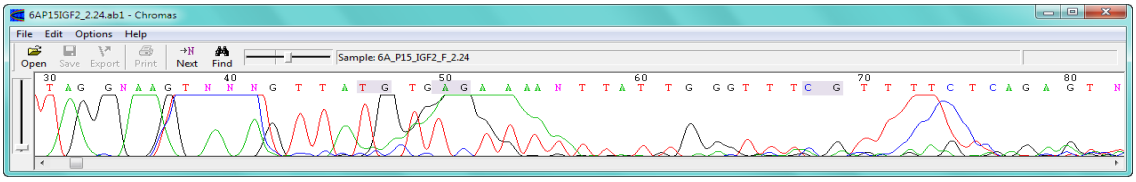

21. CL8 P8 IGF2

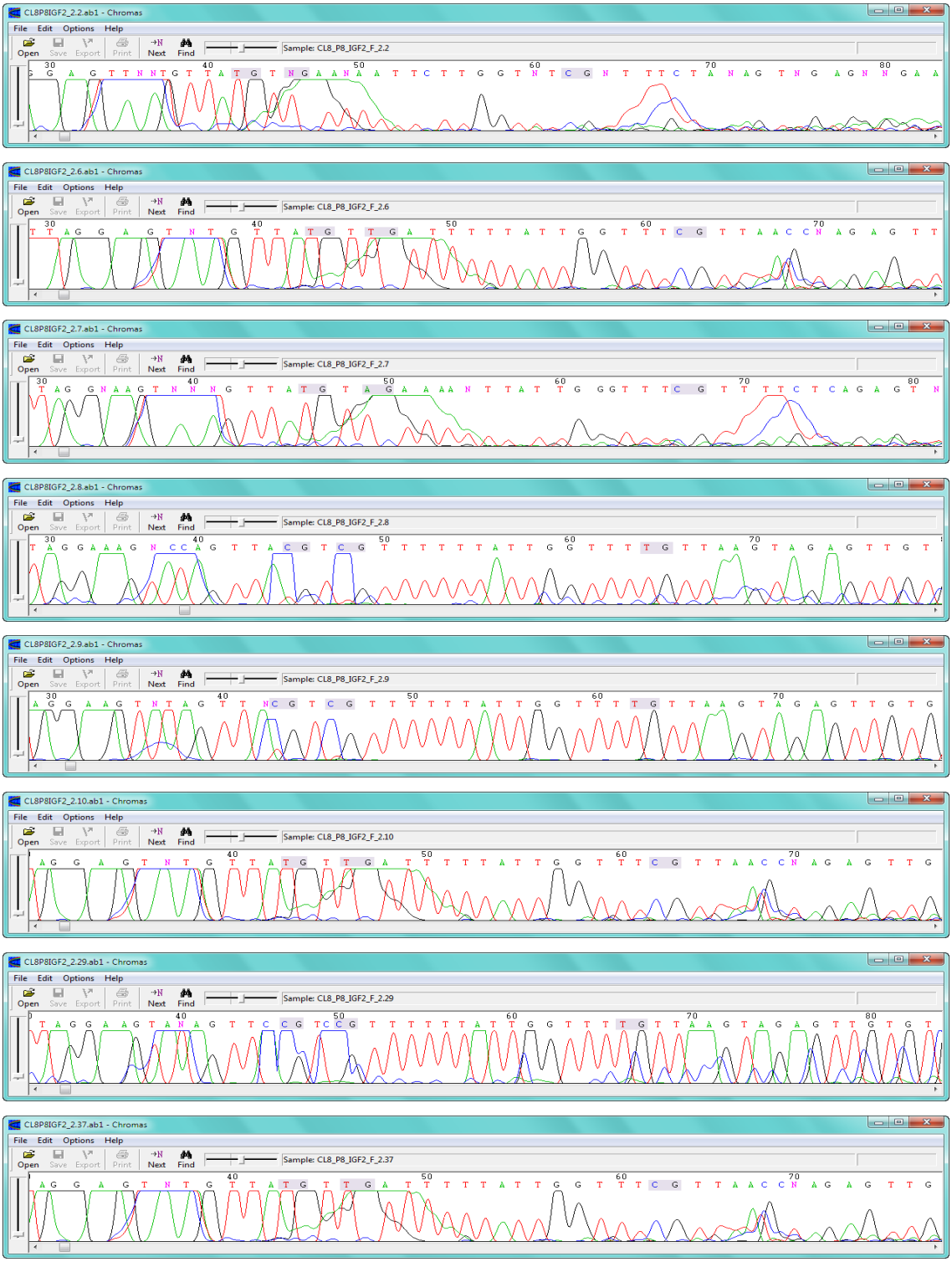

22. CL8 P15 IGF2

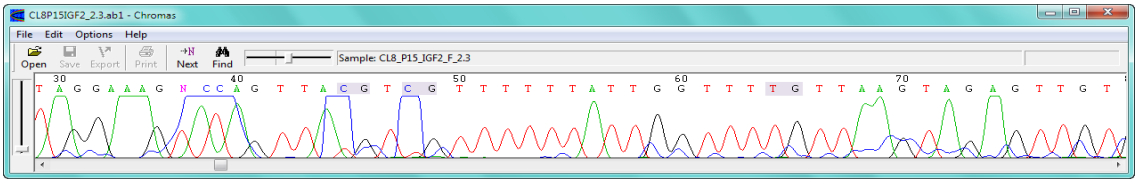

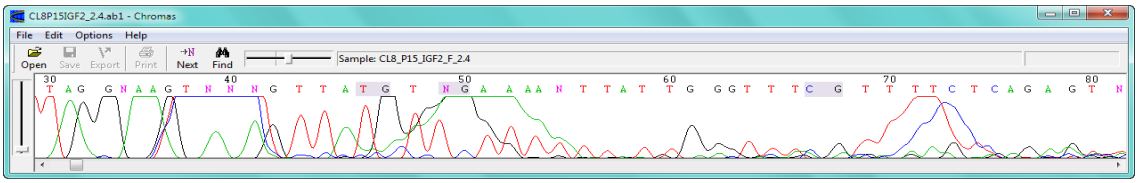

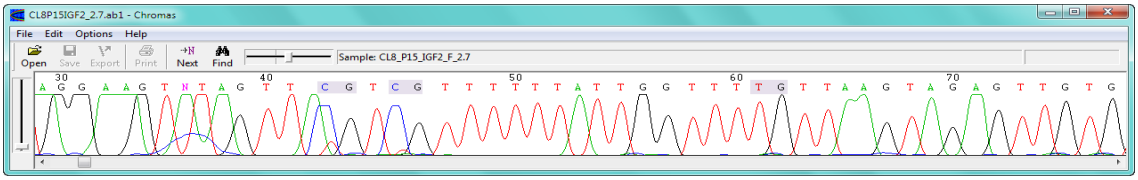

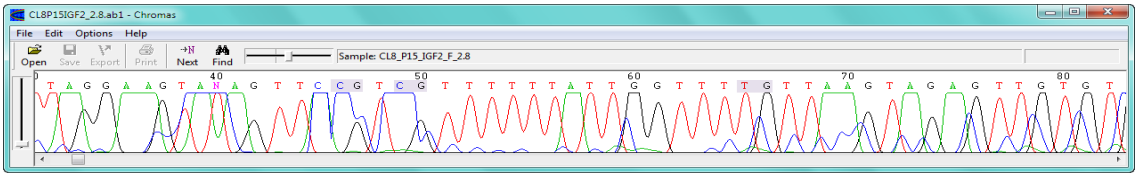

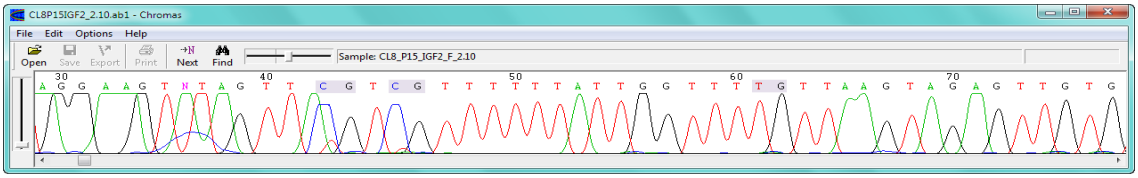

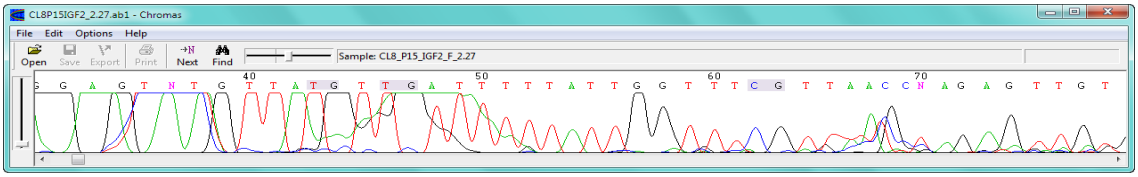

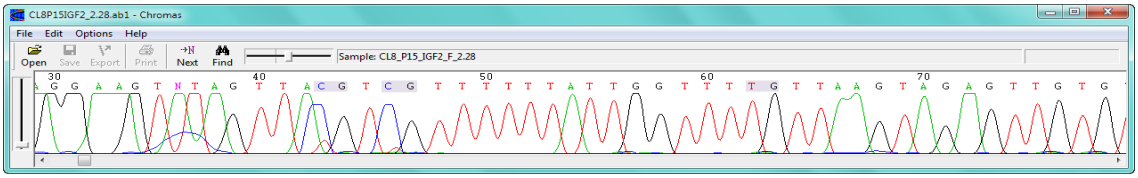

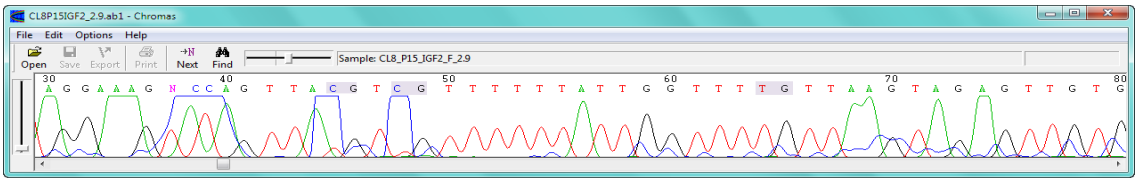

23. CL9 P8 IGF2

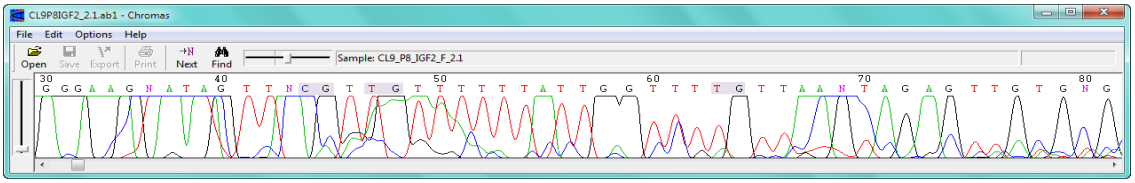

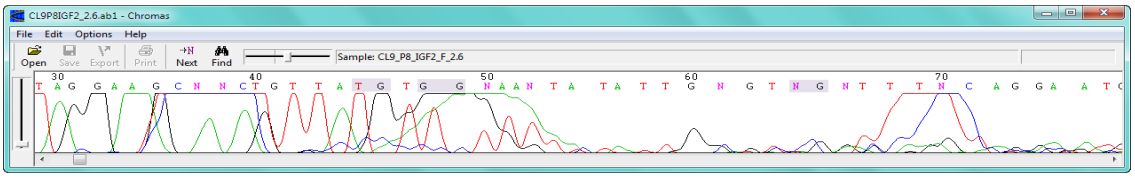

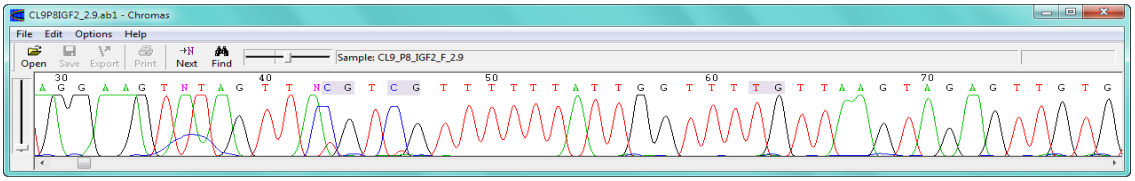

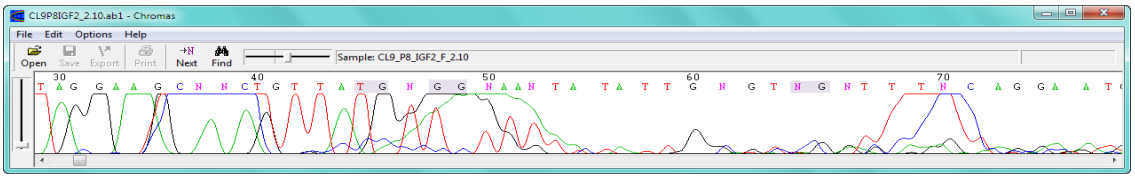

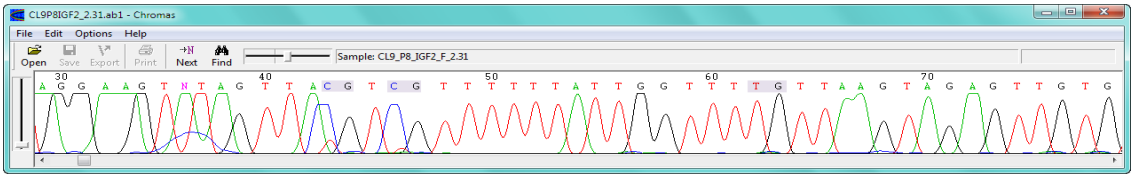

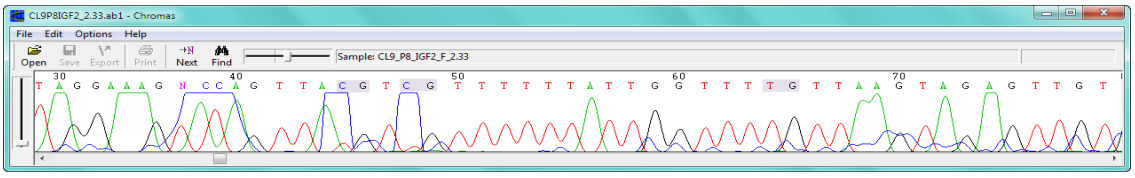

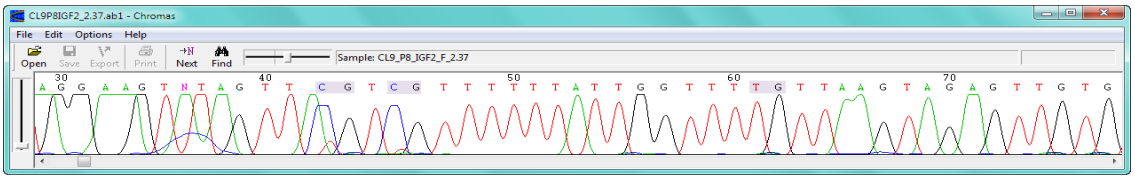

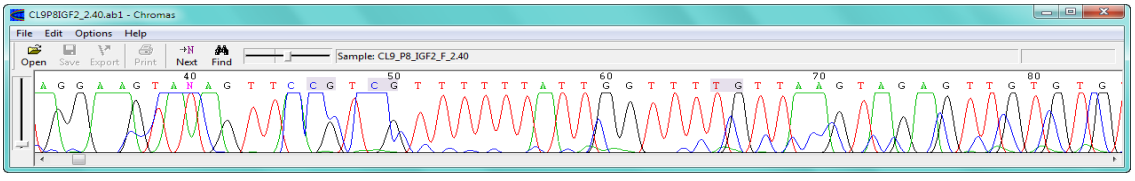

24. CL9 P15 IGF2

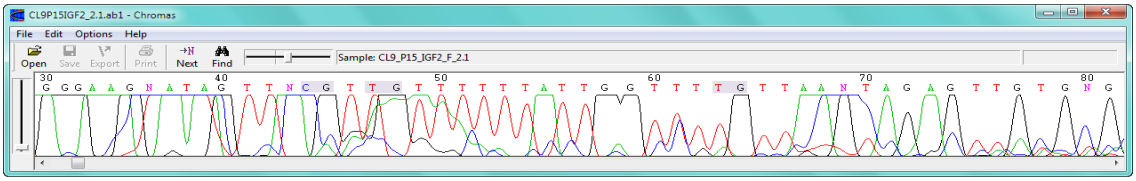

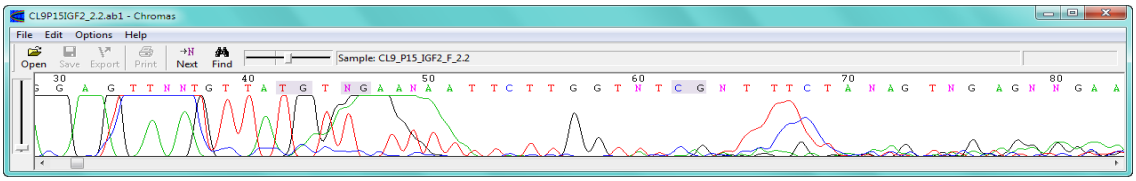

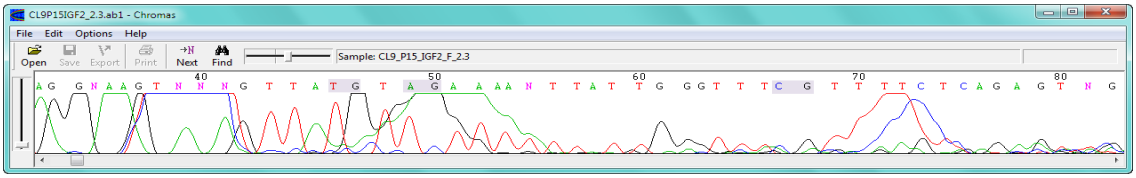

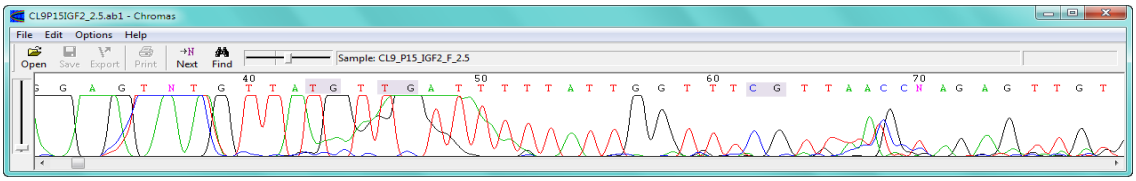

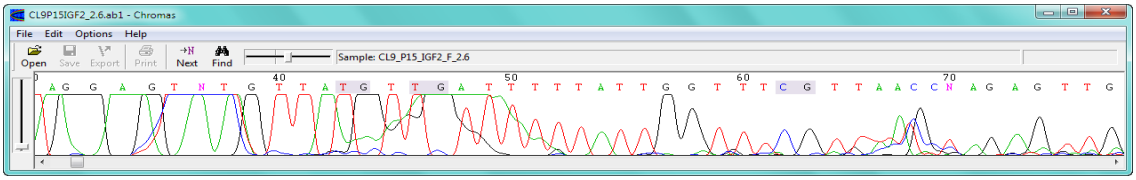

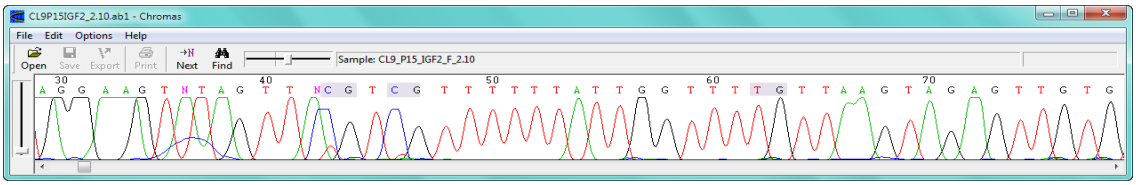

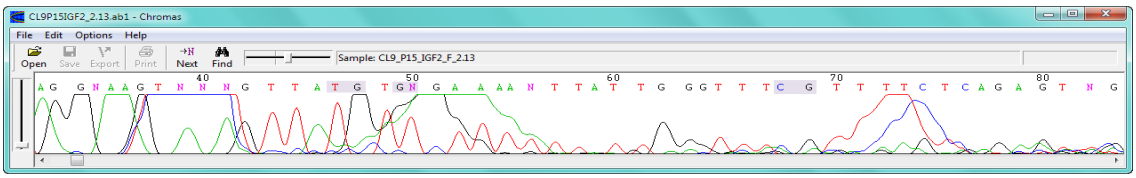

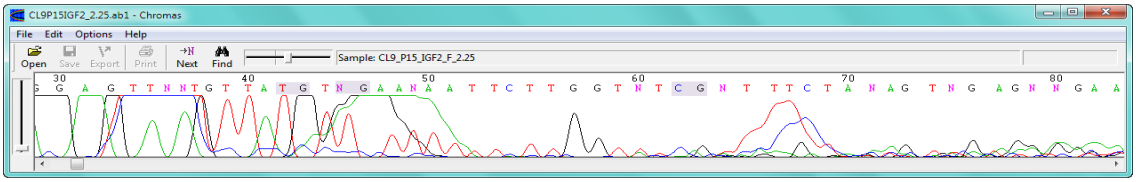

25. T8 P8 IGF2

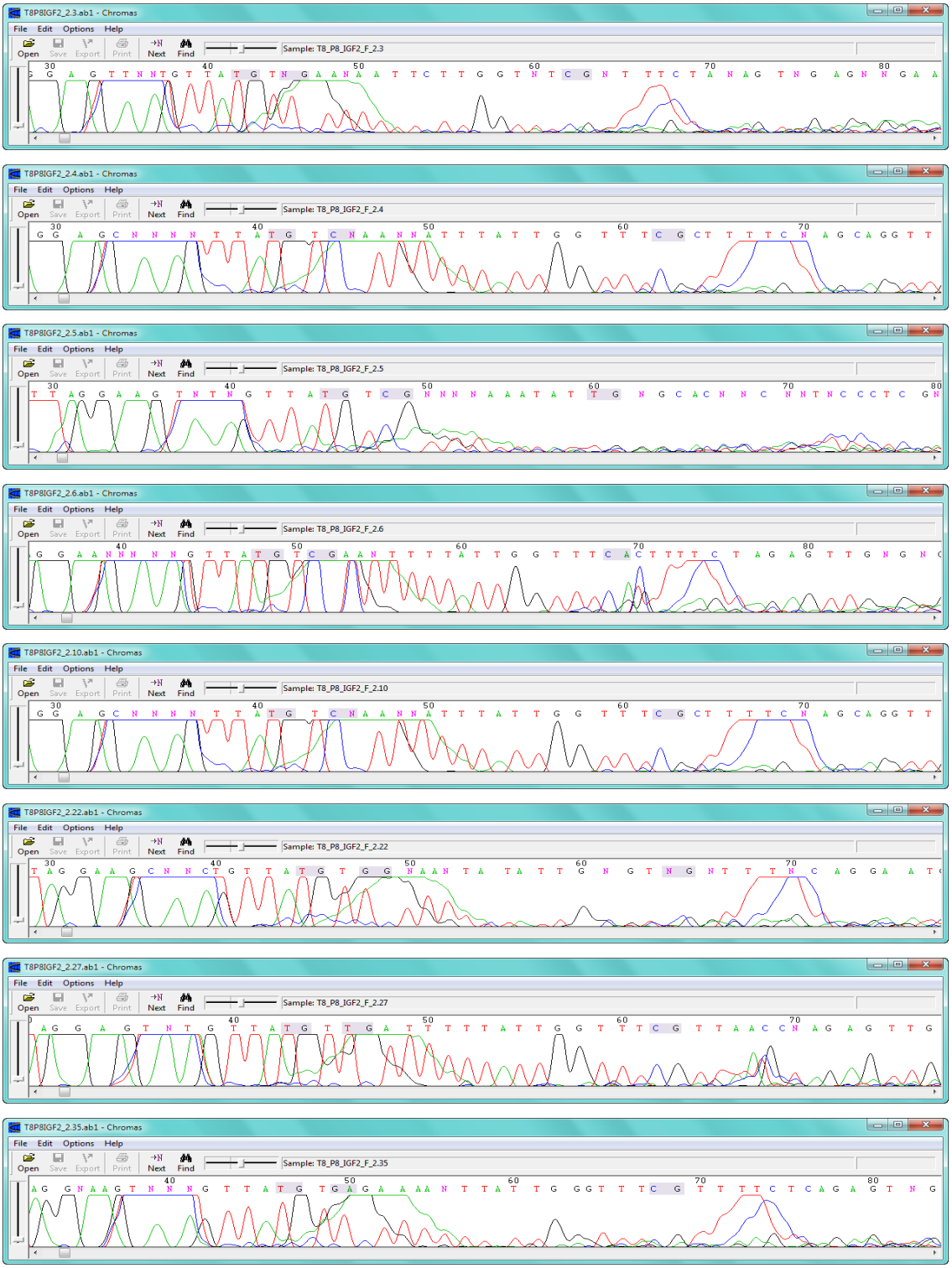
T8P8IGF2_2.3.ab1 - Chromas
Sample: T8_P8_IGF2_F_2.3
T8P8IGF2_2.4.ab1 - Chromas
Sample: T8_P8_IGF2_F_2.4
T8P8IGF2_2.5.ab1 - Chromas
Sample: T8_P8_IGF2_F_2.5
T8P8IGF2_2.6.ab1 - Chromas
Sample: T8_P8_IGF2_F_2.6
T8P8IGF2_2.10.ab1 - Chromas
Sample: T8_P8_IGF2_F_2.10
T8P8IGF2_2.22.ab1 - Chromas
Sample: T8_P8_IGF2_F_2.22
T8P8IGF2_2.27.ab1 - Chromas
Sample: T8_P8_IGF2_F_2.27
T8P8IGF2_2.35.ab1 - Chromas
Sample: T8_P8_IGF2_F_2.35

26. T8 P15 IGF2

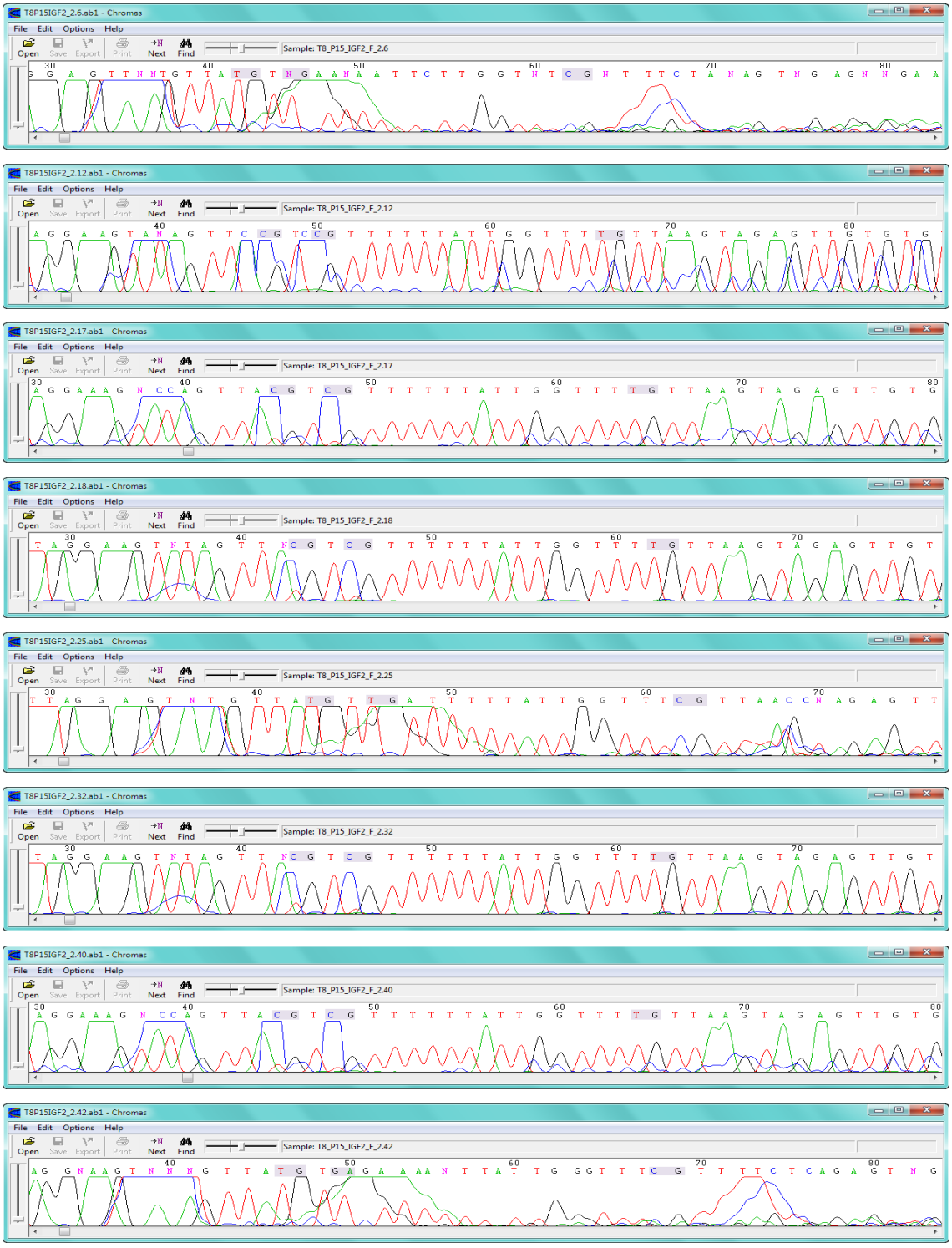

27. T11 P8 IGF2

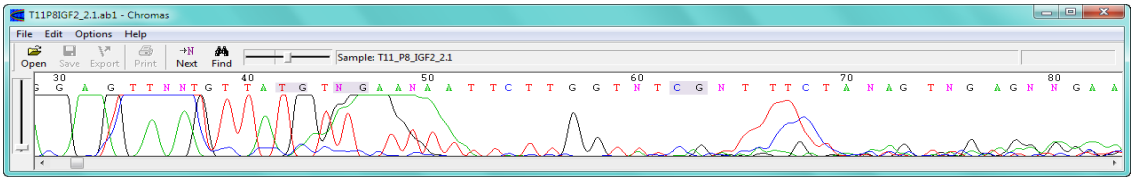

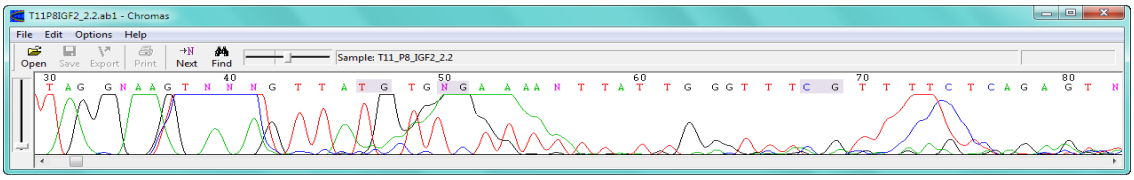

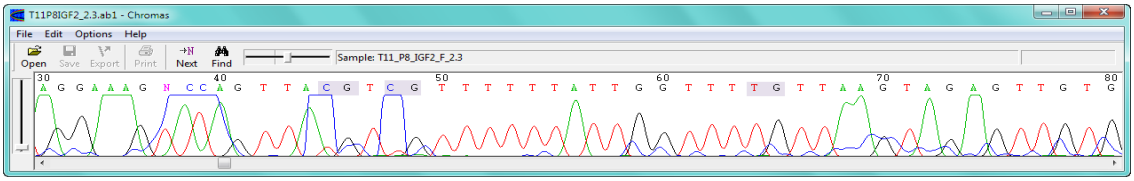

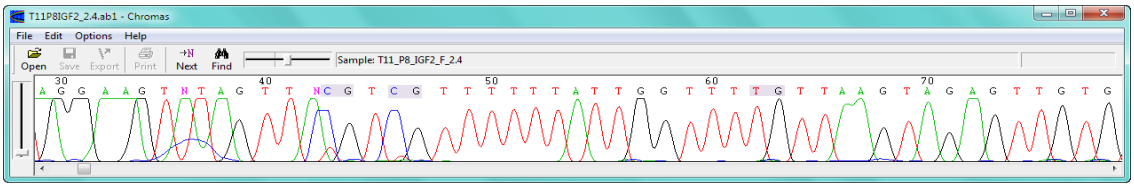

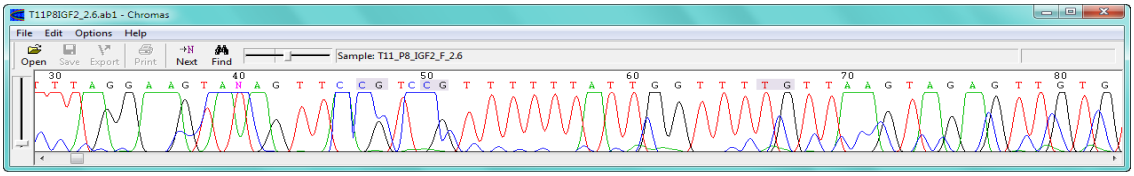

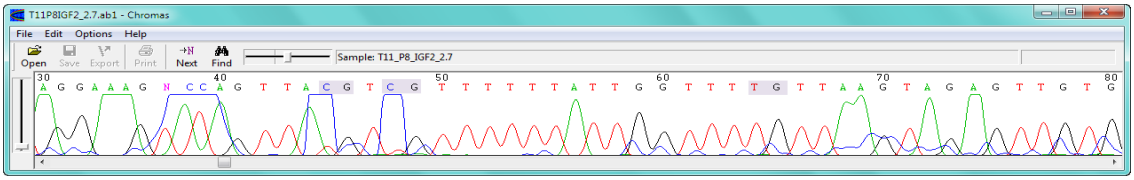

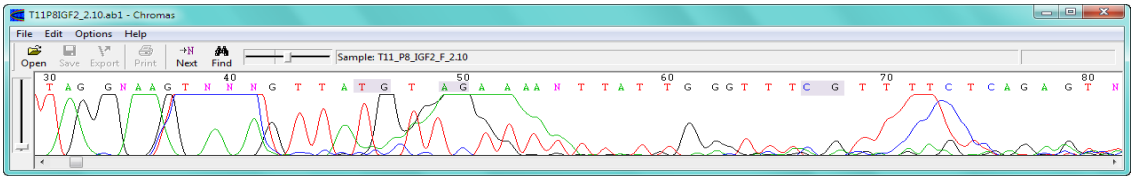

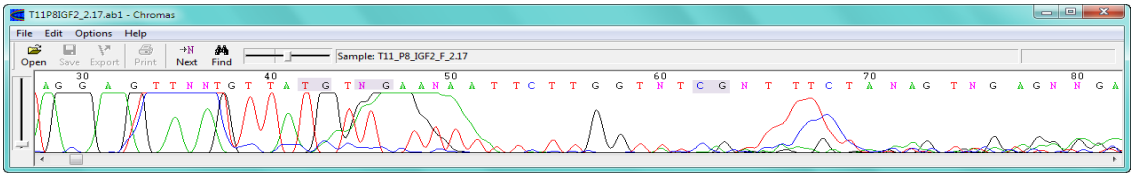

28. T11 P15 IGF2

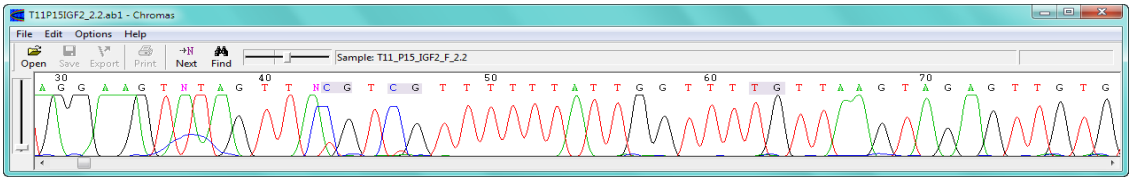

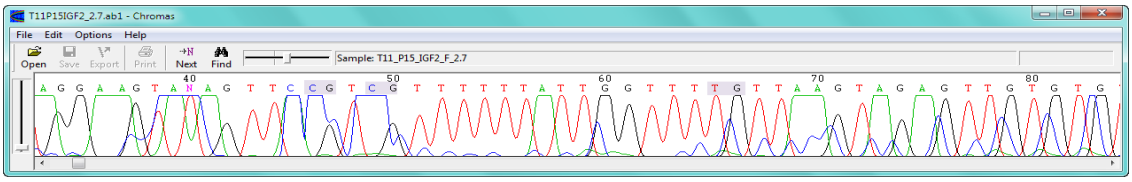

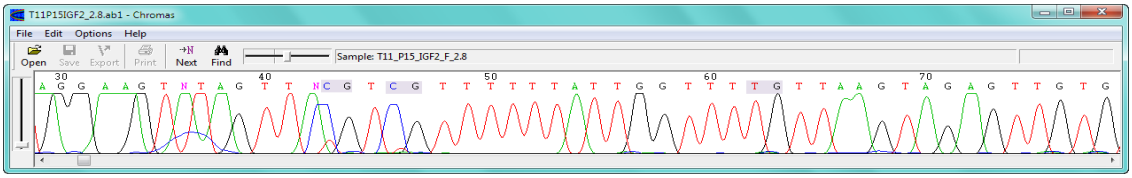

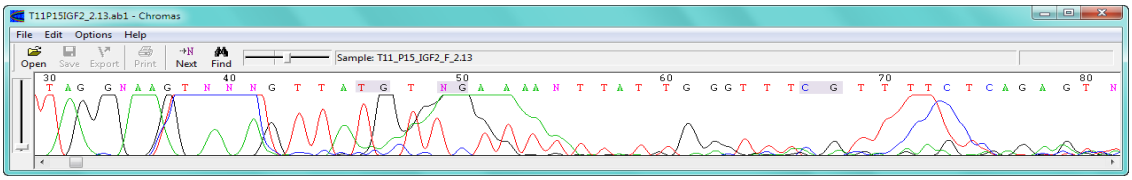

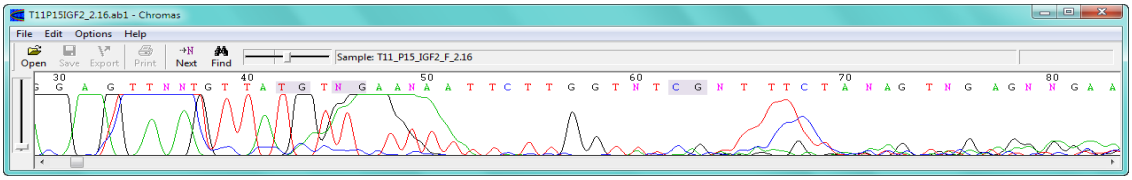

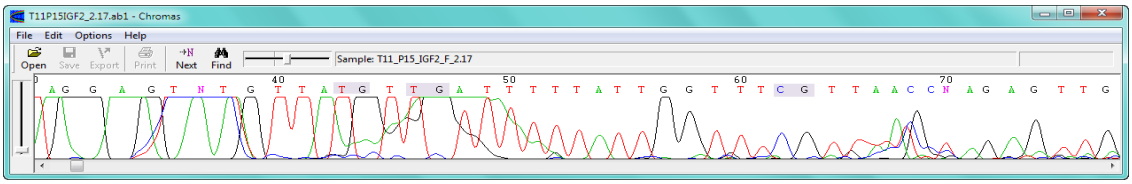

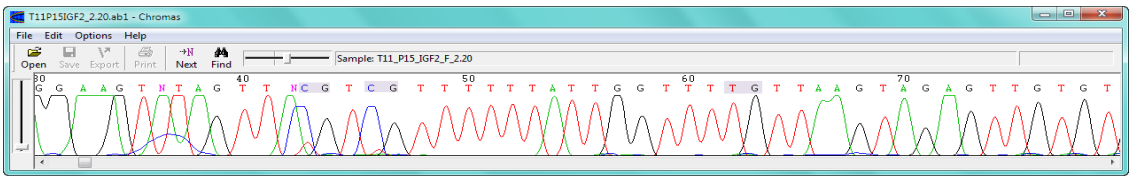

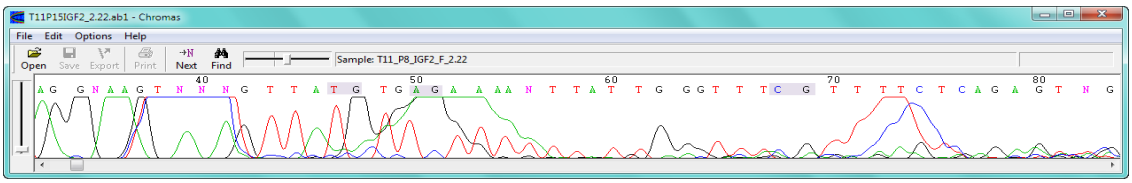

29. T18 P8 IGF2

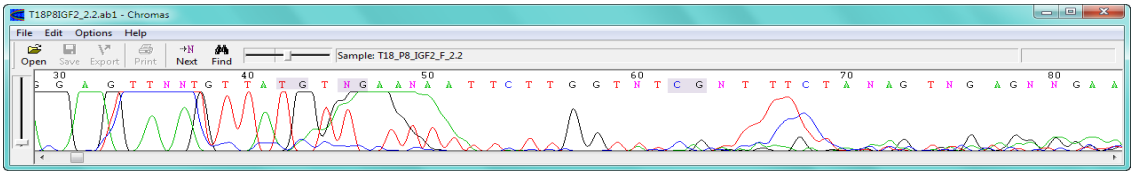

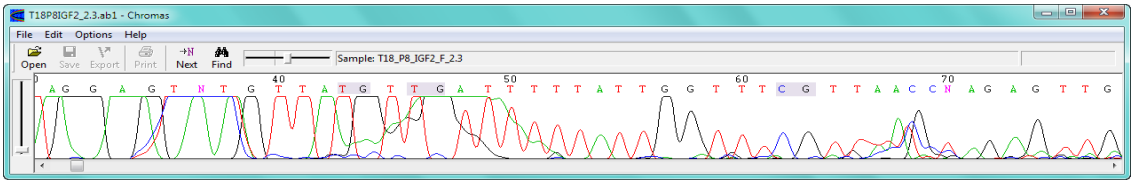

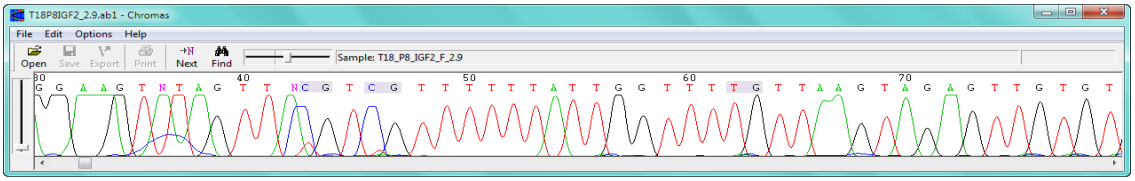

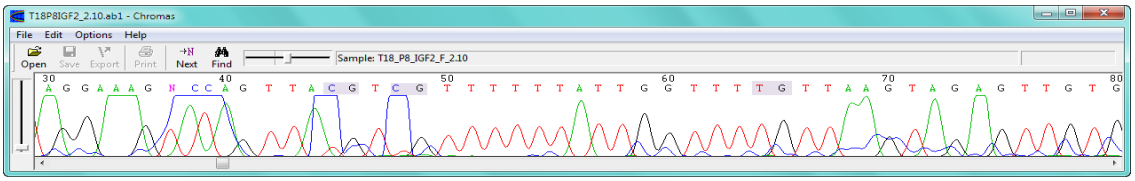

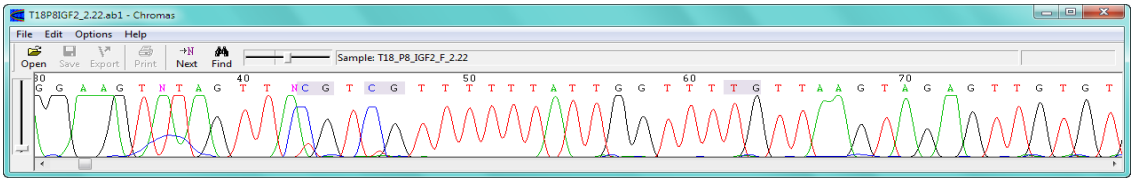

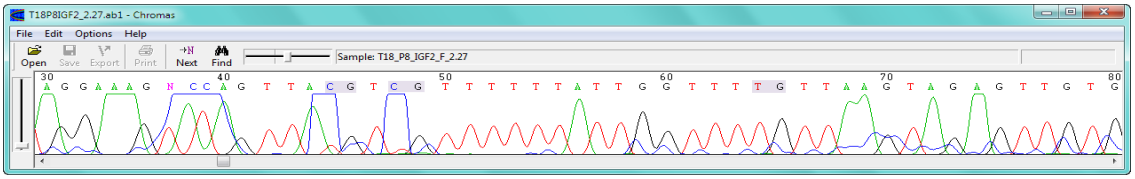

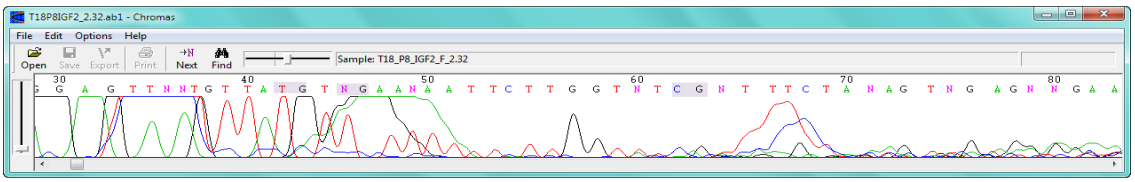

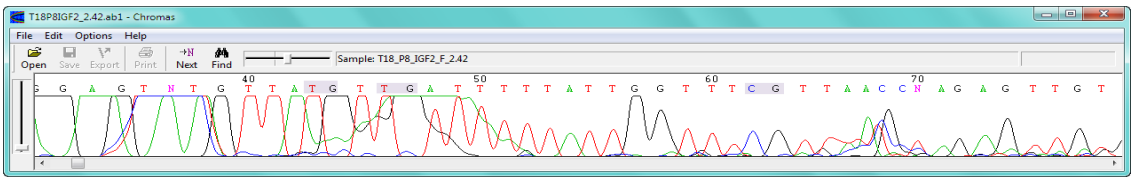

30. T18 P15 IGF2

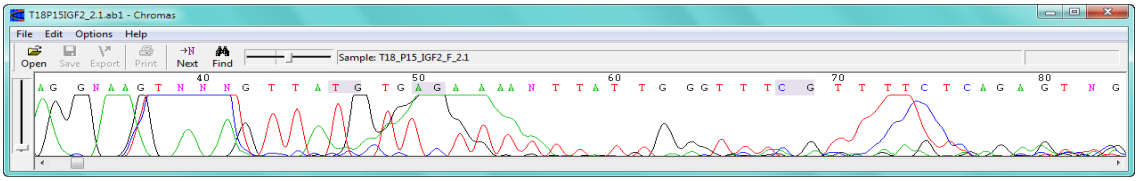

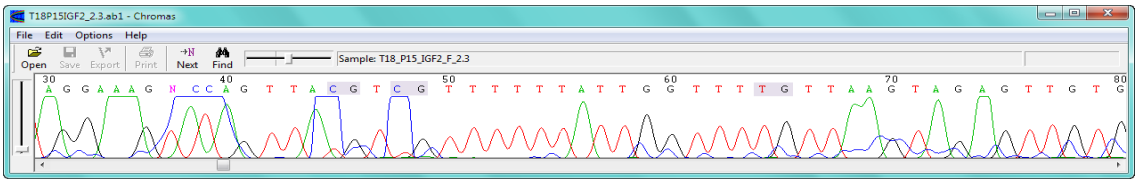

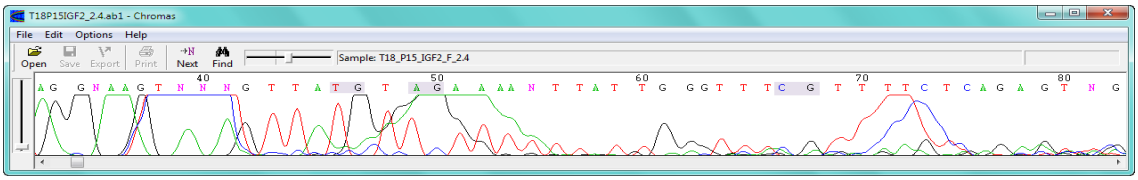

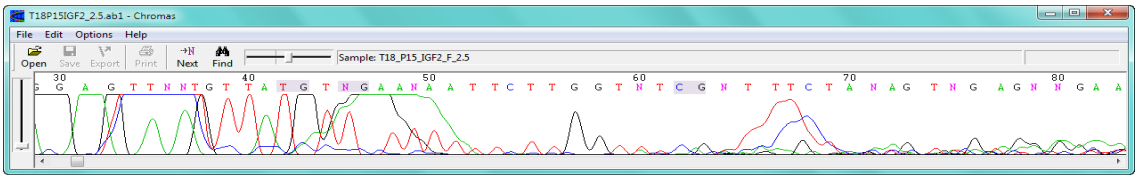

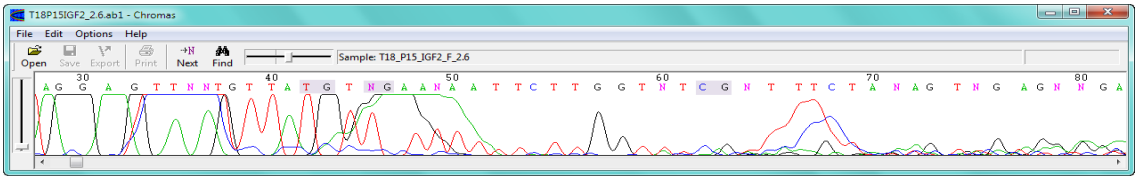

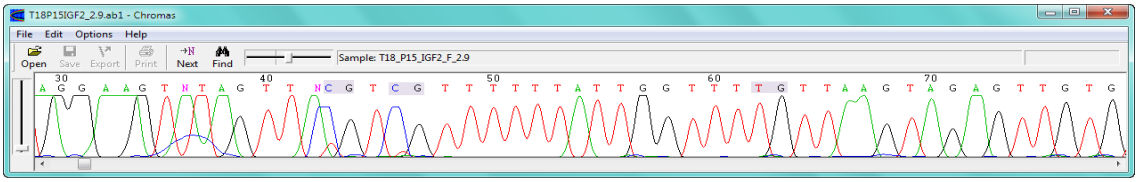

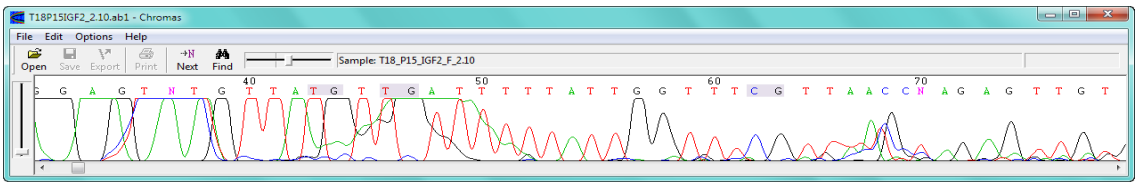

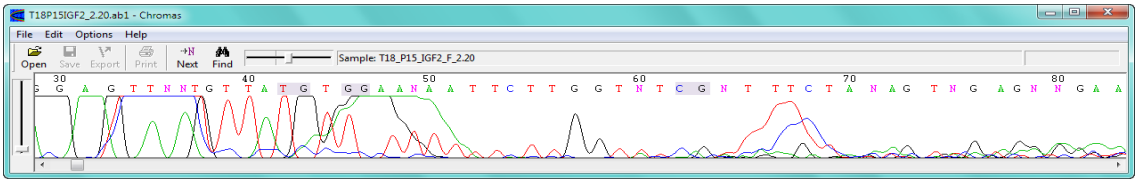

31. T21 P8 IGF2

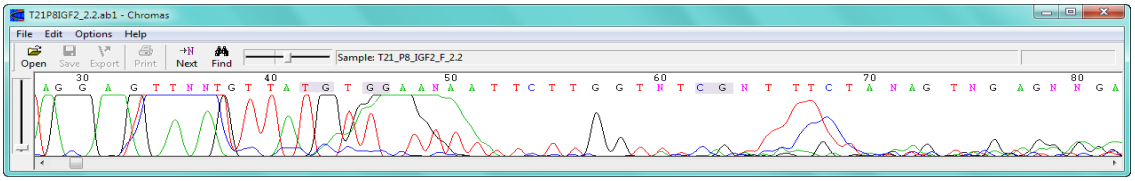

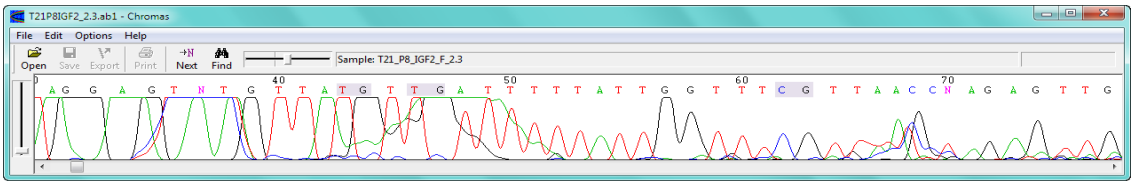

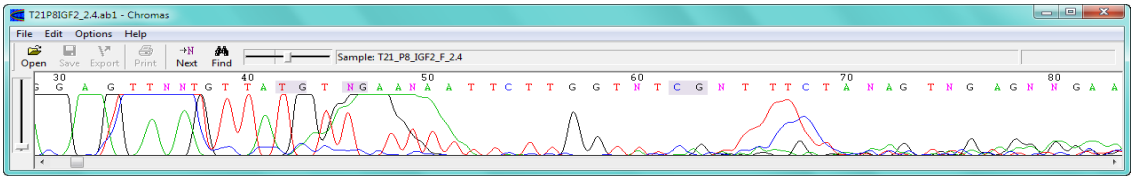

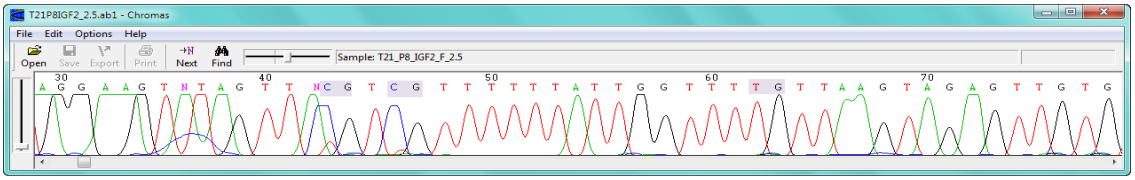

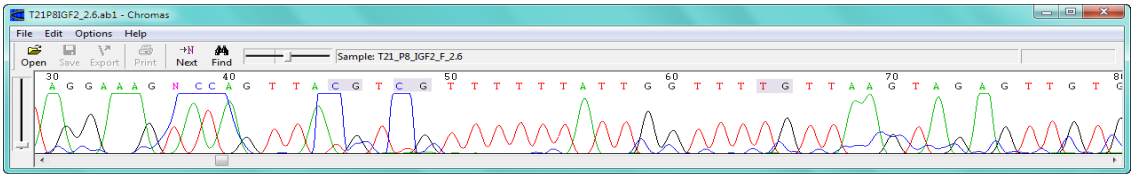

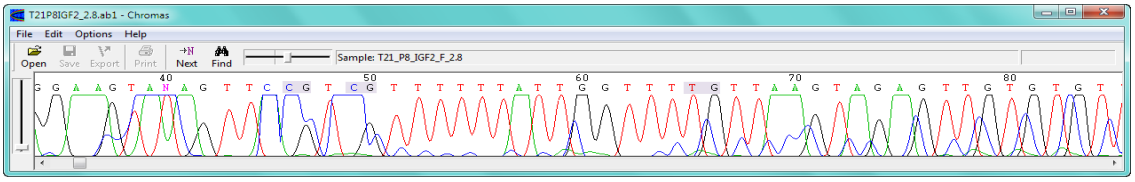

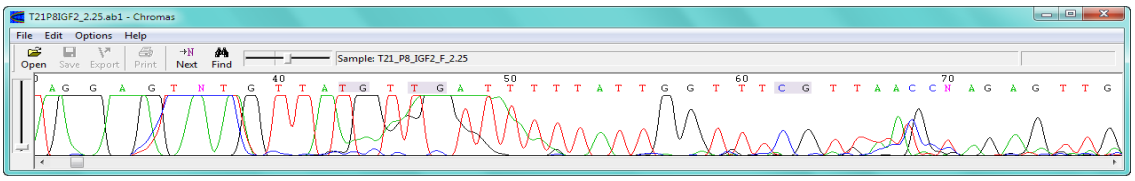

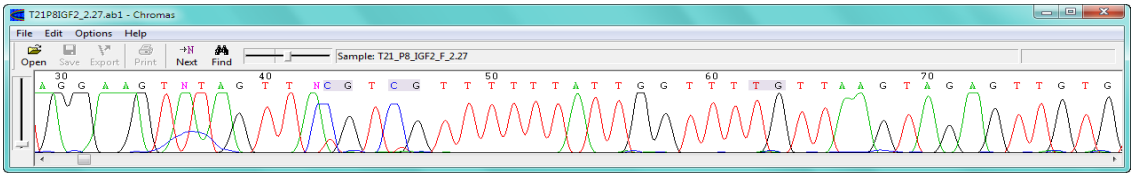

32. T21 P15 IGF2

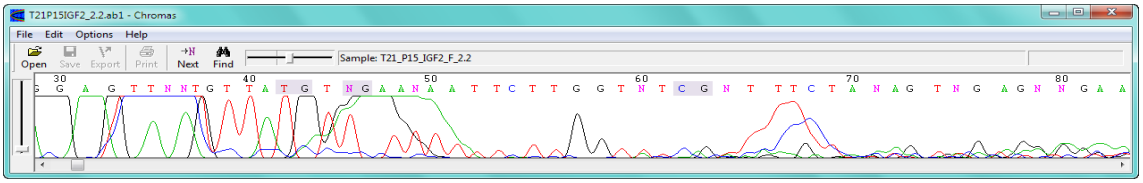

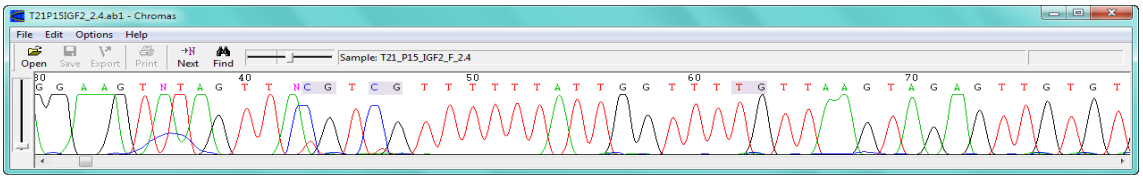

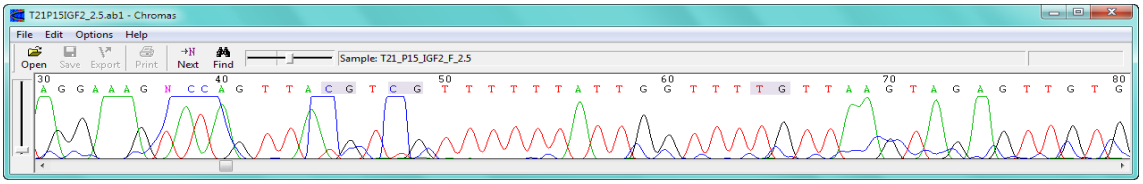

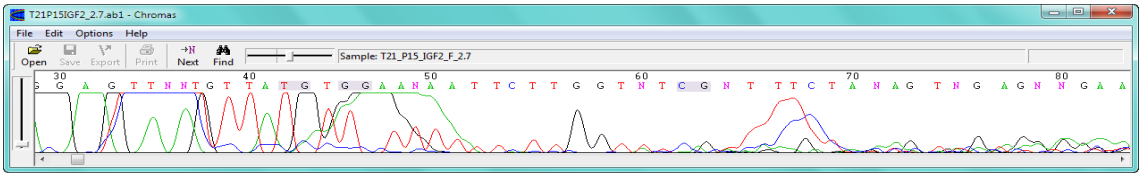

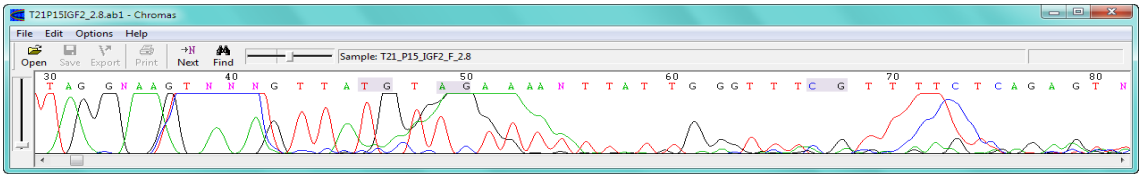

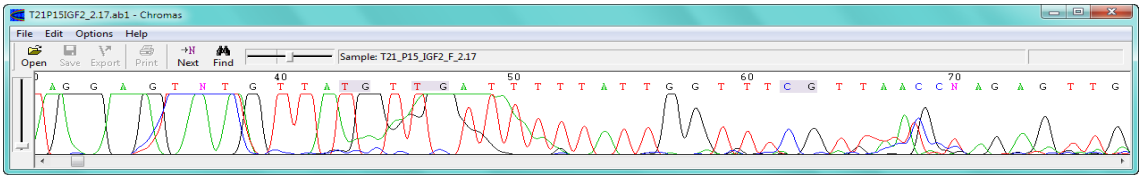

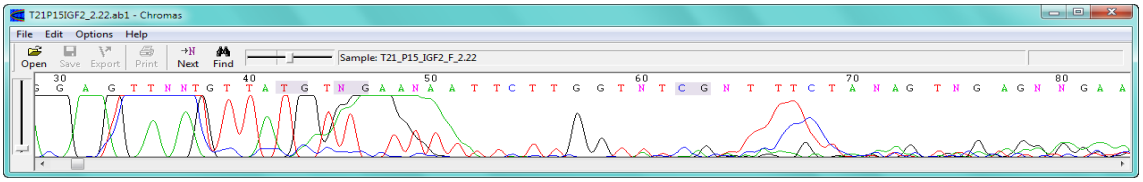

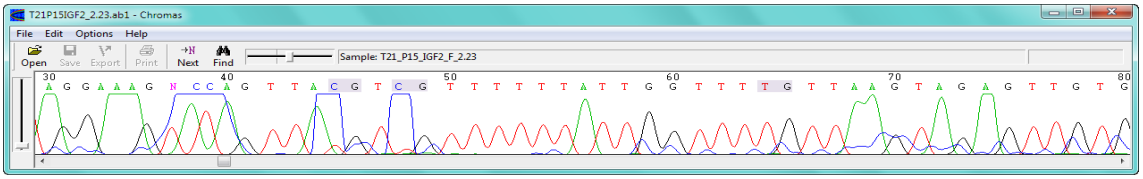

BIOGRAPHY

NAME	Miss Sujeeporn Sripradite
DATE OF BIRTH	5 January 1984
PLACE OF BIRTH	Nakhonphanom, Thailand
INSTITUTIONS ATTENDED	Srinakharinwirot University 2002-2005 Bachelor of Science (Biology) Mahidol University 2006-2009 Master of Science (Biochemistry)
RESEARCH GRANTS	Partial Thesis Writing Grant supported From Faculty of Graduate Studies, Mahidol University
HOME ADDRESS	30/1, Thamrongprasit Rd., Tumbon Nai-Mueng, Amphur Mueng, Nakhonphanom, Thailand**.**